DEVELOPMENT OF BALLISTIC-DAMAGE-TOLERANT FLIGHT CONTROL COMPONENTS MOLDED OF A SHORT-FIBER REINFORCED COMPOSITE MATERIAL. PHASE I. SUMMARY REPORT: COMPOSITE MATERIAL FORMATION, EVALUATION, AND CHARACTERIZATION.

Donald C. Cully

Goodyear Aerospace Corporation

Prepared for:

Army Air Mobility Research and Development Laboratory

September 1972

AD

USAAMRDL TECHNICAL REPORT 72-28
DEVELOPMENT OF BALLISTIC-DAMAGE-TOLERANT FLIGHT CONTROL COMPONENTS MOLDED OF A SHORT-FIBER REINFORCED COMPOSITE MATERIAL

PHASE I SUMMARY REPORT: COMPOSITE MATERIAL FORMATION, EVALUATION, AND CHARACTERIZATION

By

D. C. Cully

R. V. Kolarik

T. J. Boller

W. F. Conley

September 1972

EUSTIS DIRECTORATE

U. S. ARMY AIR MOBILITY RESEARCH AND DEVELOPMENT LABORATORY

FORT EUSTIS, VIRGINIA

CONTRACT DAAJ02-70-C-0062

GOODYEAR AEROSPACE CORPORATION

AKRON, OHIO

274

DISCLAIMERS

The findings in this report are not to be construed as an official Department of the Army position unless so designated by other authorized documents.

When Government drawings, specifications, or other data are used for any purpose other than in connection with a definitely related Government procurement operation, the U.S. Government thereby incurs no responsibility nor any obligation whatsoever; and the fact that the Government may have formulated, furnished, or in any way supplied the said drawings, specifications, or other data is not to be regarded by implication or otherwise as in any manner licensing the holder or any other person or corporation, or conveying any rights or permission, to manufacture, use, or sell any patented invention that may in any way be related thereto.

Trade names cited in this report do not constitute an official endorsement or approval of the use of such commercial hardware or software.

DISPOSITION INSTRUCTIONS

Destroy this report when no longer needed. Do not return it to the originator.

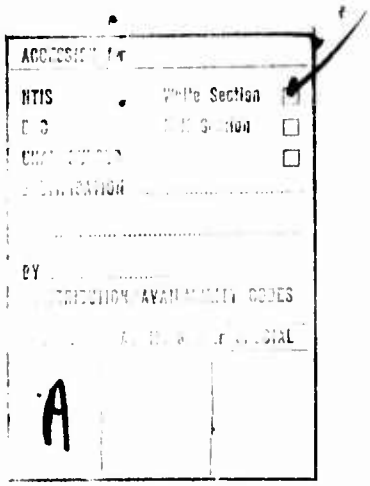

Unclassified

Security Classification

DOCUMENT CONTROL DATA - R & D

(Security classification of title, body of abstract and indexing annotation must be entered when the overall report is classified)

1 ORIGINATING ACTIVITY (Corporate author)	2a. REPORT SECURITY CLASSIFICATION
Goodyear Aerospace Corporation Akron, Ohio	Unclassified
	2b. GROUP

3 REPORT TITLE

DEVELOPMENT OF BALLISTIC-DAMAGE-TOLERANT FLIGHT CONTROL COMPONENTS MOLDED OF A SHORT-FIBER REINFORCED COMPOSITE MATERIAL

PHASE I SUMMARY REPORT: COMPOSITE MATERIAL FORMATION, EVALUATION, AND CHARACTERIZATION

4 DESCRIPTIVE NOTES *(Type of report and inclusive dates)*

Phase I Summary Report, June 1970 thru December 1971

5 AUTHOR(S) *(First name, middle initial, last name)*

Donald C. Cully and Robert V. Kolarik

6. REPORT DATE	7a. TOTAL NO. OF PAGES	7b. NO. OF REFS
September 1972	272	2

8a. CONTRACT OR GRANT NO.	9a. ORIGINATOR'S REPORT NUMBER(S)
DAAJ02-70-C-0062	
b. PROJECT NO	USAAMRDL Technical Report 72-28
c. Task 1F162203A15003	9b. OTHER REPORT NO(S) *(Any other numbers that may be assigned this report)*
d.	GER 15518

10 DISTRIBUTION STATEMENT

Approved for public release; distribution unlimited.

11. SUPPLEMENTARY NOTES	12. SPONSORING MILITARY ACTIVITY
	Eustis Directorate, U.S. Army Air Mobility Research and Development Laboratory Fort Eustis, Virginia

13. ABSTRACT

The purpose of this program was to select and characterize the most efficient discontinuous fiber glass-epoxy composite for use in ballistically tolerant flight control components. The effects of various constituent parameters on the extent of damage and residual tensile load capacity were determined after tumbled caliber .30 ball M2 projectile impacts at 0-degree obliquity and 1800 ft/sec. These parameters included fiber glass and resin types, interfacial properties, fiber length, and fiber content. The three most promising composites for further study were identified as: (1) 1-inch S-2 glass fibers in an epoxy novalac matrix, (2) 1/2-inch S-2 glass fibers in an epoxy novalac matrix, and (3) 1-inch E glass fibers in a flexibilized epoxy matrix. The study involved determination of ballistic test and composite variables on extent of damage and residual load capacity. The variables were projectile type and velocity and specimen temperature and thickness. The fatigue characteristics of undamaged and damaged specimens and the combined effects of prestress and ballistic impact conditions are reported. An "effective damage length" was computed that accounts for the loss in specimen load capacity under various test conditions. The 1/2-inch S-2 glass fibers with an epoxy-compatible finish in an epoxy novalac matrix exhibited the best overall performance. The design allowable properties of this composite were then determined. The mechanical properties (tensile, compressive, flexural, shear, and bearing) required for reliable component design were established on two data bases.

Ia

DD FORM 1 NOV 65 1473

Unclassified

Security Classification

14 KEY WORDS	LINK A		LINK B		LINK C	
	ROLE	WT	ROLE	WT	ROLE	WT
Aircraft Equipment - Control Systems						
Aircraft Safety						
Ballistic Damage						
Ballistically Tolerant Bell Crank						
Composites - Fiber Glass Reinforced						
Composites - Discontinuous Fiber Reinforced						
Helicopter - Survivability						
Impact Damage						
Small-Arms Fire						
Fracture						
Penetration						
Design Allowables						

I-6

DEPARTMENT OF THE ARMY
U. S. ARMY AIR MOBILITY RESEARCH & DEVELOPMENT LABORATORY
EUSTIS DIRECTORATE
FORT EUSTIS, VIRGINIA 23604

This report was prepared by Goodyear Aerospace Corporation under the terms of Contract DAAJ02-70-C-[illegible]2.

This effort is the first phase of a three-phase program to advance the state of the art of providing small-arms ballistic protection for Army aircraft critical components. The approach consists of using a short-fiber plastic composite and a compression-molded fabrication technique to develop ballistic-damage-tolerant flight control components that are competitive with current standard components from the standpoint of weight, strength, ease of fabrication, reliability, and cost. The Phase I effort reported herein involved an evaluation and optimization of the material system by parametric changes in several material property variables at various ballistic and environmental conditions, the selection of the optimum composite material, and its characterization for performance -- ballistically, environmentally, and structurally -- including design allowable data.

The technical monitor for this contract was Mr. Stephen Pociluyko of the Safety and Survivability Division.

TC

Task 1F162203A15003
Contract DAAJ02-70-C-0062
USAAMRDL Technical Report 72-28
September 1972

DEVELOPMENT OF BALLISTIC-DAMAGE-TOLERANT FLIGHT CONTROL COMPONENTS MOLDED OF A SHORT-FIBER REINFORCED COMPOSITE MATERIAL

Phase I Summary Report: Composite Material Formation, Evaluation, and Characterization

GER 15518

By
D. C. Cully
R. V. Kolarik
T. J. Boller
W. F. Conley

Prepared by

Goodyear Aerospace Corporation
Akron, Ohio

for

EUSTIS DIRECTORATE
U.S. ARMY AIR MOBILITY RESEARCH AND DEVELOPMENT LABORATORY
FORT EUSTIS, VIRGINIA

II

ABSTRACT

The basic purpose of the Phase I program was to select and characterize the most efficient discontinuous fiberglass-epoxy resin composite for ultimate use in ballistically tolerant flight control components. This program was conducted in three major tasks as follows:

Task I - Selection of Composite Constituents

Task II - Ballistic Damage and Crack Propagation Study

Task III - Design Allowable Properties Evaluation Study

In Task I the effects of various constituent parameters on the extent of damage and residual tensile load capacity were determined on standard specimens after tumbled caliber .30 ball M2 projectile impacts at 0-degree obliquity and 1800 ft/sec. These parameters included fiber glass and resin types, interfacial properties, fiber length, and fiber content. The three most promising composites from this task were identified for further evaluation in Task II. These candidate composites were:

1. 1-inch-long S-2 glass fibers with an epoxy-compatible finish in an epoxy novalac matrix
2. 1/2-inch-long S-2 glass fibers with an epoxy-compatible finish in an epoxy novalac matrix
3. 1-inch-long E glass fibers with an epoxy/polyester-incompatible finish in a flexibilized epoxy matrix

The Task II study involved determination of ballistic test and composite variables on extent of damage and residual load capacity. These variables included projectile type and velocity as well as specimen temperature and thickness. Also established were the fatigue characteristics of undamaged and damaged specimens and the combined effects of composite prestress and ballistic impact conditions. From these data and the static tensile strength of the undamaged composites, an "effective damage length" was computed that accounts for the loss in specimen load capacity under various test conditions. From this investigation, it was established that 1/2-inch-long S-2 glass fibers with an epoxy-compatible finish in an epoxy novalac matrix exhibited the best overall performance.

The design allowable properties of this composite were then determined at -80°F, room temperature, and 160°F in Task III. The mechanical properties (tensile, compressive, flexural, shear, and bearing) required for reliable component design were established on two data bases having associated statistical assurances.

FOREWORD

This document was prepared by Goodyear Aerospace Corporation, Akron, Ohio, under U. S. Army Contract DAAJ02-70-C-0062, Task 1F162203A15003, for the Eustis Directorate, U. S. Army Air Mobility Research and Development Laboratory. Mr. Stephen Pociluyko was the Contracting Officer's Technical Representative.

This report covers the work accomplished in Phase I - Composite Material Formation, Evaluation, and Characterization - of the project for the Development of Ballistic-Damage-Tolerant Flight Control Components Molded of a Short-Fiber Reinforced Composite Material. The contract period under which this report was prepared extended from June 1970 through December 1971.

Mr. D. C. Cully, Technical Manager, and Mr. R. V. Kolarik, Project Engineer, were the principal investigators for Goodyear Aerospace Corporation. Messrs. T. J. Boller and W. F. Conley provided the data evaluation and analysis, and Mr. G. Nagy provided technical support for the statistical data analysis. Messrs. E. Fargo and A. H. Kariotis were responsible for ballistic and physical property test engineering, respectively.

Acknowledgement is given to Mr. J. K. Burkley of GAC for his management support during the program and to Messrs. Barry Elson and Al Isham of Owens-Corning Fiberglas Corp. for their technical support.

Preceding page blank

TABLE OF CONTENTS

	Page
ABSTRACT.	iii
FOREWORD	v
LIST OF ILLUSTRATIONS	ix
LIST OF TABLES	xv
INTRODUCTION	1
TEST AND EVALUATION TECHNIQUES	3
Materials	3
Impregnation	5
Chopping	6
Staging	6
Standard Test Specimen	7
Test Methods and Equipment	10
Evaluation Criteria	21
TASK I - SELECTION OF COMPOSITE CONSTITUENTS	29
General	29
Subtask 1 - Screening Test Program	30
Subtask 2 - Fiber Diameter Effects Program	74
Subtask 3 - Fiber Strength Effects Program	84
Subtask 4 - Fiber Content Effects Program	93
Subtask 5 - Selection of Three Composite Systems	106
Subtask 6 - Transition Section Failure Program	109
TASK II - BALLISTIC DAMAGE AND CRACK PROPAGATION STUDY	124
General	124
Subtask 1 - Static Tensile Properties of Undamaged Composites	125
Subtask 2 - Effect of Ballistic Impact Conditions on Composite Damage and Load Capacity.	134
Subtask 3 - Cyclic Tensile Fatigue Properties of Undamaged and Damaged Composites	148
Subtask 4 - Composite Fracture Toughness	166

Page

Subtask 5 - Effect of Composite Thickness on Ballistic Damage and Residual Load Capacity 172
Subtask 6 - Effect of Combined Stress and Ballistic Impact Conditions 195
Subtask 7 - Selection of the Most Promising Composite 200

TASK III - DESIGN ALLOWABLE PROPERTIES EVALUATION STUDY 217

General 217
Approach to the Problem 217
Discussion of Results 225
Conclusions and Recommendations 238

SUMMARY OF RESULTS 240

APPENDIX - TENSILE FATIGUE DATA ANALYSIS 243

DISTRIBUTION 253

LIST OF ILLUSTRATIONS

Figure		Page
1	Dimensions of Standard Ballistic/Tensile Test Specimen	8
2	Test Specimen With Hole Pattern and End Plates	9
3	Ballistic Test Arrangement for Tumbled Caliber .30 Ball M2 Projectile Impacts at 1800 Ft/Sec	12
4	Load Fixture With Hydraulic Actuator	14
5	Hydraulic System for Preload Application During Ballistic Tests	15
6	Ballistic Arrangement for Caliber .30 Ball M2 Projectile Tests	16
7	Ballistic Arrangement for Caliber .50 AP M2 Projectile Tests	17
8	Simulated Crack in a Fracture Toughness Test Specimen	19
9	Sonntag Fatigue Machine With Test Specimen Mounted	20
10	Damage Measurements	22
11	Model for Off-Center Impacts	26
12	Influence of Off-Center Impacts	28
13	Typical Stress-Strain Curves for Candidate Resins	34
14	Ultimate Tensile Strength of Undamaged Specimens	38
15	Effect of Material Parameters on the Initial Tensile Modulus of Undamaged Specimens	39
16	Effect of Material Parameters on the Frequency of Transition Section Failures	41

Figure		Page
17	Hypothetical Strength Distribution Across a Specimen	44
18	Effect of Material Parameters on Ballistic Damage Areas and Volume	49
19	Typical Front Surface Ballistic Damage - Specimens With 836 Fiber Finish	50
20	Typical Front Surface Ballistic Damage - Specimens With 891 Fiber Finish	51
21	Typical Front Surface Ballistic Damage - Specimens With 897 Fiber Finish	52
22	Relationship Between Back Surface Ballistic Damage Area and Fiber Length	53
23	Typical Back Surface Ballistic Damage - Specimens With 836 Fiber Finish	54
24	Typical Back Surface Ballistic Damage - Specimens With 891 Fiber Finish	55
25	Typical Back Surface Ballistic Damage - Specimens With 897 Fiber Finish	56
26	Relationship Between Ballistic Damage Volume and Fiber Length	57
27	Effect of Material Parameters on Transverse Ballistic Damage	60
28	Relationship Between Back Surface Transverse Ballistic Damage and Fiber Length	61
29	Relationship Between Post-Damage Tensile Properties (Load Capacity) and Fiber Length	64
30	Effect of Material Parameters on Post-Damage Tensile Properties	65
31	Relationship Between Post-Damage Tensile Properties (Strength-to-Weight Ratio) and Fiber Length	67

Figure		Page
32	Typical Front and Back Surface Ballistic Damage - Specimens Reinforced With G/P683C Fibers	78
33	Comparison of Ballistic Damage Areas and Volume - Composites Reinforced With G/P683C and K/897 Fibers	79
34	Comparison of Transverse Ballistic Damage - Composites Reinforced With G/P683C and K/897 Fibers.	81
35	Comparison of Post-Damage Tensile Properties - Composites Reinforced With G/P683C and K/897 Fibers	83
36	Comparison of Ballistic Damage Areas and Volume - Composites Reinforced With S-2 and E Glass	88
37	Typical Front and Back Surface Ballistic Damage - Specimens Reinforced With S-2 Glass (470 Fiber Finish).	89
38	Comparison of Transverse Ballistic Damage - Composites Reinforced With S-2 and E Glass	90
39	Comparison of Post-Damage Tensile Properties - Composites Reinforced With S-2 and E Glass	92
40	Effect of Fiber Content on Tensile Modulus - 836/438 Composites	97
41	Effect of Fiber Content on Ballistic Damage Areas and Volume - 836/438 Composites	99
42	Typical Front Surface Ballistic Damage - 836/438 Composites With 50 and 70 V/O Nominal Fiber Content	100
43	Typical Back Surface Ballistic Damage - 836/438 Composites With 50 and 70 V/O Nominal Fiber Content	101

Figure		Page
44	Effect of Fiber Content on Transverse Ballistic Damage - 836/438 Composites	103
45	Effect of Fiber Content on Strength-to-Weight Ratio - 836/438 Composites	105
46	Severe Distortion of Transition Section Fibers as Evidenced by Tracer Material	117
47	Slight Distortion of Transition Section Fibers as Evidenced by Tracer Material	122
48	Effect of Thickness on Tensile Strength of Undamaged 470/438-1 Specimens	128
49	Effect of Temperature on Tensile Strength of Undamaged Specimens	130
50	Effect of Temperature on Tensile Modulus of Undamaged Specimens	131
51	Tensile Cyclic Fatigue Test of Undamaged 470/438-1 Specimen	151
52	Tensile Cyclic Fatigue Test of Undamaged 470/438-1/2 Specimen	152
53	Tensile Cyclic Fatigue Test of Undamaged 897/332-732-1 Specimen	153
54	Load-N Curves for Undamaged Specimens of the Three Candidate Composites	155
55	Tensile Cyclic Fatigue Test of Ballistically Damaged 470/438-1 Specimen	157
56	Tensile Cyclic Fatigue Test of Ballistically Damaged 470/438-1/2 Specimen	159
57	Tensile Cyclic Fatigue Test of Ballistically Damaged 897/332-732-1 Specimen	160
58	S-N Curves for Ballistically Damaged Specimens of the Three Candidate Composites	164

Figure		Page
59	Fatigue Curves of the Three Candidate Composites (Percentage of Damaged Load Capacity)	165
60	Fracture Toughness Test of 897/332-732-1 Composite.	168
61	Relationship Between Specimen Thickness and Predicted Residual Load Capacity for 470/438-1 Composites	180
62	Relationship Between Impact and Residual Velocity for 470/438-1 Composites	181
63	Relationship Between Ballistic Limit and Areal Density for 470/438-1 Composites.	183
64	Relationship Between Specimen Thickness and Visual Ballistic Damage Areas for the Three Candidate Composites.	186
65	Relationship Between Specimen Thickness and Visual Transverse Ballistic Damage for the Three Candidate Composites.	188
66	Relationship Between Specimen Thickness and Residual Stress Capacity for the Three Candidate Composites	191
67	Relationship Between Specimen Thickness and Estimated Ballistic Limit for the Three Candidate Composites.	192
68	Effective Damage Length From Ultimate Load Data.	208
69	Mechanical Property Specimens and Test Setups	219
70	Panel Layout for Mechanical Property Specimens.	223
71	Typical Tensile Stress-Strain Curves for 470/438-1/2 Composite	231
72	Typical Compressive Stress-Strain Curves for 470/438-1/2 Composite	233
73	Typical Panel Shear Stress-Strain Curves for 470/438-1/2 Composite	236

Figure		Page
74	Fatigue Curves for Undamaged 470/438-1/2 Composite Load Capacity Showing A- and B-Basis Tolerance Limits	248
75	Fatigue Curves for Damaged 470/438-1/2 Composite Load Capacity Showing A- and B-Basis Tolerance Limits	249
76	Fatigue Curves for 470/438-1/2 Composite as a Percentage of Static Load	250
77	Fatigue Design Curves (A Basis) for 470/438-1/2 Composite	251
78	Typical Fatigue Design Curve for 470/438-1/2 Composite (Based on 3.5-Inch Minimum Width)	252

LIST OF TABLES

Table		Page
1	Tumble Plate Locations	11
2	Test Data Rejection Criteria	24
3	Mechanical Properties of Candidate Epoxy Resins	33
4	Test Specimen Measurements - Screening Test Program	36
5	Ultimate Tensile Strength of Undamaged Specimens - Screening Test Program	37
6	Initial Tensile Modulus of Undamaged Specimens - Screening Test Program	39
7	Tensile Strength of Narrow Specimens - Screening Test Program	43
8	Initial Tensile Modulus of Narrow Specimens - Screening Test Program	45
9	Summary of Visual Ballistic Damage - Screening Test Program	48
10	Summary of Visual Transverse Ballistic Damage - Screening Test Program	59
11	Summary of Post-Damage Tensile Properties - Screening Test Program	63
12	Effect of Experimental Variables on Undamaged and Ballistically Damaged Composites - Screening Test Program	69
13	Test Specimen Measurements - Composites Reinforced With P683C-Finished E Glass	75
14	Ultimate Tensile Strength of Undamaged Specimens Reinforced With G/P683C and K/897 Fibers	76

Table		Page
15	Tensile Modulus of Undamaged Specimens Reinforced With G/P683C and K/897 Fibers	77
16	Summary of Visual Ballistic Damage - Composites Reinforced With G/P683C and K/897 Fibers	77
17	Summary of Visual Transverse Ballistic Damage - Composites Reinforced With G/P683C and K/897 Fibers.	80
18	Summary of Post-Damage Tensile Properties - Composites Reinforced with G/P683C and K/897 Fibers	82
19	Test Specimen Measurements - Composites Reinforced With 470-Finished S-2 Glass.	85
20	Ultimate Tensile Strength of Undamaged Specimens Reinforced With S-2 and E Glass	86
21	Tensile Modulus of Undamaged Specimens Reinforced With S-2 and E Glass	86
22	Summary of Visual Ballistic Damage - Composites Reinforced With S-2 and E Glass	87
23	Summary of Visual Transverse Ballistic Damage - Composites Reinforced With S-2 and E Glass	91
24	Summary of Post-Damage Tensile Properties - Composites Reinforced With S-2 and E Glass	93
25	Test Specimen Measurements - 836/438 Composites With 50, 60, and 70 V/O Nominal Fiber Content	95
26	Ultimate Tensile Strength of Undamaged 836/438 Specimens With 50, 60, and 70 V/O Nominal Fiber Content	96
27	Tensile Modulus of Undamaged 836/438 Specimens With 50, 60, and 70 V/O Nominal Fiber Content	97

Table		Page
28	Summary of Visual Ballistic Damage - 836/438 Composites With 50, 60, and 70 V/O Nominal Fiber Content	98
29	Summary of Visual Transverse Ballistic Damage - 836/438 Composites With 50, 60, and 70 V/O Nominal Fiber Content	102
30	Summary of Post-Damage Tensile Properties - 836/438 Composites With 50, 60, and 70 V/O Nominal Fiber Content	104
31	Variables Examined in the Transition Section Failure Program	110
32	Preliminary Transition Section Failure Program	112
33	Basic Transition Section Failure Program	114
34	Effect of Variables on Ultimate Tensile Strength - Transition Section Failure Program	115
35	Supplemental Transition Section Failure Program	116
36	Results of Supplemental Tests on "Minimum Movement" Preform Concept.	121
37	Results of Confirmation Tests on "Minimum Movement" Preform Concept.	121
38	Room-Temperature Tensile Properties of Undamaged Standard Specimens	126
39	Effect of Thickness on Tensile Properties of Undamaged 470/438-1 Specimens.	127
40	Effect of Temperature on Tensile Properties of Undamaged Specimens	129
41	Tensile Strength and Modulus Ratios (Temperature Basis) for Undamaged Specimens.	129
42	Edge-to-Center Tensile Strength and Modulus Ratios for Undamaged Specimens	132

Table		Page
43	Summary of Visual Ballistic Damage - Caliber .50 AP M2 Impacted Specimens	135
44	Summary of Visual Transverse Ballistic Damage - Caliber .50 AP M2 Impacted Specimens	136
45	Summary of Residual Load Capacities for Caliber .50 AP M2 Impacted Specimens	138
46	Preliminary Summary of Residual Load Capacities for Tumbled Caliber .30 Ball M2 Impacted Specimens	140
47	Multiple Regression Coefficients for Preliminary Residual Load Capacity Data	141
48	Summary of Predicted Residual Load Capacities for Tumbled Caliber .30 Ball M2 Impacted Specimens . .	141
49	Summary of Visual Ballistic Damage - Tumbled Caliber .30 Ball M2 Impacted Specimens	143
50	Summary of Visual Transverse Ballistic Damage - Tumbled Caliber .30 Ball M2 Impacted Specimens . .	144
51	Summary of Residual Load Capacities for Tumbled Caliber .30 Ball M2 Impacted Specimens	145
52	Ranking of Residual Load Capacities for Tumbled Caliber .30 Ball M2 Impacted Specimens	147
53	Summary of Fatigue Test Results on Undamaged Specimens	150
54	Comparison of Damage and Residual Load Capacity Data for 470/438-1 Composites - Tumbled Caliber .30 Ball M2 Impacts at 1500 Ft/Sec (Room Temperature)	156
55	Comparison of Damage and Residual Load Capacity Data for 470/438-1/2 Composites - Tumbled Caliber .30 Ball M2 Impacts at 1500 Ft/Sec (Room Temperature)	158

Table		Page
56	Comparison of Damage and Residual Load Capacity Data for 897/332-732-1 Composites - Tumbled Caliber .30 Ball M2 Impacts at 1500 Ft/Sec (Room Temperature)	161
57	Summary of Fatigue Test Results on Ballistically Damaged Specimens	162
58	Fracture Toughness Data for the Three Candidate Composites	169
59	Stress Concentration Factors From Fracture Toughness Data	170
60	Test Plan for Initial Phase of Thickness Effects Program	173
61	Test Plan for Second Phase of Thickness Effects Program	173
62	Summary of Visual Ballistic Damage - Thickness Effects Program (Initial Phase)	175
63	Summary of Visual Transverse Ballistic Damage - Thickness Effects Program (Initial Phase)	176
64	Summary of Measured Residual Load Capacities - Thickness Effects Program (Initial Phase)	177
65	Predicted Residual Load Capacities - Thickness Effects Program (Initial Phase)	178
66	Ballistic Limit Estimates Based on Thickness Effects Program (Initial Phase)	182
67	Summary of Visual Ballistic Damage - Thickness Effects Program (Second Phase)	185
68	Summary of Visual Transverse Ballistic Damage - Thickness Effects Program (Second Phase)	187
69	Summary of Residual Load Capacities - Thickness Effects Program (Second Phase)	190

Table		Page
70	Summary of Estimated Ballistic Limits - Thickness Effects Program (Second Phase)	190
71	Grand Summary of Damage and Residual Load Capacity Data for Standard Candidate Composites Impacted With Tumbled Caliber .30 Ball M2 Projectiles at 1500 Ft/Sec and 0-Degree Obliquity.	194
72	Summary of Threshold Stress Test Data for the Three Candidate Composites	197
73	Terms of the Multiple Regression Equation	202
74	Environment and Loading Effects on Tensile Properties of Undamaged Composites	204
75	Influence of Test Variables on the Residual Load Capacity and Effective Damage Length of Tumbled Caliber .30 Ball M2 Impacted Specimens	205
76	Constant and Coefficients for the Regression Equation - Tumbled Caliber .30 Ball M2 Impacted Specimens	206
77	Environment and Loading Effects on Tensile Properties of Tumbled Caliber .30 Ball M2 Impacted Specimens	211
78	Comparison of Load-Carrying Abilities of the Three Candidate Composites	212
79	Constant and Coefficients for the Regression Equation - Caliber .50 AP M2 Impacted Specimens	214
80	Influence of Test Variables on the Residual Load Capacity and Effective Damage Length of Caliber .50 AP M2 Impacted Specimens	215
81	Specific Gravity, Density, and Fiber Content of 470/438-1/2 Composite	226
82	Constant and Coefficients for the Mechanical Property Regression Equations	227
83	Results of Interlaminar Shear Strength Tests on 470/438-1/2 Composite	228

Table		Page
84	Results of Flexure Strength Tests on 470/438-1/2 Composite	228
85	Results of Flexure Modulus Tests on 470/438-1/2 Composite	230
86	Results of Tensile Strength Tests on 470/438-1/2 Composite	230
87	Results of Tensile Modulus Tests on 470/438-1/2 Composite	232
88	Results of Compressive Strength Tests on 470/438-1/2 Composite	232
89	Results of Compressive Modulus Tests on 470/438-1/2 Composite	235
90	Results of Panel Shear Strength Tests on 470/438-1/2 Composite	235
91	Results of Panel Shear Modulus Tests on 470/438-1/2 Composite	237
92	Results of Bearing Yield Strength Tests on 470/438-1/2 Composite	237
93	Results of Ultimate Bearing Strength Tests on 470/438-1/2 Composite	238
94	Design Allowables for 470/438-1/2 Composite	239
95	General Trends in Regard to Major Parameters	242

INTRODUCTION

This Phase I report describes the efforts of Goodyear Aerospace Corporation under U. S. Army Contract DAAJ02-70-C-0062 to characterize and optimize compression-molded, discontinuous fiber-reinforced plastic composites for ultimate use in ballistically tolerant flight control components for rotary- and fixed-wing aircraft.

Combat damage reports on U. S. Army aircraft operating in Southeast Asia indicate that rotary-wing aircraft are highly vulnerable to hostile small-arms fire. The flight control system components constitute a particularly vulnerable area. It has been conservatively estimated that 30 to 35 percent of aircraft losses can be attributed to ballistic impacts in this area. Of the various approaches available for increasing aircraft survivability, the ballistic-damage-tolerant component concept, which utilizes multi-load path designs and fiber glass composite material, offers the greatest potential with minimum weight penalty. In this concept the impacting projectile is permitted to perforate the component with minimum energy transfer and, consequently, minimum structural damage. The feasibility of this concept was clearly and dramatically demonstrated in 1965 in a USAAVLABS-sponsored program.

Considerable effort has recently been expended to develop ballistic damage-tolerant flight components using plastic composites reinforced with fiber glass cloth. The current methods for fabricating components with this type of composite involve extensive hand lay-up operations that are generally not amenable to low-cost, high-rate production. This disadvantage can be overcome by using discontinuous fiber glass composite materials that can be compression molded, essentially to the final part configuration. Limited testing of such materials by Goodyear Aerospace Corporation in 1969 produced encouraging ballistic results.

Since the gross behavior of discontinuous fiber composites is governed to a great extent by the characteristics of the constituent materials (fiber, matrix, and interface), the composites can be tailored to best meet the overall operational requirements. However, the use of short-fiber composites in structural components operating in a ballistic environment represents a new and unique application. Therefore, a need existed to evaluate various constituent materials for the purpose of optimizing the composite for ballistically tolerant component application. The optimization and subsequent structural characterization of the most promising composite material were accomplished during the Phase I program.

The Phase I program was divided into the following three major tasks:

Task I - Selection of Composite Constituents

Task II - Ballistic Damage and Crack Propagation Study

Task III - Design Allowable Properties Evaluation Study

This report is organized on a task basis. However, discussions of the three major tasks under Phase I are preceded by a description of several items that are generally common to either or both of the first two tasks. These items are:

1. Materials (Selection and Formation)

2. Test Specimens (Design and Fabrication)

3. Test Methods and Equipment

4. Evaluation Criteria

TEST AND EVALUATION TECHNIQUES

MATERIALS

The basic constituent materials and the formation of the short-fiber molding compounds utilized in the Phase I investigation are discussed in the following paragraphs. The molding compound formation includes fiber impregnation techniques as well as the chopping and staging of the impregnated stock.

Resin

The following three epoxy resin systems were selected for evaluation:

1. DEN 438*
2. DER 332* -DER 732* (70/30 blend by weight)
3. ERLA 4617* *

DEN 438 resin, an epoxy novalac, was chosen because it is a standard type commonly used in the production of the composite structures. The specific formulation selected for evaluation was:

DEN 438	100.0 pbw (parts by weight)
Methyl NADIC anhydride (MNA)* * * . .	97.0 pbw
Benzyl dimethylamine (BDMA)	1.5 pbw

This resin is characterized by an intermediate ultimate tensile strength and modulus. Because of its comparatively low elongation at failure, the resin is relatively brittle.

DER 332, an epoxy bisphenol-A resin flexibilized with DER 732, a long-chain polyglycol diepoxide, was chosen because it exhibits higher elongation at failure and greater toughness than the epoxy novalac. The following formulation was selected for evaluation:

---

* Manufactured by Dow Chemical Co., Midland, Mich.

* * Manufactured by Union Carbide Corp., Bound Brook, N.J.

* * * Manufactured by Allied Chemical Corp., Morristown, N.J.

DER 332	70.0 pbw
DER 732	30.0 pbw
Methylene dianiline (MDA)	23.0 pbw
DMP-30 (tertiary amine)*	1.5 pbw

ERLA 4617 resin, an epoxy-biscyclo pentyl ether/ethylene glycol copolymer, was chosen because of its high ultimate tensile strength and modulus compared to both the DEN 438 and DER 332-DER 732 resins. The following formulation was used in this program:

ERLA 4617	100.0 pbw
Metaphenylene diamine (m-PDA)	27.0 pbw
Boron trifluoride complex (BF_3 · MEA)	1.5 pbw

Fiber Glass

The three fiber glass materials selected for evaluation in the screening test program were identical in every respect except for the type of finish applied. The fiber glass finish is the principal factor that governs the glass-to-resin bond strength. All fiber glass materials were procured from Owens-Corning Fiberglas Corp., Toledo, Ohio. The specific Owens-Corning proprietary finishes used were:

1. 836 - Epoxy resin compatible
2. 891 - Polyester resin compatible
3. 897 - Epoxy/polyester resin incompatible

With an epoxy matrix, the glass-to-resin bond strength will be highest with the 836 finish and lowest with the 897 finish.

The basic fiber glass material chosen for examination was a Type 30 roving (2080 filaments per strand) produced from K filaments (0.00050 to 0.00055 inch in diameter) of E glass. Each pound of glass with this construction yields approximately 675 yards of roving.

---

* Manufactured by Rohm and Haas Co., Philadelphia, Pa.

Two other fiber glass materials were examined in the Task I program to determine the effects of filament diameter and fiber glass strength on the extent of ballistic damage and the residual strength of the epoxy-fiber glass composites. The data generated in these studies were compared with information obtained on appropriate composites described in the screening test program in Task I.

A 427-yd/lb roving produced from G filaments (0.00035 to 0.00040 inch in diameter) of E glass was employed to establish filament diameter effects. This roving had an epoxy/polyester-incompatible finish (P683C) that is essentially identical from a chemistry standpoint, with the 897 finish used in the screening test program. The effect of fiber glass strength was determined from an evaluation of a 20-end S-2 fiber glass roving produced from K diameter filaments. This roving yielded 750 yd/lb of glass with an epoxy-compatible finish (Type 470).

S-2 glass differs from S glass in two respects - the finish applied and the extent of quality control documentation. All basic materials used in the production of S glass are completely traceable to their source. The same degree of documentation is not maintained on the S-2 glass, nor for that matter, on any E glass produced.

IMPREGNATION

Resin impregnation of the various fiber glass rovings was accomplished on in-house equipment that consisted of the following elements:

1. Variable-speed takeoff rolls
2. Resin bath
3. Wiper with adjustable orifice
4. Staging oven
5. Cooling chamber
6. Winder with variable-torque control

The rate of roving impregnation was controlled by the speed of the takeoff rolls. The speed was maintained at a level that permitted B-staging, that is, partial polymerization of the epoxy resin. The actual speed was dependent upon the kinetics of the polymerization reaction under operating conditions of the staging oven.

The epoxy resins were diluted with methyl ethyl ketone to a nominal resin-to-solvent weight ratio of 70/30 to facilitate impregnation. This dilution also provided a means of controlling the resin/reinforcement ratio to the desired level. Further resin content control was achieved by drawing the impregnated roving through a polyethylene wiper having an adjustable orifice.

The wet roving then entered the staging oven operating at 380° to 410°F for solvent removal and partial resin polymerization. The total exposure time of the roving in the oven was generally 15 to 30 seconds, depending upon the epoxy resin type. The impregnated roving then passed through a 60° to 65°F chamber to cool the roving to room temperature. The B-staged roving was wound on a core under sufficient tension to draw the roving through the impregnation equipment.

Periodic checks were made on the resin content of the impregnated roving to ensure that the resin/reinforcement ratio was maintained within acceptable limits. This was done by weighing 20-foot lengths of impregnated roving and subtracting the weight of a comparable length of dry roving. The resin content was then determined by dividing this weight difference by the weight of the impregnated roving. Any significant deviation from nominal content could rapidly be detected and appropriate action promptly taken.

CHOPPING

The epoxy-impregnated roving was chopped to the required lengths with a Turner Rotary Carbide Tow Cutter, Model 600. The length of cut was varied by changing the speed of the feed rolls. Air injection was used to carry the roving from the feed rolls to the shear plate and to hold the fibers in line for cutting. Each roll of impregnated roving was chopped into a separate container. The molding compound was then stored at 0°F to prevent resin polymerization.

STAGING

Before combining material from a particular composition into a master molding batch, random samples were drawn from each container for gel time determination. This property defines the time that the material can be maintained at a given temperature before the resin becomes immobile. This test was performed at 300°F with a Fisher-Johns Melting Point Apparatus.

The molding compound in each container was kept at room temperature until its measured gel time ranged from 25 to 35 seconds. The material was then stored at 0°F to prevent any further reduction in gel time. When all materials of a particular composition were compatible from a gel time standpoint, they were blended into a master batch.

STANDARD TEST SPECIMEN

The design and fabrication of the standard ballistic/tensile test specimen (coupon) utilized in Tasks I and II are discussed in the following paragraphs. A description of the end plates used to transmit the load during ballistic and structural tests is also presented.

Design

The standard test specimen was designed with primary emphasis on ballistic considerations. Since most proposed tests involve fully tumbled caliber .30 Ball M2 projectiles, an adequate but reasonable specimen width had to be provided to minimize the possibility of total specimen destruction upon impact. Consequently, the specimen was designed with a test area 3.5 inches wide.

The standard specimen (see Figure 1) was nominally 1/8 inch thick, 10 inches long, and 4.5 inches wide at the ends. The 3.5-inch-long test area was provided to allow for some flexibility in impact location from an elevation standpoint. The ends of the specimen were 1/8 inch thicker than the test area with a 7-degree taper in the thickness transition section. A thickness study was conducted during Task II on specimens that were 1/4 and 3/8 inch thick in the test area and 3/8 and 1/2 inch thick, respectively, at the ends. These specimens in all other respects were identical with the 1/8-inch-thick specimens.

Each end of the standard specimen contained a double row of 0.377-inch-diameter holes as shown in Figure 2. The holes were drilled in a fixture having the identical hole pattern as the end plates. The load was transmitted from the end plates to the specimen by 0.372-inch-diameter steel pins. A 1-inch-diameter hardened steel pin was used to transmit loads from the ballistic test fixture or test machine to the end plates.

Split end plates were used for the 1/4- and 3/8-inch-thick specimens. Two 3/8-inch-diameter bolts were used in each pair of end plates to properly align the specimen during testing. See Figure 2.

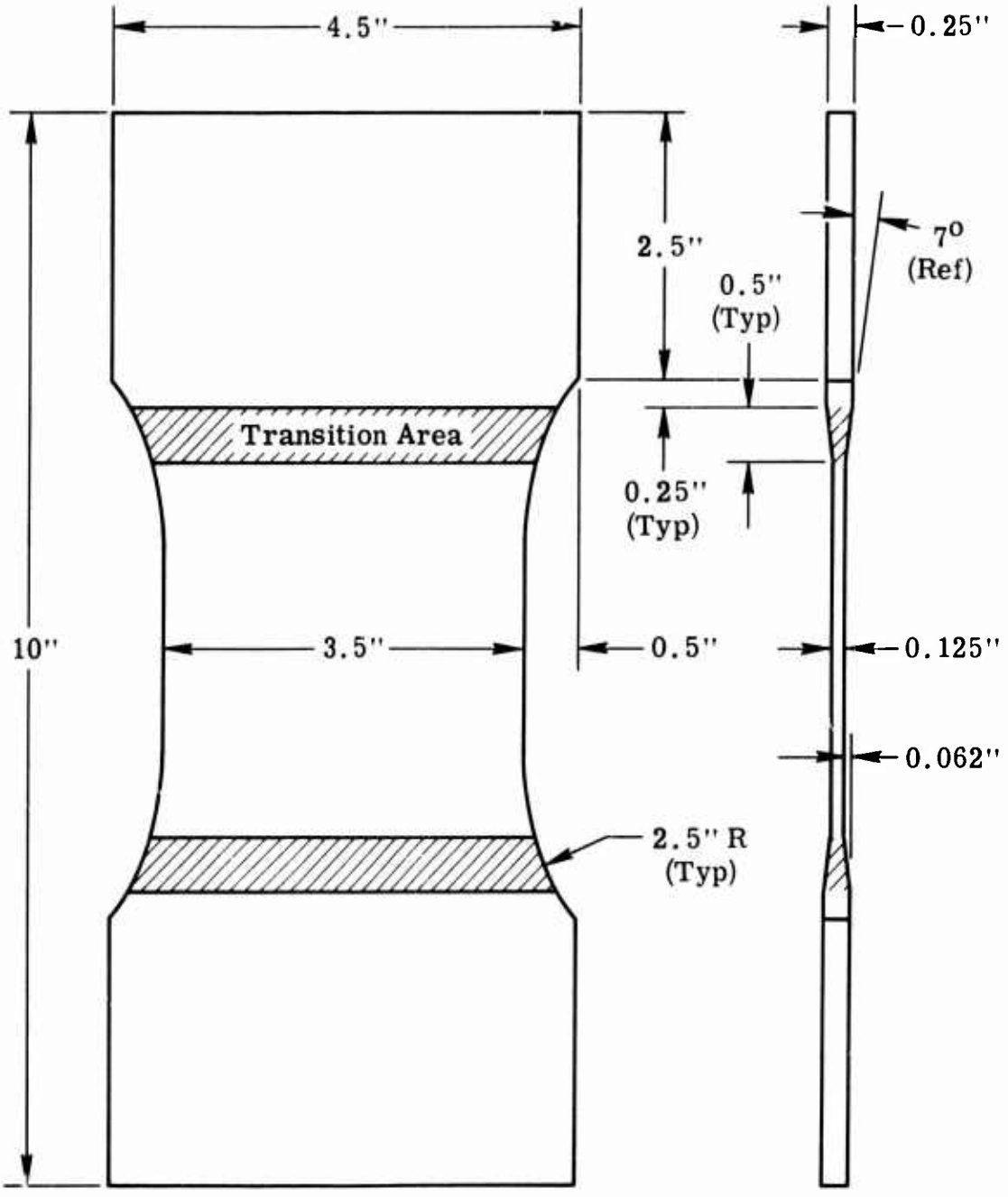

Figure 1. Dimensions of Standard Ballistic/Tensile Test Specimen.

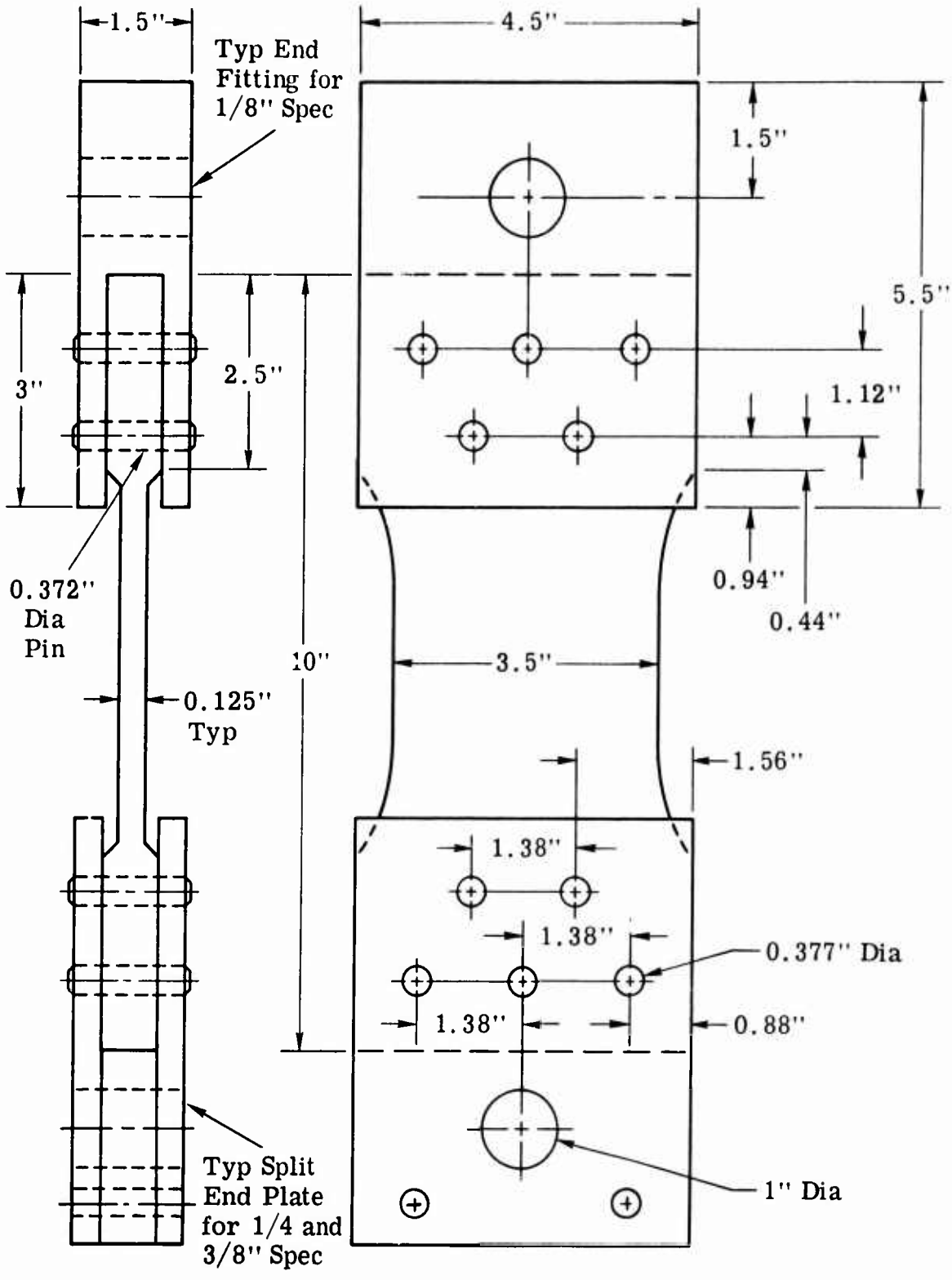

Figure 2. Test Specimen With Hole Pattern and End Plates.

Fabrication

All specimens in the Task I and II investigations were fabricated from preforms that had the same plan view configuration as the molded specimen. The proper amount of molding compound was distributed in a split preform mold and subsequently densified. In Task I the sections of the preform, i.e., the center and the ends, were built up independently, and the preform was then compacted under a light load. A high frequency of transition section failures was experienced with Task I specimens, necessitating a change in specimen fabrication techniques. Transition section failures were virtually eliminated by the adoption of a modified method of preforming that involved a different method of material distribution and higher compaction pressures. The transition area of the specimen is shown in Figure 1. The Task II specimens were fabricated using preforms that had a continuous layer of material that extended the full length of the specimen. The preform was then compacted at a pressure of approximately 40 psi.

The preform was placed in the matched metal die mold operating at 300°F. The basic cure cycle consisted of 1000-psi pressure applied for 20 minutes. Pressure was applied very rapidly in Task I, but at a moderate rate during Tas II. Upon completion of the molding cycle, the specimen was taken from the mold and cooled to ambient temperature; then all resin-fiber glass flash was carefully removed. Tables 35, 36, and 37 give details of the processing changes incorporated in Task II.

The specimens with the ERLA 4617 epoxy matrix were post-cured for 16 hours at 360°F to develop the ultimate structural properties. The specimens were clamped between thick metal plates during post-cure to prevent distortion.

TEST METHODS AND EQUIPMENT

The standard test methods and equipment utilized in conducting the Task I and II investigations are described in the following paragraphs.

Specimen Characteristics

Thickness measurements were taken at four locations in the test area, and the average value was computed for each specimen produced. Density measurements were made using the water-displacement technique. The fiber content was determined by pyrolysis of the resin at 1050°F in an oxidizing atmosphere.

Tensile Testing of Undamaged Specimens

The tensile strength and modulus of standard specimens were measured at room temperature on a Baldwin Tensile Tester at a crosshead separation rate of 0.05 in./min. A 2-inch gage length extensometer was mounted on each specimen during tensile tests to provide a load-deflection curve. The tensile modulus of the composite was determined from the initial slope of this curve.

Ballistic Testing

The primary ballistic threat for the Phase I program was the fully tumbled caliber .30 ball M2 projectile impacting at 0-degree obliquity. The tumbled condition was attained by firing the projectile through a 0.40-inch-thick sheet of stretched Plexiglas oriented at 20 degrees to the flight path. To achieve a fully tumbled condition with the projectile oriented transverse to the longitudinal axis of the specimen, it was necessary to precisely locate the tumble plate with respect to the target face. This location varied as indicated in Table 1 for each of the nominal impact velocities.

TABLE 1. TUMBLE PLATE LOCATIONS

Nominal Impact Velocity (ft/sec)	Distance Between Faces of Tumble Plate and Target (in.)
900	18.0
1200	18.0
1500	18.0
1800	19.5
2100	19.5
2400	18.0

The ballistic test arrangement showing the relative location of the weapon, chronograph grids, tumble plate, and specimen is shown in Figure 3. Avtron chronographs, Models T309A and T333B, were used to measure incremental times during projectile flight. The projectile striking velocity was computed from the following expression:

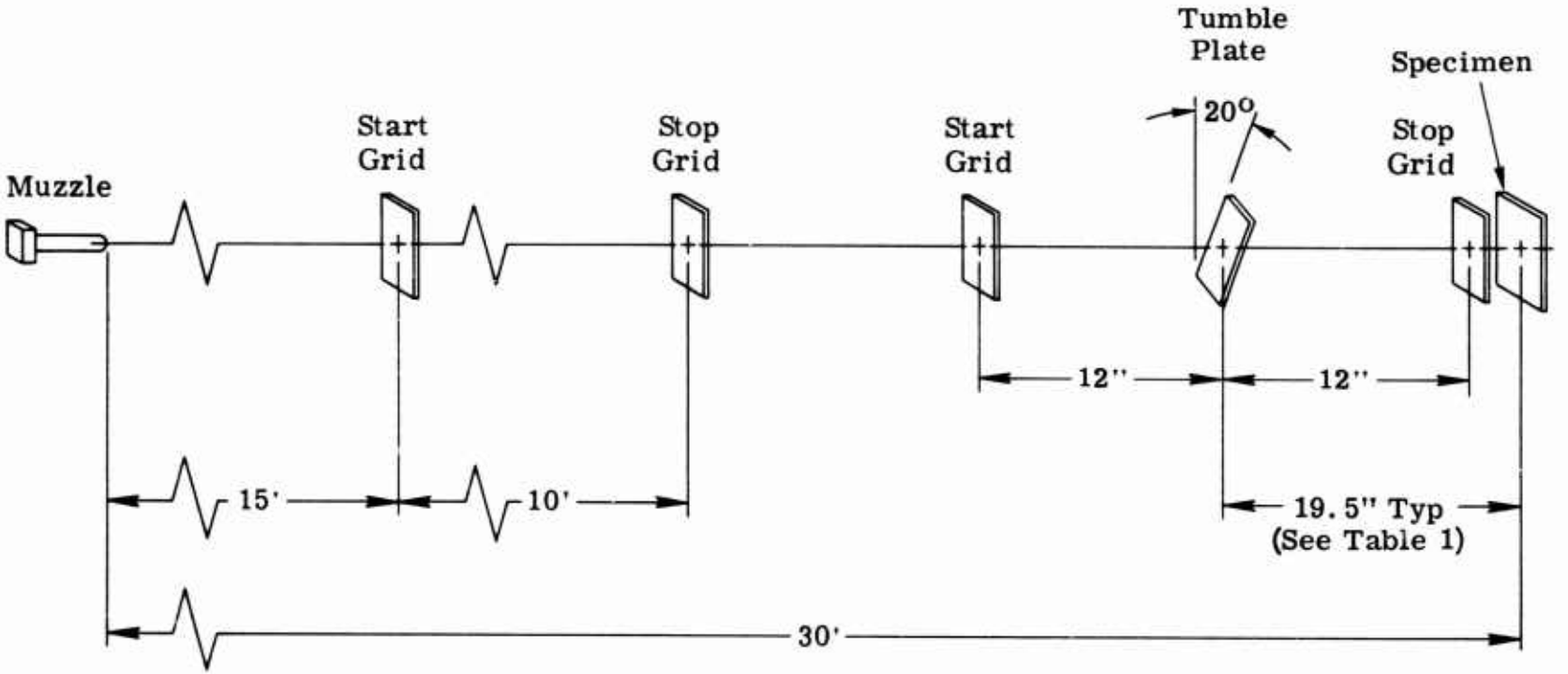

Figure 3. Ballistic Test Arrangement for Tumbled Caliber .30 Ball M2 Projectile Impacts at 1800 Ft/Sec.

$$V_s = 2V_a - V_m \quad (1)$$

where V_s = striking velocity, ft/sec

V_a = velocity, ft/sec, measured over the 2-foot base line

V_m = muzzle velocity, ft/sec, measured over the 10-foot base line

Equation (1) demands that the chronograph grids for determining velocity for the short base line are centered about the tumbled plate. For all caliber .30 ball M2 tests, a 24-inch spacing was used between start and stop grids.

Ballistic tests were also performed with untumbled caliber .50 AP M2 projectiles at 0-degree obliquity and nominal impact velocities of 1500, 1800, and 2100 ft/sec. The ballistic arrangement shown in Figure 3 was modified by removing the tumble plate and associated grids for the tests with caliber .50 AP M2 projectiles.

All ballistic testing was conducted while the specimen was under tensile preload. The lever-type fixture shown in Figure 4 uses an 8-inch-diameter hydraulic actuator for applying the load to the test specimen. The actuator was calibrated to establish the load on the fixture as a function of actuator pressure so that an accurate determination of specimen prestress could be obtained. Although the load fixture has three specimen mounting locations, only the central position was used. The actuator was pressurized to the required level using a Blackhawk hydraulic hand pump. A one-gallon-capacity accumulator was installed in the hydraulic system to ensure constant pressure on the actuator during ballistic testing. A photograph of the hydraulic system is shown in Figure 5.

During the Task I investigations, the specimen was preloaded to 35 percent of the average ultimate tensile strength of undamaged specimens measured at room temperature. During the latter stages of the Task II program, the preload was changed to 35 percent of the average undamaged strength at 160°F. This modification was prompted by the fact that a number of specimens tested at 160°F showed evidence of damage away from the actual ballistic impact point. The away-from-perforation damage was attributed to high stresses present in the test specimen because of tensile strength degradation of the composite systems at 160°F.

Photographs of the ballistic arrangement during caliber .30 ball M2 and caliber .50 AP M2 projectile tests are shown in Figures 6 and 7, respectively. These photographs show the Hycam camera and associated lighting

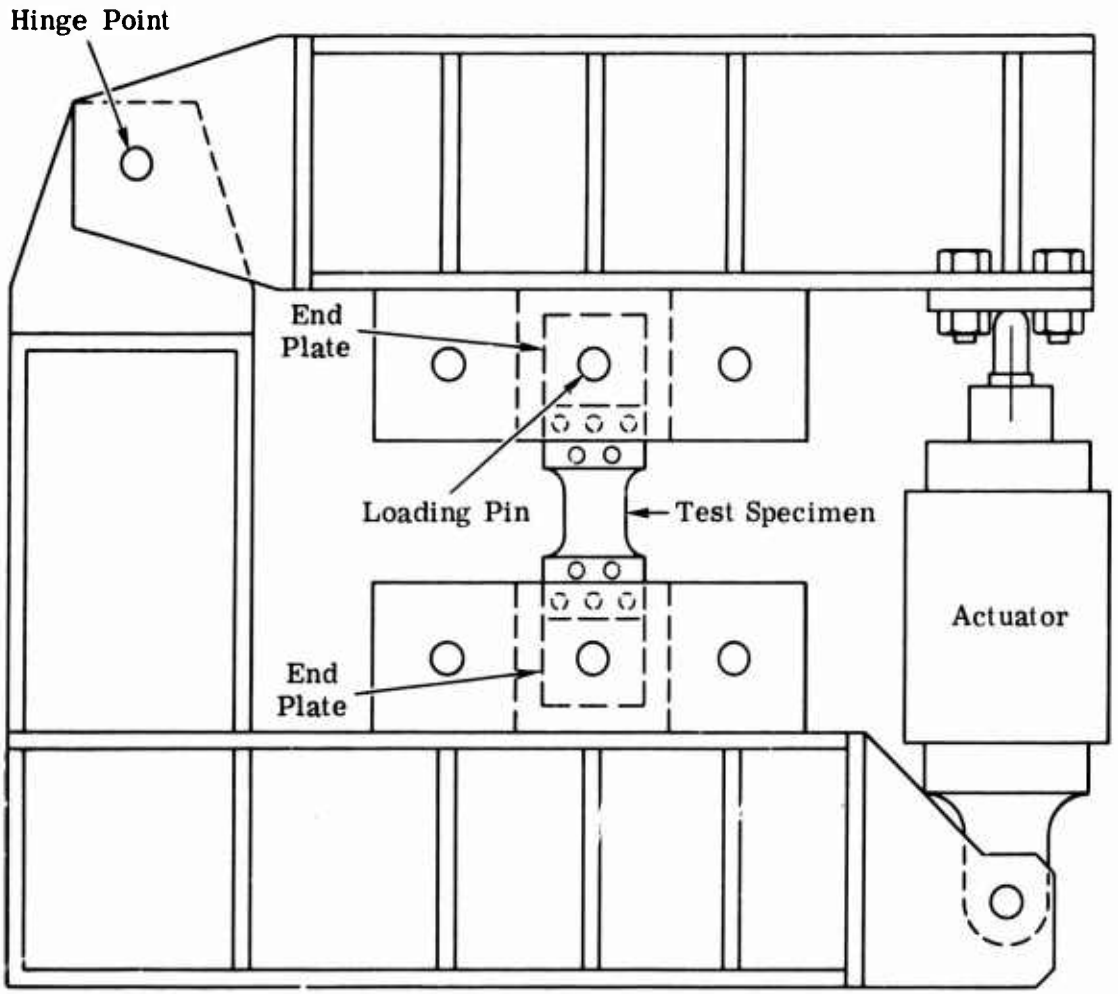

Figure 4. Load Fixture With Hydraulic Actuator.

equipment used during high-speed (10, 000 frames per second) motion-picture filming of projectile impacts on a few selected test specimens. The lever-type load fixture and mounted specimen are clearly visible in these photographs.

During the thickness investigation study in Task II, measurements were made of the residual velocity of the projectile after perforation (complete penetration) of the test specimen. The remaining velocity was determined over a 2-foot base line with the start grid located on the back of the test specimen.

Ballistic testing at extreme temperatures was accomplished by installing a temperature-controlled enclosure in the load fixture. Liquid nitrogen

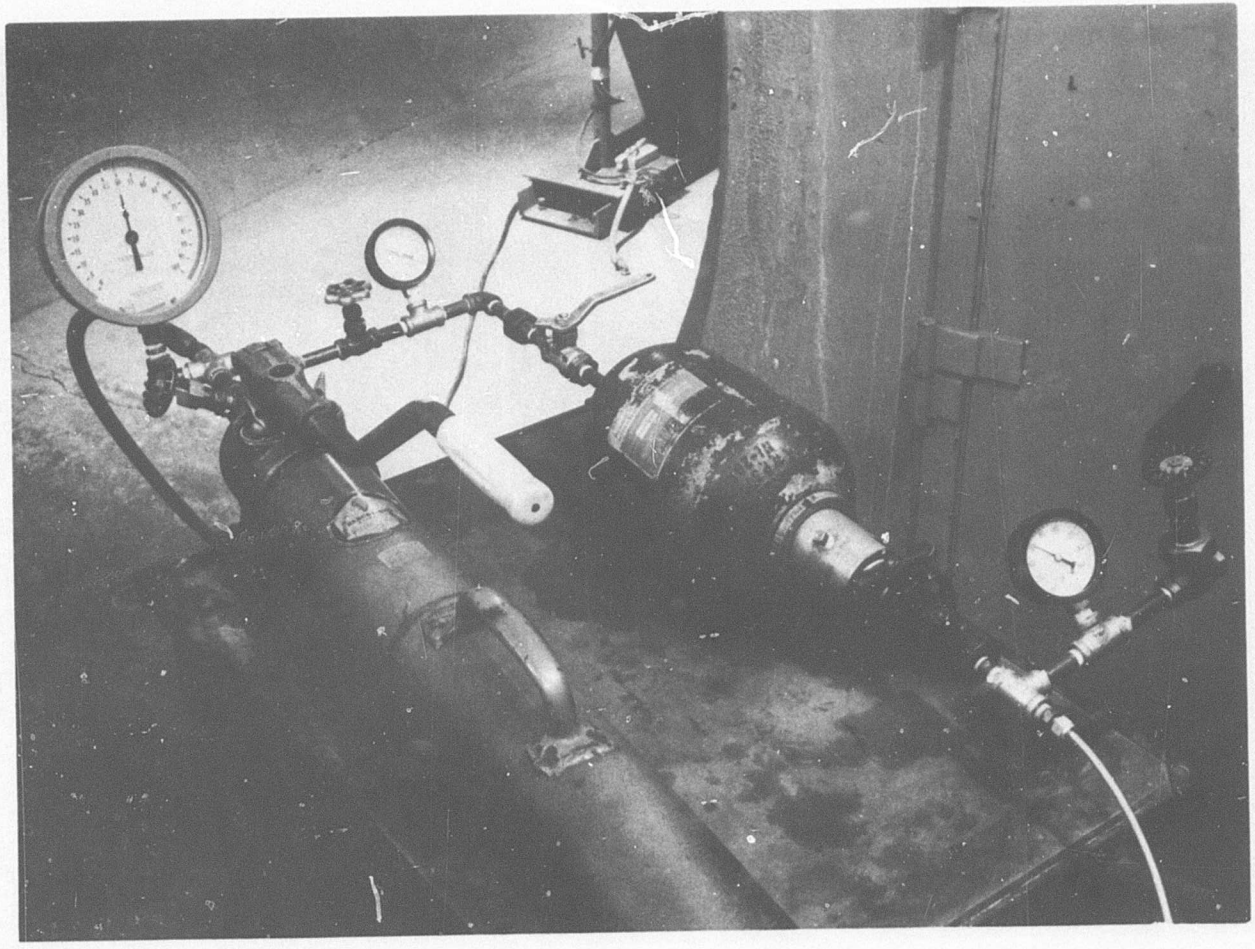

Figure 5. Hydraulic System for Preload Application During Ballistic Tests.

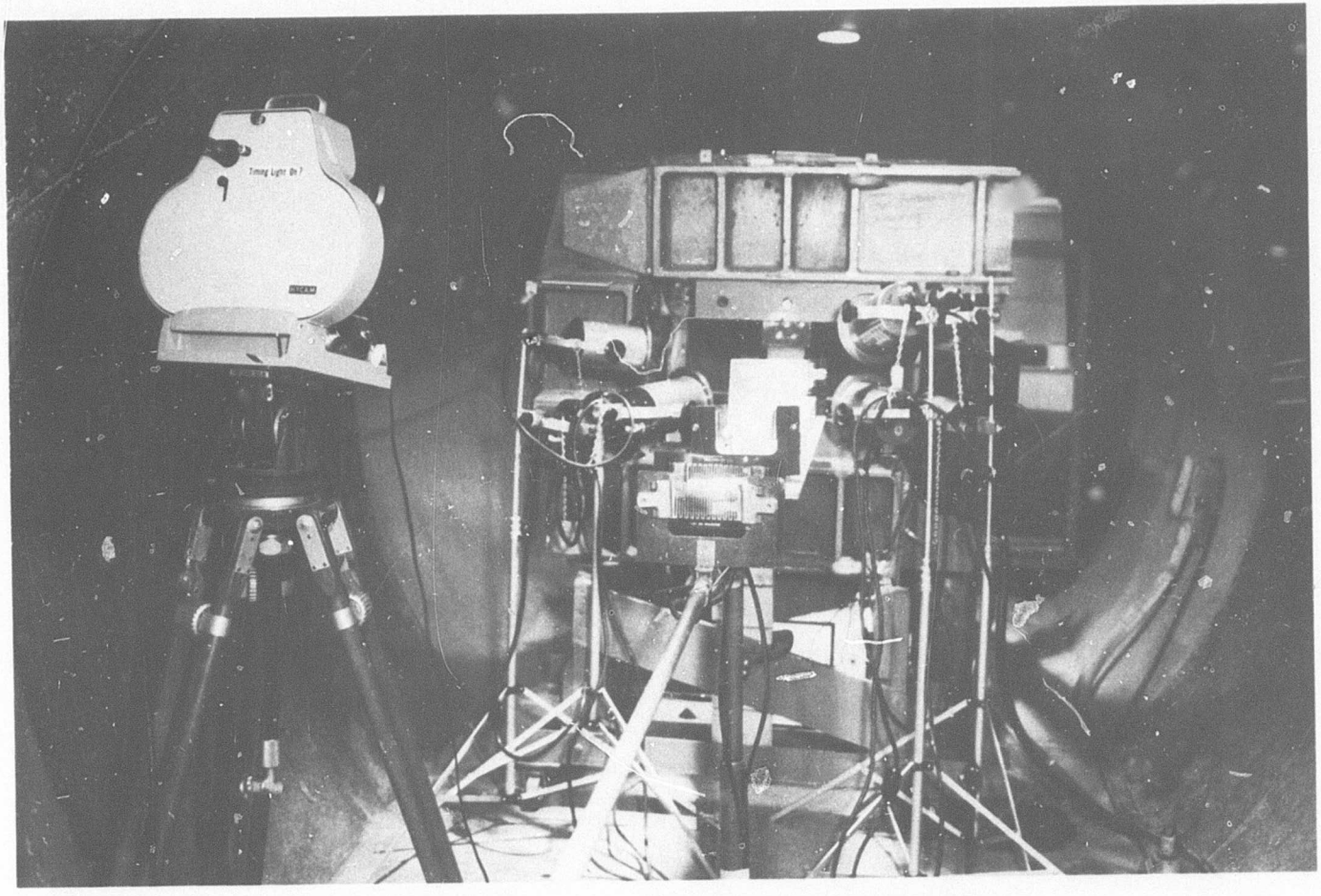

Figure 6. Ballistic Arrangement for Caliber .30 Ball M2 Projectile Tests.

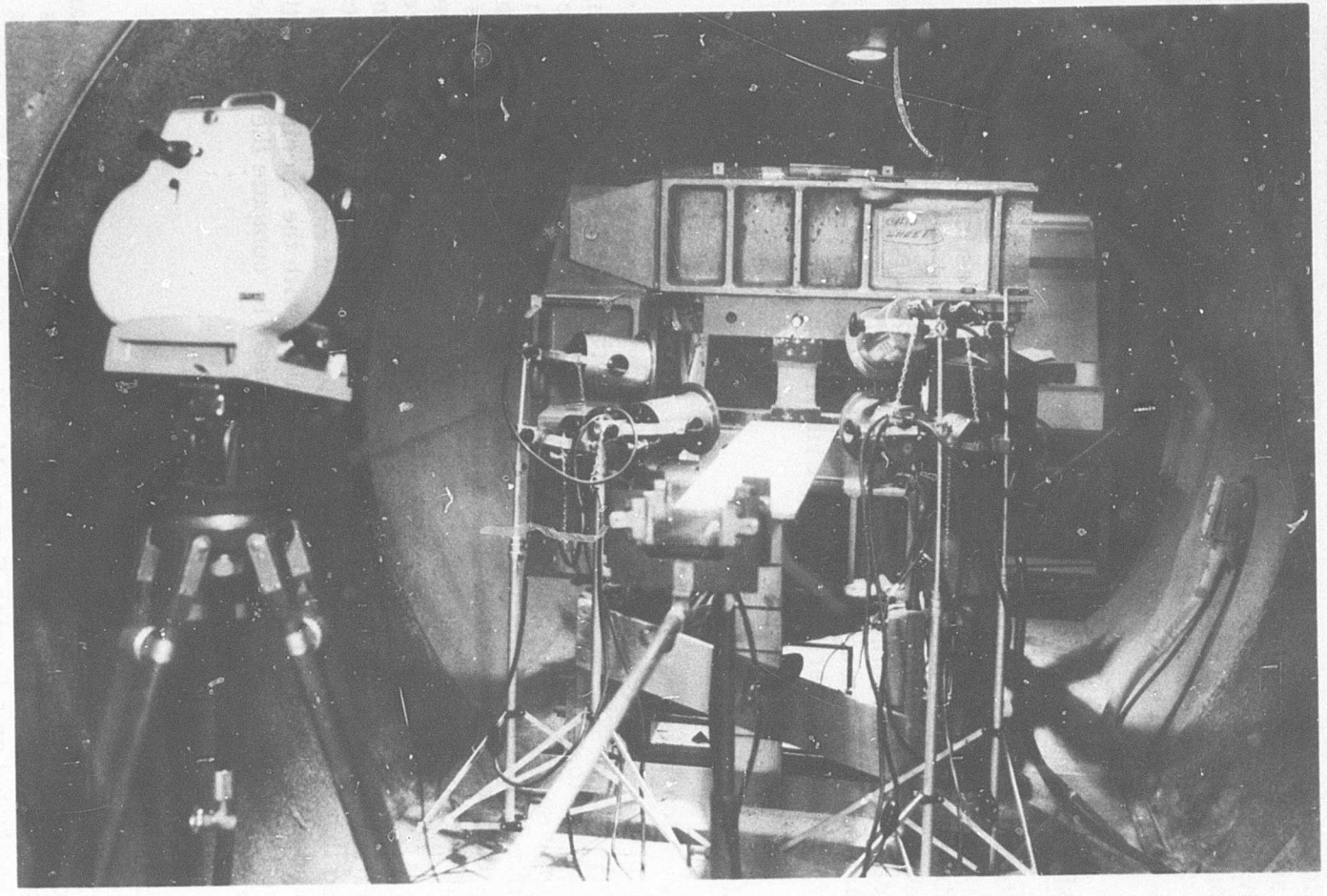

Figure 7. Ballistic Arrangement for Caliber .50 AP M2 Projectile Tests.

was used to achieve the -80°F temperature level, and self-contained heating elements were used for the 160°F condition. A thermocouple was mounted on the specimen, and the temperature was recorded with a Minneapolis-Honeywell Multipoint Recorder. Prior to ballistic testing, the specimens were soaked for a minimum of 30 minutes at the test temperature to ensure that equilibrium conditions existed. The specimens were prestressed just before ballistic impact.

Tensile Testing of Damaged Specimens

The test procedure and equipment for determining residual load capacity were identical with those discussed in "Tensile Testing of Undamaged Specimens." Prior to conducting the residual load capacity tests, the extent of ballistic damage in terms of area, volume, and transverse width was determined on both the front and back surfaces of the specimen. A discussion of the damage measurement technique is presented in a subsequent paragraph under "Evaluation Criteria."

Fracture Toughness Testing

Fracture toughness testing was performed during Task I to determine the crack propagation resistance of short-fiber glass-epoxy composites. The standard test specimen was modified with a simulated crack to determine the fracture toughness. A 1/2-inch-diameter hole was drilled in the center of the specimen test area. A hacksaw cut approximately 3/16 inch long transverse to the loading direction was made on each side of the hole. These cuts were then extended an additional 1/16 inch with a jeweler's saw blade (size 4/0). The total initial crack length was nominally 1 inch long. Figure 8 shows a close-up of the simulated crack. The specimens were then loaded in tension at a crosshead separation rate of 0.05 in./min. The rate of slow crack propagation was continually marked on the specimen so that the effective crack length at the onset of rapid propagation could be established. This measurement along with the specimen width, failure load, and specimen thickness was used to compute the toughness factor.

Fatigue Testing

The cyclic tensile fatigue property of the discontinuous epoxy-fiber glass composites was determined on 1/8-inch-thick standard test specimens in both the undamaged and ballistically damaged conditions. These tests were conducted on a Sonntag Fatigue Machine, Model SF-10-0, which has

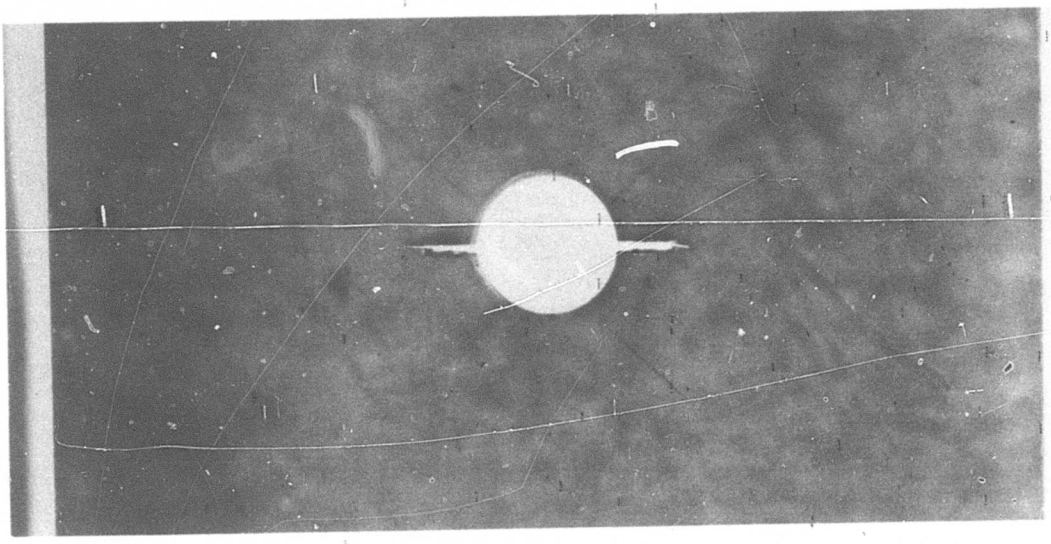

Figure 8. Simulated Crack in a Fracture Toughness Test Specimen.

a capacity of 10,000 pounds and operates at a frequency of 30 cps. Figure 9 shows the specimen mounted in the fatigue machine.

$R < 0.1$ fatigue tests were conducted at stress levels that would provide meaningful data for the preparation of S-N curves. The fatigue life region of particular interest ranged from 10^4 to 10^7 cyles. Generally, a maximum of 15 specimens of any composite type were evaluated; the distribution of specimens from a stress standpoint depended upon data reproducibility. During all fatigue testing the minimum cyclic load was maintained at approximately 150 pounds to ensure against compressive or zero stress conditions and the resultant undesirable relaxation in bearing that would occur at the end pins.

Combined Stress-Impact Testing (Ballistic Threshold Testing)

Combined stress-impact testing was performed at 160°F on 1/8-inch-thick standard ballistic/tensile specimens. These specimens were impacted with fully tumbled caliber .30 ball M2 projectiles at 0-degree obliquity and a nominal velocity of 1500 ft/sec. The initial specimen of each composite type was preloaded to 70 percent of the average tensile strength of undamaged specimens at the test temperature. An up-and-down method was employed wherein the test stress level was selected

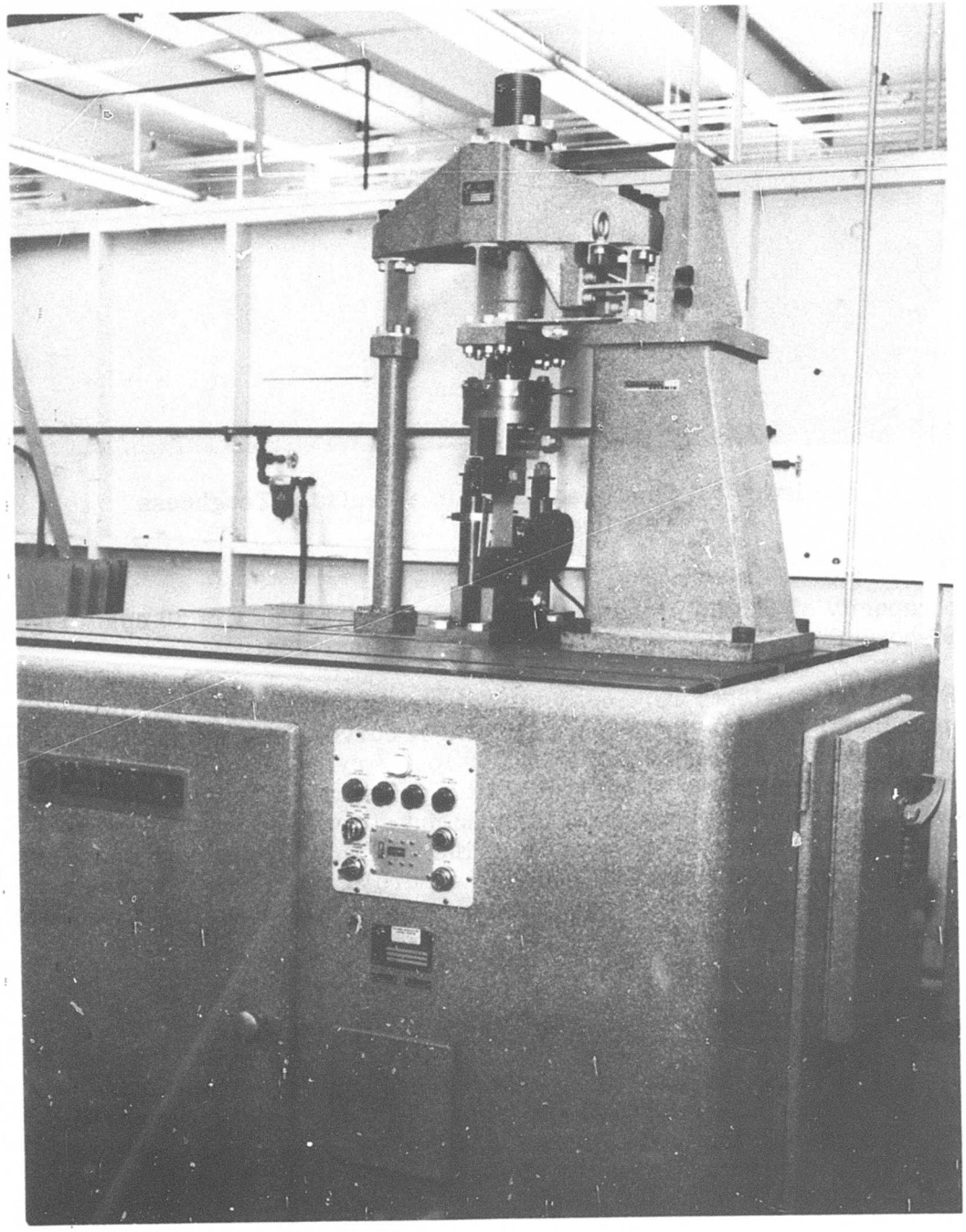

Figure 9. Sonntag Fatigue Machine With Test Specimen Mounted.

based on the response of the previous test specimen. If the previous specimen failed catastrophically at a particular stress level, the preload was reduced for the next specimen. Conversely, if the previous specimen survived, the stress level was increased for the following test.

EVALUATION CRITERIA

The following paragraphs describe ballistic damage and residual load capacity criteria used to assess the performance of the various epoxy-fiber glass composites after projectile impact. In addition, rejection criteria that were applied to all test data are discussed.

Outline tracings were prepared showing the extent of visual ballistic damage on both the entrance and exit surfaces of the specimen as well as the location of this damage relative to the test area. In addition, the orientation and length of the projectile wound were noted. Because this constituted a very laborious and time-consuming operation, a more rapid technique was developed that involved the reproduction of the damaged specimen surfaces on a copying machine. Since all specimens were tested to failure after ballistic impact, these copies provided a permanent record of the extent of ballistic damage.

Front and back surface measurements as shown in Figure 10 were made of transverse and area damage caused by projectile impact. In addition, measurements were taken of the projectile footprint length and orientation on the front surface.

Damage Areas

The damage areas, particularly on the back surface, generally had very irregular edges. These irregularities were caused by fiber pullout or displacement from the test specimen. A damage envelope was drawn that averaged out these irregularities on the specimen surfaces. The area of the damage envelope was then measured on the outline tracings or the reproduction machine copies with a planimeter.

Damage Volume

The front and back surface damage areas coupled with the specimen thickness were used to calculate the damage volume, assuming a conical frustrum, from the following equation:

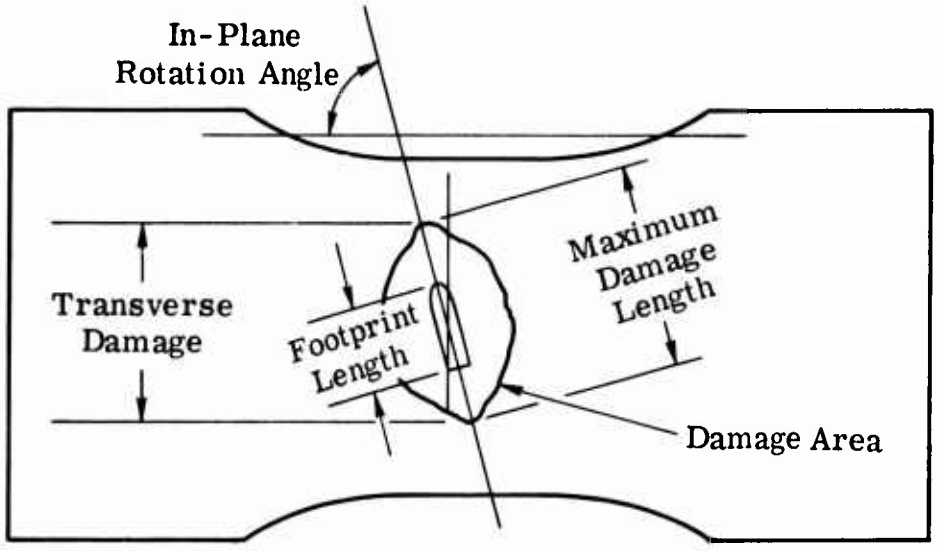

A. Front Surface

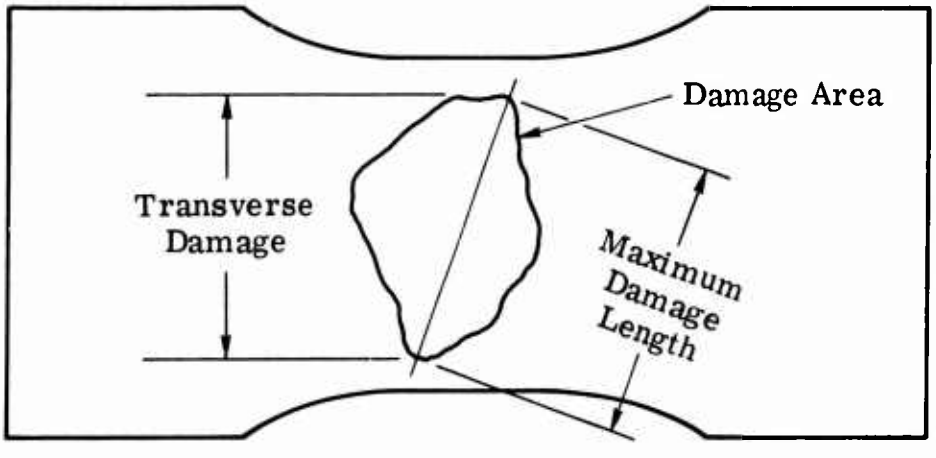

B. Back Surface

Figure 10. Damage Measurements.

$$V = \frac{t}{3}\left(A_1 + A_2 + \sqrt{A_1 A_2}\right) \qquad (2)$$

where V = damage volume, $in.^3$

t = specimen thickness, in.

A_1 = front surface damage area, $in.^2$

A_2 = rear surface damage area, $in.^2$

Maximum Damage Length

This parameter represents the maximum linear dimension of damage irrespective of orientation within the damage envelope on both the front and back specimen surfaces.

Transverse Damage Length

The transverse damage length is the maximum linear dimension of damage oriented normal to the longitudinal axis of the test specimen.

Residual Load Capacity

The residual load capacity of the test specimens was determined from ultimate tensile tests. Because of differences that existed in specimen thickness, the residual load capacity values were adjusted by linear normalization to a nominal specimen thickness of 1/8 inch.

Residual Strength-to-Weight Ratio (Breaking Length)

Because of differences in the density of the constituent materials and in the resin/reinforcement ratio, measurable differences in composite density were obtained. Therefore, the residual strength-to-weight ratio was computed to simultaneously appraise the post-damage load capacity advantage and the weight penalty associated with the composite system. The strength-to-weight ratio is also referred to as the "breaking length." This represents the length of material with a 1/8-by-3.5-inch cross section that would cause failure when suspended below the damaged area.

Data Rejection Criteria

Certain test values were excluded in the analysis of data generated on

ballistically damaged specimens. The four categories for data rejection are presented in Table 2 along with the criteria, the measurements affected, and the exceptions. A brief explanation of the rationale used in the development of the rejection criteria is given below.

The axial length of a fully tumbled caliber .30 ball M2 projectile is 1.10 inches. If the observed footprint length was less than 0.90 inch, all post-damage measurements were excluded unless the damage was actually greater than the average of acceptable impacts within the group. The second category, in-plane projectile rotation, was a cause for data rejection since maximum damage tends to occur in the direction of the projectile axis. Unless the projectile was oriented normal to the tensile load

TABLE 2. TEST DATA REJECTION CRITERIA

Category	Rejection Criterion	Measurements Affected	Exceptions
Projectile not fully tumbled	Axial length is less than 0.90 inch for the projectile wound on the impacted surface.	Damage areas, damage volume, transverse damage, damage strength	General damage is greater than the average of other acceptable impacts within the group.
In-plane projectile rotation	Maximum damage length is greater than 1.2 times transverse damage length.	Transverse damage, damage strength	Damage strength is less than the average of acceptable impacts within the group.
Transition section failures	End failures.	Damage strength	Value is higher than the average of acceptable failures within the group.
Ballistic damage symmetry	P_{sym}/P factor exceeds value of 1.15.	Damage strength	Value is higher than the average of acceptable impacts within the group.

path, transverse damage was generally reduced. When the maximum damage length was greater than 1.2 times the transverse damage length, the transverse damage length values were rejected. The exception to this rule is when the damage strength was less than the average strength of the specimens having acceptable ballistic impacts.

In a limited number of cases, transition section failures occurred despite the presence of a ballistic perforation in the central portion of the test specimen. In these cases, the damage strength data were rejected unless the value was higher than the average of acceptable failures within the group.

Another cause for data rejection was associated with off-center ballistic damage. If the projectile caused front surface damage that was closer to one edge than the other, failure would be initiated in the narrow edge. The measured load capacity would be lower than that obtained with symmetrically located damage.

The model used for this criterion is shown in Figure 11. For the condition where no bending is introduced into the specimen, the moment about the center line must be zero. Therefore, for a 3.5-inch-wide specimen,

$$T_L \left(\frac{3.5}{2} - \frac{e_L}{2}\right) - T_S \left(\frac{3.5}{2} - \frac{e_S}{2}\right) = 0 \qquad (3)$$

where T_L = load carried by long side

T_S = load carried by short side

e_L = undamaged length of long side

e_S = undamaged length of short side

Simplifying Equation (3) results in

$$T_L = T_S \left(\frac{3.5 - e_S}{3.5 - e_L}\right) \qquad (4)$$

Since the total load (P) carried by the specimen is equal to the sum of the loads carried by each side, then

$$P = T_S + T_L \qquad (5)$$

When the expression for T_L is used from Equation (4), then Equation (5) becomes

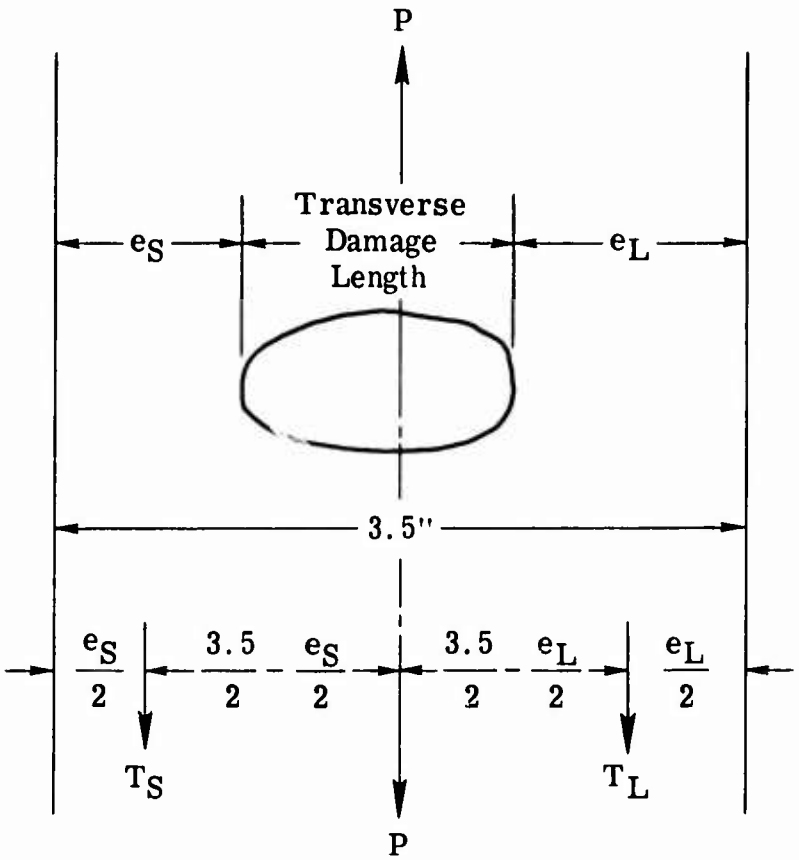

Figure 11. Model for Off-Center Impacts.

$$P = T_S + T_S\left(\frac{3.5 - e_S}{3.5 - e_L}\right) \tag{6}$$

or

$$P = T_S\left(1 + \frac{3.5 - e_S}{3.5 - e_L}\right) \tag{7}$$

If σ is the failing stress of the material, then

$$T_S = \sigma t\, e_S \tag{8}$$

where t = specimen thickness

Substituting the expression for T_S from Equation (8) into Equation (7) results in

$$P = \sigma t e_S \left(1 + \frac{3.5 - e_S}{3.5 - e_L}\right) \tag{9}$$

For the symmetrical damage condition, the undamaged area (A_U) is

$$A_U = t(e_S + e_L) \tag{10}$$

and the load capacity is

$$P_{sym} = \sigma t(e_S + e_L) \tag{11}$$

The ratio of the load carried by a specimen with symmetrical damage to one with off-center damage is

$$\frac{P_{sym}}{P} = \frac{\sigma t\,(e_S + e_L)}{\sigma t\, e_S \left(1 + \dfrac{3.5 - e_S}{3.5 - e_L}\right)} \tag{12}$$

In simplified form, Equation (12) becomes

$$\frac{P_{sym}}{P} = \frac{e_S + e_L}{e_S \left(1 + \dfrac{3.5 - e_S}{3.5 - e_L}\right)} \tag{13}$$

The relationship between P_{sym}/P and long-side edge distance (e_L) is shown graphically in Figure 12. The arbitrarily selected acceptance region for P_{sym}/P values ranged from 1.00 to 1.15. If the P_{sym}/P value exceeded 1.15, the residual load capacity data were excluded unless the specimen strength with off-center damage was greater than the average of specimens with centered damage.

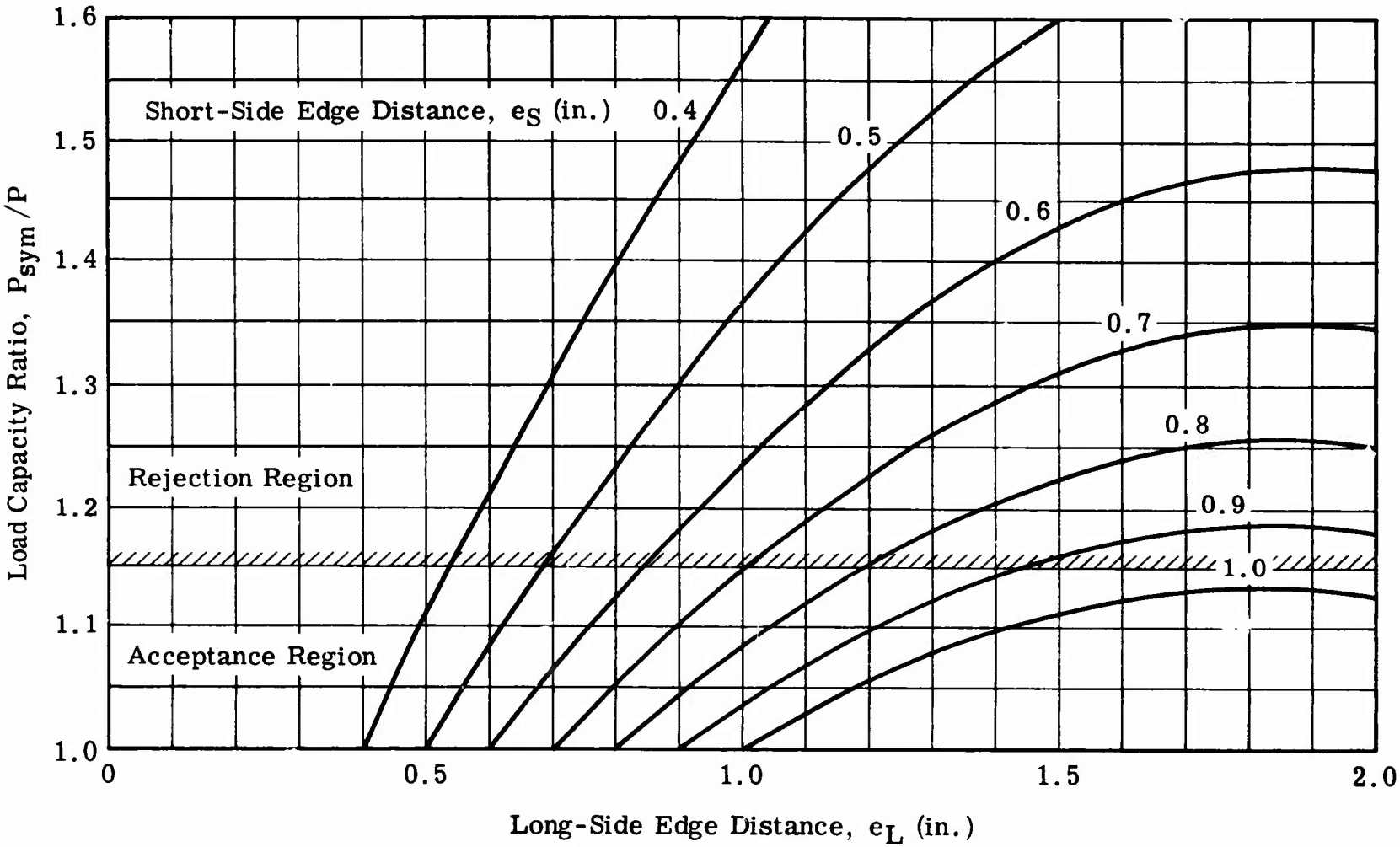

Figure 12. Influence of Off-Center Impacts.

TASK I - SELECTION OF COMPOSITE CONSTITUENTS

GENERAL

Standard metallic flight control components are susceptible to ballistic impact failure, particularly under operational stress. Aircraft survivability can be increased most effectively by utilizing ballistically tolerant components. These components are designed to permit ballistic penetration with minimum energy transfer and structural degradation. Molded, short-fiber glass-epoxy composites, in limited testing, have demonstrated such properties. This application represents a novel and potentially significant usage for discontinuous composites.

Since the gross behavior of discontinuous composites is primarily governed by the characteristics of the constituent materials (fiber, matrix, and interface), the composites can be tailored to best satisfy the overall operational requirements. Because the effects of these constituent characteristics were unknown, it was necessary to conduct an empirical program, Task I, to evaluate these characteristics for the purpose of optimizing the composite for ballistically tolerant component application.

The Task I program was divided into the following subtasks:

1. Screening Test Program
2. Fiber Diameter Effects Program
3. Fiber Strength Effects Program
4. Fiber Content Effects Program
5. Selection of Three Composite Systems

The purpose of the screening test program was to define the effects of epoxy resin type, fiber glass finish, and fiber length on the tensile properties of undamaged and damaged composites. The fiber diameter effects program was intended to establish which of two commercially available glass filament diameters, K or G, would exhibit the more favorable ballistic response. The objective of the fiber strength effects program was to determine whether improved ballistic tolerance would be achieved with a high-strength glass (S-2) compared to the commonly used lower strength E glass. The fiber content effects study was intended to discover whether an optimum fiber content level exists at which residual tensile properties of the composite are maximized. Based on the results of these subtasks, the most promising systems would be identified for subsequent evaluation in Task II.

The Task I activity was augmented to include a transition section failure

program for the purpose of eliminating the problem of end failures that plagued the basic Task I investigations.

Each of the subtasks under Task I is discussed in detail in this section of the report.

SUBTASK 1 - SCREENING TEST PROGRAM

General

Considerable latitude is available in the selection of constituent materials for composite construction. When high strength, structural efficiency, and economics are prime considerations, fiber glass is most commonly chosen as the reinforcing material. The resin matrix must carry out several important functions to allow the composite to effectively resist structural loads. These functions include transferring the load between filaments and providing strength and rigidity in directions normal to the filaments. The resin must be capable of sustaining high shear deformation to accommodate strain concentrations caused by the high-modulus reinforcement and low-modulus resin. Epoxy-type resins provide an optimum combination of properties based on the above considerations and, consequently, are most appropriate as matrix materials for high-strength composites.

The structural response of fiber-reinforced composites is dependent not only on constituent material properties but also on the form and orientation of the reinforcement, the fiber-matrix interfacial strength, and the relative proportions of the constituents. In discontinuous composites the physical characteristics of the reinforcement, such as fiber length and bundle size, are also important factors. Some of these parameters have a pronounced effect on structural behavior, whereas others have relatively minor influences. However, the effects of these factors on the extent of ballistic damage and the post-damage structural properties are not currently known.

The objective of this subtask was to investigate the effects of certain constituent material parameters on the tensile strength and modulus of discontinuous fiber glass-epoxy composites in both the undamaged and ballistically damaged conditions.

Approach to the Problem

A complete evaluation of all possible parametric combinations that might

affect the structural response of undamaged and ballistically impacted composites was economically prohibitive. It was necessary, therefore, to restrict the screening test program to the three parameters considered to have the greatest potential influence on structural properties. A number of variables considered to have less influential effects would be evaluated in subsequent Task I investigations. The variables selected for investigation were:

1. Resin Type
2. Fiber Finish
3. Fiber Length

Each of these variables would be evaluated at three experimental levels.

A broad range of experimental levels was selected to increase the probability of discovering the true effect of the variables on damaged composite properties. If only subtle changes were made in these levels, the true effect might be obscured because of variability (material and test) and/or the small sample size used.

The following epoxy resins were chosen for examination:

1. DEN 438
2. DER 332-DER 732 (70/30 blend by weight)
3. ERLA 4617

DEN 438, an epoxy novalac resin, has intermediate tensile strength and modulus but low elongation and toughness. DER 332-DER 732 blend is a flexibilized epoxy with intermediate strength and low modulus but high elongation and toughness. ERLA 4617 resin exhibits high strength and modulus, low elongation, and intermediate toughness.

The following fiber finishes were selected for evaluation:

1. 836 - Epoxy compatible
2. 891 - Polyester compatible
3. 897 - Epoxy/polyester incompatible

The resin and fiber glass interfacial strength should be highest for the epoxy-compatible (836) finish and lowest for the epoxy/polyester-incompatible (897) finish. Examination of this broad range of glass-to-resin strenths should provide insight into the significance of this variable on both the extent of ballistic damage and residual strength of the fiber glass-epoxy composites.

The fiber finishes were applied to a fiber glass roving having the following characteristics:

Glass Type	E
Filament Diameter	K (0.00050 to 0.00055 inch)
Filaments/Strand	2080 (Type 30)
Yield	.675 yd/lb

The three fiber lengths chosen for investigation in the screening test program were 1/4, 1/2, and 1 inch. These lengths are typical of those commonly used in constructing high-strength, discontinuous composites. The extremes (1/4 to 1 inch) represent a fourfold difference in length (from 1/4 to 1 inch), which should be adequate for determining whether fiber length has a significant effect on structural properties of ballistically damaged composites.

A full parametric investigation was conducted in which all possible combinations of the independent variable levels were explored. This resulted in 3^3 (three variables at three experimental levels each), or 27 combinations. All tests were performed at room temperature on the standard tensile/ballistic specimens described in "Test and Evaluation Techniques." The specimens were net compression molded to a thickness of 1/8 inch and had a nominal fiber content of 60 volume percent (v/o).

A total of eight replicates (three for determining the tensile properties of undamaged specimens and five for measuring ballistic impact effects) were produced for each of the 27 combinations. The ballistic evaluation was conducted with fully tumbled caliber .30 ball M2 projectiles at 0-degree obliquity and a nominal striking velocity of 1800 ft/sec. During the ballistic tests, the specimens were preloaded to 35 percent of their undamaged strength. After impact, the extent of ballistic damage and the residual load capacity were determined. The effect of the independent variables on damaged composite properties was then established from an analysis of post-damage measurements.

Results of Tensile Tests on Undamaged Specimens

The mechanical properties of the three candidate resin types (DEN 438, DER 332-DER 732, and ERLA 4617) as measured on unfilled, cast specimens are reported in Table 3. (A discussion of resin formulations and chemistry along with bath compositions for fiber glass impregnation is given in "Test and Evaluation Techniques.") Typical stress-strain curves for these resins are given in Figure 13. Tensile testing was conducted on

TABLE 3. MECHANICAL PROPERTIES OF CANDIDATE EPOXY RESINS

Property	Units	DEN 438	DER 332-DER 732	ERLA 4617
Ultimate Tensile Strength	psi	9,300	9,500	14,500
Tensile Modulus	psi x 10^3	540	420	800
Elongation at Failure	pct	1.9	7.1	2.3
Stress Intensity Factor, K_{IC}	in./$lb^{3/2}$	475	1,080	725
Toughness	in.-lb/$in.^3$	100	512	187

Type I specimens (1/4 inch thick or under) at room temperature in accordance with Federal Test Standard No. 406, Method 1011.

The stress intensity factors reported in Table 3 were determined on precracked 1/8-by-2-by-6 inch specimens. To initiate the crack, a 3/16-inch-diameter hole was drilled in the center of the specimen. A knife blade was then inserted through the hole and tapped until a crack was started through the full specimen thickness at right angles to the specimen length on both sides of the hole. The specimen was loaded in tension until crack instability (rapid fracture) occurred. The stress intensity factor (K_{IC}) was calculated from the following mathematical expressions:

$$Y = X/B \tag{14}$$

where X = crack length at onset of rapid fracture, in.

B = specimen width, in.

$$Z = \frac{Y\,(2 + Y^4)}{(2 - Y^2 - Y^4)^2} \tag{15}$$

$$K_{IC} = \frac{P}{t}\sqrt{\frac{\pi Z}{B}} \tag{16}$$

where P = failure load, lb

t = specimen thickness, in.

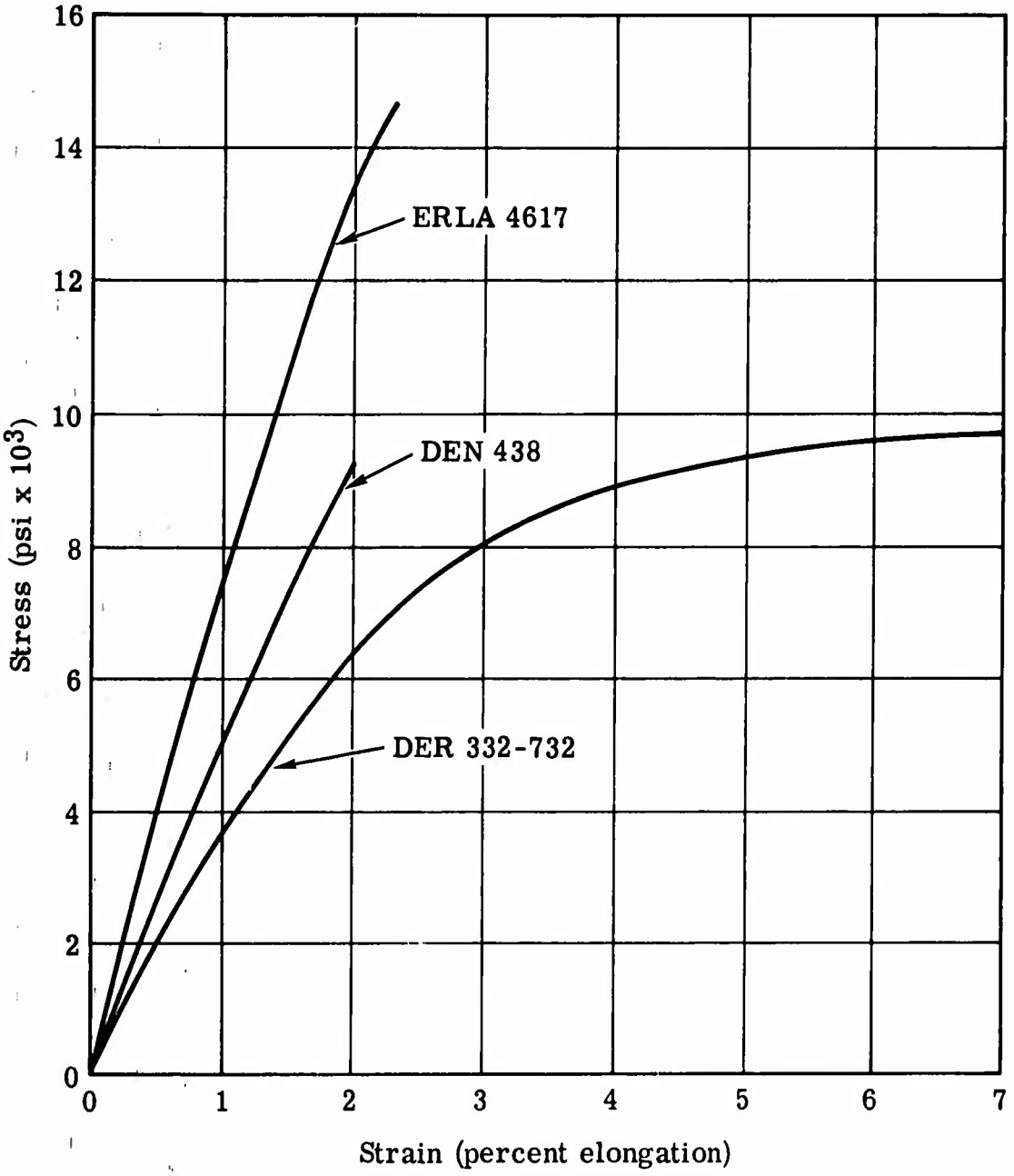

Figure 13. Typical Stress-Strain Curves for Candidate Resins.

The toughness values listed in Table 3 were obtained by measuring the area under the stress-strain curves shown in Figure 13.

DEN 438 resin is characterized by ultimate strength and modulus values that are typical of epoxy resins. Because of its relatively low elongation at failure, the resin has comparatively poor toughness. The low stress intensity factor indicates that the resin has relatively poor resistance to rapid crack propagation.

DER 332-DER 732 resin (70/30 blend by weight) exhibits high elongation at failure (7.1 percent). This property coupled with its intermediate tensile strength produces a tough resin. The resistance of this low-modulus epoxy resin to rapid crack propagation is high.

ERLA 4617 resin is unique because of its extremely high tensile strength (14,500 psi) and modulus (800×10^3 psi). Because of its relatively low elongation at failure (2.3 percent), the resin has comparatively poor toughness as defined by the area under the stress-strain curve. The resistance of ERLA 4617 to rapid crack propagation is intermediate between the DEN 438 and DER 332-DER 732 resins.

The screening test program involved evaluation of 216 [illegible] compression molded specimens (eight replicates at each of 27 material combinations). It was subsequently necessary to increase the quantity of specimens to 218 because tensile modulus data had not been obtained on two of the material combinations. Density and thickness measurements were taken on each specimen prior to tensile or ballistic testing, and fiber content determinations were performed on representative specimens after undamaged or post-damaged tensile testing. The water-displacement method was used to determine the specimen densities. The thickness measurements were taken at four locations within the 3.5-inch-square test area of the specimen. The fiber content was determined by the loss-on-ignition technique whereby the resin is eliminated by pyrolysis in an oxidizing atmosphere at 1050°F.

The average thickness, density, and fiber content values for the 27 material combinations are reported in cell form in Table 4. The data indicate that density and fiber content generally increase with decreasing fiber length because of better packing attainable with the shorter fibers. The average fiber content of the 27 material combinations was 57.9 v/o, which was slightly below the 60 v/o target level.

The average undamaged ultimate tensile strength measurements of three replicates at each of 25 material combinations and four replicates at two

TABLE 4. TEST SPECIMEN MEASUREMENTS - SCREENING TEST PROGRAM

Type of Fiber Finish	1-Inch Fiber Length			1/2-Inch Fiber Length			1/4-Inch Fiber Length		
	Resin Type			Resin Type			Resin Type		
	438	332-732	4617	438	332-732	4617	438	332-732	4617
	A. Thickness (in.)								
836	0.127	0.125	0.126	0.122	0.128	0.124	0.122	0.129	0.126
891	0.123	0.122	0.126	0.123	0.122	0.124	0.125	0.124	0.126
897	0.123	0.125	0.122	0.122	0.127	0.122	0.126	0.123	0.124
	B. Density ($lb/in.^3$)								
836	0.070	0.070	0.072	0.073	0.070	0.072	0.073	0.071	0.072
891	0.072	0.072	0.072	0.072	0.074	0.073	0.073	0.073	0.072
897	0.073	0.070	0.073	0.073	0.073	0.073	0.074	0.073	0.074
	C. Fiber Content (v/o)								
836	53.3	54.9	56.9	59.4	55.0	56.2	59.5	55.1	57.4
891	55.8	59.5	54.9	57.4	62.0	57.9	59.0	59.7	57.0
897	57.8	55.0	59.3	58.6	59.5	59.2	62.2	60.9	61.1

combinations are summarized in cell form in Table 5. The number of specimens that failed in the tapered transition section and the number of replicates are noted for each cell. (The problem of end failures will be discussed in subsequent paragraphs of this section of the report.)

A bar-graph presentation of the ultimate strength data is shown in Figure 14. It is apparent that undamaged tensile stength is directly related to fiber length. As fiber length is increased from 1/4 to 1 inch, a 40-percent increase in strength results despite the fact that the incidence of end failures was significantly higher with 1-inch composites.

The strength data shown in Figure 14 for the various resin and fiber finish combinations were obtained by averaging values across the three fiber length levels. The results indicate, as expected, that the highest undamaged tensile strength is achieved when the fiber glass has an epoxy-compatible finish (836). The composites reinforced with the polyester-compatible finish (891) exhibited strength values that were consistently less than the grand average. The lowest composite strength of all resin and fiber finish combinations evaluated was obtained with the 897 fiber

TABLE 5. ULTIMATE TENSILE STRENGTH OF UNDAMAGED SPECIMENS - SCREENING TEST PROGRAM

Type of Fiber Finish	1-Inch Fiber Length			1/2-Inch Fiber Length			1/4-Inch Fiber Length		
	Resin Type			Resin Type			Resin Type		
	438	332-732	4617	438	332-732	4617	438	332-732	4617
	A. Ultimate Tensile Strength (psi)[a]								
836	26,740	23,060	23,100	18,670[b]	21,140	21,200	13,650[b]	16,390	18,270
891	20,930	17,430	21,100	13,670	15,860	14,870	16,800	14,280	14,210
897	20,900	21,790	18,230	17,320	17,990	12,970	15,290	17,030	13,300
	B. No. of Center Failures per Cell								
836	1	0	0	4	1	0	3	2	1
891	0	0	0	3	0	0	3	1	0
897	0	0	0	3	0	0	3	3	2

[a]Values are based on three replicates per cell except as noted.

[b]Values are based on four replicates.

finish (epoxy/polyester incompatible) in a 4617 resin matrix. The tensile strength of the composites does not appear to be significantly influenced by the resin matrix across all fiber finishes.

The initial tensile modulus of undamaged specimens representing the 27 material combinations is summarized in cell form in Table 6. The modulus values were determined from stress-strain records made during ultimate tensile strength testing. A bar-graph presentation of these data (Figure 15) indicates that initial modulus is essentially independent of fiber length. The deviation from the grand average (3.78×10^6 psi) is less than 2 percent for any of the three fiber lengths examined.

The initial modulus of the composites is highly correlated to the resin modulus, as anticipated. The low-modulus 332-732 resin contributed to low composite modulus values regardless of fiber finish. The specimens with the high-modulus 4617 resin exhibited the highest initial tensile modulus values irrespective of fiber finish.

The initial modulus values of composites with the 897 (epoxy/polyester-incompatible) fiber finish were higher with all three candidate resins than corresponding specimens with either the 836 or 891 fiber finishes. This unexpected response may be attributable, in some degree, to the organic

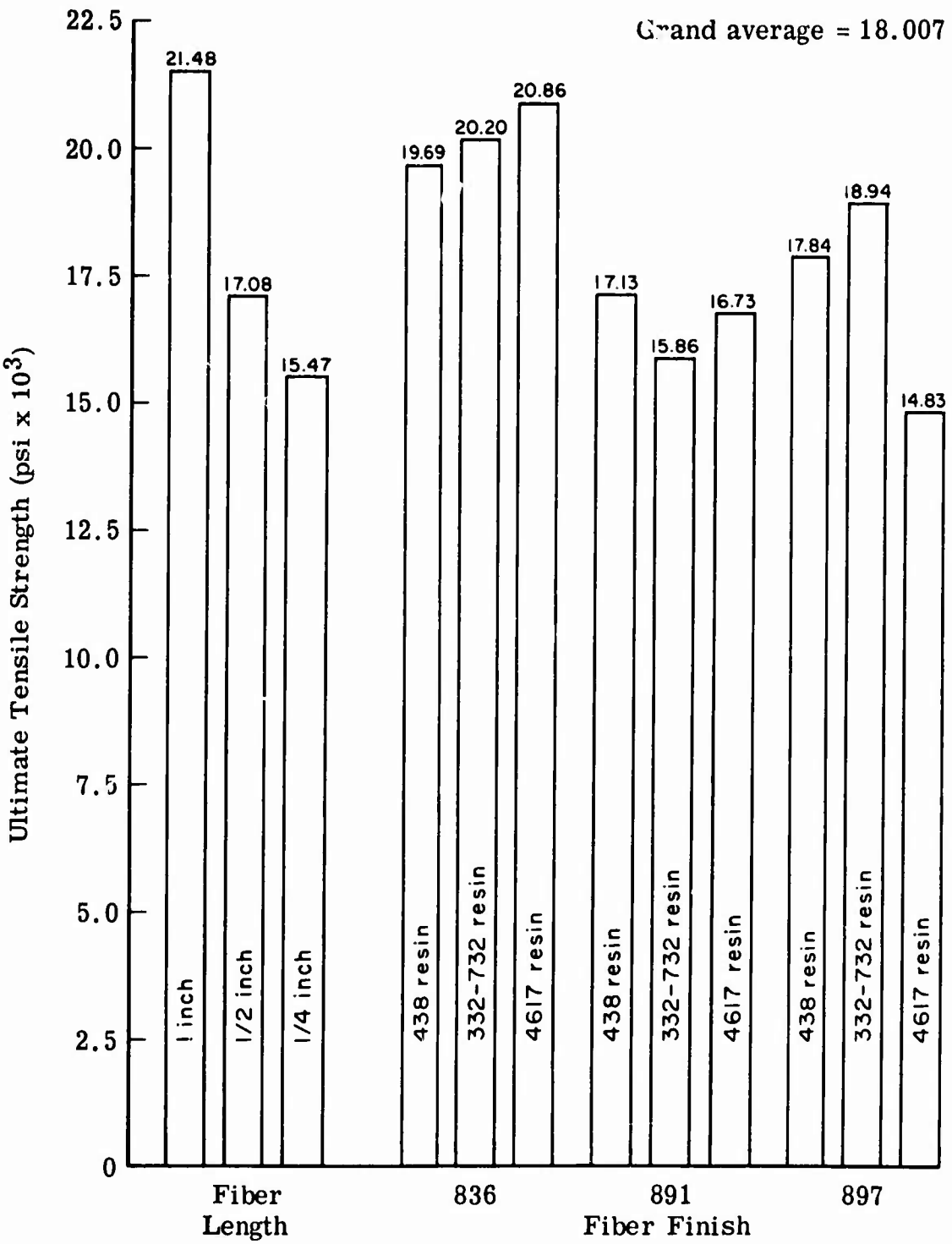

Figure 14. Ultimate Tensile Strength of Undamaged Specimens.

TABLE 6. INITIAL TENSILE MODULUS[a] OF UNDAMAGED SPECIMENS - SCREENING TEST PROGRAM

Type of Fiber Finish	1-Inch Fiber Length			1/2-Inch Fiber Length			1/4-Inch Fiber Length		
	Resin Type			Resin Type			Resin Type		
	438	332-732	4617	438	332-732	4617	438	332-732	4617
836	3.12	3.40	4.64	3.33[b]	2.91	4.39	4.04[b]	3.07	4.07
891	3.52[b]	3.27	4.40	3.44[c]	3.68	4.39	3.68	3.25	3.91
897	3.95	3.68	4.69	3.38	3.77	4.26	3.94	3.41[b]	4.51

[a]Values (in psi x 10^6) are based on three replicates per cell except as noted.

[b]Values are based on one replicate.

[c]Values are based on two replicates.

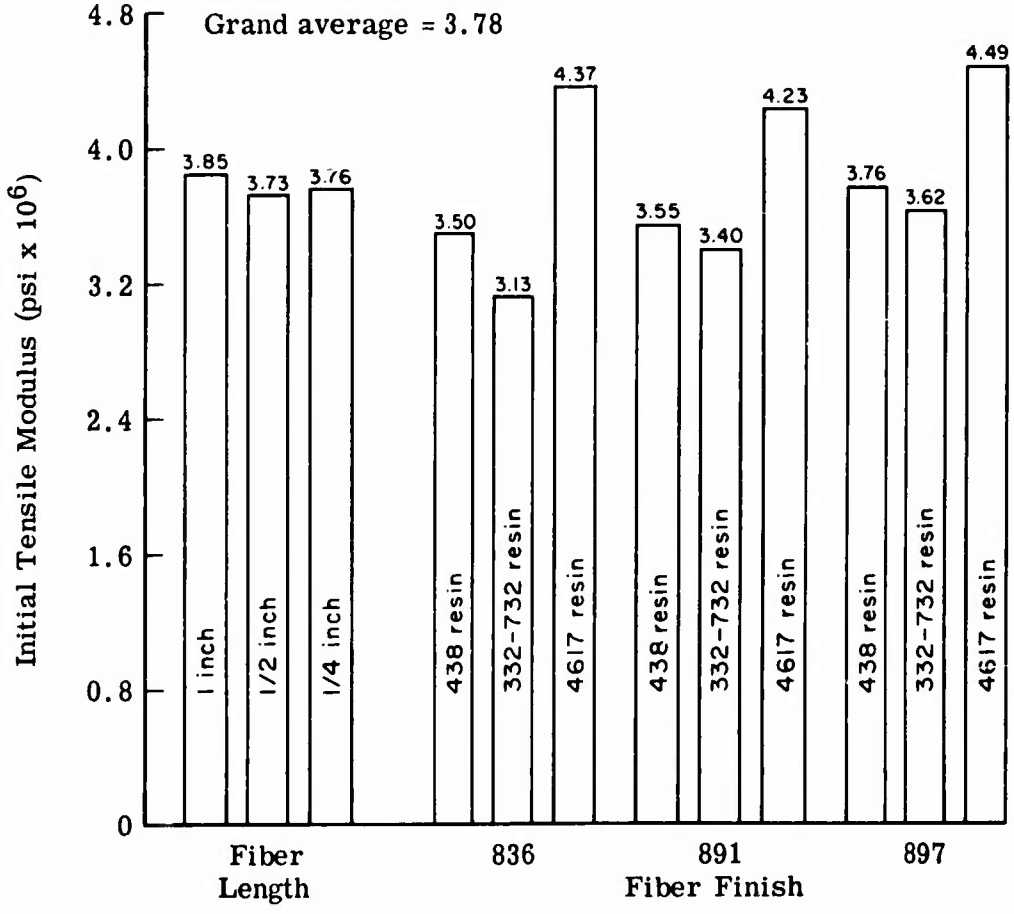

Figure 15. Effect of Material Parameters on the Initial Tensile Modulus of Undamaged Specimens.

solvent in the impregnation bath extracting the 897 finish from the fibers and exposing raw glass. Coupling of epoxy resins to bare glass is generally outstanding, and high modulus values could result. The response may also be a result, in part, of the generally higher fiber content of composites with the 897 fiber finish. The average fiber content of all specimens with the 897 fiber finish was 59.3 v/o compared to 56.4 and 58.1 v/o for the specimens with 836 and 891 fiber finishes, respectively.

As previously noted, a relatively high frequency of transition section failures was experienced during ultimate tensile strength testing of undamaged specimens. The frequency of such failures on a percentage basis is shown in Figure 16 as a function of fiber length and resin type-fiber finish combinations. In determining the effect of fiber length, the frequency of end failures was averaged for all specimens of a particular fiber length regardless of resin type and fiber finish. The frequency of transition section failures for the various resin and fiber finish combinations was obtained by averaging failure rates for all three fiber lengths.

It is readily apparent that test specimens with 1-inch fibers are particularly susceptible to transition section failures. Of the 27 specimens with 1-inch fibers, only one (or 3.7 percent) failed in the gage area during tensile testing. The vulnerability to end failures decreases directly with fiber length. The end failure rates for the specimens with 1/2- and 1/4-inch fibers were 57.1 and 35.7 percent, respectively.

From a resin standpoint, the lowest transition section failure rates were experienced with the 438 resin regardless of fiber finish. On the other hand, the frequency of end failures was greater than 75 percent with the 4617 resin irrespective of fiber finish. The specimens with the 332-732 resin also exhibited a high end failure rate compared to the 438 resin.

The polyester-compatible fiber finish (891) contributed to a high frequency of end failures compared to the other two fiber finishes. No signficant difference in the rate of transition section failures was observed between the 836 and 897 fiber finishes.

The design of the standard ballistic/tensile specimen was based primarily on ballistic considerations. The physical dimensions, particularly the length-to-width ratio, differ significantly from those recommended for tensile strength determination and may have been responsible for the high incidence of end failures. Since all specimens did not fail in the transition section, the problem is not exclusively design oriented. Other factors, such as material distribution in the preform and flow characteristics of the molding compound, may have contributed to end failures.

Transition section failures were a continuing problem throughout Task I. Because of the potential impact that this problem could have on flight

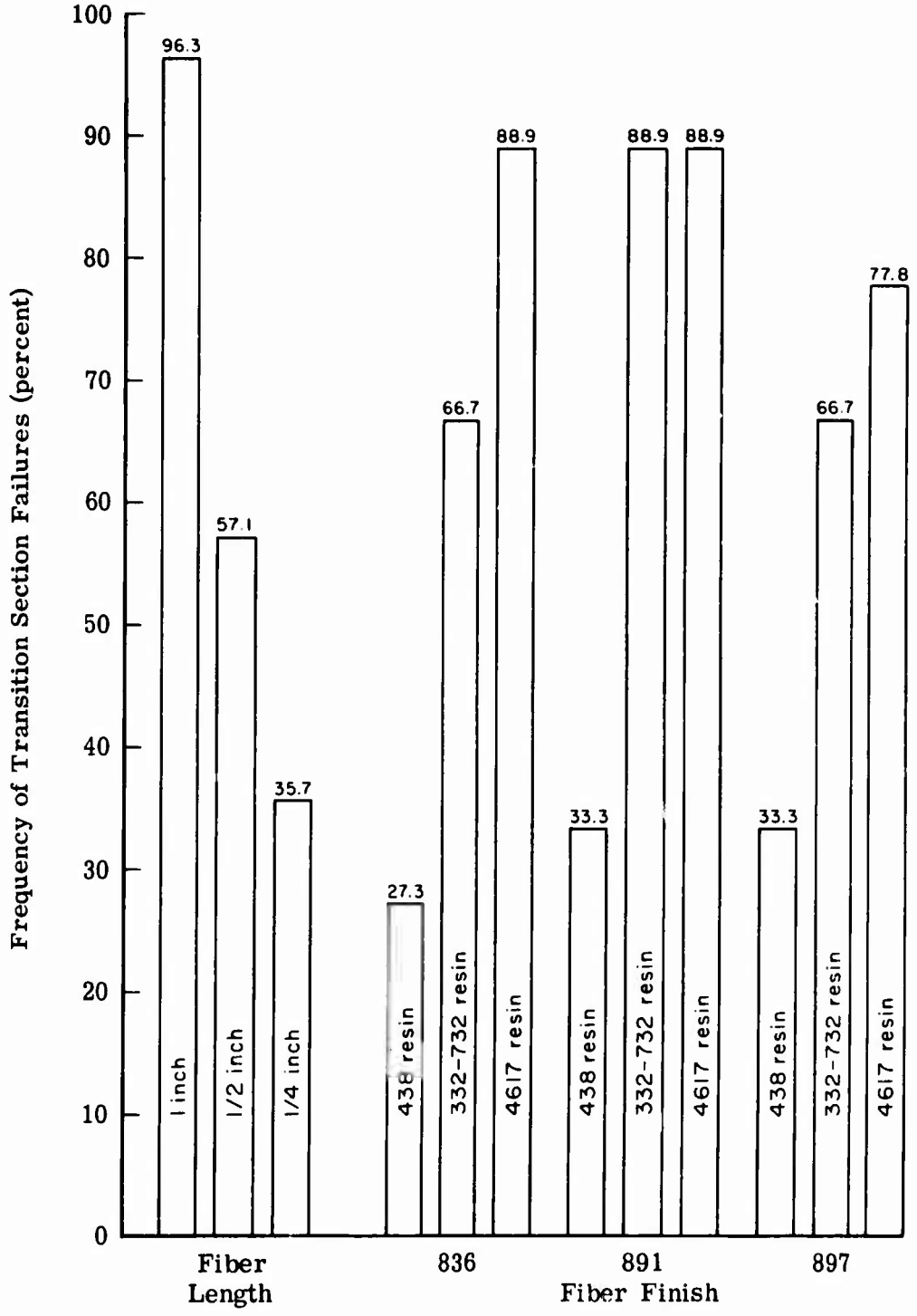

Figure 16. Effect of Material Parameters on the Frequency of Transition Section Failures.

control component design and production, a concentrated program was undertaken at the conclusion of Task I to eliminate such failures.

The tensile strength of 11 of the 27 material combinations was obtained from narrow specimens cut from standard ballistic/tensile specimens. These narrow specimens were nominally 1/2 inch wide in the gage area (3/4 inch wide at the ends), 8-1/2 inches long, and 1/8 inch thick. Four specimens, two each from the center and edge areas, were prepared from each standard specimen.

A summary of tensile strength data is given in Table 7 for both the center- and edge-cut specimens. Certain test values were excluded from consideration if the specimen failed in the transition section at a strength level that would have a downward bias on the average results. If all narrow specimens of a particular composite system failed in the transition section, then only the highest strength value was reported.

During tensile testing of the narrow specimens, no transition section failures were experienced with center-cut specimens regardless of fiber length. However, the incidence of end failures with edge-cut specimens was significantly affected by fiber length. End failures were obtained in 9 of 12 specimens cut from the edges of 3.5-inch-wide specimens reinforced with 1-inch fibers. Only 10 percent of the edge-cut specimens with 1/2-inch fibers exhibited transition section failures. None of the eight edge-cut specimens with 1/4-inch fibers experienced end failures.

The data reported in Table 7 clearly indicate that tensile strength varies across the width of the standard test specimen because of edge fiber alignment. The effect of this alignment on strength becomes increasingly more pronounced as fiber length increases. For 1-inch fibers the average ratio of edge-to-center strength was 1.491 if the questionable ratio of 2.40 for the 891/438 composite system is excluded. This essentially means that the 1/2-inch width at the edges of the 3.5-inch-wide specimen will carry 49.1 percent more load than a similar specimen cut from the randomly oriented material in the center area. The edge-to-center ratios for specimens with 1/2- and 1/4-inch fibers are 1.398 and 1.036, respectively.

A simple hypothetical model that is applicable regardless of fiber length is presented in Figure 17 to describe the variation in strength across a wide specimen. In this model the 3.5-inch-wide specimen is divided into seven equal-width sections. Test results were obtained on specimens from four of these regions. This model assumes that the three center regions are identical in strength (σ_c) to that measured on center-cut specimens. The measured edge strength (σ_e) is assumed to represent the average strength across those two sections. The remaining two regions are assumed to have strengths intermediate to the edge and center sections. The average strength (σ_{avg}) of the standard 3.5-inch-wide

TABLE 7. TENSILE STRENGTH OF NARROW SPECIMENS - SCREENING TEST PROGRAM

Composite System			Ultimate Tensile Strength (psi)		Strength Ratio, σ_e/σ_c	Ultimate Tensile Strength (psi)	
Fiber Finish	Resin Type	Fiber Length	Edge, σ_e	Center, σ_c		Predicted, σ_p[a]	Measured, σ_m
836	438	1 in.	31,350	20,750	1.511	25,290	28,790
836	332-732	1 in.	>44,100[b]	28,220	1.564	35,030	>24,030
836	4617	1 in.	37,500[b]	29,250	1.281	32,790	>25,200
891	438	1 in.	26,700[b]	11,120	2.387	17,800	>23,000
897	438	1 in.	35,280[b]	21,930	1.609	27,650	>23,300
					Avg = 1.673[c]	$\sigma_p = 0.878\,\sigma_m$[d]	
836	438	1/2 in.	18,800	13,000	1.446	15,490	18,670
891	438	1/2 in.	17,680	13,990	1.264	15,570	13,670
897	438	1/2 in.	20,310	13,480	1.507	16,410	17,320
897	4617	1/2 in.	18,290	13,320	1.373	15,450	>14,800
					Avg = 1.398	$\sigma_p = 0.956\,\sigma_m$[e]	
891	4617	1/4 in.	13,900	15,180	0.916	14,630	14,210
897	438	1/4 in.	13,670	11,810	1.157	12,610	15,290
					Avg = 1.036	$\sigma_p = 0.937\,\sigma_m$	

[a] Based on $\sigma_p = \frac{3\sigma_e + 4\sigma_c}{7}$.

[b] Rejection criteria applied.

[c] Avg = 1.491 if specimen 891/438 ratio is excluded.

[d] Specimen 836/438 data only.

[e] Specimen 897/4617 data excluded.

specimen would then be described by the following equation:

$$\sigma_{avg} = \frac{4}{7}\,\sigma_c + \frac{3}{7}\,\sigma_e \qquad (17)$$

A comparison of strength values predicted by Equation (17) with those measured on the standard 3.5-inch-wide specimen is presented in Table 7. Direct comparisons are possible with only six systems - one with 1-inch fibers, three with 1/2-inch fibers, and two with 1/4-inch fibers - where center failures were obtained. The reported value for the measured strength of the 836/438 specimen with 1-inch fibers is based on the average strength of two specimens, one of which failed in the transition section. This particular specimen, however, failed at a higher strength than the companion specimen. No meaningful comparisons are possible between predicted and observed strengths for the other five specimens with 1-inch fibers since all specimens failed in the transition section.

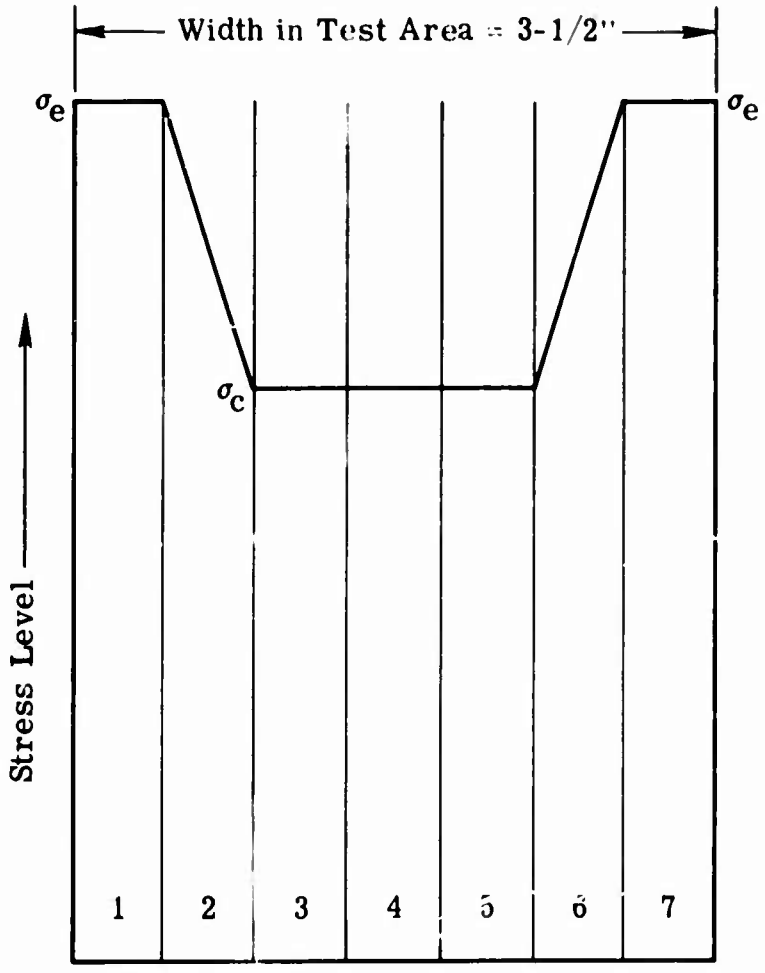

Figure 17. Hypothetical Strength Distribution Across a Specimen.

The predicted strength for the 836/438 specimen with 1-inch fibers was 25,290 psi, or 87.8 percent of the measured strength of 28,790 psi. For the three composite systems with 1/2-inch fibers where all wide specimens failed in the center area, the average predicted strength was 15,820 psi compared with 16,550 psi for the average measured strength. This difference of 730 psi represents a deviation of 4.4 percent from the average measured strength. The average predicted and measured strength values for the composites with 1/4-inch fibers are 13,620 and 14,750 psi, respectively. This represents a difference of 7.7 percent, based on the measured strength.

The relatively good agreement between predicted and measured tensile strength indicates that the model is a fairly accurate representation of the true strength.

During ultimate tensile testing an extensometer was mounted on each specimen to obtain stress-strain curves for narrow specimens cut from both the edge and center of moldings 3.5 inches wide. Modulus of elasticity values were then determined from the initial slope of these curves. The resultant data for the 11 material combinations tested are reported in Table 8.

The initial tensile modulus data indicate that fibers are definitely aligned along the edges of the net molded, 3.5-inch-wide standard specimen. The edge alignment effect is most pronounced with specimens containing 1-inch fibers. This effect decreases as fiber length decreases. The ratios of edge-to-center modulus for specimens with 1-, 1/2-, and 1/4-inch fibers are 1.368, 1.256, and 1.131, respectively. If the modulus ratio for the 891/438 specimen with 1-inch fibers is excluded, the resultant average is 1.321. This composite exhibited edge-to-center strength and modulus ratios that deviated significantly from other composites reinforced with 1-inch fibers.

TABLE 8. INITIAL TENSILE MODULUS OF NARROW SPECIMENS - SCREENING TEST PROGRAM

Composite System			Initial Tensile Modulus (psi x 10^6)		Modulus Ratio, E_e/E_c	Initial Tensile Modulus (psi x 10^6)	
Fiber Finish	Resin Type	Fiber Length	Edge, E_e	Center, E_c		Predicted, E_p[a]	Measured, E_m
836	438	1 in.	3.59	2.92	1.229	3.21	3.12
836	332-732	1 in.	4.32	3.11	1.394	3.62	3.40
836	4617	1 in.	5.32	3.86	1.386	4.48	4.64
891	438	1 in.	4.21	2.62	1.607	3.30	3.52
897	438	1 in.	4.42	3.47	1.274	3.88	3.95
					Avg = 1.368[b]	E_p = 1.000 E_m	
836	438	1/2 in.	3.68	2.90	1.269	3.23	3.33
891	438	1/2 in.	3.66	3.00	1.223	3.28	3.44
897	438	1/2 in.	4.14	3.19	1.298	3.60	3.38
836	4617	1/2 in.	4.96	4.00	1.242	4.42	4.26
					Avg = 1.256	E_p = 1.012 E_m	
891	4617	1/4 in.	4.13	3.80	1.086	3.94	3.91
897	438	1/4 in.	3.85	3.27	1.177	3.52	3.94
					Avg = 1.131	E_p = 0.951 E_m	

[a]Based on $E_p = \frac{3E_e + 4E_c}{7}$

[b]Avg = 1.321 if specimen 891/438 ratio is excluded.

Predictions of the initial tensile modulus for 3.5-inch-wide specimens were made from data generated on narrow specimens. This was accomplished by substituting modulus terms for the strength terms in the hypothetical distribution model. This yields the following predictive equation for initial tensile modulus:

$$E_{avg} = \frac{4}{7} E_c + \frac{3}{7} E_c \qquad (18)$$

A summary of predicted and measured initial tensile modulus for the 11 material combinations is given in Table 8. The agreement between predicted and measured modulus values for each composite system is good - better, in fact, than that observed with tensile strength data. The average predicted-to-measured modulus ratios for all composites with a particular fiber length closely approach unity. The average ratios of 1.000, 1.012, and 0.951 for specimens with 1-, 1/2-, and 1/4-inch fibers, respectively, are further evidence that the hypothetical model is a reasonably accurate representation of the true tensile properties of wide specimens.

Results of Ballistic Tests

Five replicates of each of the 27 material combinations were ballistically impacted at room temperature with fully tumbled caliber .30 ball M2 projectiles at 0-degree obliquity and a nominal striking velocity of 1800 ft/sec. The specimens were stressed during ballistic testing to 35 percent of the average undamaged ultimate tensile strength. The average strength was determined at room temperature on 3.5-inch-wide specimens of each material combination.

After ballistic testing, a permanent record was made of the visual damage sustained by the specimen on both the impact and exit surfaces. This record initially consisted of a full-scale outline tracing showing the extent of damage and its physical relationship to the test area. This procedure was subsequently replaced by a simpler and more descriptive method involving reproduction machine copies. Before making these copies, the damage envelope was marked on each surface along with the projectile footprint length and orientation on the impact surface. This was done because the extent of damage could be more accurately assessed from the actual specimens rather than the machine copies.

The extent of area damage was measured directly from the reproduction machine copy with a planimeter. The volume damage was computed assuming that the damage is a frustrum of a cone with the front and back

surface areas representing the top and bottom areas of the frustrum. The formula for the volume of a conical frustrum is defined in Equation (2) of the "Test and Evaluation Techniques" discussion.

A summary of damage areas and volume for the 27 material combinations is presented in cell form in Table 9. The damage measurements are based on five replicates except for the 891/438 composites with 1/4-inch fibers. Damage data from two of these composite specimens were rejected because the projectile was not properly tumbled.

A bar-graph presentation of the effect of fiber length and resin type-fiber finish combinations on the extent of ballistic damage is shown in Figure 18. These data indicate that front surface area damage increases from 0.81 to 1.01 $in.^2$ as fiber length increases from 1/4 to 1 inch. These values represent the average damage areas of all specimens of a particular fiber length regardless of resin type or fiber finish. It was further observed that composites with the 438 resin matrix generally exhibit the greatest damage irrespective of fiber finish and fiber length. On the other hand, specimens with a 4617 resin matrix in combination with any of the three fiber finishes sustained less damage, on the average, than the grand front surface damage area of 0.923 $in.^2$

Photographs of front surface ballistic damage to representative specimens of each of the 27 material combinations are shown in Figures 19, 20, and 21. The subtle differences in front surface damage areas are difficult to discern from these photographs. However, the photographs do reveal that the projectile wound is relatively clean for all specimens with 1/4-inch fibers.

The graphical presentation of back surface damage area as a function of fiber length shown in Figure 22 clearly indicates that fiber length has a strong influence on damage area. When the back surface damage area is averaged across all fiber lengths as shown in Figure 18, the damage is seen to increase with fiber length. For 1-inch fiber composites, the average back surface damage was 3.77 $in.^2$ and the grand average was 2.594 $in.^2$ The average back surface damage areas for specimens with 1/2- and 1/4-inch fibers were 2.39 and 1.62 $in.^2$, respectively.

The resin type also appears to have a definite effect on back surface damage area. The influence is identical with that observed from the front surface damage area; namely, specimens with a 438 resin matrix exhibit greatest damage regardless of fiber finish and those with the 4617 resin sustain below-average back surface area damage. The results also suggest that composites with the epoxy/polyester-incompatible finish (897) sustain the greatest back surface area damage irrespective of resin type.

TABLE 9. SUMMARY OF VISUAL BALLISTIC DAMAGE - SCREENING TEST PROGRAM

Type of Fiber Finish	1-Inch Fiber Length			1/2-Inch Fiber Length			1/4-Inch Fiber Length		
	Resin Type			Resin Type			Resin Type		
	438	332-732	4617	438	332-732	4617	438	332-732	4617
	A. Front Surface Area (in.^{2})[a]								
836	1.07	0.93	0.97	0.95	0.84	0.88	0.83	0.83	0.78
891	1.23	0.87	0.86	1.06	0.84	0.73	1.00[b]	0.73	0.72
897	1.13	0.96	1.03	1.30	1.03	0.94	0.76	0.91	0.75
	B. Back Surface Area (in.^{2})[a]								
836	4.06	2.87	3.36	2.25	2.20	2.38	1.56	1.46	1.62
891	3.92	3.85	3.77	2.55	2.33	2.04	2.13[b]	1.59	1.52
897	4.31	3.62	4.17	2.96	2.63	2.15	1.52	1.81	1.40
	C. Volume (in.^{3})[a]								
836	0.304	0.227	0.255	0.189	0.186	0.195	0.143	0.147	0.147
891	0.299	0.273	0.268	0.213	0.185	0.166	0.193[b]	0.141	0.138
897	0.313	0.271	0.297	0.246	0.223	0.185	0.138	0.164	0.131

[a]Values are based on five replicates except as noted.

[b]Values are based on three replicates.

Photographs of back surface ballistic damage to representative specimens of the 27 material combinations evaluated are shown in Figures 23, 24, and 25. The powerful influence of fiber length on back surface area damage is readily apparent. The resin type and fiber finish effects are more subtle and are not apparent from the photographs.

Since damage volume is a direct function of front and back surface damage areas, any parameter that affects the latter values in a common manner will also influence the damage volume in a similar way. Consequently, fiber length had a pronounced effect on damage volume because it significantly affected front and back surface damage areas. The curves presented in Figure 26 show the relationship between damage volume and

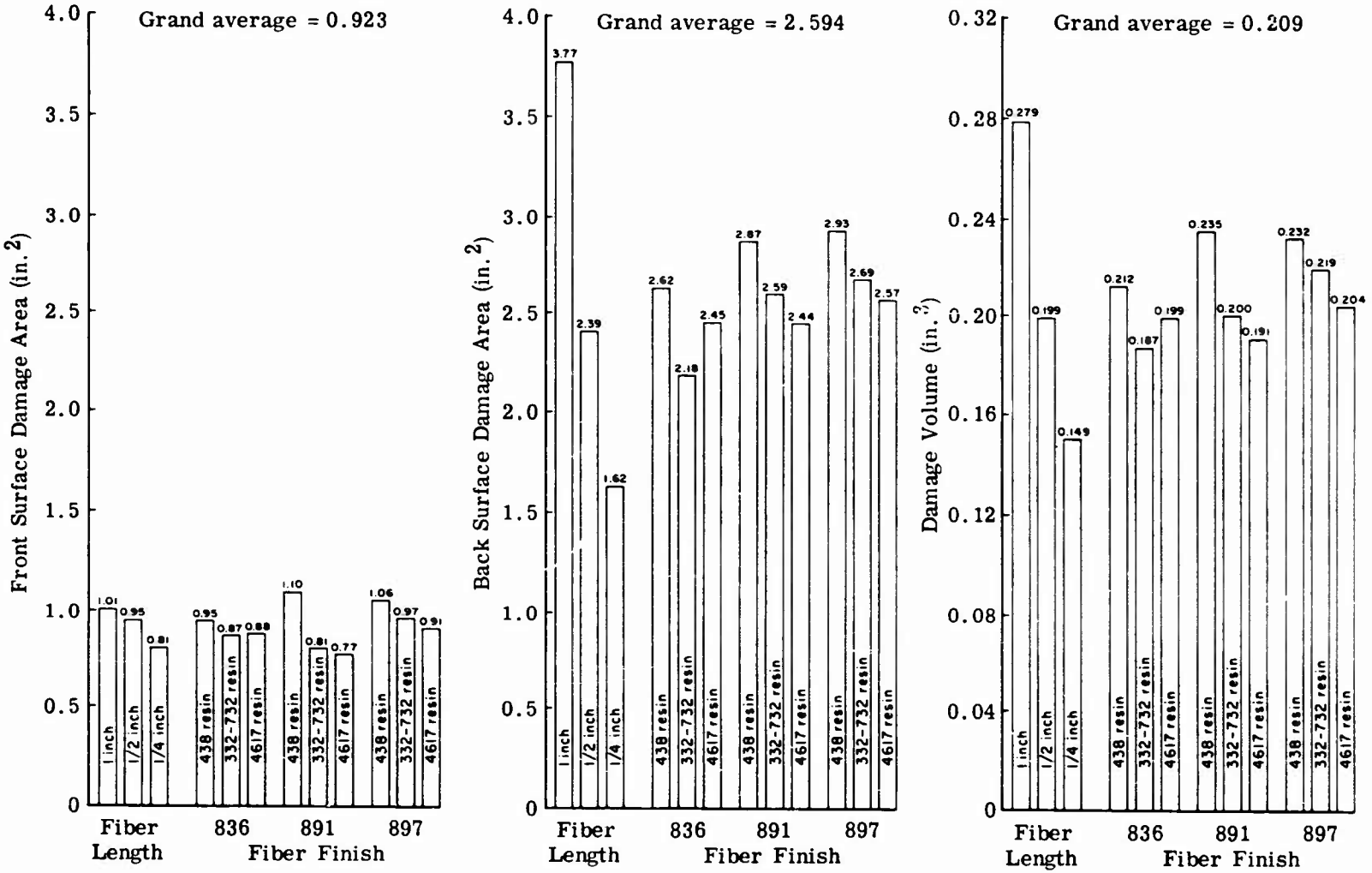

Figure 18. Effect of Material Parameters on Ballistic Damage Areas and Volume.

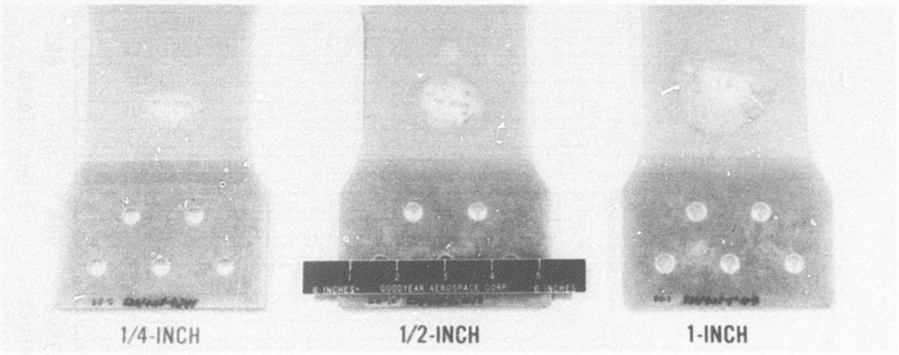

A. Type 438 Resin

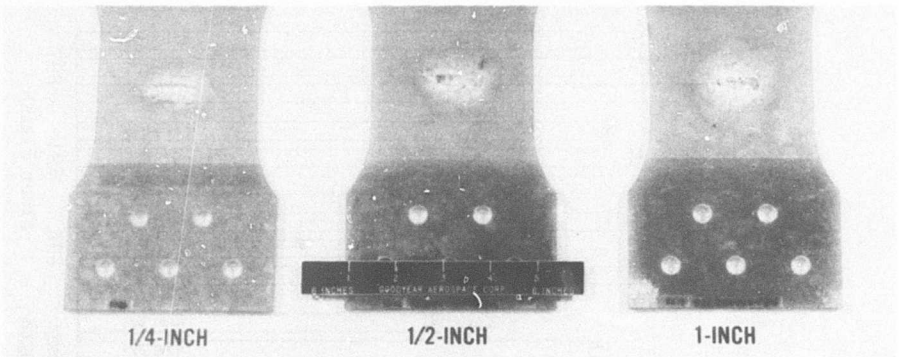

B. Type 332-732 Resin

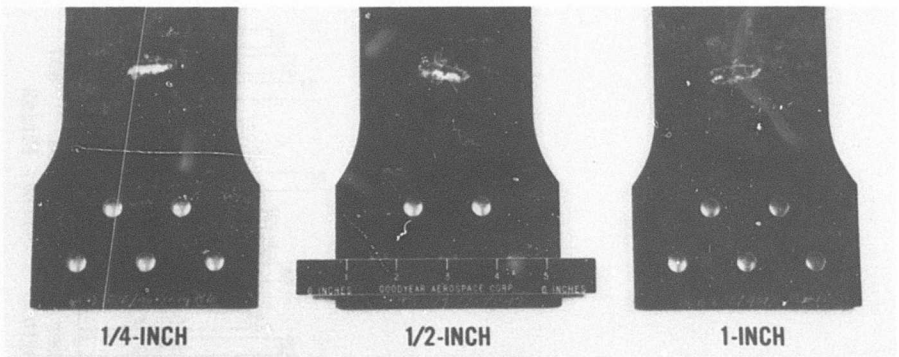

C. Type 4617 Resin

Figure 19. Typical Front Surface Ballistic Damage - Specimens With 836 Fiber Finish.

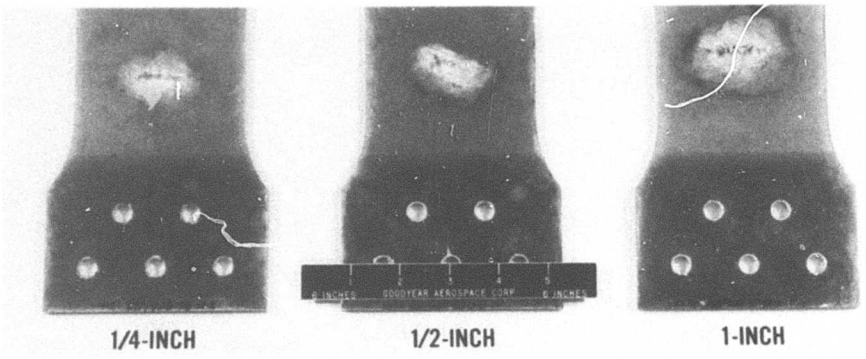

A. Type 438 Resin

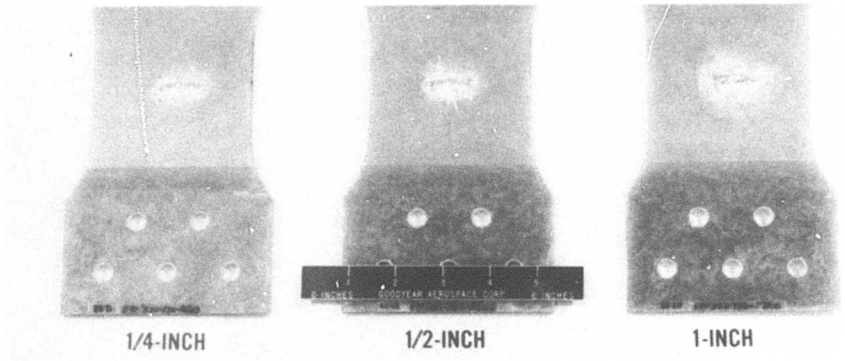

B. Type 332-732 Resin

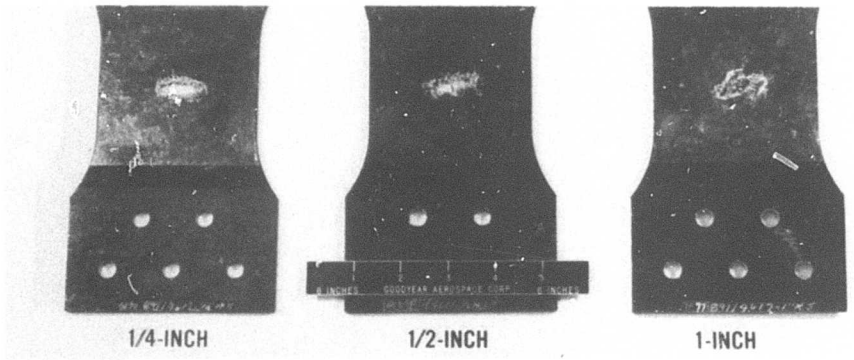

C. Type 4617 Resin

Figure 20. Typical Front Surface Ballistic Damage - Specimens With 891 Fiber Finish.

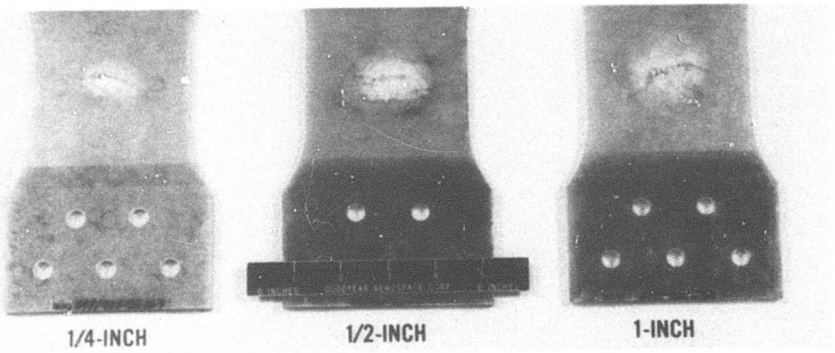

A. Type 438 Resin

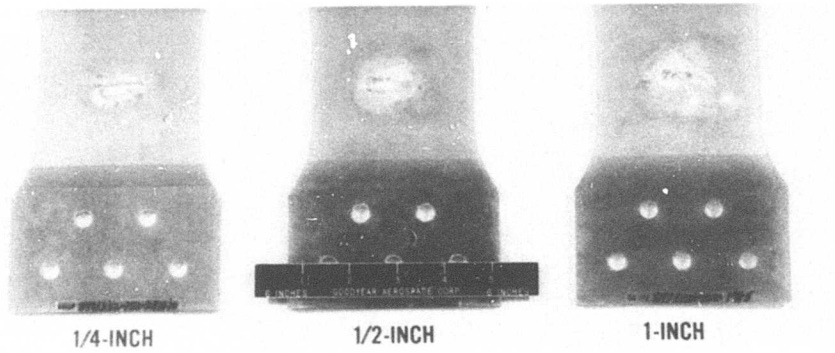

B. Type 332-732 Resin

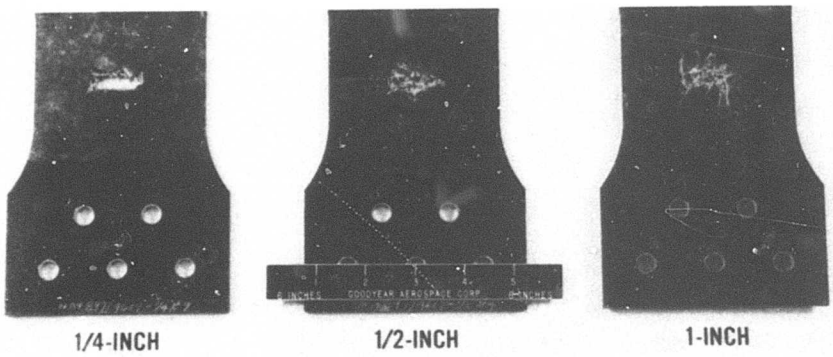

C. Type 4617 Resin

Figure 21. Typical Front Surface Ballistic Damage - Specimens With 897 Fiber Finish.

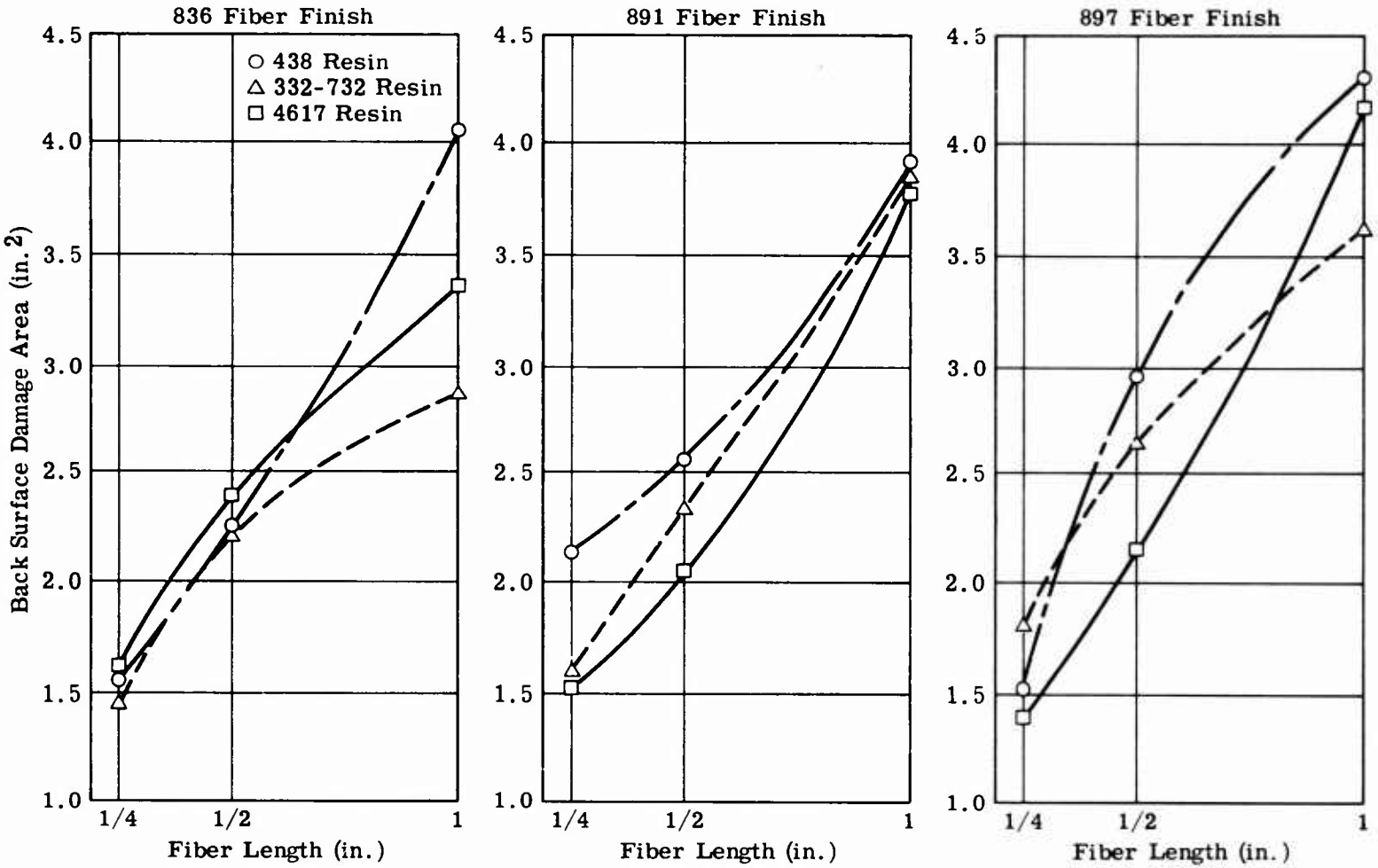

Figure 22. Relationship Between Back Surface Ballistic Damage Area and Fiber Length.

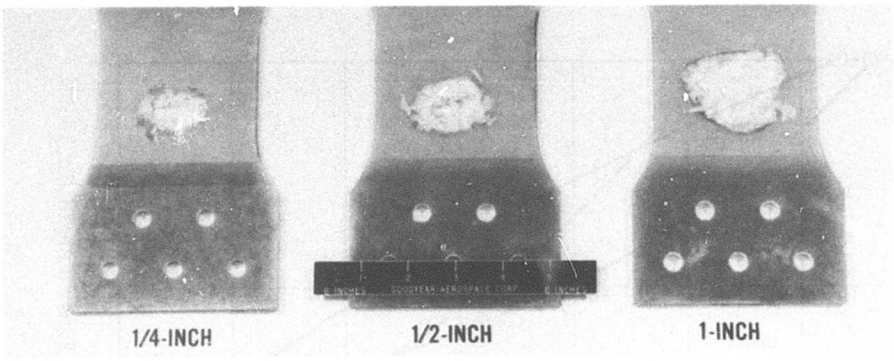

A. Type 438 Resin

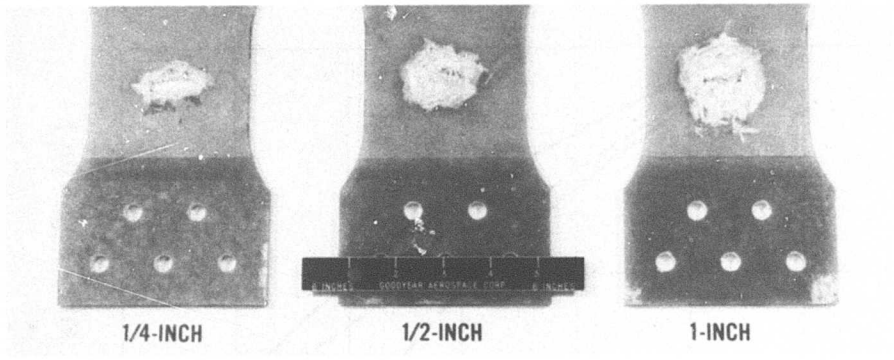

B. Type 332-732 Resin

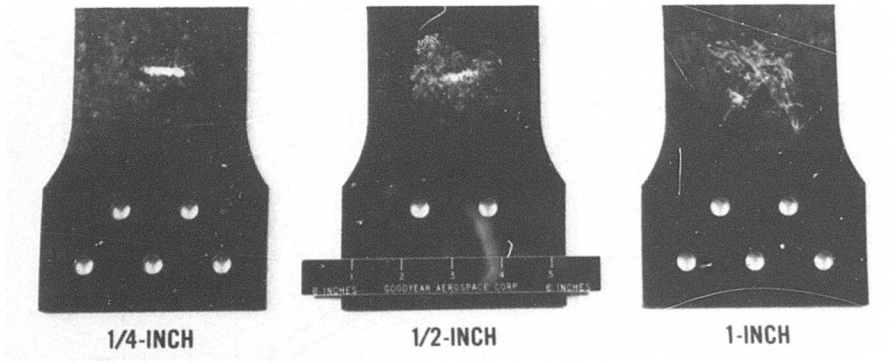

C. Type 4617 Resin

Figure 23. Typical Back Surface Ballistic Damage - Specimens With 836 Fiber Finish.

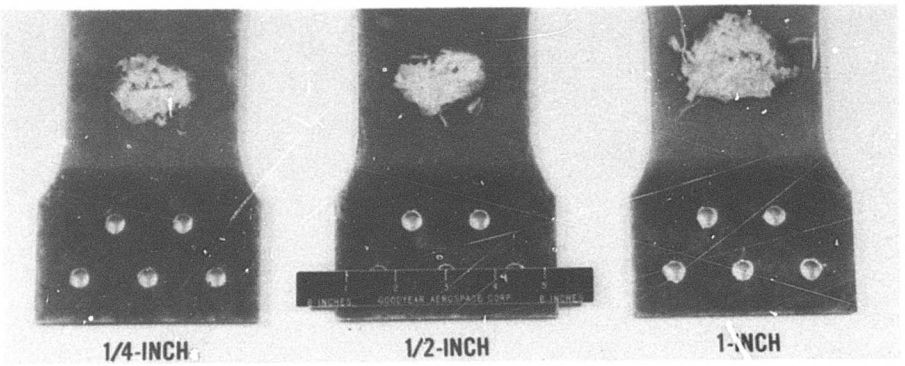

A. Type 438 Resin

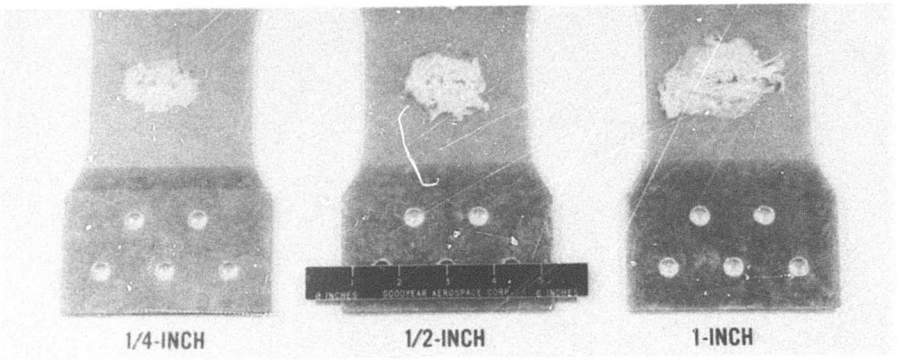

B. Type 332-732 Resin

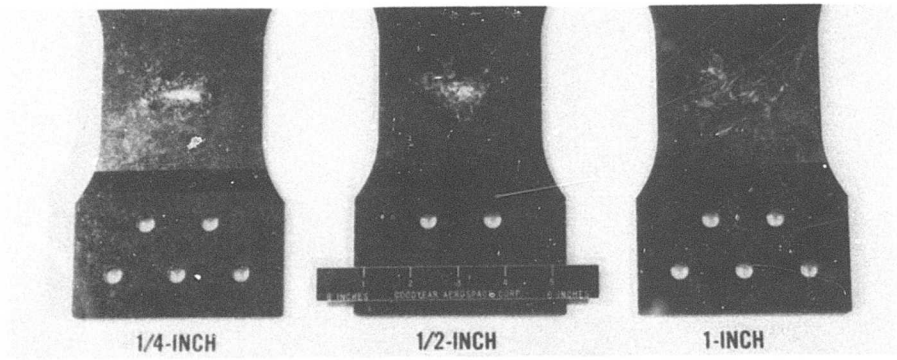

C. Type 4617 Resin

Figure 24. Typical Back Surface Ballistic Damage - Specimens With 891 Fiber Finish.

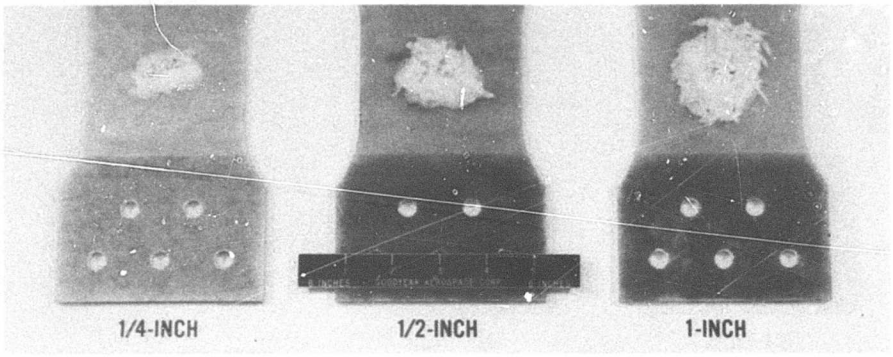

A. Type 438 Resin

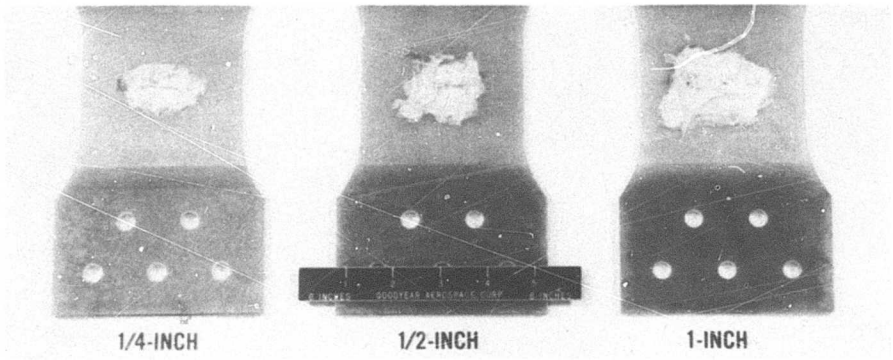

B. Type 332-732 Resin

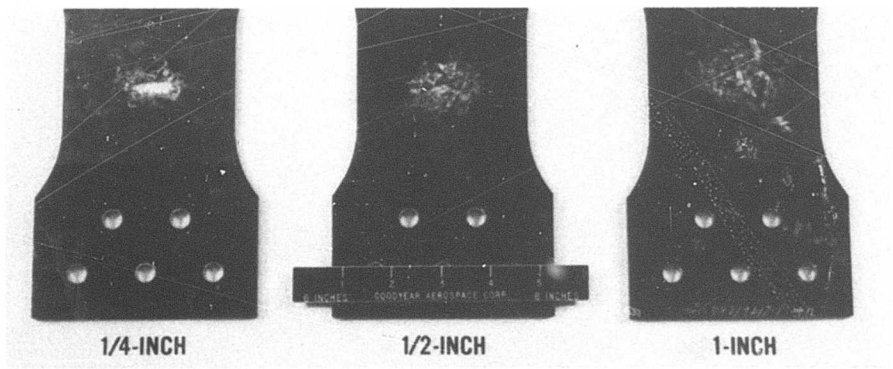

C. Type 4617 Resin

Figure 25. Typical Back Surface Ballistic Damage - Specimens With 897 Fiber Finish.

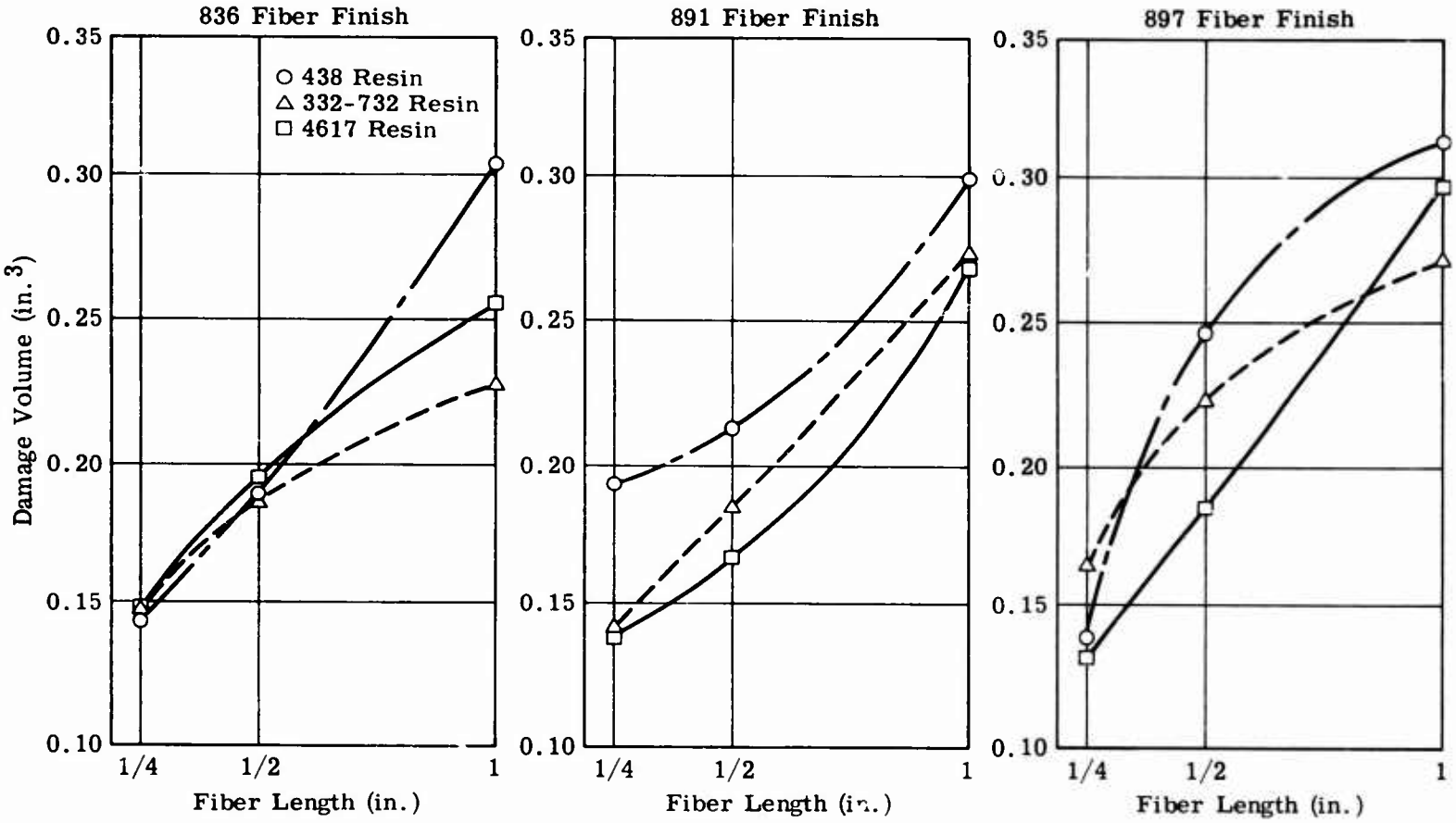

Figure 26. Relationship Between Ballistic Damage Volume and Fiber Length.

fiber length for the nine resin and fiber finish combinations examined. These data indicate that damage volume increases directly with fiber length. This effect is also evident in Figure 18, where the damage volumes are averaged for all resin type and fiber finish combinations of a particular fiber length. The average damage volume for 1-inch fiber composites was 0.279 $in.^3$, and the grand average was 0.209 $in.^3$ The composites with 1/2- and 1/4-inch fibers exhibited damage volumes of 0.199 and 0.149 $in.^3$, respectively.

The common trends associated with the 438 and 4617 resin matrices with respect to damage areas were also manifest in the damage volume results. The 438 resin exhibited the greatest damage volume regardless of fiber finish when the data were averaged across all fiber lengths. Below-average volume damage was experienced by composites with a 4617 resin matrix irrespective of fiber finish. These effects can be seen from the bar-graph presentation of damage volume shown in Figure 18.

The values reported in cell form in Table 10 define the extent of transverse damage sustained by the specimens as a result of ballistic impact. The front, back, and average transverse damage are presented for each of the 27 material combinations examined. Each transverse damage value is based on five replicates at each combination unless otherwise noted. Certain values were excluded from consideration based on two rejection criteria - projectile not fully tumbled and in-plane projectile rotation - discussed in "Test and Evaluation Techniques."

The bar graphs presented in Figure 27 depict the effects of fiber length and resin type-fiber finish combinations on the extent of transverse ballistic damage. The influence of fiber length was determined by averaging all transverse damage values for specimens of common fiber length regardless of resin type or fiber finish. The effect of resin type and fiber finish was obtained by averaging damage values across all fiber lengths for a particular resin type and fiber finish combination.

The average front surface transverse damage exhibited by specimens representing all 27 material combinations was 1.357 inches. The effect of fiber length on this damage parameter is negligible as evidenced by the values of 1.37, 1.37, and 1.33 inches for composites with 1-, 1/2-, and 1/4-inch fibers, respectively. With regard to the effect of resin type on front surface transverse damage, no universal trend is evident across the full spectrum of fiber finishes. The results suggest that fiber finish has an apparent effect on transverse damage. This observation is based on the fact that, regardless of resin type, the composites with 836 (epoxy-compatible) fiber finish exhibited below-average front surface transverse damage and those with 897 (epoxy/polyester-incompatible) fiber finish produced above-average damage.

TABLE 10. SUMMARY OF VISUAL TRANSVERSE BALLISTIC DAMAGE - SCREENING TEST PROGRAM

Type of Fiber Finish	1-Inch Fiber Length			1/2-Inch Fiber Length			1/4-Inch Fiber Length		
	Resin Type			Resin Type			Resin Type		
	438	332-732	4617	438	332-732	4617	438	332-732	4617
	A. Front Surface Transverse Damage (in.)[a]								
836	1.41	1.28[b]	1.37	1.27[c]	1.30	1.32	1.25[b]	1.35	1.33
891	1.52	1.26	1.27[b]	1.48[b]	1.28	1.33[b]	1.39	1.24[b]	1.31
897	1.45	1.40	1.40	1.61	1.39	1.37	1.30[b]	1.44	1.32[b]
	B. Back Surface Transverse Damage (in.)[a]								
836	2.54	2.06[b]	2.29	1.89[c]	1.95	2.00	1.74[b]	1.69	1.77
891	2.44	2.40	2.40[b]	2.12[b]	1.82	1.87[b]	1.82	1.69[b]	1.67
897	2.31	2.29	2.34	2.21	2.02	1.95	1.72[b]	1.87	1.65[b]
	C. Avg Front/Back Surface Transverse Damage (in.)[a]								
836	1.97	1.67[b]	1.83	1.58[c]	1.62	1.66	1.74[b]	1.52	1.55
891	1.98	1.83	1.84[b]	1.80[b]	1.55	1.60[b]	1.61	1.46[b]	1.49
897	1.88	1.85	1.87	1.91	1.70	1.66	1.51[b]	1.65	1.48[b]

[a]Values are based on five replicates except as noted.

[b]Values are based on four replicates.

[c]Values are based on three replicates.

Back surface transverse damage is significantly affected by fiber length as indicated by the bar graphs in Figure 27. For 1-inch fiber composites, the average damage was 2.34 inches as opposed to a grand average of 2.019 inches. The 1/2- and 1/4-inch fiber composites exhibited transverse damage of 1.98 and 1.74 inches, respectively. The pronounced effect of fiber length on back surface transverse damage is also apparent from the series of curves presented in Figure 28. These curves are based on average damage for each of the 27 material combinations examined.

The results given in Figure 27 also indicate that the composites with a 438 resin matrix sustain above-average back surface transverse damage irrespective of fiber finish. The effect of fiber finish is negligible across the three resin types.

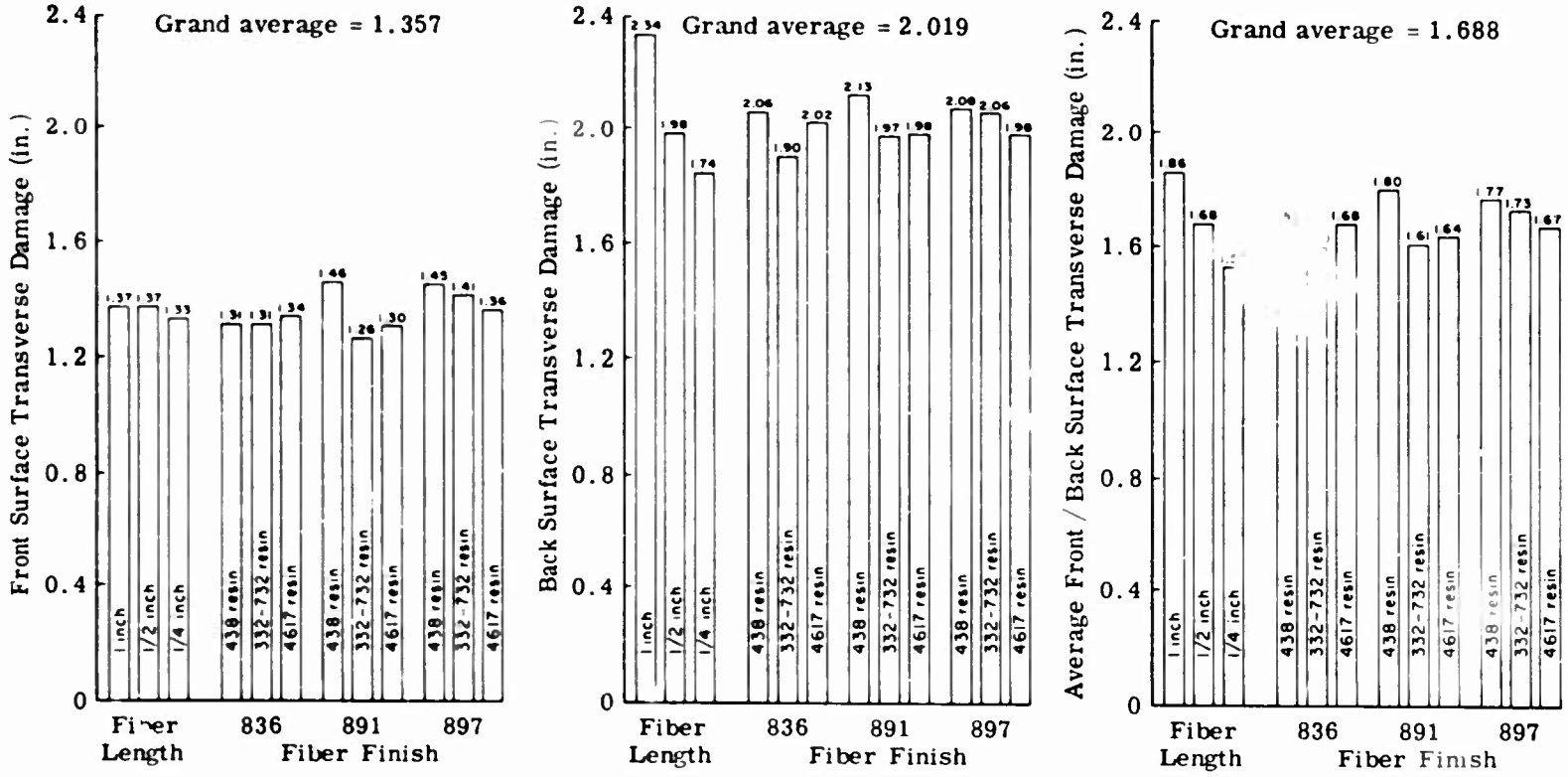

Figure 27. Effect of Material Parameters on Transverse Ballistic Damage.

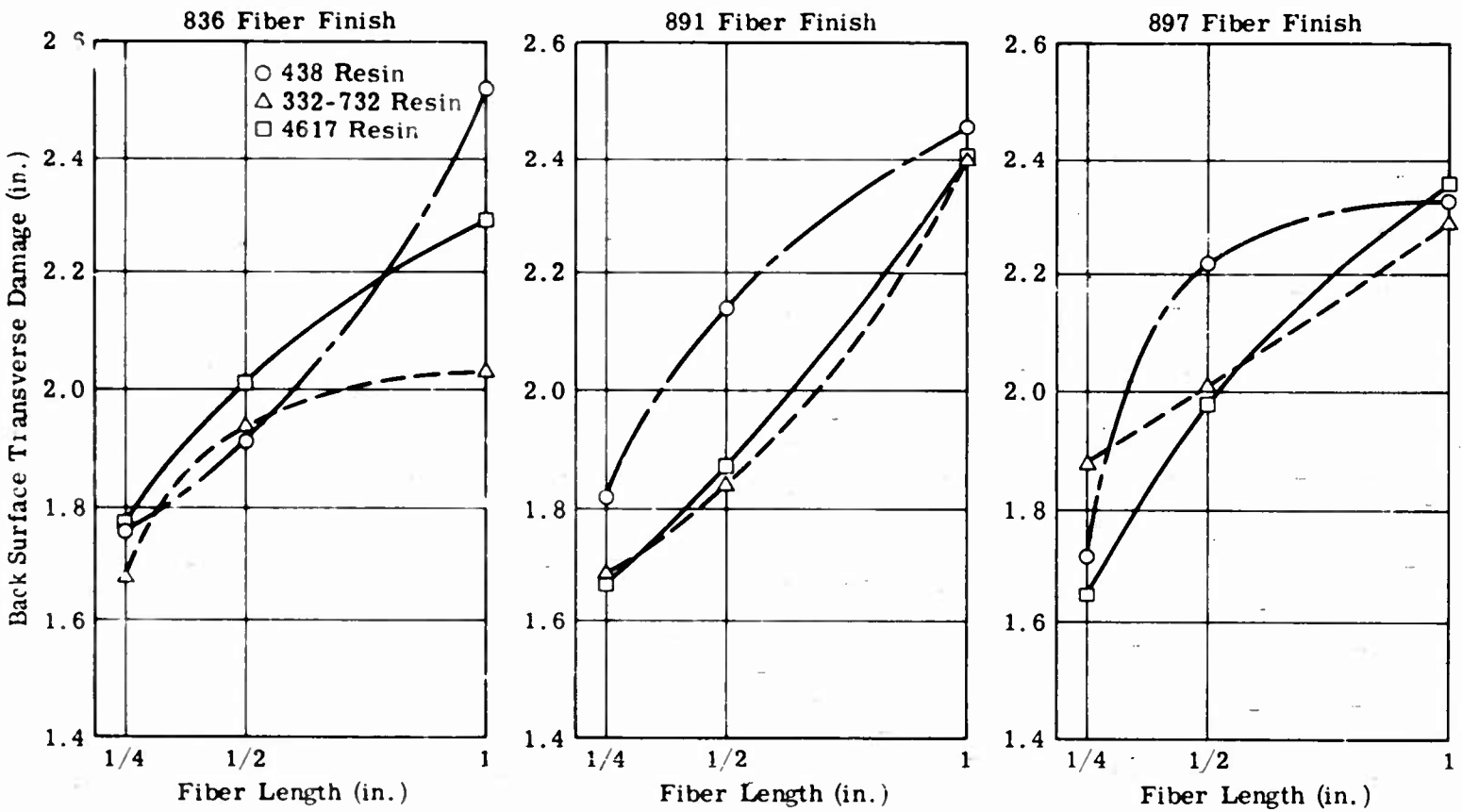

Figure 28. Relationship Between Back Surface Transverse Ballistic Damage and Fiber Length.

The average transverse damage values reported in Table 10 represent the mean of the front and back surface damage values. The effects of fiber length as well as resin type and fiber finish on average transverse damage are shown in Figure 27. The procedure employed for isolating the effects of these variables was identical with that previously described. The results indicate, as expected, that an increase in fiber length produces an increase in average transverse damage. This effect is less pronounced than observed from back surface transverse damage since the influence has been moderated by the front surface measurements. The average transverse damage was 1.86, 1.68, and 1.53 inches for 1-, 1/2-, and 1/4-inch composites, respectively, compared with a grand average of 1.688 inches. With regard to resin type and fiber finish, no significant trend was evident between these variables and average transverse damage.

Results of Tensile Tests on Ballistically Damaged Specimens

After ballistic damage assessment, the impacted specimens were subjected to tensile testing to determine their residual load capacities. A cell-form summary of average load capacities and computed strength-to-weight ratios based on individual specimen densities is presented in Table 11 for each of the 27 material combinations. A number of individual load capacity test values were excluded from the cell averages based on the rejection criteria described in "Test and Evaluation Techniques." The corresponding strength-to-weight ratios were also excluded from the calculation of the cell means.

The average residual load capacities are plotted in Figure 29 as a function of fiber length for each of the resin type and fiber finish combinations evaluated. It is obvious that residual load capacity increases significantly with increasing fiber length despite the fact that greater damage is experienced with the longer fibers. The highest value for post-damage load capacity, 9759 pounds, was obtained with 1-inch, 897-finished (epoxy/polyester-incompatible) fibers in a 332-732 resin matrix.

The curves for the 836-finished (epoxy-compatible) fibers indicate that the 4617 resin matrix produces superior results at all fiber lengths. The lowest residual load capacities with this fiber finish were associated with the 438 resin irrespective of fiber length. For composites reinforced with 897-finished fibers, the 332-732 resin produced the highest post-damage load capacities at all fiber lengths examined.

An alternate method for determining the effect of the experimental variables on the response is to average all available data for a particular

TABLE 11. SUMMARY OF POST-DAMAGE TENSILE PROPERTIES - SCREENING TEST PROGRAM

Type of Fiber Finish	1-Inch Fiber Length			1/2-Inch Fiber Length			1/4-Inch Fiber Length		
	Resin Type			Resin Type			Resin Type		
	438	332-732	4617	438	332-732	4617	438	332-732	4617
	A. Load Capacity (lb)[a]								
836	7464	8487	8667	5101[b]	5436	6955	3765[b]	4299	5449
891	7211[b]	8255[c]	8625[d]	4740[b]	6182	4967[b]	4217[d]	3724[b]	3961
897	8840[b]	9759[b]	7532[d]	5000[b]	5988	5355	3720[b]	4625	3511
	B. Strength-to-Weight Ratio (in. x 10^3)[a]								
836	243	276	276	161[b]	177	223	117[b]	139	173
891	229[b]	261[c]	276[d]	150[b]	192	156[b]	132[d]	112[b]	125
897	278[b]	318[b]	236[d]	156[b]	189	167	115[b]	145	109

[a] Data normalized to a 1/8-inch specimen thickness. Values are based on five replicates except as noted.

[b] Values are based on four replicates.

[c] Values are based on two replicates.

[d] Values are based on three replicates

variable level. For example, the influence of fiber length on residual load capacity can be established by averaging the cell values for specimens of a common fiber length (1, 1/2, or 1/4 inch). The effect of combinations of variables, such as resin type and fiber finish, can be determined in the same basic manner; i.e., average the residual load capacities for a particular resin type and fiber finish combination across all three fiber lengths.

The results of this alternate method are presented in bar-graph form in Figure 30. It is evident that fiber length has a powerful and direct effect on residual load capacity. The 1-inch fiber composites exhibited an average post-damage load capacity of 8318 pounds compared to a grand average of 5994.6 pounds. The average residual load capacities of 1/2- and 1/4-inch composites were 5525 and 4141 pounds, respectively. With respect to resin type effects, the results indicate that the composites with a 438 resin matrix exhibit below-average post-damage load capacities regardless of fiber finish. On the other hand, composites with a 332-732 resin matrix exhibited above-average residual load capacities.

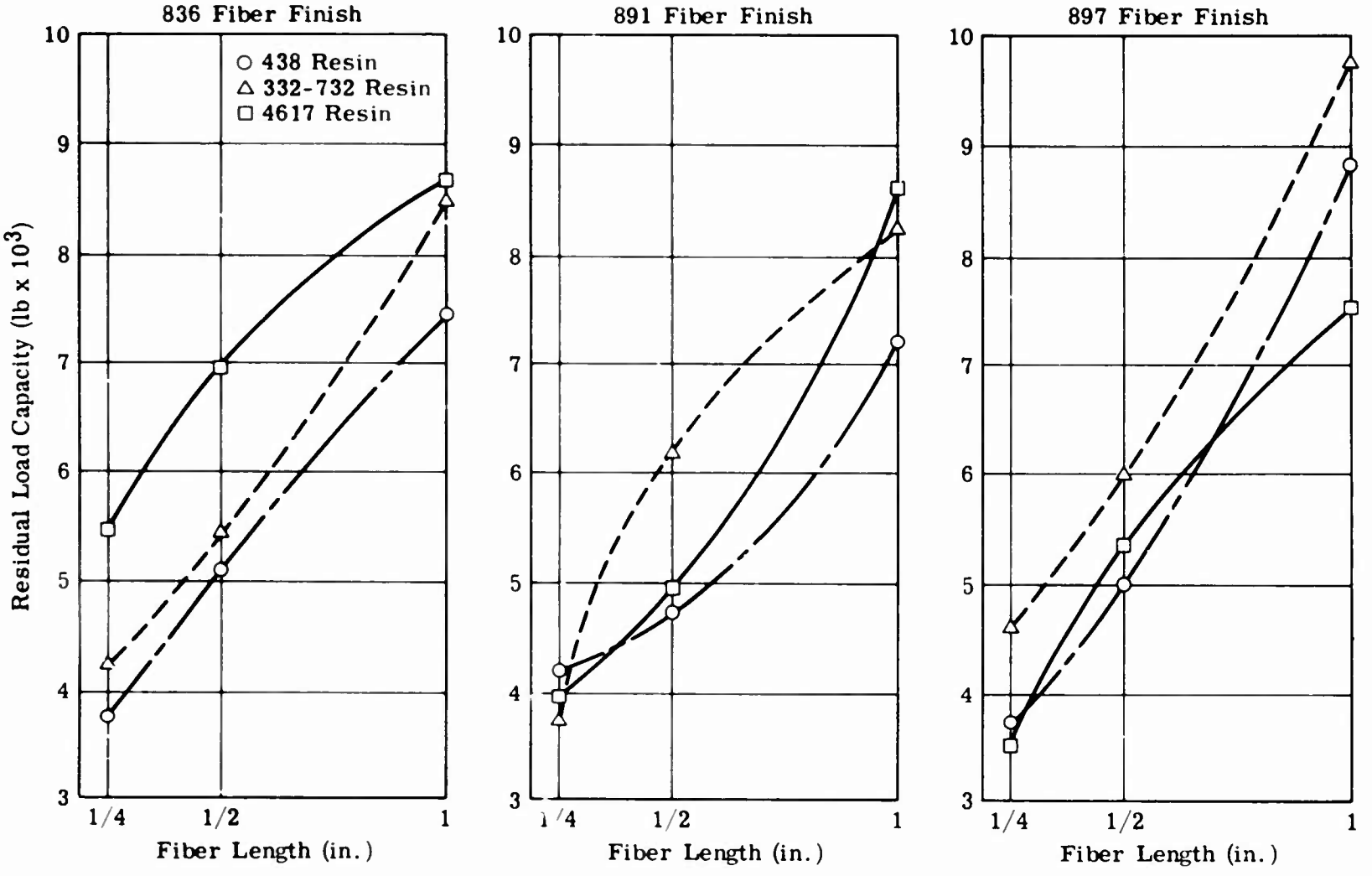

Figure 29. Relationship Between Post-Damage Tensile Properties (Load Capacity) and Fiber Length.

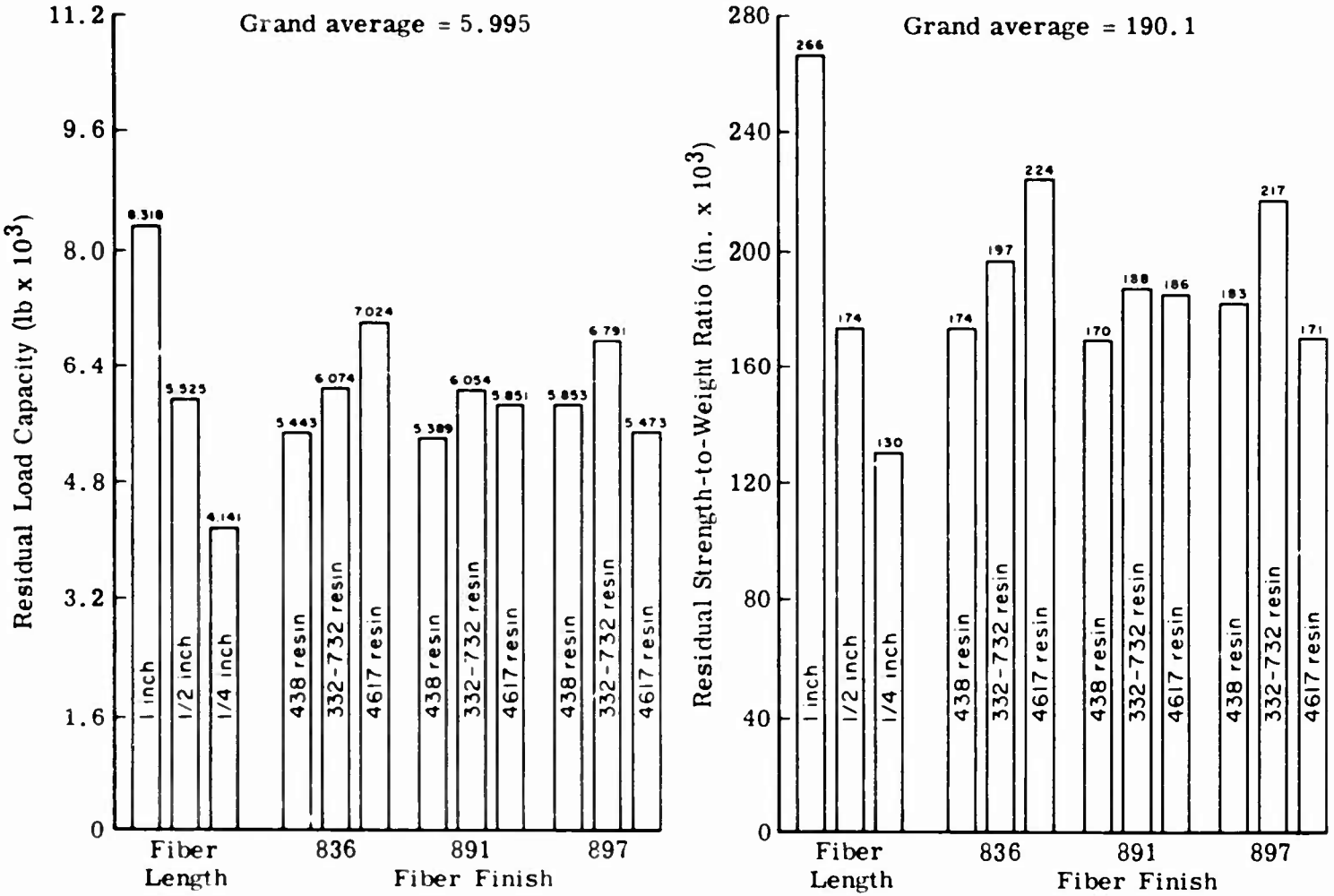

Figure 30. Effect of Material Parameters on Post-Damage Tensile Properties.

The results indicate that two resin type and fiber finish combinations are clearly superior to all others based on average residual load capcities across all fiber lengths. These two combinations, 836/4617 and 897/332-732, exhibited average post-damage load capacities of 7024 and 6791 pounds, respectively. The balance of the combinations exhibited near- or below-average residual load capacities.

The post-damage strength-to-weight ratio (breaking length) is an extremely important term that simultaneously appraises the strength advantage and weight penalty associated with each composite system. The breaking length represents the length of composite material with a 1/8-by-3.5-inch cross section that can be suspended below the damage zone before failure occurs. The breaking length is computed by dividing the residual load capacity by the specimen density.

A graphical presentation of residual strength-to-weight ratios as a function of fiber length is shown in Figure 31 for each of the nine resin type and fiber finish combinations evaluated. Because the density of the 332-732 resin blend is slightly lower than either of the other two candidate resins, the relative breaking lengths of composites with this resin matrix are generally improved. The highest residual strength-to-weight ratio, 318 x 10^3 inches, was obtained with the 897/332-732 composite reinforced with 1-inch fibers.

It is evident from the curves presented in Figure 31 that breaking length increases directly with fiber length in spite of the greater damage associated with longer fibers. It can also be seen that the composites with the 4617 resin matrix exhibit equivalent or higher breaking lengths in combination with 836-finished fibers than the corresponding composites with either 438 or 332-732 resins. Actually, the 836/438 composite has the lowest residual breaking length at all fiber lengths examined. Irrespective of fiber length, the 897-finished fiber composites with a 332-732 resin matrix are clearly superior from a strength-to-weight ratio standpoint than those with either 438 or 4617 resins.

The influence of the experimental variables on average residual breaking length is shown by the bar graphs in Figure 30. Fiber length has a strong and direct influence as evidenced by the fact that 1-inch fiber composites exhibited an average residual strength-to-weight ratio approximately twice that of 1/4-inch fiber composites. The average breaking lengths for composites with 1-, 1/2-, and 1/4-inch fibers were 266, 174, and 130 x 10^3 inches, respectively. The grand average breaking length across all 27 experimental cells was 190.1 x 10^3 inches.

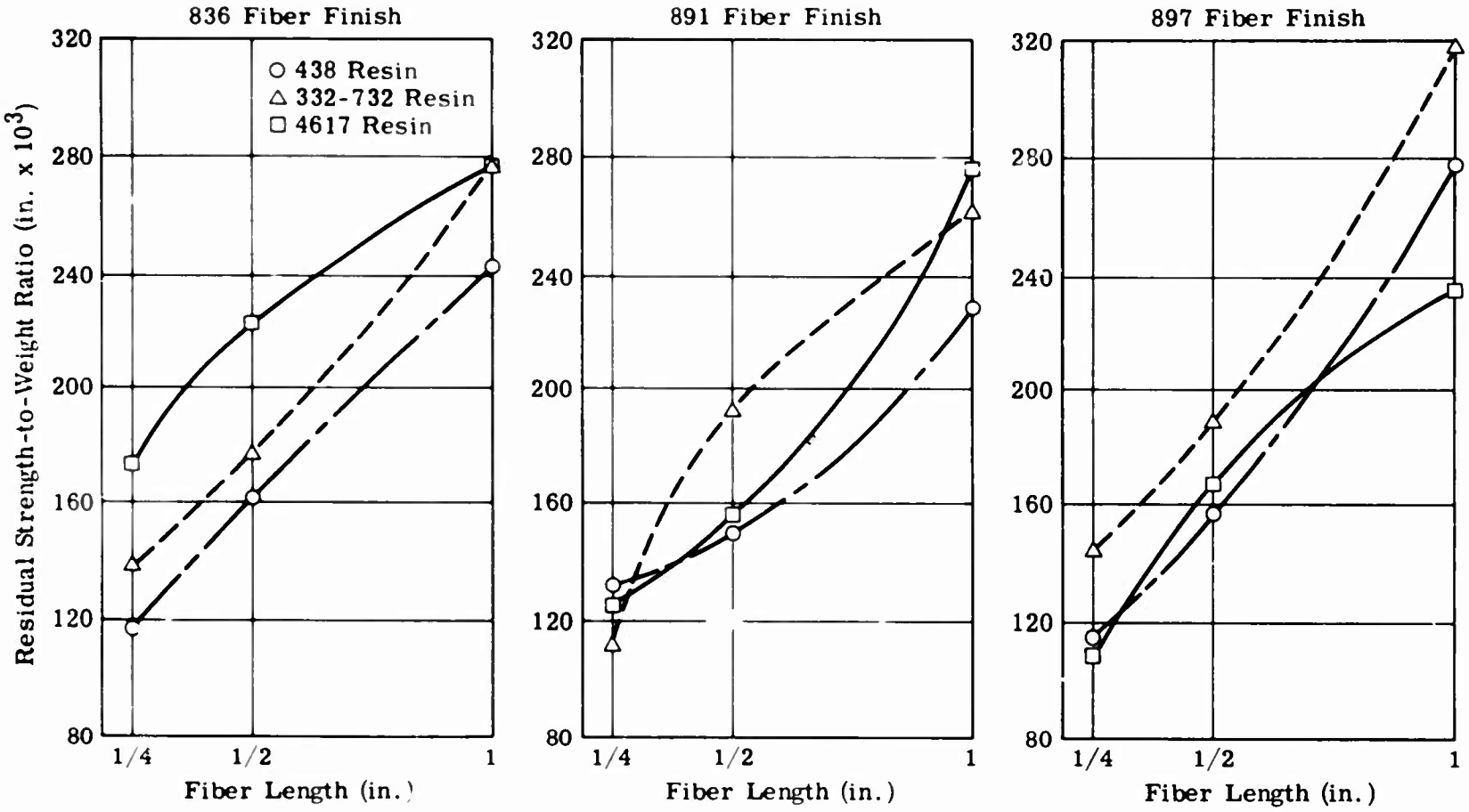

Figure 31. Relationship Between Post-Damage Tensile Properties (Strength-to-Weight Ratio) and Fiber Length.

The composites containing a 438 resin matrix exhibited average breaking lengths that were below the grand average regardless of fiber finish. Below-average performance was also exhibited by composites reinforced with 891-finished (polyester-compatible) fibers. The two resin type and fiber finish combinations that exhibited superior residual breaking lengths were 836/4617 and 897/332-732.

Conclusions and Recommendations

The results of the screening test program are presented in summary form in Table 12 to indicate the effect of the experimental variables (fiber length, resin type, and fiber finish) on each of the following parameters:

1. Undamaged Tensile Properties
   a. Ultimate Strength
   b. Initial Modulus

2. Extent of Ballistic Damage
   a. Area (Front and Back Surfaces)
   b. Volume
   c. Transverse (Front and Back Surfaces and Average)

3. Post-Damage Tensile Properties
   a. Load Capacity
   b. Strength-to-Weight Ratio

The effect of fiber length on each parameter was determined by averaging the response values for each particular fiber length across all resin types and fiber finishes. Because of interaction between resin and fiber finish, the average results across the three fiber lengths are reported for each of the nine resin type and fiber finish combinations.

The following criteria were employed in establishing the significance of the test results:

1. Values within ±5 percent of the grand average are not significant. These values are represented by 0 in Table 12.

2. Values that vary by 5 to 15 percent from the grand average are significant. These values are represented by + or -, depending on whether the effect is beneficial (+) or adverse (-). Where undamaged or damaged tensile properties are concerned, the + is always used with above-average values. When damage parameters are involved, the + is used to represent less-than-average damage.

TABLE 12. EFFECT OF EXPERIMENTAL VARIABLES ON UNDAMAGED AND BALLISTICALLY DAMAGED COMPOSITES - SCREENING TEST PROGRAM

	Fiber Length (in.)			Fiber Finish and Resin Type								
				836			891			897		
	1	1/2	1/4	438	332-732	4617	438	332-732	4617	438	332-732	4617
Ultimate Tensile Strength (Undamaged)	++	-	-	+	+	++	0	-	-	0	+	--
Initial Tensile Modulus (Undamaged)	0	0	0	-	--	++	-	-	+	0	0	++
Front Surface Ballistic Damage Area	-	0	+	0	+	0	--	+	++	-	-	0
Back Surface Ballistic Damage Area	--	+	++	0	++	+	-	0	+	-	0	0
Ballistic Damage Volume	--	0	++	0	+	0	-	0	+	-	0	0
Front Surface Transverse Ballistic Damage	0	0	0	0	0	0	-	+	0	-	0	0
Back Surface Transverse Ballistic Damage	--	0	+	0	+	0	-	0	0	0	0	0
Avg Front/Back Surface Transverse Ballistic Damage	-	0	+	0	+	0	-	0	0	0	0	0
Residual Load Capacity	++	-	--	-	0	++	-	0	0	0	+	-
Strength-to-Weight Ratio	++	-	--	-	0	++	-	0	0	0	+	-

Sym	Value (%)	Sym	Value (%)	Sym	Value (%)
--	>-15	0	±5	+	+5 to +15
-	-5 to -15			++	>+15

3. Values that differ by more than 15 percent from the average are considered highly significant. The values are represented by ++ or --, depending on whether the resultant effect was beneficial (++) or adverse (--).

In discussing the summary data in Table 12, the effect of either resin type or fiber finish will be reported as significant if a trend is observed across all experimental levels of the other variable. For example, above-average ultimate tensile strength (undamaged) was exhibited by composites with 836-finished (epoxy-compatible) fibers irrespective of resin type. Consequently, the 836 fiber finish has a significant effect on undamaged tensile strength. If a consistent trend in response is evident at two experimental levels and a neutral effect is observed at the third level, then the effect of the variable will be noted, but on a more restrained basis.

The conclusions drawn from the data in Table 12 are summarized below for each parameter investigated.

1. Ultimate Tensile Strength (Undamaged)

   a. Strength increases significantly with increasing fiber length.

   b. The 836-finished (epoxy-compatible) fibers contribute to significantly higher strength.

   c. The 891-finished (polyester-compatible) fibers produce near- or below-average strength.

   d. No consistent trend was apparent relative to the effects of resin type on strength.

   e. The highest average strength was exhibited by the 836/4617 composites.

   f. The lowest strength values were obtained with the 897/4617 composites.

2. Initial Tensile Modulus (Undamaged)

   a. Fiber length has a negligible effect on tensile modulus.

   b. Fiber finish has some effect on modulus.

   c. Composites with the high-modulus 4617 resin matrix exhibit values that are significantly higher than the grand average.

d. Composites with either a 438 or a 332-732 matrix provide near- or below-average modulus values.

3. Front Surface Ballistic Damage Area

a. Damage decreases signficantly with decreasing fiber length.

b. Composites with the 897 (epoxy/polyester-incompatible) fiber finish experience near- or above-average damage.

c. The 438 resin matrix contributes to near- or above-average damage. The most significant damage was experienced with this resin in combination with the 891 (polyester-compatible) fiber finish.

d. The 891/4617 composites exhibited less damage, on the average, than any of the other resin type and fiber finish combinations.

4. Back Surface Ballistic Damage Area

a. Fiber length has a highly significant effect on the back surface damage area. Damage decreases indirectly with fiber length.

b. Composites reinforced with 836-finished fibers show near- or less-than-average visual damage.

c. Composites with a 4617 resin matrix experience near- or below-average back surface damage.

d. The 438 resin matrix contributes to near- or above-average damage.

e. The smallest back surface area damage was experienced, on the average, with the 836/332-732 composites.

5. Ballistic Damage Volume

a. The effect of fiber length on damage volume is highly significant. A decrease in fiber length results in reduced damage volume.

b. The fiber finish has an insignificant effect on damage.

c. Composites with a 438 resin matrix experience near- or above-average damage volumes.

6. Front Surface Transverse Ballistic Damage

a. The effects of fiber length and finish are negligible.

b. Composites with a 438 resin matrix sustain near- or above-average front surface transverse damage.

7. Back Surface Transverse Ballistic Damage

a. Damage decreases significantly with decreasing fiber length.

b. The fiber finish and resin type have negligible effects on back surface transverse damage.

8. Average Front/Back Surface Transverse Ballistic Damage

a. Fiber length has a significant inverse effect on transverse damage.

b. The effects of fiber finish and resin type are insignificant.

9. Residual Load Capacity (Post-Damage)

a. Fiber length has a highly significant and direct effect on residual load capacity.

b. Fiber finish does not have a significant effect on load capacity.

c. Composites with a 438 resin matrix evidence near- or below-average post-damage load capacity.

d. The highest load capacity values were obtained, on the average, with 836/4617 composites.

10. Strength-to-Weight Ratio (Post-Damage)

a. As fiber length increases, a highly significant increase in strength-to-weight ratio results.

b. Fiber finish has a negligible effect on breaking length.

c. The composites with a 438 resin matrix exhibited near- or below-average residual strength-to-weight ratios.

d. The highest post-damage breaking lengths were achieved, on the average, with the 836/4617 composites.

It is evident from the data summary in Table 12 that composites with 1-inch fibers exhibit significantly higher undamaged tensile strengths than those with shorter fibers. Furthermore, the residual properties of 1-inch fiber composites are superior to those with 1/2- and 1/4-inch fibers despite the fact that ballistic damage is greater for the longer fibers.

With respect to resin type and fiber finish combinations, the residual tensile properties in a number of instances conform to the expected result based on undamaged strength and extent of visual damage. For example, the 891/438 composites exhibited average undamaged tensile strength but greater than average ballistic damage. Consequently, the residual properties, as anticipated, were below average. However, several cases are evident where the response was unexpected based on undamaged strength and extent of damage. The 836/438 composites, for instance, exhibited below-average residual properties in spite of the fact that the undamaged strength was high and the damage nominal. Therefore, visual damage per se is not a totally reliable criterion on which to judge the post-damage properties of discontinuous fiber-epoxy composites.

The 836/4617 and 897/332-732 composites exhibited residual tensile properties that were significantly higher than any of the other resin type and fiber finish combinations evaluated. The net molded, 3.5-inch-wide specimens produced with the 897/332-732 composites with 1-inch fibers yielded the highest residual load capacity (9759 pounds) and strength-to-weight ratio (318×10^3 inches).

It can also be concluded from the screening test program that the high frequency of transition section failures experienced, particularly with longer fibers, constitutes a potentially serious production problem. This arises from the fact that production flight control components will probably contain transition sections that are more severe than the 7-degree taper in the standard 3.5-inch-wide test specimen.

It is recommended that a program be undertaken to identify the causes for the high incidence of end failures and to develop a practical means for their elimination that is applicable to the production of control components.

It is also recommended that the 836/4617 and 897/332-732 composite systems (particularly the 897/332-732 composite with 1-inch fibers), which exhibited such outstanding residual tensile properties, be given serious consideration when selecting the three most promising materials for more extensive evaluation in Task II.

SUBTASK 2 - FIBER DIAMETER EFFECTS PROGRAM

General

Essentially all fiber glass roving currently manufactured for molding compound application is produced with K filaments (0.00050 to 0.00055 inch in diameter). Only a small percentage is made from the smaller G filaments (0.00035 to 0.00040 inch in diameter). The trend toward larger diameter fibers began in the sixties, primarily for economic reasons. Although some divergence of opinion still exists, it is generally agreed that the structural properties of composites prepared from the larger diameter fibers are equivalent or marginally superior to those reinforced with smaller diameter fibers. However, no data currently exist on the effect of fiber diameter on the ballistic response of reinforced plastic composites.

The goal of this investigation, therefore, was to determine the influence of fiber diameter on undamaged and damaged tensile strength as well as the physical size of the ballistic damage.

Approach to the Problem

The initial screening test program described in Subtask 1 involved K diameter fibers in roving form with three fiber finishes having varying degrees of compatibility with epoxy resins. In the fiber diameter effects study, the plan was to evaluate G diameter fibers that were identical in finish and form with a previously evaluated material. Unfortunately, roving with G diameter fibers that had such a finish was not commercially available. Consequently, it was necessary to identify a finish that was as nearly similar as possible to one of the finishes evaluated on K diameter fibers. An epoxy/polyester-incompatible finish (P683C), which is chemically similar to the 897 finish previously tested, was finally selected for investigation.

The P683C-finished fiber glass roving was evaluated in the three material combinations (resin type and fiber length) at which the 897 finish had been examined. These test combinations were selected because of the low susceptibility of the 897-finished fiber glass composites to transition section failure. This would permit direct comparisons between G diameter and K diameter fiber-reinforced specimens with respect to undamaged tensile properties as well as the loss in load capacity due to ballistic damage. The following choices were obvious since all specimens reinforced with 897-finished fibers failed in the center section:

1. 332-732 epoxy resin, 1/4-inch fiber length
2. 438 epoxy resin, 1/4-inch fiber length
3. 438 epoxy resin, 1/2-inch fiber length

All composites would have a nominal fiber content of 60 v/o.

The test plan for evaluating the G diameter fibers was identical with that conducted with K diameter fibers. This plan involved the measurement of undamaged tensile properties (strength and modulus), extent of ballistic damage, and residual tensile load capacity. The specimens would be preloaded to 35 percent of the undamaged tensile strength during ballistic testing with fully tumbled caliber .30 ball M2 projectiles at 0-degree obliquity and 1800 ft/sec nominal impact velocity.

Discussion of Results

The average thickness, density, and fiber content of the composites reinforced with P683C-finished E glass are given in Table 13. These values represent the average of eight specimens fabricated at each of the three material combinations.

TABLE 13. TEST SPECIMEN MEASUREMENTS - COMPOSITES REINFORCED WITH P683C-FINISHED E GLASS

Resin Type	Fiber Length (in.)	Thickness (in.)	Density ($lb/in.^3$)	Fiber Content (v/o)
332-732	1/4	0.126	0.068	55.0
438	1/4	0.129	0.069	54.5
438	1/2	0.126	0.070	56.8

The average fiber content of the specimens reinforced with G/P683C fibers was consistently lower than the corresponding specimens reinforced with K/897 fibers. The actual differences in fiber content for the 897/438 composites ranged from 1.8 v/o for the 1/2-inch fibers to 7.7 v/o for the 1/4-inch fibers. Consequently, the densities of the P683C specimens are lower than those of the corresponding 897 specimens.

The comparative undamaged tensile strengths measured on three replicates each with G and K diameter fibers are summarized in Table 14. All G diameter fiber specimens failed in the transition section, whereas the K diameter fiber specimens exhibited center failures. Therefore, the effect of fiber diameter on undamaged strength cannot be established from the experimental data.

TABLE 14. ULTIMATE TENSILE STRENGTH OF UNDAMAGED SPECIMENS REINFORCED WITH G/P683C AND K/897 FIBERS

Resin Type	Fiber Length (in.)	Avg Tensile Strength (psi)	
		G/P683C	K/897
332-732	1/4	13,540	17,030
438	1/4	12,500	15,290
438	1/2	12,540	17,320

The tensile modulus values given in Table 15 for the G/P683C specimens were computed from the initial slopes of stress-strain curves generated during undamaged specimen testing. The modulus data for the K/897 specimens are presented for comparison. The strain measurements were obtained from an extensometer (2-inch gage length) attached in the gage area of the specimen.

The reported tensile moduli of the K/897 specimens reinforced with 1/4-inch fibers are significantly higher than those of the corresponding G/P683C specimens. This relative behavior was expected, however, because of the 5.9 to 7.7 v/o greater fiber loading in the K/897 specimens. Actually, no significant difference in modulus was anticipated due to fiber diameter effects. For the specimens with 438 resin and 1/2-inch fibers, where the fiber contents of G/P683C and K/897 were similar (56.8 and 58.6 v/o, respectively), the tensile modulus values were essentially identical.

TABLE 15. TENSILE MODULUS OF UNDAMAGED SPECIMENS REINFORCED WITH G/P683C AND K/897 FIBERS

Resin Type	Fiber Length (in.)	Avg Tensile Modulus (psi x 10^6)	
		G/P683C	K/897
332-732	1/4	3.10	3.41
438	1/4	3.19	3.94
438	1/2	3.42	3.38

Typical ballistic damage sustained by specimens of the three composites reinforced with G/P683C fibers is shown photographically in Figure 32 for the front and back surfaces. Area and volume damage data are summarized in Table 16 along with comparative K/897 data. The results depicted by the bar graphs in Figure 33 indicate that the G/P683C-reinforced composites exhibit significantly less area and volume damage at two material combinations than the corresponding K/897-reinforced composites. With the other material combination, i.e., the 438 resin and the 1/4-inch fiber length, the difference in ballistic damage for the two fiber diameters is relatively small.

TABLE 16. SUMMARY OF VISUAL BALLISTIC DAMAGE - COMPOSITES REINFORCED WITH G/P683C AND K/897 FIBERS

Resin Type	Fiber Length (in.)	Fiber Type	Ballistic Damage[a]		
			Front Area ($in.^2$)	Back Area ($in.^2$)	Volume ($in.^3$)
332-732	1/4	G/P683C	0.71	1.59	0.142
		K/897	0.91	1.83	0.165
438	1/4	G/P683C	0.81	1.50	0.148
		K/897	0.76	1.53	0.139
438	1/2	G/P683C	0.92[b]	2.46[b]	0.208[b]
		K/897	1.30	3.00	0.256

[a]Values are based on five replicates except as noted.
[b]Values are based on four replicates.

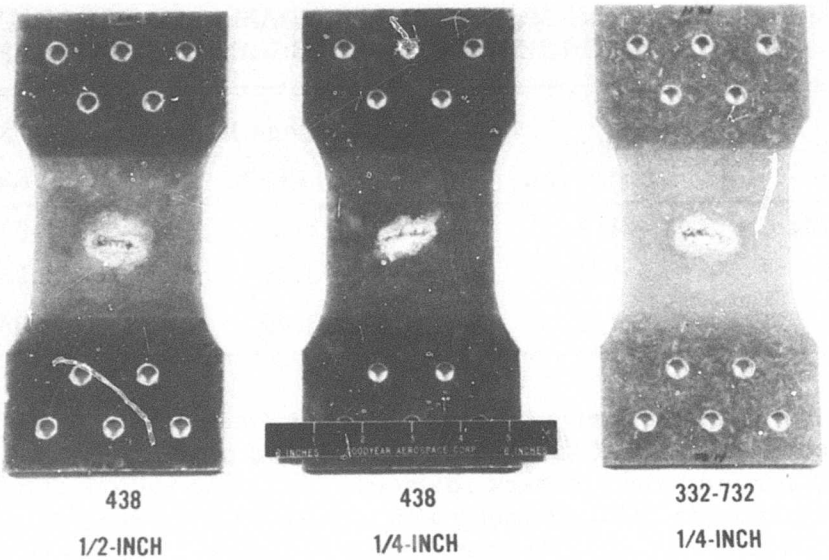

A. Front Surface

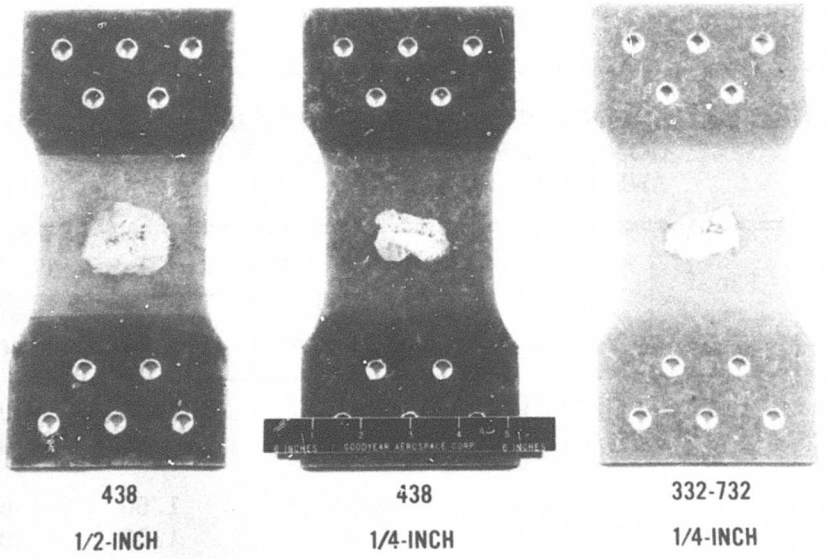

B. Back Surface

Figure 32. Typical Front and Back Surface Ballistic Damage - Specimens Reinforced With G/P683C Fibers.

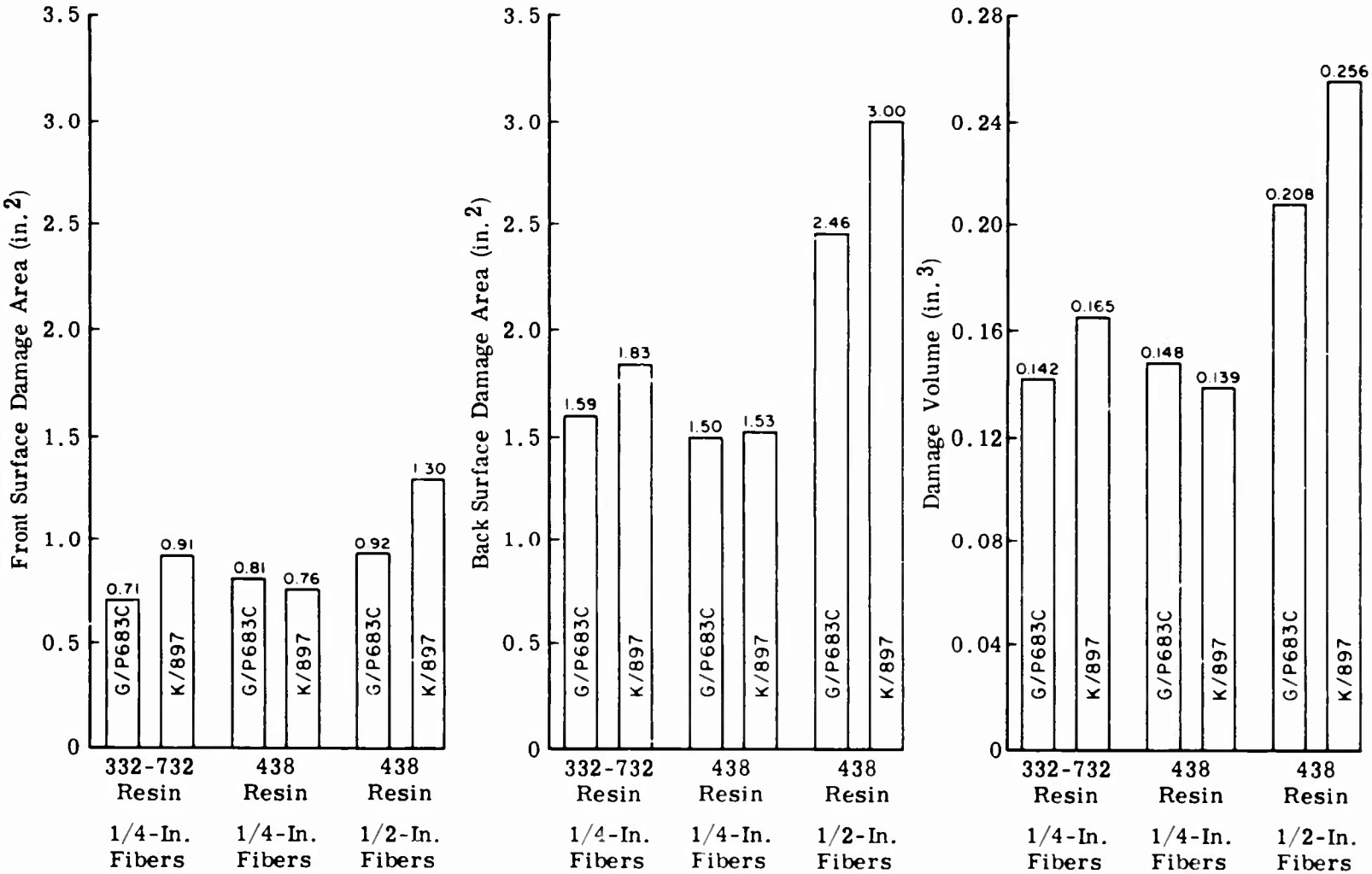

Figure 33. Comparison of Ballistic Damage Areas and Volume - Composites Reinforced With G/P683C and K/897 Fibers.

The front, back, and average transverse damage data resulting from ballistic impacts on 3.5-inch-wide specimens reinforced with either G/P683C or K/897 fibers are summarized in Table 17. These data are also presented in bar-graph form in Figure 34. These results indicate that both the back surface and average (front and back) transverse damage are significantly greater for the K/897-reinforced composites than for the corresponding G/P683C-reinforced composites. With respect to the front surface, the K/897-reinforced composites experienced substantially more damage than the G/P683C-reinforced composites in two of the three systems tested. Only with the 438 resin and 1/4-fiber material combination did the G/P683C composites exhibit slightly greater transverse damage. Based on these results, it is reasonable to conclude that composites with larger diameter (K) fibers are more vulnerable to transverse damage than corresponding composites with smaller diameter (G) fibers.

Post-damage tensile property data for the G/P683C composites are summarized in Table 18 along with comparative information for the corresponding K/897 composites. A bar-graph presentation of these data is

TABLE 17. SUMMARY OF VISUAL TRANSVERSE BALLISTIC DAMAGE - COMPOSITES REINFORCED WITH G/P683C AND K/897 FIBERS

Resin Type	Fiber Length (in.)	Fiber Type	Transverse Ballistic Damage (in.)[a]		
			Front Surface	Rear Surface	Avg
332-732	1/4	G/P683C	1.26[b]	1.65[b]	1.46[b]
		K/897	1.44	1.87	1.66
438	1/4	G/P683C	1.38[b]	1.54[b]	1.46[b]
		K/897	1.30[b]	1.72[b]	1.51[b]
438	1/2	G/P683C	1.30[c]	2.01[c]	1.65[c]
		K/897	1.61	2.21	1.92

[a]Values are based on five replicates except as noted.

[b]Values are based on four replicates.

[c]Values are based on three replicates.

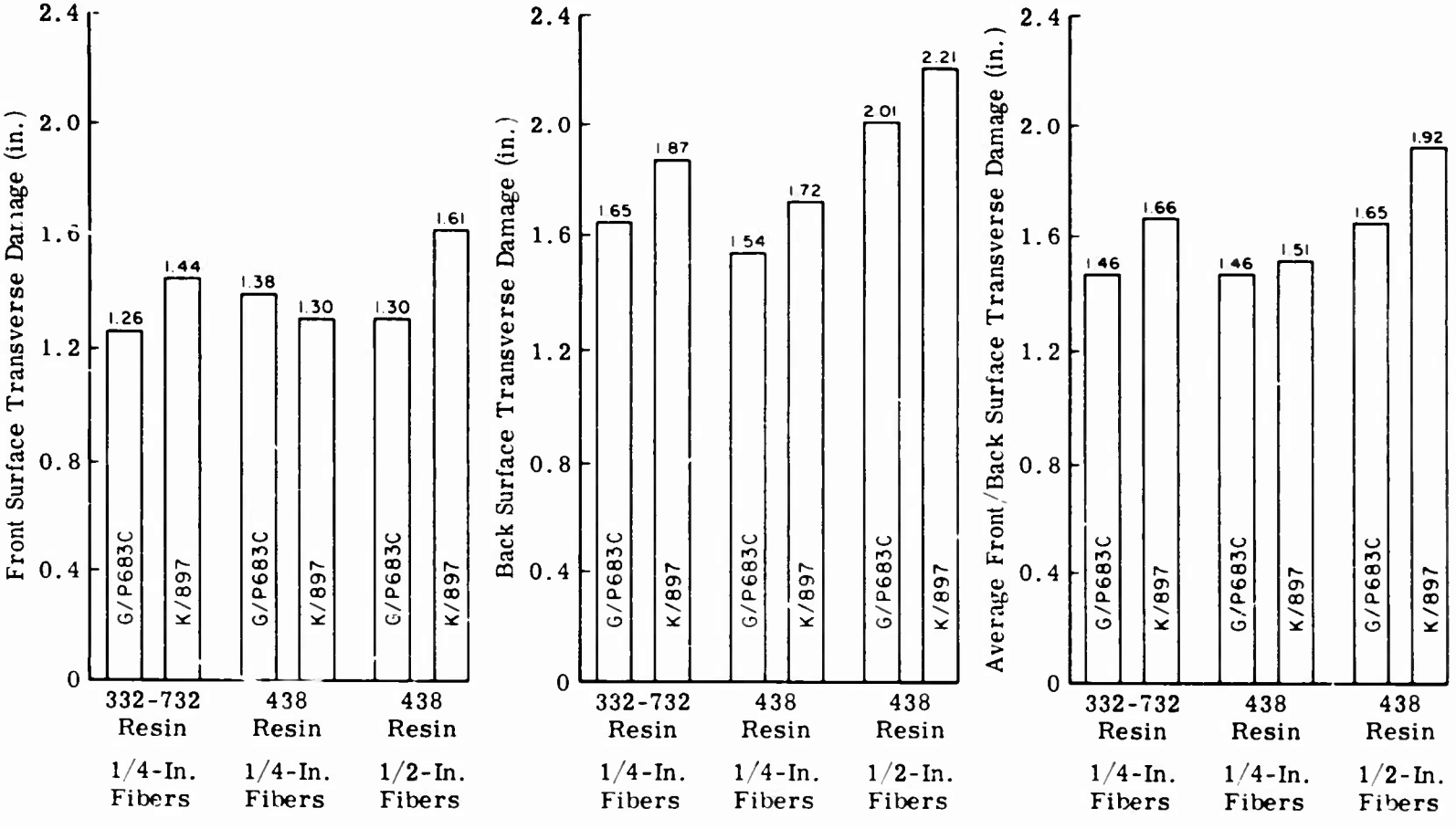

Figure 34. Comparison of Transverse Ballistic Damage - Composites Reinforced With G/P683C and K/897 Fibers.

TABLE 18. SUMMARY OF POST-DAMAGE TENSILE PROPERTIES - COMPOSITES REINFORCED WITH G/P683C AND K/897 FIBERS

Resin Type	Fiber Length (in.)	Fiber Type	Post-Damage Tensile Properties[a]	
			Load Capacity (lb)	Strength-to-Weight Ratio (in. x 10^3)
332-732	1/4	G/P683C	3920[b]	128[b]
		K/897	4625	145
438	1/4	G/P683C	3510[b]	113[b]
		K/897	3720[b]	115[b]
438	1/2	G/P683C	4690[c]	149[c]
		K/897	5000[b]	157[b]

[a] Data normalized to a 1/8-inch specimen thickness. Values are based on five replicates except as noted.

[b] Values are based on four replicates.

[c] Values are based on two replicates.

given in Figure 35. It is evident that 3.5-inch-wide specimens with K/897 fibers exhibit greater residual load capacities and strength-to-weight ratios than G/P683C-reinforced specimens in all material combinations evaluated. Since K/897 specimens generally exhibit higher residual strength despite greater damage, this suggests that the undamaged strength of the K/897 composites is greater than that of the corresponding G/P683C composites.

Conclusions and Recommendations

The following conclusions can be drawn from the results of the fiber diameter effects program:

1. The undamaged tensile strengths of composites reinforced with larger diameter (K) fibers is probably greater than those with smaller diameter (G) fibers.

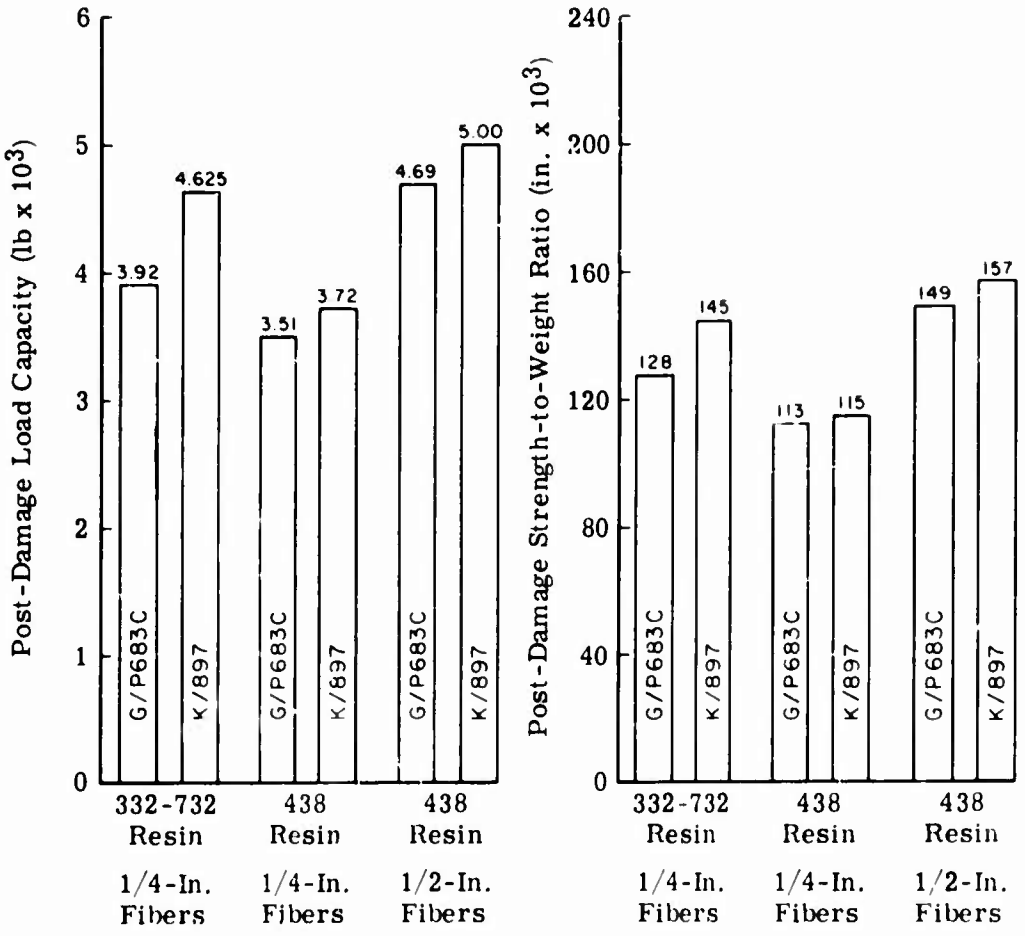

Figure 35. Comparison of Post-Damage Tensile Properties - Composites Reinforced With G/P683C and K/897 Fibers.

2. Composites with G diameter fibers generally exhibit less area, volume, and transverse damage from ballistic impact than corresponding composites with larger diameter fibers.

3. The residual tensile properties, i.e., load capacity and strength-to-weight ratio, of K/897 composites are superior to those of corresponding G/P683C composites.

Based on the results of this investigation, it is recommended that no further consideration be given to the use of G diameter fibers of E glass as the reinforcement in composites intended for ballistically tolerant component application.

SUBTASK 3 - FIBER STRENGTH EFFECTS PROGRAM

General

The purpose of this investigation was to establish the effect of fiber glass filament strength on the undamaged and damaged properties of net compression molded composite test specimens. The high-strength reinforcement selected for evaluation was S-2 glass with a 470 (epoxy-compatible) finish. This material was procured in the form of a 20-end roving. Each end of this commercially available product contains 204 G filaments (0.00035 to 0.00040 inch in diameter). A pound of S-2 glass yields 750 yards of roving. The S-2 glass was chosen rather than S glass because of a significant cost advantage. Actually, the materials are identical in composition, differing only in the finish employed. S-2 glass reportedly exhibits only marginally lower structural properties than S glass. The performance of composites with the high-strength glass reinforcement will be compared with the previously generated data on E glass with an 836 (epoxy-compatible) finish.

The tensile strength of S-2 glass filaments is approximately 33 percent higher than that of E glass filaments. In addition, S-2 glass exhibits an 18 percent higher tensile modulus and 2 percent lower density than E glass.

Approach to the Problem

The fiber strength effect on undamaged and damaged properties was established from an evaluation of S-2 and E glass reinforcements at three common material combination levels. The specific material combinations (resin type and fiber length) were selected on the basis of the low susceptibility of undamaged E glass (836 finish) specimens to transition section failure in the screening test program. Of the nine resin type and fiber length combinations previously evaluated with 836-finished E glass, six combinations exhibited at least 67 percent end failures. The following three combinations that produced a low frequency of transition section failures were chosen for investigation:

1. 438 epoxy resin, 1/4-inch fiber length
2. 438 epoxy resin, 1/2-inch fiber length
3. 332-732 epoxy resin, 1/4-inch fiber length

The nominal fiber content of the molded specimens was established at 60 v/o so that the resultant undamaged and damaged properties could be directly compared to existing data.

Ultimate tensile testing was performed on three replicates of undamaged specimens at each material combination. Five specimens of each combination were then subjected to ballistic impacts with fully tumbled caliber .30 ball M2 projectiles at 0-degree obliquity and a nominal velocity of 1800 ft/sec. During testing, the specimens were preloaded to 35 percent of the average ultimate tensile strength of undamaged specimens measured at room temperature. After impact, the extent of area, volume, and transverse damage was measured. The residual load capacity of the damaged specimens was then determined at room temperature.

Discussion of Results

The thickness, density, and fiber content of the composites reinforced with 470-finished S-2 glass are given in Table 19. The values represent the average of eight specimens produced at each of the three material combinations.

TABLE 19. TEST SPECIMEN MEASUREMENTS - COMPOSITIES REINFORCED WITH 470-FINISHED S-2 GLASS

Resin Type	Fiber Length (in.)	Thickness (in.)	Density ($lb/in.^3$)	Fiber Content (v/o)
332-732	1/4	0.126	0.067	58.0
438	1/4	0.126	0.068	57.1
438	1/2	0.126	0.069	58.7

The undamaged tensile strengths of the S-2 and E glass specimens are summarized in Table 20. Since all S-2 glass specimens failed in the transition section, no absolute strength comparison with E glass specimen data is possible. However, despite transition section failures, the S-2 glass specimens exhibited higher strength values in two of the three material combinations examined.

TABLE 20. ULTIMATE TENSILE STRENGTH OF UNDAMAGED SPECIMENS REINFORCED WITH S-2 AND E GLASS

Resin Type	Fiber Length (in)	Avg Tensile Strength (psi)	
		S-2 Glass/470	E Glass/836
332-732	1/4	17, 130*	16, 390
438	1/4	17, 830*	13, 650
438	1/2	19, 100*	20, 650

* All transition area failures

During undamaged ultimate tensile testing, an extensometer (2-inch gage length) was mounted on the S-2 glass specimens to obtain a stress-strain curve. The tensile modulus values presented in Table 21 were computed from the initial slopes of the curves. Modulus data previously measured and reported on E glass composites of similar construction (resin type and fiber length) are also presented for comparison. The modulus values for the S-2 glass composites as well as the 1/4-inch fibers of E glass in a 332-732 resin matrix are based on averages of three replicates each. The moduli for the 1/4- and 1/2-inch fibers of E glass in a 438 resin matrix are values measured on only one specimen of each type. Because of the limited data on the latter two systems, comparisons with modulus values of corresponding S-2 glass composites are not considered appropriate. For 1/4-inch fibers of S-2 and E glass in a 332-732 resin matrix, the reported values indicate that the S-2 glass composites exhibit a significantly higher tensile modulus (3.70×10^6 psi versus 3.07×10^6 psi). This relative performance was anticipated because of the higher modulus of the S-2 glass fibers.

TABLE 21. TENSILE MODULUS OF UNDAMAGED SPECIMENS REINFORCED WITH S-2 AND E GLASS

Resin Type	Fiber Length (in.)	Avg Tensile Modulus (psi x 10^6)	
		S-2 Glass/470	E Glass/836
332-732	1/4	3.70	3.07
438	1/4	3.66	4.04
438	1/2	3.97	3.33

A summary of area and volume ballistic damage sustained by the composites reinforced with S-2 and E glass is given in Table 22. A bar-graph comparison of ballistic damage at the three material combination levels is presented in Figure 36. Typical front and back surface ballistic damage to the specimens reinforced with S-2 glass is shown photographically in Figure 37. From an area standpoint, the data indicate that the S-2 glass composites experience equivalent or less front surface damage than the corresponding E glass composites. No definite trend was observed at all three material combinations examined that indicated either the S-2 or the E glass composite consistently exhibiting greater volume or back surface area damage. Differences in volume damage between the fiber glass types were, in fact, relatively small at each of the three material combination levels.

TABLE 22. SUMMARY OF VISUAL BALLISTIC DAMAGE -- COMPOSITES REINFORCED WITH S-2 AND E GLASS

Resin Type	Fiber Length (in.)	Fiber Type	Ballistic Damage[a]		
			Front Area ($in.^2$)	Back Area ($in.^2$)	Volume ($in.^3$)
332-732	1/4	S-2/470	0.69	1.68	0.146
		E/836	0.83	1.46	0.147
438	1/4	S-2/470	0.69[b]	1.58[b]	0.141[b]
		E/836	0.83	1.56	0.143
438	1/2	S-2/470	0.95	2.62	0.221
		E/836	0.95	2.21	0.189

[a] Values are based on five replicates except as noted.

[b] Values are based on four replicates.

The front, back, and average transverse damage exhibited by the S-2 and E glass composites is presented in Table 23. The results shown in bar-graph form in Figure 38 indicate that only minor differences exist in transverse damage between the fiber glass types at each material combination examined.

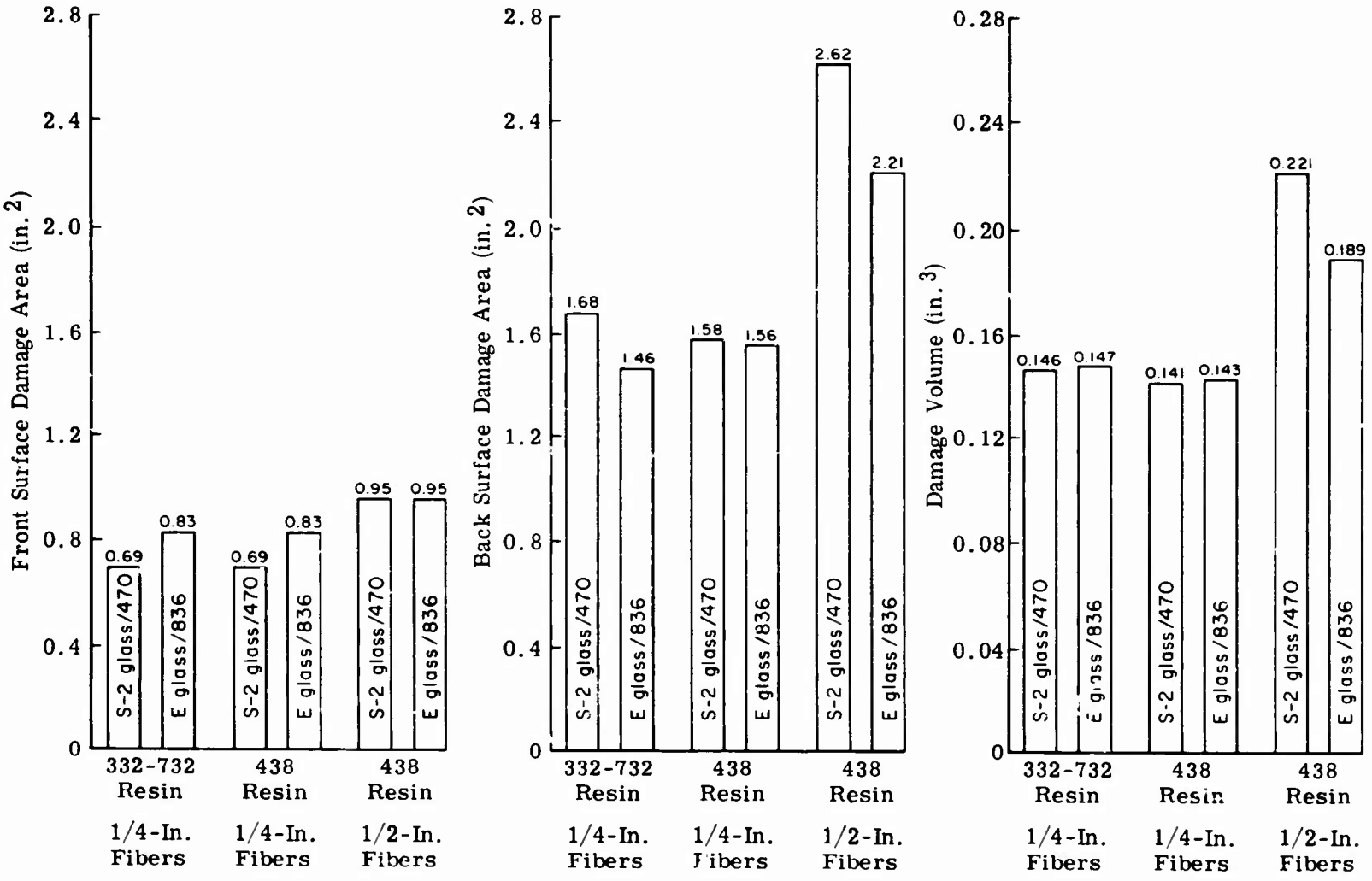

Figure 36. Comparison of Ballistic Damage Areas and Volume - Composites Reinforced With S-2 and E Glass.

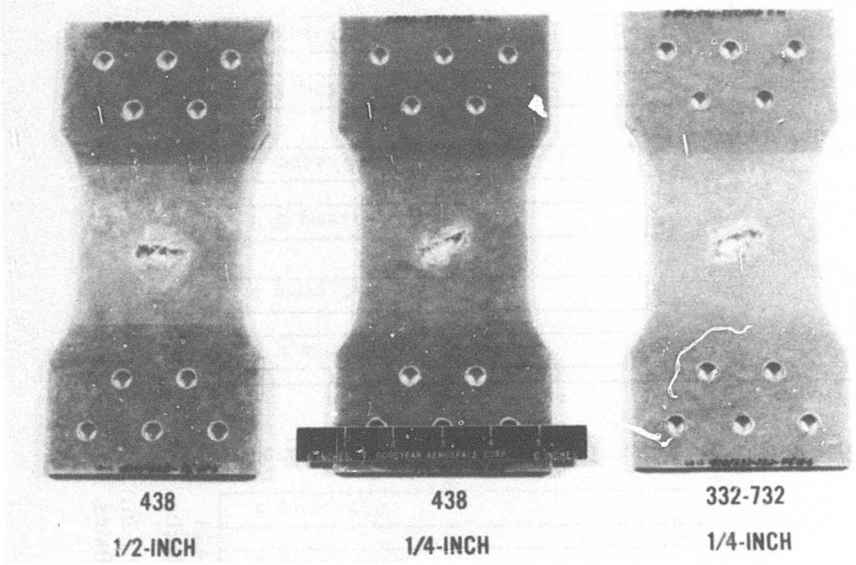

A. Front Surface

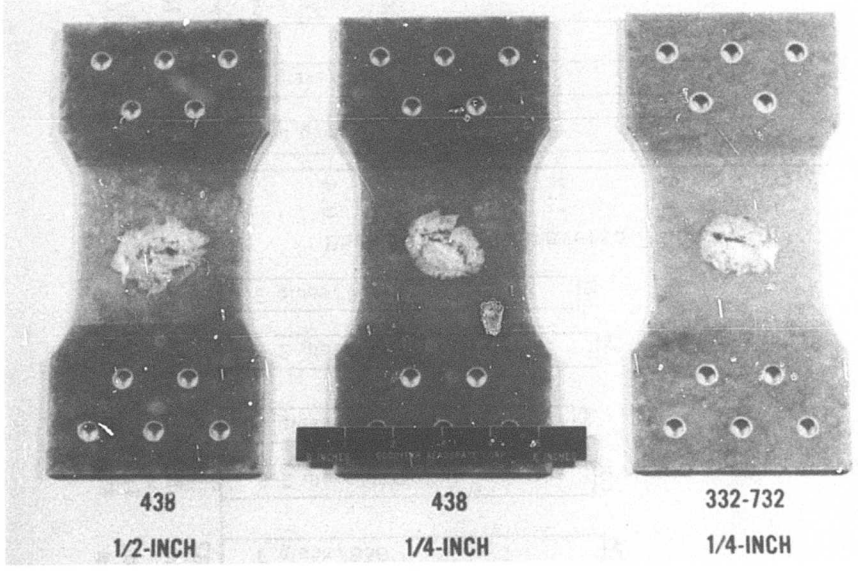

B. Back Surface

Figure 37. Typical Front and Back Surface Ballistic Damage - Specimens Reinforced With S-2 Glass (470 Fiber Finish).

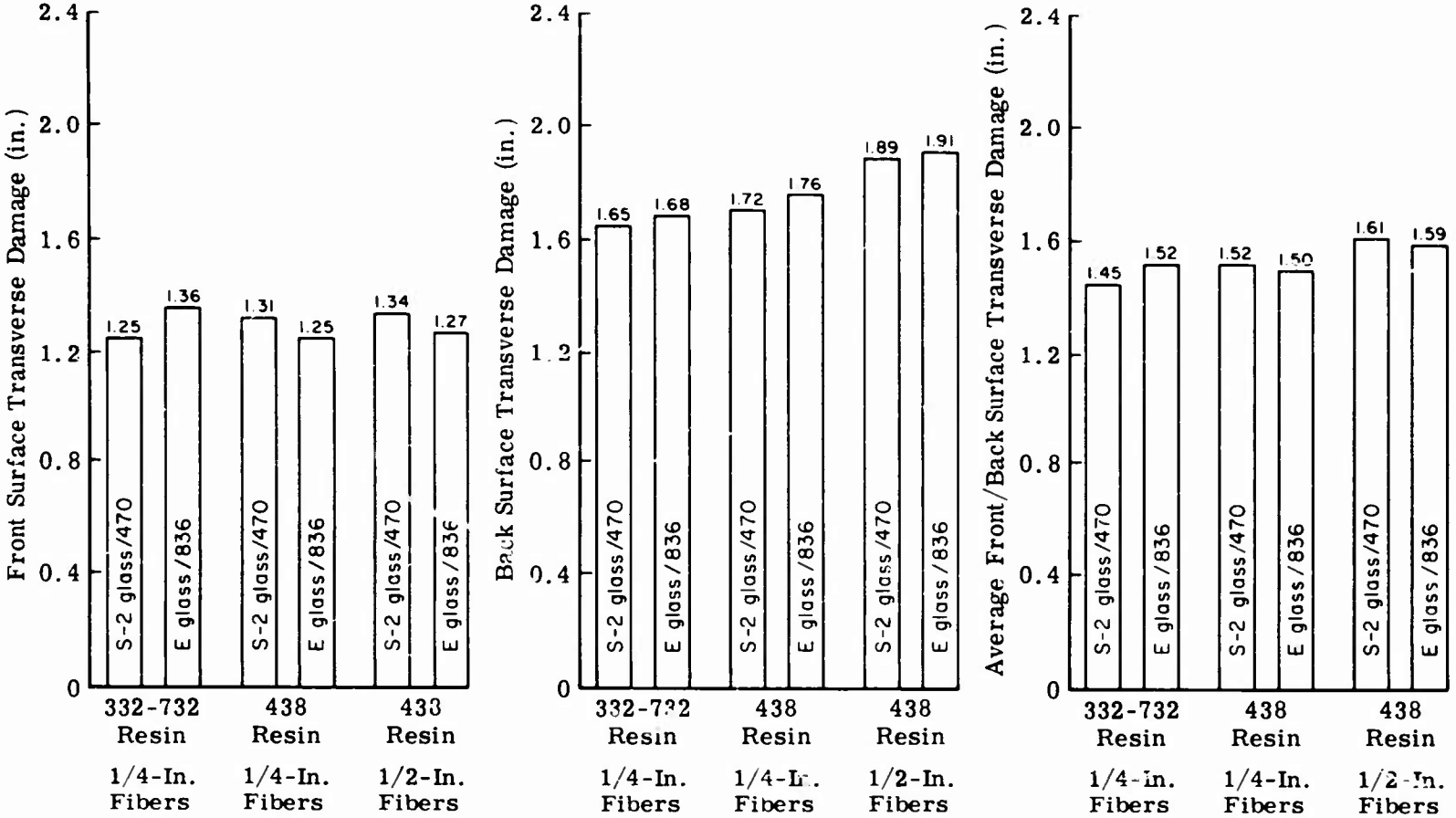

Figure 38. Comparison of Transverse Ballistic Damage - Composites Reinforced With S-2 and E Glass.

TABLE 23. SUMMARY OF VISUAL TRANSVERSE BALLISTIC DAMAGE - COMPOSITES REINFORCED WITH S-2 AND E GLASS

Resin Type	Fiber Length (in.)	Fiber Type	Transverse Ballistic Damage (in.)[a]		
			Front Surface	Rear Surface	Avg
332-732	1/4	S-2/470	1.25[b]	1.65[b]	1.45[b]
		E/836	1.36	1.68	1.52
438	1/4	S-2/470	1.31[c]	1.72[c]	1.52[c]
		E/836	1.25[b]	1.76[b]	1.50[b]
438	1/2	S-2/470	1.34	1.89	1.61
		E/836	1.27[d]	1.91[d]	1.59[d]

[a] Values are based on five replicates except as noted.

[b] Values are based on four replicates.

[c] Values are based on two replicates.

[d] Values are based on three replicates.

The load capacities and strength-to-weight ratios of ballistically damaged S-2 and E glass composites are summarized in Table 24 and shown in bar-graph form in Figure 39. The residual load capacity data clearly show the superiority of the S-2 glass over corresponding E glass composites. Increases of 17 to 43 percent in damaged load capacity over E glass composites were realized, with the most significant increases occurring in the composites with the 438 epoxy resin system.

The difference in post-damage performance between S-2 and E glass composites is even more pronounced on a strength-to-weight ratio basis because of the lower density (approximately 6 percent) of the S-2 glass composites. Strength-to-weight ratio increases were 19 to 50 percent over the corresponding E glass composites.

Conclusions and Recommendations

Composites with S-2 or E glass reinforcements exhibit similar

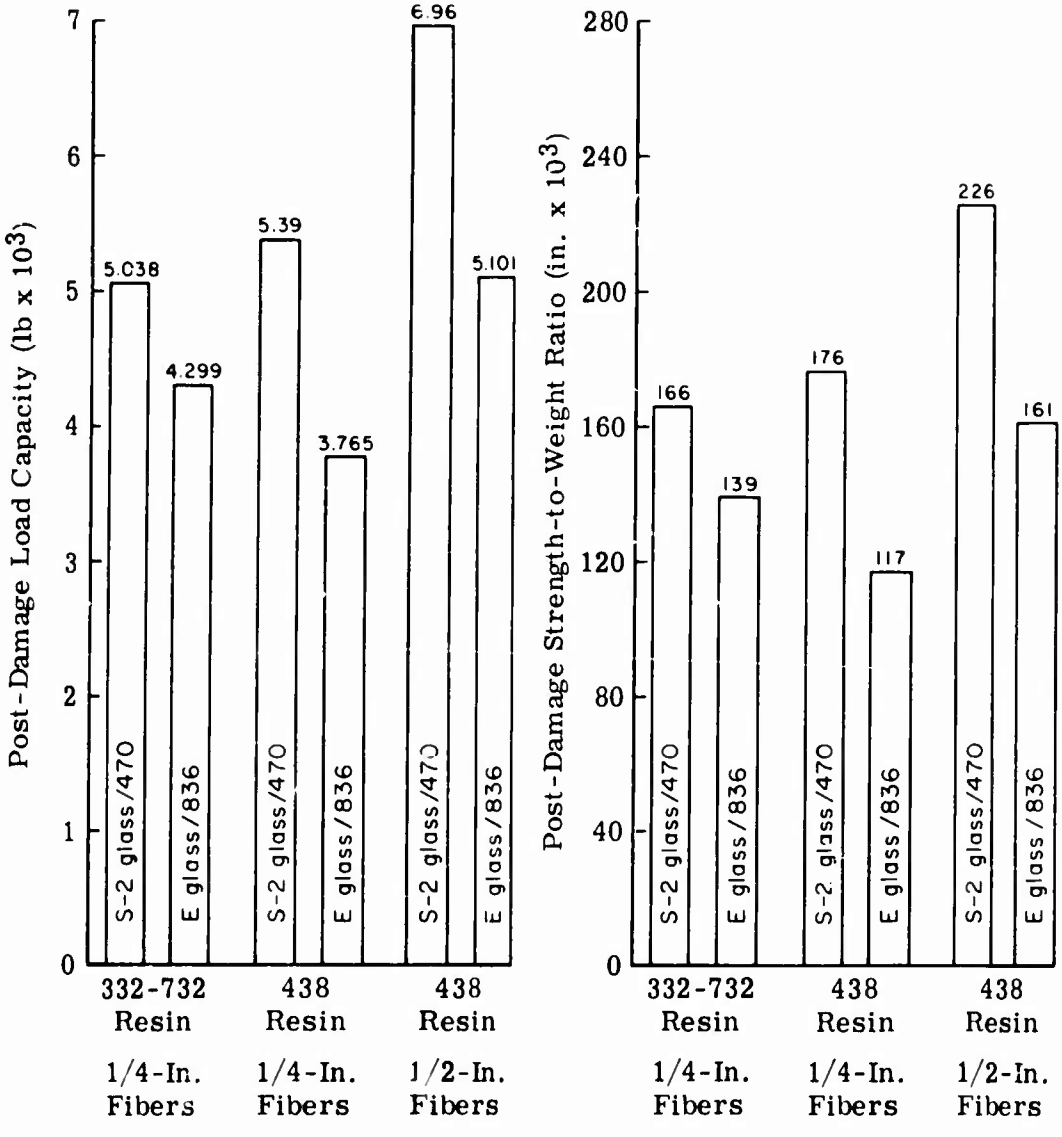

Figure 39. Comparison of Post-Damage Tensile Properties - Composites Reinforced With S-2 and E Glass.

TABLE 24. SUMMARY OF POST-DAMAGE TENSILE PROPERTIES - COMPOSITES REINFORCED WITH S-2 AND E GLASS

Resin Type	Fiber Length (in.)	Fiber Type	Post-Damage Tensile Properties[a]	
			Load Capacity (lb)	Strength-to-Weight Ratio (in. x 10^3)
332-732	1/4	S-2/470	5038[b]	166[b]
		E/836	4299	139
438	1/4	S-2/470	5390[c]	176[c]
		E/836	3765[b]	117[b]
438	1/4	S-2/470	6960[b]	226[b]
		E/836	5101[b]	161[b]

[a]Data normalized to a 1/8-inch specimen thickness. Values are based on five replicates except as noted.

[b]Values are based on four replicates.

[c]Values are based on two replicates.

ballistic damage when impacted by fully tumbled caliber .30 ball M2 projectiles at 0-degree obliquity and 1800 ft/sec. A significant improvement in post-damage load capacity and breaking length was achieved by the direct substitution of S-2 glass for E glass in composite construction. These observations also suggest greater undamaged strength - a fact that was verified with two of the material combinations despite transition section failures.

The outstanding performance associated with the high-strength S-2 glass indicates that this material deserves serious consideration in the final selection of composite systems for Task II evaluation.

SUBTASK 4 - FIBER CONTENT EFFECTS PROGRAM

General

The density and strength of composite materials are affected by changes in the relative proportions of the constituents, i.e., matrix and

reinforcement. Since density is governed by the rule of mixtures, the relationship between density and fiber content (or resin content) can readily be calculated. In the fiber glass-epoxy system, increased fiber content produces higher densities because the glass is approximately twice the density of the resin. With regard to strength, it is generally agreed that maximum tensile properties are achieved when the fiber content is in the range of 50 to 60 v/o. However, the effect of fiber content on the extent of damage and residual strength of ballistically impacted discontinuous fiber composites is currently unknown.

The objective of this investigation, therefore, was to establish the influence of fiber content on undamaged and damaged tensile strength as well as the extent of area, volume, and transverse ballistic damage.

Approach to the Problem

Selection of the three material combinations for evaluation of fiber content effects was based on the following factors:

1. High undamaged ultimate tensile strength.
2. Low susceptibility to transition section failures.
3. Desirability of having a continuous variable to aid in data analysis.

The material combinations that best satisfied these factors were 1/4-, 1/2-, and 1-inch fibers of 836-finished fiber glass in a 438 epoxy resin matrix. The nominal fiber content levels selected for evaluation were 50 and 70 v/o. The resultant test data would be directly comparable to 60 v/o fiber content data previously generated.

The 50 and 70 v/o fiber content specimens were subjected to the following series of measurements and tests:

1. Thickness
2. Density
3. Fiber Content
4. Undamaged Tensile Properties
5. Ballistic Damage Assessment
6. Damaged Tensile Properties

Discussion of Results

The initial attempts to mold the 70 v/o fiber content materials were unsuccessful in all fiber lengths because of insufficient resin. Therefore, it was necessary to reduce the fiber content to approximately 63 v/o to obtain consistently high quality moldings.

The average density, thickness, and fiber content values based on eight replicates of the various groups of specimens prepared in this program are summarized in Table 25. The fiber content values were obtained on samples taken from the center area of the specimens after ultimate tensile testing. These values were determined by converting loss-on-ignition data (weight basis) to a volume basis, using fiber and resin densities of 2.54 and 1.26 g/cc, respectively. The 60 v/o fiber data generated in the screening test program are also given in Table 25 for comparison.

TABLE 25. TEST SPECIMEN MEASUREMENTS - 836/438 COMPOSITES WITH 50, 60, AND 70 V/O NOMINAL FIBER CONTENT

Fiber Length (in.)	Fiber Content (v/o)		Avg Thickness (in.)	Density ($lb/in.^3$)
	Nominal	Actual (Avg)		
1/4	50	45.5	0.127	0.066
1/2	50	44.1	0.126	0.065
1	50	44.2	0.127	0.065
1/4	60	59.5	0.122	0.073
1/2	60	59.4	0.122	0.073
1	60	53.3	0.127	0.070
1/4	70	63.8	0.124	0.074
1/2	70	62.8	0.126	0.074
1	70	62.6	0.124	0.074

The undamaged tensile strengths based on three replicates each of the 50, 60, and 70 v/o fiber content specimens are summarized in Table 26. All specimens tested with the 1/2-inch fiber materials at the 60 and 70 v/o fiber content levels exhibited center failures. In addition, one specimen each with 1/4- and 1-inch fibers at the 60 v/o fiber content level failed in the center area. The balance of the specimens failed in the transition section. Consequently, no significance can be attached to either the absolute tensile strength values or strength differences at the various fiber content or fiber length levels.

TABLE 26. ULTIMATE TENSILE STRENGTH OF UNDAMAGED 836/438 SPECIMENS WITH 50, 60, AND 70 V/O NOMINAL FIBER CONTENT

Fiber Length (in.)	Avg Tensile Stength (psi)		
	45 v/o	60 v/o	63 v/o
1/4	11, 840	13, 650	14, 280
1/2	12, 550	20, 650	16, 240
1	14, 740	26, 740	21, 350

Stress-strain curves were obtained from an extensometer (2-inch gage length) mounted on undamaged specimens during ultimate tensile testing. The tensile modulus values given in Table 27 were determined from the initial slopes of the curves. These data, plotted in Figure 40, indicate that tensile modulus increases, as expected, with increasing fiber content at all fiber length levels. The increase in modulus associated with increasing fiber length is primarily attributed to the higher degree of fiber alignment that is present along the edges of specimens with longer fibers.

Five replicates of each material combination were then impacted at room temperature with fully tumbled caliber .30 ball M2 projectiles at 0-degree obliquity and a nominal velocity of 1800 ft/sec. During the ballistic tests, the specimens were preloaded to 35 percent of the ultimate tensile strength measured at room temperature on undamaged specimens.

The area and volume damage measurements taken on the 50 and 70 v/o fiber content specimens are summarized in Table 28 along with previously reported data at the 60 v/o level. These values represent the

TABLE 27. TENSILE MODULUS OF UNDAMAGED 836/438 SPECIMENS WITH 50, 60, AND 70 V/O NOMINAL FIBER CONTENT

Fiber Length (in.)	Avg Tensile Modulus (psi x 10^6)[a]		
	45 v/o	60 v/o	63 v/o
1/4	2.36	4.04[b]	3.71
1/2	2.44	3.33[b]	3.70
1	2.55	3.12	4.38

[a] Values are based on three replicates except as noted.

[b] Values are based on one specimen.

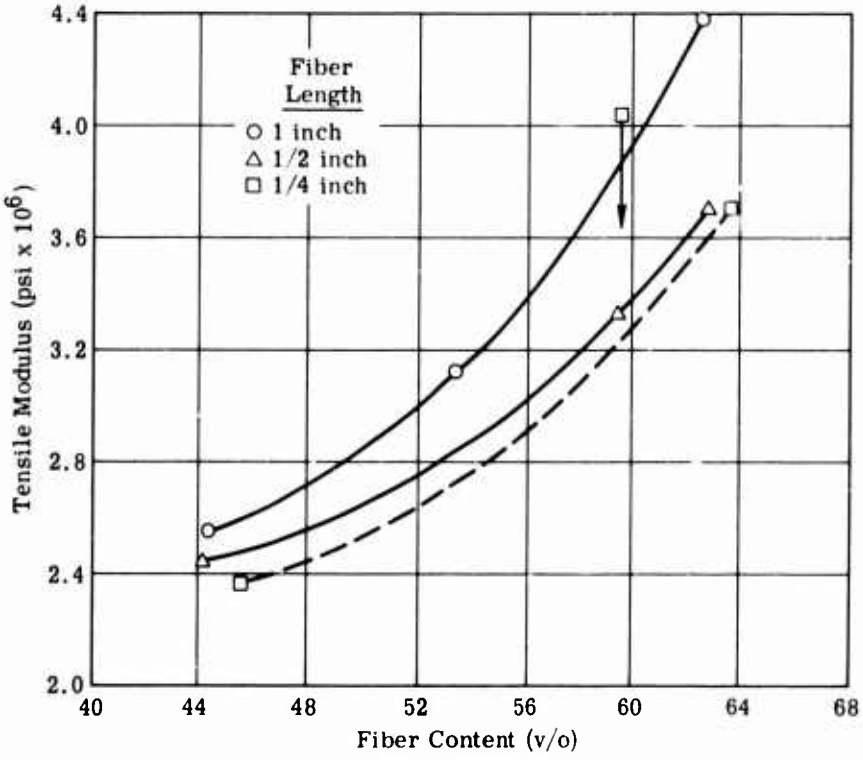

Figure 40. Effect of Fiber Content on Tensile Modulus - 836/438 Composites.

TABLE 28. SUMMARY OF VISUAL BALLISTIC DAMAGE - 836/438 COMPOSITES WITH 50, 60, and 70 V/O NOMINAL FIBER CONTENT

Nominal Fiber Content (v/o)	Fiber Length		
	1 Inch	1/2 Inch	1/4 Inch
	A. Front Surface Area ($in.^2$)		
50	0.97	0.91	0.75
60	1.07	0.95	0.83
70	1.22	1.05	0.86
	B. Back Surface Area ($in.^2$)		
50	4.15	2.46	1.58
60	4.06	2.25	1.56
70	4.16	2.17	1.51
	C. Volume ($in.^3$)		
50	0.300	0.209	0.146
60	0.304	0.189	0.143
70	0.318	0.199	0.145

average damage based on five replicates at each fiber content level. A graphical presentation of the area and volume damage data is shown in Figure 41. These data indicate that the front surface damage area tends to increase slightly with increasing fiber content regardless of fiber length. With respect to back surface damage area, the effect of fiber content does not follow any consistent trend across all fiber lengths examined. Actually, the differences in area damage at any particular fiber length are relatively small even in the most extreme case. Mixed results were also obtained with regard to volume damage as influenced by fiber content variations. The extreme differences in volume damage at a given fiber length were smaller on a percentage basis than differences in back surface damage area.

The damage area summary as well as the post-impact photographs shown in Figures 42 and 43 indicate that damage area increases

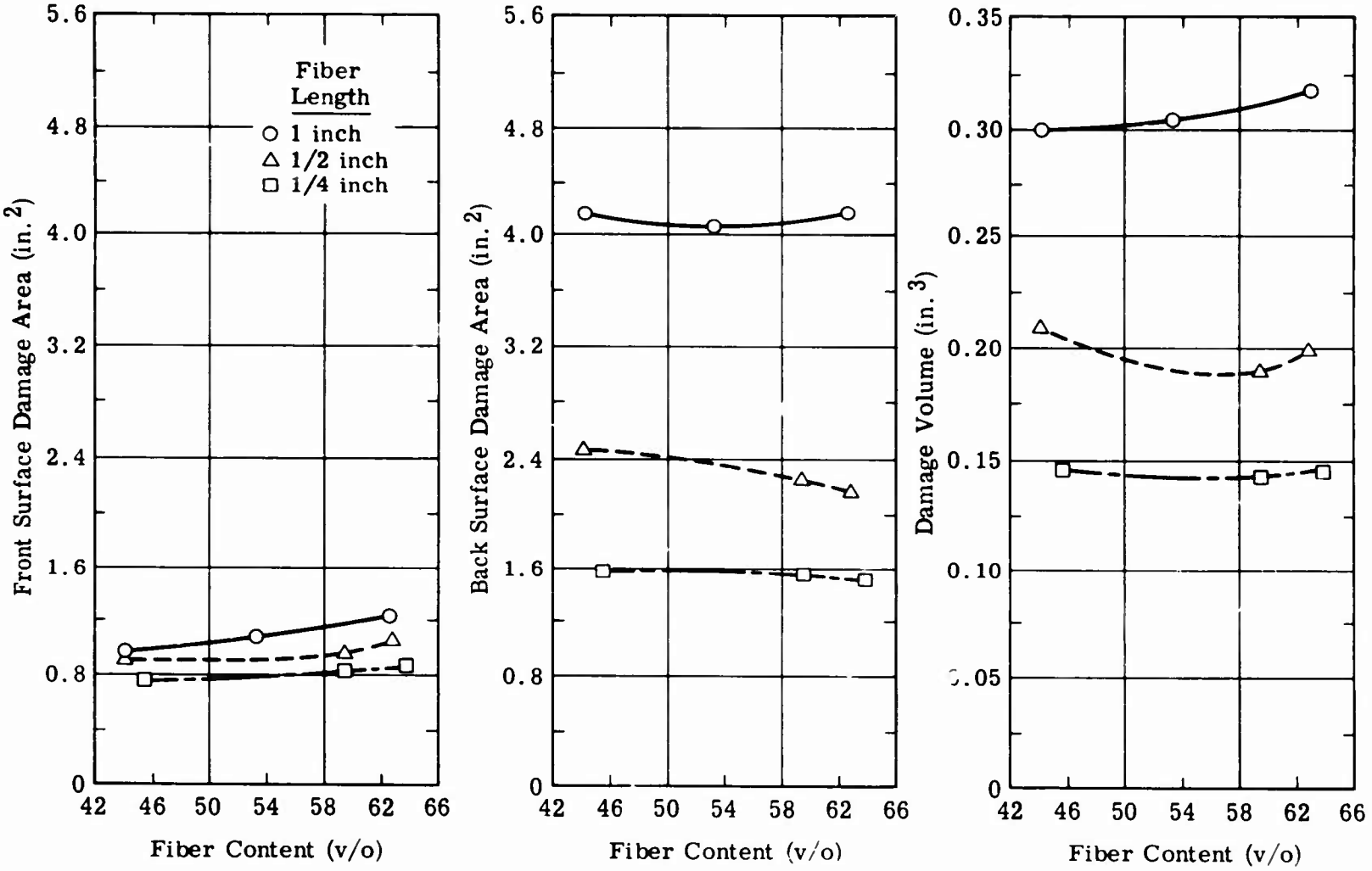

Figure 41. Effect of Fiber Content on Ballistic Damage Areas and Volume - 836/438 Composites.

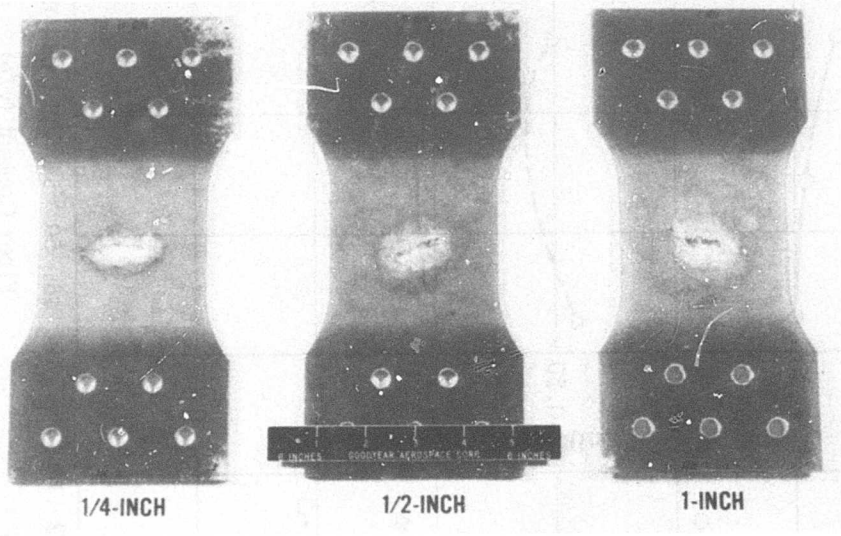

A. 50 V/O Fiber Content

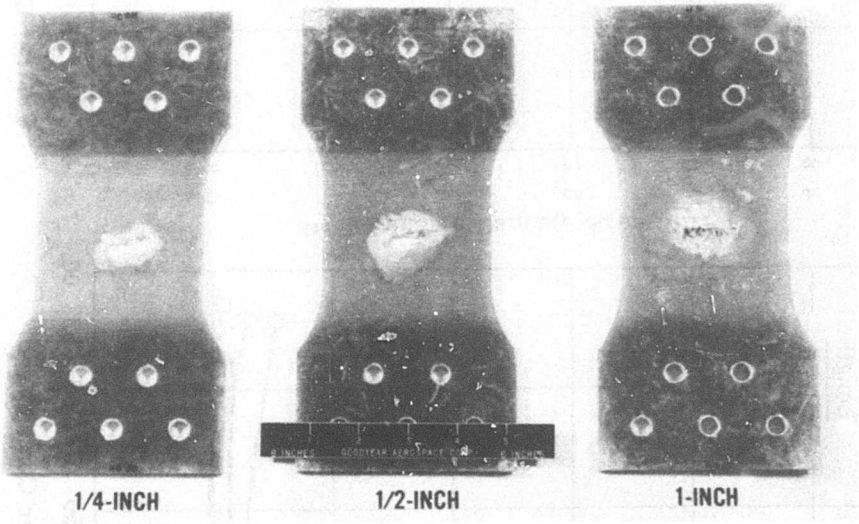

B. 70 V/O Fiber Content

Figure 42. Typical Front Surface Ballistic Damage - 836/438 Composites With 50 and 70 V/O Nominal Fiber Content.

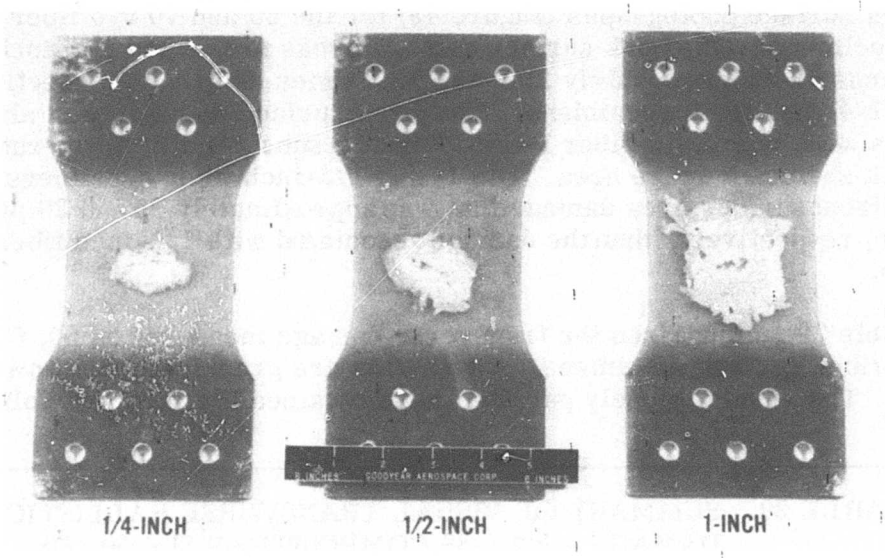

A. 50 V/O Fiber Content

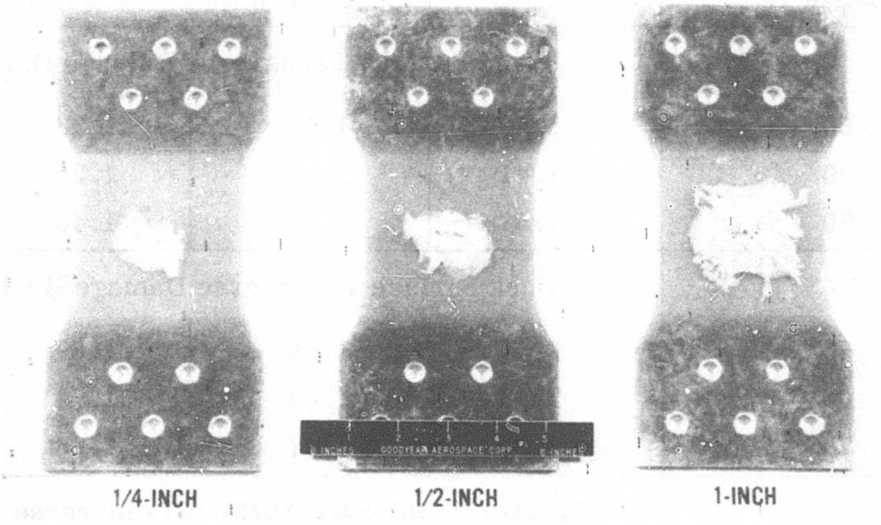

B. 70 V/O Fiber Content

Figure 43. Typical Back Surface Ballistic Damage - 836/438 Composites With 50 and 70 V/O Nominal Fiber Content.

significantly with increasing fiber length. This is particularly evident in the back surface photographs (Figure 43) for the 50 and 70 v/o fiber content specimens. The back surface damage areas for 1- and 1/2-inch fiber specimens are approximately 2.62 and 1.45 times as great, respectively, as the 1/4-inch fiber specimens. The front surface damage area also increases with increasing fiber length, but at a substantially lower rate than the back surface damage area. The 1- and 1/2-inch fiber specimens exhibited front surface area damage that was approximately 35 and 20 percent greater, respectively, than the damage associated with 1/4-inch fiber lengths.

Table 29 summarizes the transverse damage measured on 50, 60, and 70 v/o fiber content specimens. These data are graphically shown in Figure 44. The results closely parallel those obtained for area and volume

TABLE 29. SUMMARY OF VISUAL TRANSVERSE BALLISTIC DAMAGE - 836/438 COMPOSITES WITH 50, 60, AND 70 V/O NOMINAL FIBER CONTENT

Nominal Fiber Content (v/o)	Fiber Length		
	1 Inch	1/2 Inch	1/4 Inch
	A. Front Surface Transverse Damage (in.)		
50	1.39	1.40	1.38
60	1.41	1.27	1.25
70	1.53	1.46	1.40
	B. Back Surface Transverse Damage (in.)		
50	2.40	1.96	1.69
60	2.53	1.89	1.74
70	2.73	1.97	1.66
	C. Avg Front/Back Surface Transverse Damage (in.)		
50	1.90	1.68	1.54
60	1.97	1.58	1.50
70	2.13	1.72	1.53

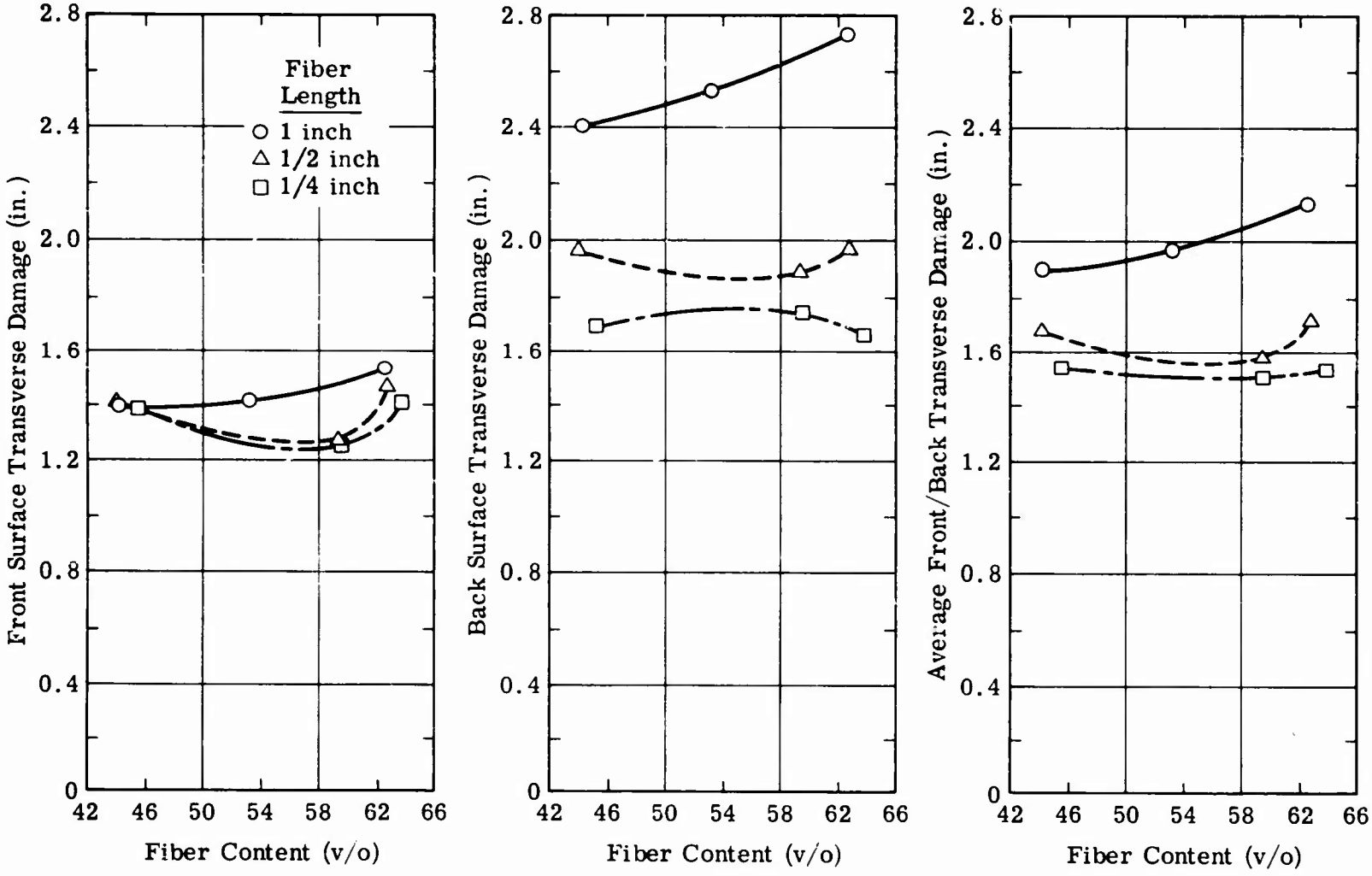

Figure 44. Effect of Fiber Content on Transverse Ballistic Damage - 836/438 Composites.

damage; i.e., fiber content does not have a powerful influence on transverse damage, but fiber length does. The maximum front and back surface transverse damage was exhibited by the 1-inch fiber specimens at the highest fiber content level (70 v/o nominal). The transverse damage values were 1.53 and 2.73 inches, respectively, for the front and back specimen surfaces.

The post-damage ultimate tensile properties of the 50, 60, and 70 v/o fiber content specimens are given in Table 30. The load capacity results indicate that the 50 v/o fiber content specimens generally failed at a lower load than the specimens with a high fiber content. For 1/2- and 1-inch fiber lengths, the 60 and 70 v/o fiber content specimens exhibited essentially identical residual load capacities.

The strength-to-weight ratio data given in Table 30 are graphically presented in Figure 45. Although no universal trend was evident between

TABLE 30. SUMMARY OF POST-DAMAGE TENSILE PROPERTIES - 836/438 COMPOSITES WITH 50, 60, AND 70 V/O NOMINAL FIBER CONTENT

Nominal Fiber Content (v/o)	Fiber Length		
	1 Inch	1/2 Inch	1/4 Inch
	A. Load Capacity (lb)[a]		
50	5905[b]	4484[c]	3770[c]
60	7464	5101[c]	3765[c]
70	7489	5081	4438
	B. Strength-to-Weight Ratio (in. x 10^3)[a]		
50	205[b]	156[c]	128[c]
60	243	161[c]	117[c]
70	229	156	135

[a] Data normalized to a 1/8-inch specimen thickness. Values are based on five replicates except as noted.

[b] Values are based on three replicates.

[c] Values are based on four replicates.

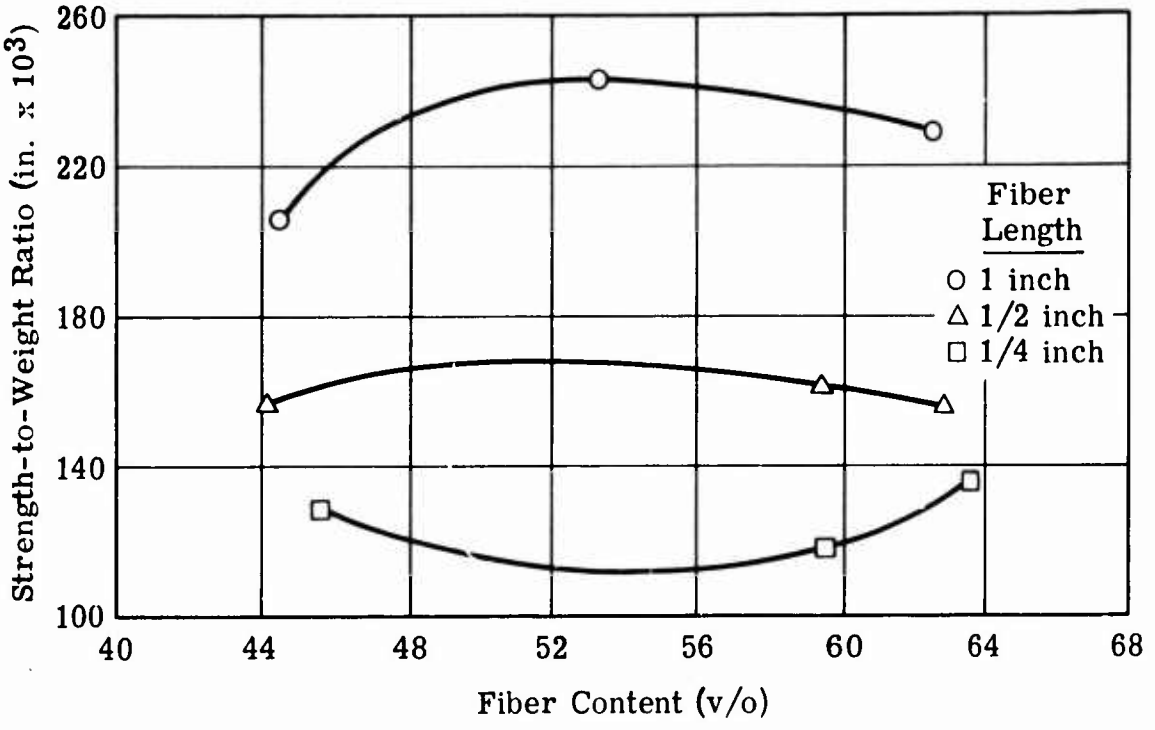

Figure 45. Effect of Fiber Content on Strength-to-Weight Ratio - 836/438 Composites

breaking length and fiber content at all three fiber length levels examined, the curve indicates that the optimum fiber content for 1/2- and 1-inch fibers falls in the 50 to 54 v/o range. Actually, the difference in breaking length for any given fiber length is relatively insensitive to fiber content changes within the range of experimental levels explored.

Conclusions and Recommendations

The following conclusions can be drawn from the fiber content investigation:

1. A fiber content limit exists above which discontinuous fiber moldings of high quality cannot be consistently produced. This upper limit appears to be about 63 v/o.

2. Ballistic damage is not significantly affected by fiber content changes within the actual range examined (44.1 to 63.8 v/o).

3. Post-damage breaking length (strength-to-weight ratio) for the three fiber lengths showed no consistent trend relative to changes in fiber volume. The maximum breaking length of the 1/2- and 1-inch fiber length occurs in the 50 to 54 v/o fiber content range.

Based on the results of this program, the target fiber content level for all subsequent specimens for Phase I evaluation will be 50 to 54 v/o. The molding compound will, of necessity, have a slightly lower fiber content because of typical resin loss during the molding operation.

SUBTASK 5 - SELECTION OF THREE COMPOSITE SYSTEMS

General

During the first four subtasks of Task I, 39 material combinations were evaluated to establish the influence of constituent characteristics on damaged and undamaged specimen properties. Based on these results, the three most promising composite systems were to be selected for more extensive evaluation in Task II.

Approach to the Problem

Primary consideration in the selection process was given to the post-damage properties of the candidate material systems. These properties, namely, extent of ballistic damage and residual load capacity, govern the design of flight control components that must continue to function after ballistic impact. Since minimum component weight is desired, the density of the composite material must also be considered. Therefore, the residual breaking length (strength-to-weight ratio) rather than the load capacity was established as one of the criteria for selecting the three composites for Task II evaluation.

It was also deemed advisable to avoid selecting material systems of similar construction. This would guard against the possibility that a common material factor would have a universally detrimental effect on all specimens during certain Task II tests such as cyclic fatigue or ballistic impact at temperature extremes.

Discussion of Results

The following three composite systems were tentatively selected for Task II evaluation:

1. 897-finished E glass, 332-732 epoxy resin, 1-inch fiber length

2. 470-finished S-2 glass, 4617 epoxy resin, 1-inch fiber length

3. 470-finished S-2 glass, 4617 epoxy resin, 1/2-inch fiber length

Specimens produced with each of these systems would have a nominal fiber content of 52 v/o.

The 897/332-732 composite with 1-inch fibers was chosen because it exhibited the highest breaking length of all damaged composites evaluated in Task I. The two systems with S-2 glass were selected on the basis of their projected outstanding properties. The rationale for considering the 470/4617 composites is presented below.

In the comparison of composites reinforced with S-2 glass and E glass, the S-2 glass was found to significantly improve post-damage tensile strength regardless of the resin type or fiber length investigated. It was further observed that the 4617 resin produced the highest post-damage breaking length values when utilized with E glass with an epoxy-compatible finish (836). Since S-2 glass has an epoxy-compatible finish (470), it was anticipated that the 470/4617 combination would produce the highest residual strength possible within the limits of the variables examined.

Before a final commitment was made on the two S-2 glass composites, a limited empirical investigation was conducted to establish whether the anticipated post-damage properties of the 470/4617 composites would be realized. Specimens were subjected to ultimate tensile testing in both the undamaged and ballistically damaged conditions. The undamaged tensile strengths of specimens with 1/2- and 1-inch fibers averaged 13,200 and 18,670 psi, respectively. All undamaged specimens failed in the transition section. The specimens with 1/2- and 1-inch fibers exhibited tensile moduli of 5.12×10^6 and 5.70×10^6 psi, respectively, the highest values achieved in all the Task I investigations. These high values were anticipated since the S-2 glass and 4617 resin individually have the highest moduli of the glasses and resins evaluated.

The post-damage load capacities of specimens fabricated from 1/2- and 1-inch fibers were 4543 and 7852 psi, respectively. The breaking lengths, based on measured densities of 0.072 and 0.073 $lb/in.^3$ for the 1/2- and 1-inch materials, were 143×10^3 and 248×10^3 inches, respectively. These post-damage load capacity and breaking length values were significantly lower than the values obtained for the corresponding E glass specimens (836/4617 composites with 1/2- and 1-inch fibers). Therefore, the anticipated improvements in damage properties were not achieved.

Because of the poor performance of the 470/4617 composites, the Task I data were reviewed, and two replacement selections were made. In making these choices, only the resin type and fiber finish combinations that had specifically been evaluated were considered. Extrapolations of existing data to other fiber lengths were considered reasonable and legitimate because of the wealth of information generated in the Task I program on fiber length effects. The two replacement systems finally selected were:

1. 470-finished S-2 glass, 438 epoxy resin, 1-inch fiber length

2. 470-finished S-2 glass, 438 epoxy resin, 1/2-inch fiber length

The 470/438 composites were selected because this combination of fiber finish and resin exhibited the highest post-damage strength properties of all composites evaluated with 1/4- and 1/2-inch fibers. Since post-damage properties increase with increasing fiber length, similar relative performance should be obtained with 1-inch fibers. The 1/2-inch fiber length was chosen to provide a system with reduced ballistic damage at some sacrifice in undamaged and damaged tensile properties.

Each of the three selected systems has at least one material characteristic that is foreign to the other systems. For example, the 897/332-732 composite with 1-inch fibers differs from the 470/438 composite with 1-inch fibers in fiber strength, finish compatibility, and resin type. Similar comparisons among other system combinations will disclose at least one significant material difference. Therefore, this precludes the possibility of all systems exhibiting poor performance due to the adverse effect of one common material factor.

Conclusions and Recommendations

Data extrapolations across the boundaries of resin type and/or fiber finish are not currently possible. When changes are contemplated in resin type or fiber finish, the system must be treated as a new material with unknown properties.

The following material systems were recommended for Task II evaluation:

1. 897-finished E glass, 332-732 epoxy resin, 1-inch fiber length

2. 470-finished S-2 glass, 438 epoxy resin, 1-inch fiber length

3. 470-finished S-2 glass, 438 epoxy resin, 1/2-inch fiber length

Selection of these three material systems for subsequent evaluation was approved by the Eustis Directorate. The target fiber content of the molded specimens was established at 52 v/o.

SUBTASK 6 - TRANSITION SECTION FAILURE PROGRAM

General

A high incidence of failures was observed in the thickness transition section of Task I undamaged specimens during ultimate tensile testing. These failures were experienced with essentially all specimens produced from 1-inch chopped fiber glass molding compounds regardless of the resin type or the strength, diameter, or finish of the fibers. The frequency of such failures generally decreased with decreasing fiber length.

The probable cause of these failures was the presence of severely distorted or misoriented fibers in the transition region. Crimped, bent, and twisted fibers were clearly evident in this area from a visual examination of sectional and "burned-out" specimens. In the case of the "burned-out" specimens, the matrix was eliminated by pyrolysis at 1050°F in an oxidizing atmosphere.

One potential factor contributing to transition section failures was the preforming method used, whereby molding compound was independently loaded in the end and center sections. Material allocated to each section was limited to the assigned preform areas. Consequently, a separation plane may have been created between sections, preventing nesting and promoting crippling of the fibers during the subsequent molding operation. Although the preforming method was considered to be the primary cause of transition failures, material and molding factors also may have been responsible. Since flight control components might contain transition sections at least as severe as the 7-degree thickness taper in the test specimen, a resolution of the failure problem was considered important.

Approach to the Problem

A concentrated program was undertaken to examine the effects of various material, molding, and preform parameters on failure location and ultimate tensile strength. This effort was devoted to an investigation of those parameters considered to be most influential in governing strength and failure location. Factors judged to be of lesser importance were held constant at a preselected level.

The variables and number of levels examined in the program are presented in Table 31.

TABLE 31. VARIABLES EXAMINED IN THE TRANSITION SECTION FAILURE PROGRAM

Variable	Description	Levels
Gel Time	Gelation time of resin measured at 300°F on a Fisher-Johns Melting Point Apparatus	2
Preform Weight	Weight allocation on an area or volume basis	2
Dwell Time	Hold time between initial and final closure cycles. Initial closure refers to the condition where center separation of die cavity was 5/8 inch.	2
Closure Time	Time from initiation of the final closure cycle to attainment of 75 percent of full molding pressure.	3

The preform weight distribution on an area basis referred to in Table 31 simply means that a constant thickness of material was distributed in the preform mold. The material was then compacted into the standard preform configuration. In the volume-based distribution, the preform was constructed with 26 grams of molding compound in each end, 161 grams distributed across the entire specimen surface area, and finally, an additional 26 grams in each end. Again, the preform was compacted to the standard configuration. The volume distribution was similar to that used in all previous Task I investigations except for the placement method. The new technique provided a full-length core of molding compound that eliminated the possible existence of an artificial wall between sections.

The following factors were held constant throughout the initial experiment:

1. Material: One-inch-long, 470-finished S-2 fiber glass in a 438 epoxy resin matrix at a nominal fiber content of 52 v/o. This was one of the materials selected for subsequent evaluation in Task II.

2. Molding Compound Charge: 265 grams

3. Preform Configuration: Similar to the molded specimen except that the thickness difference between the center and ends was 1/4 inch (1/8 inch per side).

4. Preform Compaction Pressure: 0.75 psi

5. Molding Temperature: 295 (±5)°F

6. Molding Pressure: 1000 psi (20 tons)

7. Molding Time: 20 minutes

8. Replicates: Three

Green tracer material was produced for incorporation in the preforms to determine flow patterns and extent of fiber distortion. This material was made by dyeing the fiber glass roving prior to resin impregnation and chopping the prepreg into 1-inch lengths.

The natural and dyed molding compounds were each divided into two lots of equal weight. The 300°F gel times of these lots were adjusted as necessary by room temperature staging to two levels, namely, 25 and 45 seconds. These levels were selected to provide a significant difference in resin staging to maximize the probability of discerning the true effect of gel time on failure location and tensile strength.

Discussion of Results

Prior to conducting the initial investigation, it was necessary to establish appropriate values for the experimental levels of dwell and closure times. This information was obtained from a preliminary program in which judicious changes were made in the variable levels. Adequate data were collected from 15 specimens to define reasonable experimental values for dwell and closure times within the molding capabilities of the material. The results of this preliminary program are summarized in Table 32. Based on the limited experimentation performed, the following observations can be made:

1. The molding characteristics of the two gel time materials are similar after each is exposed for a dwell time equal to its gel time.

TABLE 32. PRELIMINARY TRANSITION SECTION FAILURE PROGRAM

Test Series No.	Gel Time (sec)	Preform Weight Distribution	Dwell Time (sec)	Closure Time (sec)	Ult Tensile Strength (psi)	Failure Location[a]	Remarks[b]
DT-101	45	Area	20	15.0	26,000	C	FRA
DT-102	↓	↓	↓	90.0	29,300	C	FRA
DT-103				9.0	28,100	T	FRA
DT-104				35.0	28,400	T	
DT-105	25	Area	20	21.0	34,300	T	
DT-106	↓	↓	25	12.0	22,400	T	
DT-107			↓	54.0	36,600	T	
DT-108	45	Area	45	64.0	35,900	C	FRA
DT-109	↓	↓	↓	24.0	31,000	T	FRA
DT-110				12.0	27,100	T	
DT-111				7.5	33,300	T	FRA
DT-112	45	Volume	45	10.0	22,600	T	
DT-113	↓	↓	↓	24.0	29,200	T	
DT-114	25/45[c]	Volume	30	24.0	29,100	T	
DT-115	↓	↓	45	24.0	23,800	T	

[a]C denotes center section failure. T denotes transition section failure.

[b]FRA denotes that the specimen exhibited a fiber-rich area in the center section.

[c]A 50/50 weight mixture was used for this test series.

2. Fiber distortion decreased with increasing elapsed time (dwell and closure). This was evident from tracer fibers placed in the transition region.

3. Beyond a certain elapsed time, poor-quality moldings of high void content resulted because of little or no resin flow.

4. Both rapid and relatively slow molding cycles produced specimens with fiber-rich areas in the center section.

5. Combining materials of widely differing gel times should be avoided. This produces an undesirable condition where one material is always overstaged compared with the other and, consequently, has different flow characteristics during molding.

On the basis of this preliminary program, dwell times equal to 0.8 and 1.2 gel times were selected. This results in dwell times of 36 and 54 seconds for the 45-second gel time material and 20 and 30 seconds for the 25-second gel time material. The three nominal closure times chosen for the parametric program were 12, 24, and 36 seconds.

The results of the parametric program are given in Table 33. Of the 72 specimens evaluated, only two exhibited center failures. One of these two specimens had a fiber-rich area in the center section, which probably contributed to failure in this region.

The effect of the experimental variable levels on ultimate tensile strength is presented in Table 34. The values were obtained by averaging the strengths of all specimens at a particular variable level. The grand average is the mean value of all 24 combinations examined in this program.

The data indicate that the closure time had the most significant impact on undamaged tensile strength. The strength at a 36-second closure time is 8.4 to 9.3 percent higher than the 12- and 24-second closures. Although the gel time apparently represents the second most significant factor, the density of the higher strength, 45-second gel time material is approximately 2 percent greater. Consequently, the difference in strength-to-weight ratios for the two gel time levels is relatively small. The remaining variables, i.e., weight distribution and dwell time, have a minimal effect on strength over the experimental range investigated. It was again observed from the condition of tracer fibers in the transition section that fiber distortion decreased with increased combined dwell and closure times.

Since the desired center failures were not achieved during the parametric study, a second effort was performed that was concerned primarily with an investigation of the effect of alternative methods of preform fabrication. In addition, a limited number of experiments were conducted to evaluate molding cycle modifications.

TABLE 33. BASIC TRANSITION SECTION FAILURE PROGRAM

Test Series No.	Gel Time (sec)	Preform Weight Distribution	Dwell Time (sec)	Avg Closure Time (sec)[a]	Avg Ult Tensile Strength (psi)[a]	Failure Location[b]	Remarks[c]
DT-201	45	Area	54	11.5	26,670	3T	
DT-202	↓	↓	↓	24.3	25,370	3T	
DT-203	↓	↓	↓	32.7	30,530	3T	1 FRA
DT-204	↓	↓	36	11.7	25,700	3T	3 FRA
DT-205	↓	↓	↓	24.7	26,870	3T	
DT-206	↓	↓	↓	36.0	29,270	3T	1 FRA
DT-207	45	Volume	54	12.0	27,670	3T	
DT-208	↓	↓	↓	25.3	27,470	3T	
DT-209	↓	↓	↓	40.7	28,600	3T	
DT-210	↓	↓	36	12.3	25,100	1C & 2T	
DT-211	↓	↓	↓	24.7	27,630	3T	
DT-212	↓	↓	↓	40.7	29,730	1C & 2T	1 FRA
DT-213	25	Area	30	12.0	27,930	3T	
DT-214	↓	↓	↓	25.7	24,030	3T	
DT-215	↓	↓	↓	37.0	28,300	3T	
DT-216	↓	↓	20	15.0	25,430	3T	
DT-217	↓	↓	↓	25.3	23,430	3T	
DT-218	↓	↓	↓	37.7	23,770	3T	
DT-219	25	Volume	30	14.0	25,530	3T	
DT-220	↓	↓	↓	26.2	24,970	3T	
DT-221	↓	↓	↓	43.3	30,200	3T	
DT-222	↓	↓	20	12.7	24,700	3T	
DT-223	↓	↓	↓	25.7	28,070	3T	
DT-224	↓	↓	↓	38.0	27,370	3T	

[a]Values are based on three replicates.

[b]Digits indicate the number of transition (T) and center (C) section failures in the test series.

[c]Digits indicate the number of specimens that exhibited a fiber-rich area (FRA) in the center section.

TABLE 34. EFFECT OF VARIABLES ON ULTIMATE TENSILE STRENGTH - TRANSITION SECTION FAILURE PROGRAM

Variable	Level	Avg Ult Tensile Strength (psi)[a]	Factor[b]
Gel Time	45 sec	27,633	1.028
	25 sec	26,143	0.972
Preform Weight Distribution	Area basis	26,526	0.987
	Volume basis	27,250	1.013
Dwell Time	0.8 (gel time)	26,420	0.983
	1.2 (gel time)	27,356	1.017
Closure Time	12 sec	26,216	0.975
	24 sec	25,980	0.966
	36 sec	28,471	1.059

[a]Grand average = 26,888 psi.

[b]Ratio of average strength at variable level to grand average.

The following specific experiments were performed:

1. Extended closure times
2. Extended dwell and closure times
3. Increased charge at the transition section
4. Compacted and rf-heated preforms
5. Dump loading, i.e., no preforms
6. Reduced width preforms
7. Compacted preforms
8. Reduced molding temperature

Specimens were also prepared using the Task I preforming method and

molding cycle to provide base-line date for assessing program progress. The results of this series of tests are summarized in Table 35.

Series DT-225 and DT-226 specimens, constructed using the former preform/molding procedure, produced transition section failures at 22,030 and 20,530 psi, respectively, for the 45- and 25-second gel time materials. Severe distortion of the tracer fibers in the transition section is evident from the photograph shown in Figure 46. The average values for the comparable materials evaluated in the basic program were 27,633

TABLE 35. SUPPLEMENTAL TRANSITION SECTION FAILURE PROGRAM

Test Series No.	Gel Time (sec)	Preform Weight Distribution	Dwell Time (sec)	Closure Time (sec)	Ult Tensile Strength (psi)	Failure Location[a]	Remarks
DT-225 DT-226	45 25	Volume Volume	0 0	5.5 5.5	22,030 20,530	4T 3T	Preforms constructed using former technique i.e., separate ends and center buildups.
DT-227 DT-228	45 45	Area Volume	36 36	68.0 70.5	32,900 32,500	2T[b] 2T[b]	Extended closure time.
DT-229 DT-230	25 25	Area Volume	40 40	74.0 74.5	28,070 31,550	2T 2T	Extended dwell and closure times.
DT-231	45	Volume	54	24.0	29,400	1T	Increased charge at transition.
DT-232A DT-232B	45 25	Volume Volume	36 18	40.0 34.0	32,020 31,170	2C & 1T[c] 1C & 2T[b]	Preform compacted at 40 psi and rf-heated for 30 seconds.
DT-233A DT-233B DT-233C DT-233D DT-233E	45 45 45 25 25	None (See remarks)	0	72.5 101.0 127.0 62.0 81.0	34,000 32,900 41,500 29,700 27,630	2C 1C 1C[d] 1T[d] 3T[d]	No preform. Molding compound dumped into die cavity and leveled.
DT-234A DT-234B	45 45	Volume Volume	54 36	40.0 54.0	23,200 23,500	1C[d] 1C[d]	Preform width reduced 1/2 inch on each side. Compacted at 40 psi.
DT-235	45	Volume	54	20.0	36,500	1C & 1T	Preform compacted at 40 psi.
DT-236A DT-236B DT-236C	45 45 45	Volume Volume Volume	54 36 90	96.0 114.0 39.0	37,000 32,400 27,800	1T 1T 1T	Specimens molded at 275°F.

[a]Digits indicate the number of transition (T) and center (C) section failures in the test series.

[b]Two specimens exhibited fiber-rich areas in the center section.

[c]Three specimens exhibited fiber-rich areas in the center section.

[d]One specimen exhibited a fiber-rich area in the center section.

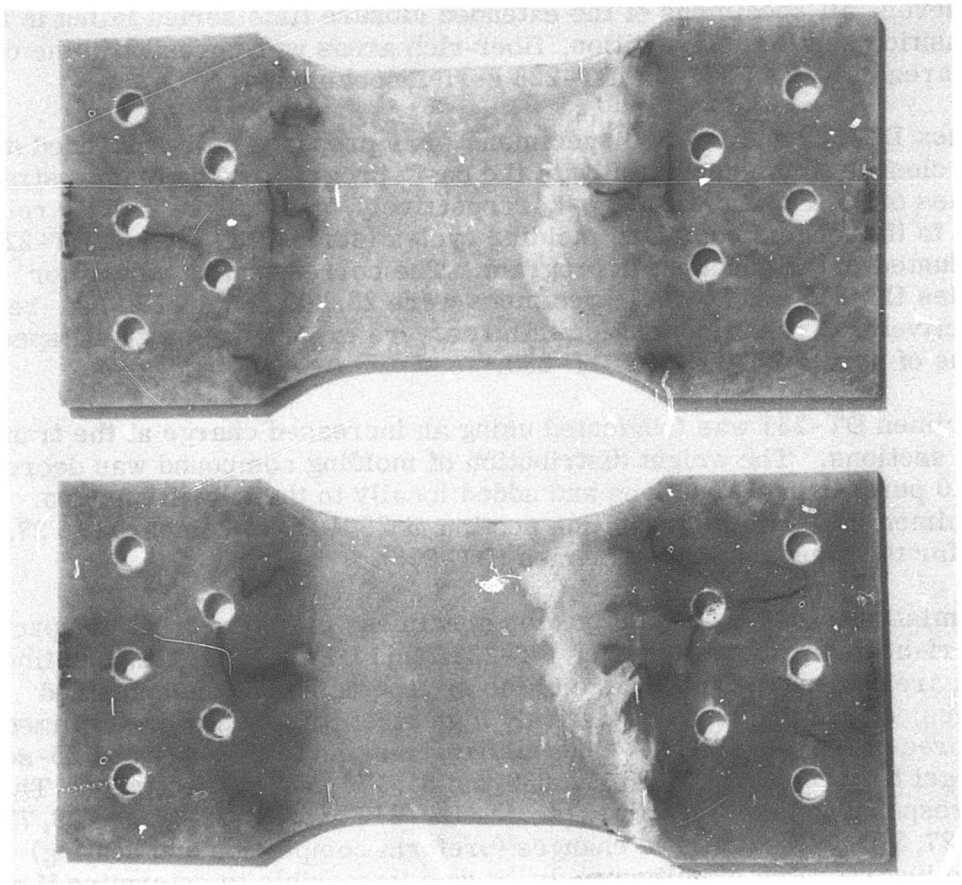

Figure 46. Severe Distortion of Transition Section Fibers as Evidenced by Tracer Material.

and 26, 143 psi, respectively. (These latter values are based on the combined response of specimens prepared with area and volume basis weight distribution preforms.) It is readily apparent that the transition section strength was increased approximately 5, 600 psi with both gel time materials. This improvement is partially attributable to a continuous layer of molding compound in the preform.

Extending the closure time approximately 100 percent beyond the maximum level examined in the basic program resulted in a significant improvment in tensile strength. Series DT-227 and DT-228 specimens exhibited strengths of 32, 900 and 32, 500 psi. The average values for the same

systems molded at one-half the closure time were 29, 270 and 29, 730 psi. However, all specimens of the extended closure time series failed in the transition section. In addition, fiber-rich areas were present in the center area of all DT-277 and DT-228 series specimens.

Series DT-229 and DT-230 specimens were prepared using extended dwell and closure times compared with the basic program. The tensile strength values of 28, 070 and 31, 550 psi, respectively, gave mixed results relative to the longest combined molding cycles (series DT-215 and DT-221) evaluated in the parametric program. The corresponding values for series DT-215 and DT-221 specimens were 28, 300 and 30, 200 psi, respectively. Transition section failures were experienced with all specimens of series DT-229 and DT-230.

Specimen DT-231 was fabricated using an increased charge at the transition sections. The weight distribution of molding compound was decreased by 10 percent in all sections and added locally to the transition area. The specimen failed in the transition section at 29, 400 psi compared to 27, 470 psi for the standard loading series (DT-208).

Promising results were obtained on specimens prepared from compacted and rf-heated preforms (series DT-232A and DT-232B). Although fiber-rich areas were evident in five of the six specimens of the combined series, center failures at relatively high strength levels were realized in three of the specimens. The failure strengths for the 45- and 25-second gel time materials were 32, 030 and 31, 170 psi, respectively. The corresponding base-line values (series DT-212 and DT-224) were 29, 730 and 27, 370 psi. Since two changes (preform compaction and heating) were incorporated simultaneously, it was impossible to determine if one or both factors contributed to improved transition section strength and to a higher frequency of center failures.

Series DT-233A through DT-233E specimens were fabricated by simply dumping the molding compound charge directly into the die cavity. The press was closed at a relatively slow rate without the customary dwell step. The average tensile strength of the four specimens with 45-second gel time material (series DT-233A through DT-233C) was 36, 100 psi. This high strength is attributed in part to greater fiber alignment along the longitudinal edges of these specimens. All four specimens failed in the center area, and one contained a fiber-rich area in the center section.

The average tensile strength of specimens prepared from 25-second gel time stock (series DT-233D and DT-233E) was 28, 650 psi. All four specimens failed in the transition section, and two exhibited fiber-rich areas in the center section. No satisfactory explanation is available for

the disparity in failure strength and location between the 45- and 25-second gel time specimens.

It was observed in numerous specimens that tracer fibers in the transition section flowing transverse to the specimen longitudinal axis experienced no significant distortion. In the same specimens, however, transition section tracer fibers oriented parallel to the longitudinal axis were frequently distorted. To maximize transverse flow and reduce longitudinal flow, two narrow preforms were constructed with the molding compound distributed on a volume basis. These preforms were nominally 1/2 inch narrower on each side than the normal preform. This was accomplished by inserting flexible foam inserts into the preform mold. The preforms were then compacted at a pressure of 40 psi.

These narrow preforms were molded at two different conditions (54-second dwell time with a 40-second closure and 36-second dwell time with a 54-second closure). The resultant specimens (DT-234A and DT-234B) exhibited center failures at relatively low strengths (23,200 and 23,500 psi, respectively). These low strengths were attributed in part to the presence of fiber-rich areas in the center section and to a greater proportion of transversely oriented fibers. Series DT-209, identical with specimen DT-234A except for preform width, exhibited an average tensile strength of 28,600 psi.

Series DT-235 specimens were evaluated to determine the effect of preform compaction on the failure strength and location. The preform was prepared using molding compound distributed on a volume basis. The preform was initially compacted at 0.75 psi and subsequently densified at 40 psi. The 40-psi level was selected based on a cursory study of the relationship between compaction pressure and final preform thickness. It was found that the thickness decreased rapidly as the pressure was increased to 40 psi. However, at higher pressures no significant thickness reduction was apparent. After 40-psi compaction, the center section thickness of the preform was approximately 0.180 inch - essentially half the thickness after the 0.75-psi compaction.

Two series DT-235 specimens were molded using a 54-second dwell time and a 20-second closure time. One specimen failed in the center section and the other in the transition section. The latter specimen was extensively crazed in the center section after tensile testing, indicating that the material was highly stressed. The average strength of these two specimens was 36,500 psi. This value was significantly higher than strengths obtained in the basic program for comparable specimens (series DT-207 and DT-208). The latter two series exhibited strengths of 27,670 psi (12-second closure time) and 27,470 psi (25.3-second closure time), respectively.

Series DT-236A through DT-236C specimens were evaluated to determine the effect of reduced molding temperature on increasing transition section strength. Reducing the die temperature to 275°F results in an increased resin viscosity and apparent stiffness of the preimpregnated fiber. The decreased temperature also reduces the polymerization rate of the epoxy resin and provides additional time for die closure. The 275°F molding temperature has one serious disadvantage - increased cure time. A 40-minute cure was utilized on the three specimens molded at 250°F.

Transition section failures were experienced with all specimens fabricated at 275°F. The tensile strengths of these specimens ranged from 27,800 to 37,000 psi (average of 32,400 psi). The average strength was similar to the long dwell, slow closure test data of 32,500 psi for series DT-228 specimens.

By reviewing all the data (flow patterns, fiber distortion, tensile strength, and failure location) generated to this point and considering the impact of the preform/molding procedure in the production of flight components, the specimens molded from compacted preforms (series DT-235) were judged to be the most promising. Therefore, additional specimens were produced to further evaluate the "minimum movement" concept.

Because the series DT-235 specimens showed evidence of some center-to-end material flow during molding, a weight distribution change was incorporated in all subsequent preforms. The uniform layer was reduced from 161 to 145 grams, and the difference was distributed equally among the four end buildups. A second modification, involving the construction of the preform on a light table, was implemented after molding the first specimen with the modified weight distribution. By using an optically transparent base plate in the preform mold in conjunction with the light table, it was possible to distribute the molding compound more uniformly than previous methods. The end buildups and the constant thickness core were constructed separately and subsequently assembled under low compaction pressure. The resultant preform was then densified at 40 psi and compression molded at 1000 psi.

The results of this evaluation are presented in Table 36. Specimen DT-237-1, prepared without the benefit of a light table, failed at the transition section at a stress of 35,600 psi. The other two specimens (DT-237-2 and DT-237-3) failed in the center section at 35,800 and 31,400 psi, respectively. The difference in strength of these latter specimens may have resulted from changes in the dwell and closure times. In all three specimens, the tracer fibers placed in the transition section in a T shape (top transverse to longitudinal axis) exhibited minimal flow and distortion.

TABLE 36. RESULTS OF SUPPLEMENTAL TESTS ON "MINIMUM" MOVEMENT" PREFORM CONCEPT

Specimen No.	Gel Time (sec)	Preform Weight Distribution	Dwell Time (sec)	Closure Time (sec)	Ult Tensile Strength (psi)	Failure Location
DT-237-1	45	Volume	54	26	35, 600	Transition
DT-237-2	45	↓	54	40	35, 800	Center
DT-237-3	45	↓	36	47	31, 400	Center

Five additional specimens were prepared to confirm that the "minimum movement" preform concept would produce center section failures. Two of the specimens were produced using 45-second gel time material and three with 25-second gel time material. The results given in Table 37 show that four center failures were experienced and that the fifth specimen (DT-237-8) failed in the transition section at 38, 100 psi, the highest strength of any of the five specimens. The strength of the four specimens with center failures ranged from 27, 800 to 36, 200 psi. The tracer fibers located in the transition section exhibited only slight distortion, as shown in Figure 47.

TABLE 37. RESULTS OF CONFIRMATION TESTS ON "MINIMUM MOVEMENT" PREFORM CONCEPT

Specimen No.	Gel Time (sec)	Preform Weight Distribution	Dwell Time (sec)	Closure Time (sec)	Ult Tensile Strength (psi)	Failure Location
DT-237-4	45	Volume	0	38	36, 200	Center
DT-237-5	45	↓	54	40	27, 800	Center
DT-237-6	25	↓	25	51	34, 100	Center
DT-237-7	25	↓	25	41	32, 200	Center
DT-237-8	25	↓	25	40	38, 100	Transition

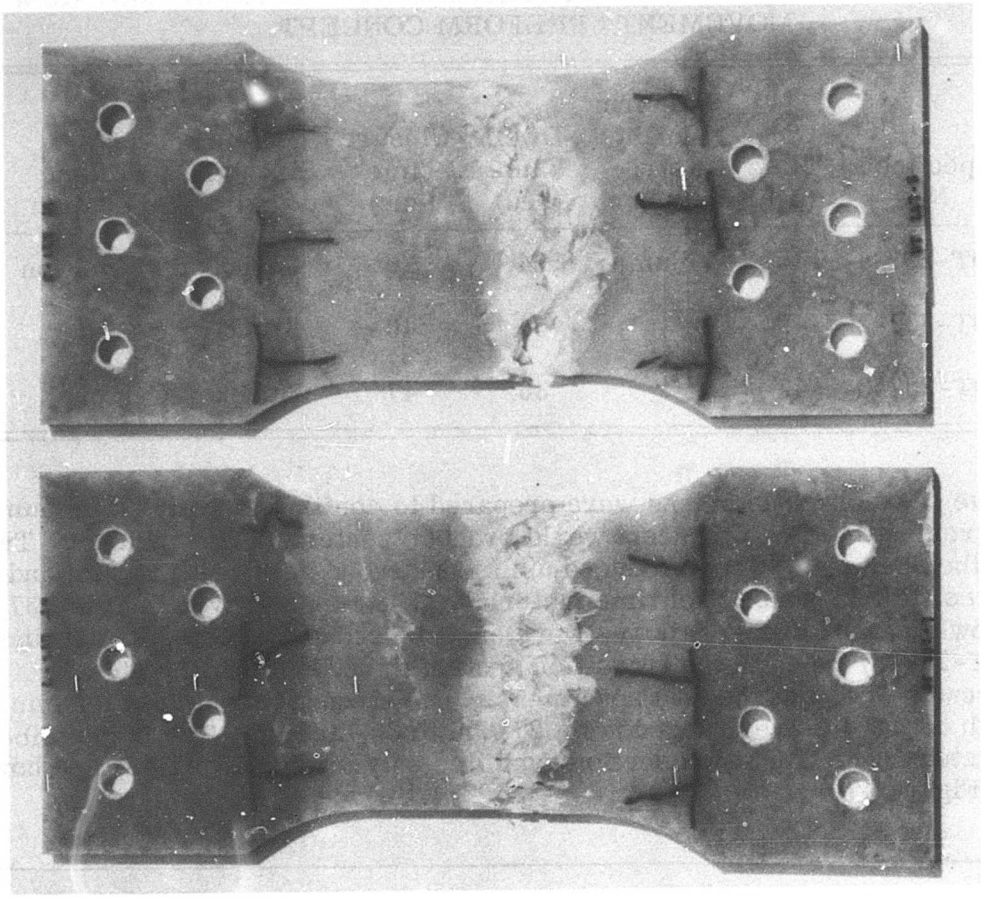

Figure 47. Slight Distortion of Transition Section Fibers as Evidenced by Tracer Material.

It is significant to note that an extremely short molding cycle (0-second dwell and 38-second closure time) produced a center failure in specimen DT-237-4 at a high stress level (36,200 psi). Although the data are extremely limited, this suggests that considerable flexibility is available within the molding parameters for producing high-quality composites if the "minimum movement" preform technique is used.

Conclusions and Recommendations

A preforming method was developed that dramatically reduced the

frequency of transition section failures. This method differs from former preforming processing in two significant aspects. First, the preform is fabricated with a full-length core of molding compound. This eliminated the artificial wall and the resulting fiber crippling that was produced by limiting materials to specific sections of the specimen. Second, the preform was compacted to reduce material movement during the molding cycle. Both changes are considered vital factors to the elimination of transition section failures.

This new "minimum movement" preform approach, coupled with a light table to aid in material distribution, produced center failures in 88 percent of the specimens. Only one specimen out of the eight tested experienced a transition section failure, and this occurred at a very high stress level.

None of the various material and molding cycle changes examined in this program consistently contributed to center failures. However, the study did provide valuable information relative to the parametric limits within which high-quality moldings could be produced.

Because of the outstanding success achieved in eliminating transition section failures, the "minimum movement" preform technique was adopted for the balance of the Phase I specimen fabrication.

TASK II - BALLISTIC DAMAGE AND CRACK PROPAGATION STUDY

GENERAL

The objective of the Task II program was to select the most promising discontinuous fiber glass-epoxy composite, based on a comprehensive empirical evaluation of the three candidate composites chosen from the Task I program. The most promising composite would subsequently be characterized in Task III and ultimately used in ballistically tolerant flight control components. The following three candidate composites were selected for evaluation:

1. 1-inch S-2 glass fibers (470 finish) in a 438 epoxy resin matrix
2. 1/2-inch S-2 glass fibers (470 finish) in a 438 epoxy resin matrix
3. 1-inch E glass fibers (897 finish) in a 332-732 epoxy resin matrix

The nominal fiber content was 52 v/o for each composite. For brevity, these three candidate composites will be referred to as 470/438-1, 470/438-1/2, and 897/332-732-1 throughout the discussion of the Task II program.

The Task II program was divided into the seven independent investigations (subtasks) listed below. The title of each subtask is indicative of the general character of the effort involved.

1. Static Tensile Properties of Undamaged Composites
2. Effect of Ballistic Impact Conditions on Composite Damage and Load Capacity
3. Cyclic Tensile Fatigue Properties of Undamaged and Damaged Composites
4. Composite Fracture Toughness
5. Effect of Composite Thickness on Ballistic Damage and Residual Load Capacity
6. Effect of Combined Stress and Ballistic Impact Conditions (Threshold)

7. Selection of the Most Promising Composite

Each of the subtasks under Task II is discussed in detail in this section of the report.

SUBTASK 1 - STATIC TENSILE PROPERTIES OF UNDAMAGED COMPOSITES

General

Subtask 1 presents a compilation of all tensile property data generated during the Task II program on undamaged composites. The fact that these data are reported as the lead topic in Task II should not be construed as having any chronological significance. Rather, this organization is intended to provide a more thorough understanding of the candidate composites prior to a discussion of the various Task II investigations.

This study involved the determination of the static tensile properties (strength and modulus) of 1/8-inch-thick specimens of the three candidate composites. In addition, the effect of composite thickness on these properties was established from an evaluation of 1/16-, 1/8-, 1/4-, and 3/8-inch-thick 470/438-1 specimens. The tensile tests for these studies were performed at room temperature on undamaged, net-molded, standard 3.5-inch-wide ballistic/tensile specimens. Finally, the distribution of tensile properties across the standard specimen was determined for the three candidate materials at -80°F, room temperature, and 160°F. This latter investigation was conducted on narrow specimens cut from 1/8-inch-thick, 3.5-inch-wide specimens.

Approach to the Problem

The ultimate tensile strength and modulus of 1/8-inch-thick, 3.5-inch-wide undamaged specimens were determined at room temperature on six replicates of each candidate composite. The modulus values were calculated from load-deflection curves generated during testing. The thickness effects study was performed at room temperature on standard specimens of the 470/438-1 composite, using four replicates at each nominal thickness level, i.e., 1/16, 1/8, 1/4, and 3/8 inch. Again, load-deflection curves were obtained during tensile testing for modulus determination.

The narrow specimens used to define the distribution of tensile strength and modulus across the standard specimen were nominally 1/2 inch wide

and 1/8 inch thick in the gage area. The specimens were 3/4 inch wide at the ends and had an overall length of 8.5 inches. Four specimens were prepared from each standard specimen - two each from the edge and center areas. The edge-cut specimens were considered representative of partially aligned material. The specimens cut from the center area were considered typical of randomly oriented material. Eighty-four specimens, 28 of each candidate material, were evaluated. Eight specimens each were tested at -80° and 160°F and 12 at room temperature. Each group of specimens contained an equal number of edge- and center-cut specimens. An extensometer with a 2-inch gage length was mounted on the narrow specimens during tensile testing to obtain a stress-strain curve.

Discussion of Results

The average tensile strength and modulus values for 1/8-inch-thick undamaged standard specimens of the three candidate composites are presented in Table 38. The modulus values were calculated from the initial slope of the load-deflection curves. The averages given for the 470/438-1 composite include the 1/8-inch-thick specimen data from Subtask 5 of Task II.

TABLE 38. ROOM-TEMPERATURE TENSILE PROPERTIES OF UNDAMAGED STANDARD SPECIMENS

Composite	Ultimate Tensile Strength (psi)	Initial Tensile Modulus (psi x 10^6)
470/438-1	27,440	3.50
470/438-1/2	22,950	3.59
897/332-732-1	29,120	3.47

The results indicate that the 897/332-732-1 composite exhibits the highest tensile strength (29,120 psi) of the three candidate composites. The lowest strength (22,950 psi) was obtained, as expected, for the composite with the shorter (1/2-inch) fibers. Of the 22 specimens tested, only two failed in the transition section, and these occurred at strength levels that exceeded the group average. This is dramatic evidence that the serious transition section failure problem encountered in Task I was satisfactorily resolved.

The modulus data for the two 470/438 composites indicate that fiber length, at least within the range examined, has no significant effect on initial tensile modulus. With respect to the 897/332-732-1 composite, the modulus is similar to the 470/438 composites despite the fact that the glass and resin moduli are lower than the constituents in the 470/438 composites. The explanation for this apparent anomaly is the higher fiber content of the 897/332-732-1 composite. The fiber content of this composite was 59.2 v/o compared with 52.2 v/o for both of the 470/438 composites. This higher fiber content may also have contributed to an increase in undamaged tensile strength.

The tensile strength and modulus data generated in the thickness effects investigation (Subtask 5) on 470/438-1 composites are summarized in Table 39 and shown graphically in Figure 48. The values are based on 10 replicates for the 1/8-inch-thick specimens and four replicates for the other three specimen thicknesses.

Based on the limited thickness testing involved, it appears that maximum strength results at or near a composite thickness of 1/4 inch. The lower strength associated with the 1/16-inch-thick specimens may be attributed to less randomness in the location of fiber ends. Any concentration of fiber ends at a common location will result in reduced strength. The possibility of such an occurrence decreases directly with specimen thickness. The differences in strength for the thicker specimens (1/8, 1/4, and 3/8 inch) are not considered significant.

TABLE 39. EFFECT OF THICKNESS ON TENSILE PROPERTIES OF UNDAMAGED 470/438-1 SPECIMENS

Thickness (in.)	Ultimate Tensile Strength (psi)	Initial Tensile Modulus (psi x 10^6)
0.062	24,770	3.74
0.126	27,440	3.50
0.253	29,550	3.68
0.371	28,880	3.67

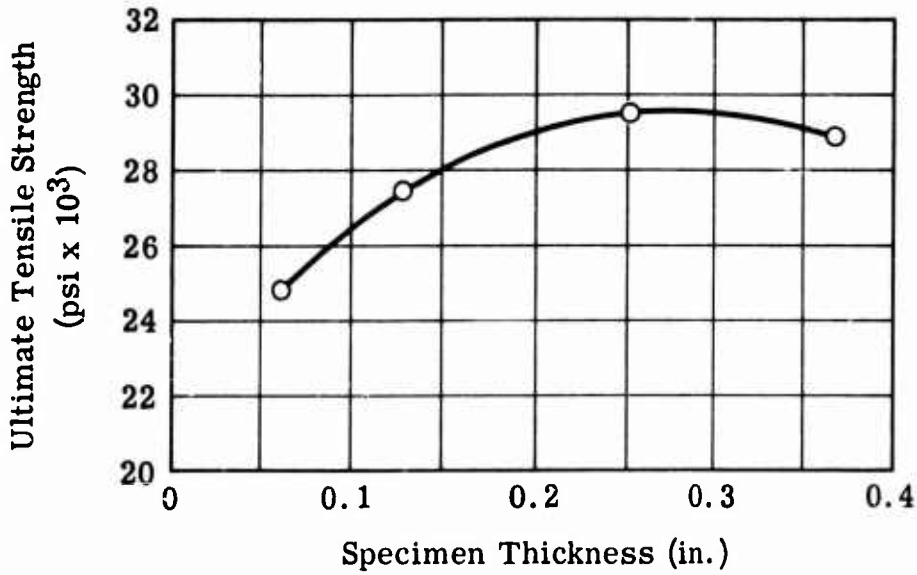

Figure 48. Effect of Thickness on Tensile Strength of Undamaged 470/438-1 Specimens.

With respect to initial tensile modulus, it would appear that specimen thickness has an insignificant effect within the range examined. Although some modulus decrease might be expected with increased thickness due to third dimension fiber randomness, this is probably minimized by the preforming technique used in specimen fabrication.

Tensile strength and modulus data for both center- and edge-cut specimens of the three candidate composites tested at -80°F, room temperature, and 160°F are summarized in Table 40. Graphical presentations of strength and modulus as a function of the test temperature are shown in Figures 49 and 50, respectively. As expected, the tensile properties generally decrease with increasing temperature.

A better appreciation of the effect of temperature on strength and modulus can be obtained from the ratios of elevated and low-temperature properties to room-temperature values given in Table 41. These data indicate that the tensile properties at 160°F are approximately 66 percent of the room-temperature values. This factor is relatively constant for all three candidate composites regardless of specimen origin, i.e., edge or center. At -80°F an increase in average strength and modulus can be observed compared with room-temperature data. The average increases amounted to approximately 15 and 8 percent, respectively, for strength and modulus.

TABLE 40. EFFECT OF TEMPERATURE ON TENSILE PROPERTIES OF UNDAMAGED SPECIMENS

Composite	Temp (°F)	Ultimate Tensile Strength (psi)		Initial Tensile Modulus (psi x 10^6)	
		Center	Edge	Center	Edge
470/438-1	-80	27,150	42,400	3.29	4.45
	75	25,370	34,130	3.00	3.83
	160	15,980	22,270	1.90	2.65
470/438-1/2	-80	20,360	21,570	3.11	3.57
	75	19,640	22,770	3.02	3.63
	160	12,590	14,170	1.84	2.26
897/332-732-1	-80	28,630	43,540	3.43	4.15
	75	21,790	33,140	2.85	3.50
	160	16,890	21,340	1.88	2.65

TABLE 41. TENSILE STRENGTH AND MODULUS RATIOS (TEMPERATURE BASIS) FOR UNDAMAGED SPECIMENS

Composite	Specimen Origin	Strength Ratios		Modulus Ratios	
		σ_{160}/σ_{75}	σ_{-80}/σ_{75}	E_{160}/E_{75}	E_{-80}/E_{75}
470/438-1	Center	0.630	1.070	0.633	1.098
	Edge	0.652	1.243	0.692	1.161
470/438-1/2	Center	0.641	1.034	0.609	1.030
	Edge	0.622	0.948	0.623	0.984
897/332-732-1	Center	0.775	1.318	0.660	1.024
	Edge	0.644	1.316	0.757	1.187
Average		0.661	1.155	0.662	1.081

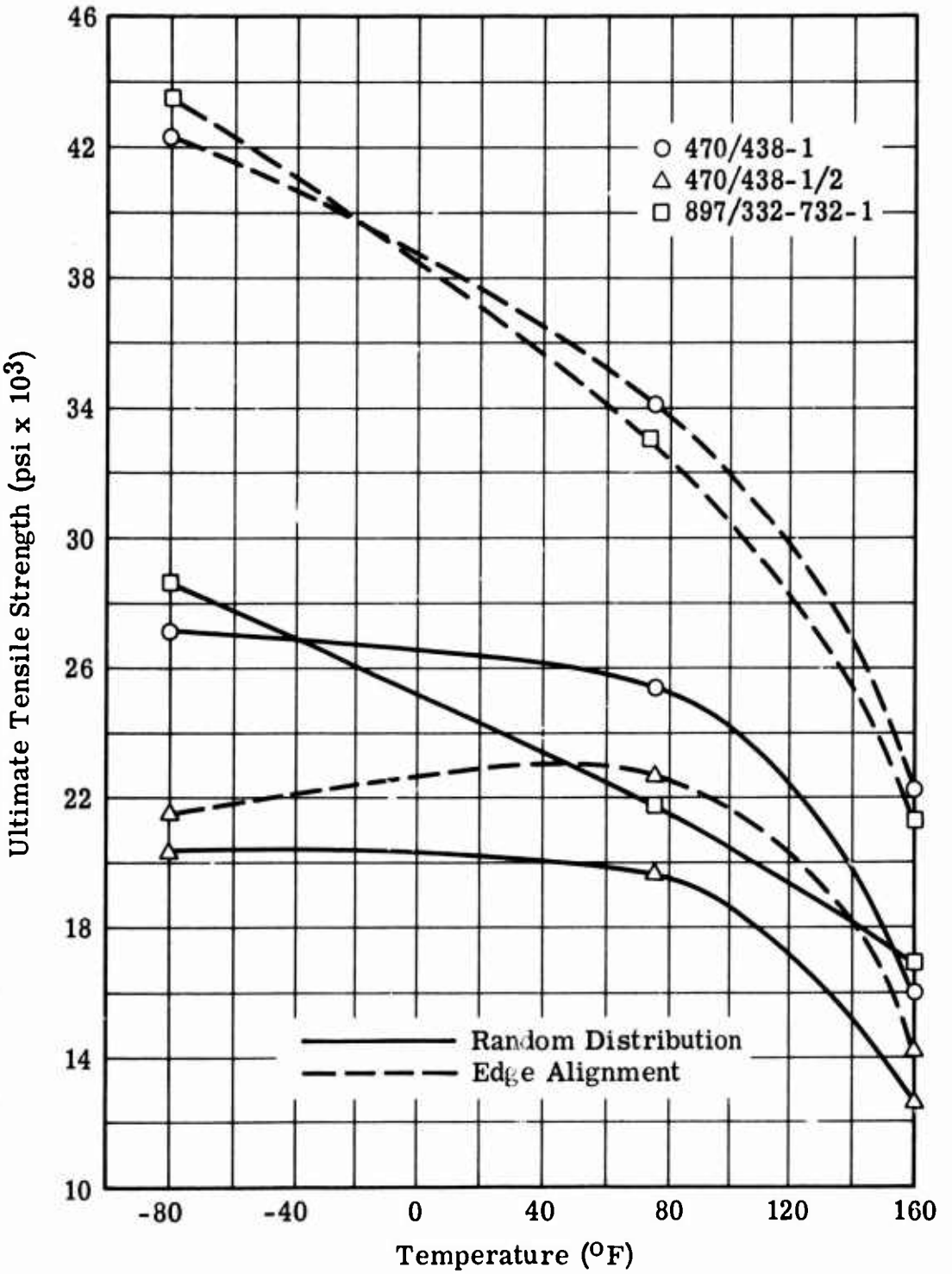

Figure 49. Effect of Temperature on Tensile Strength of Undamaged Specimens.

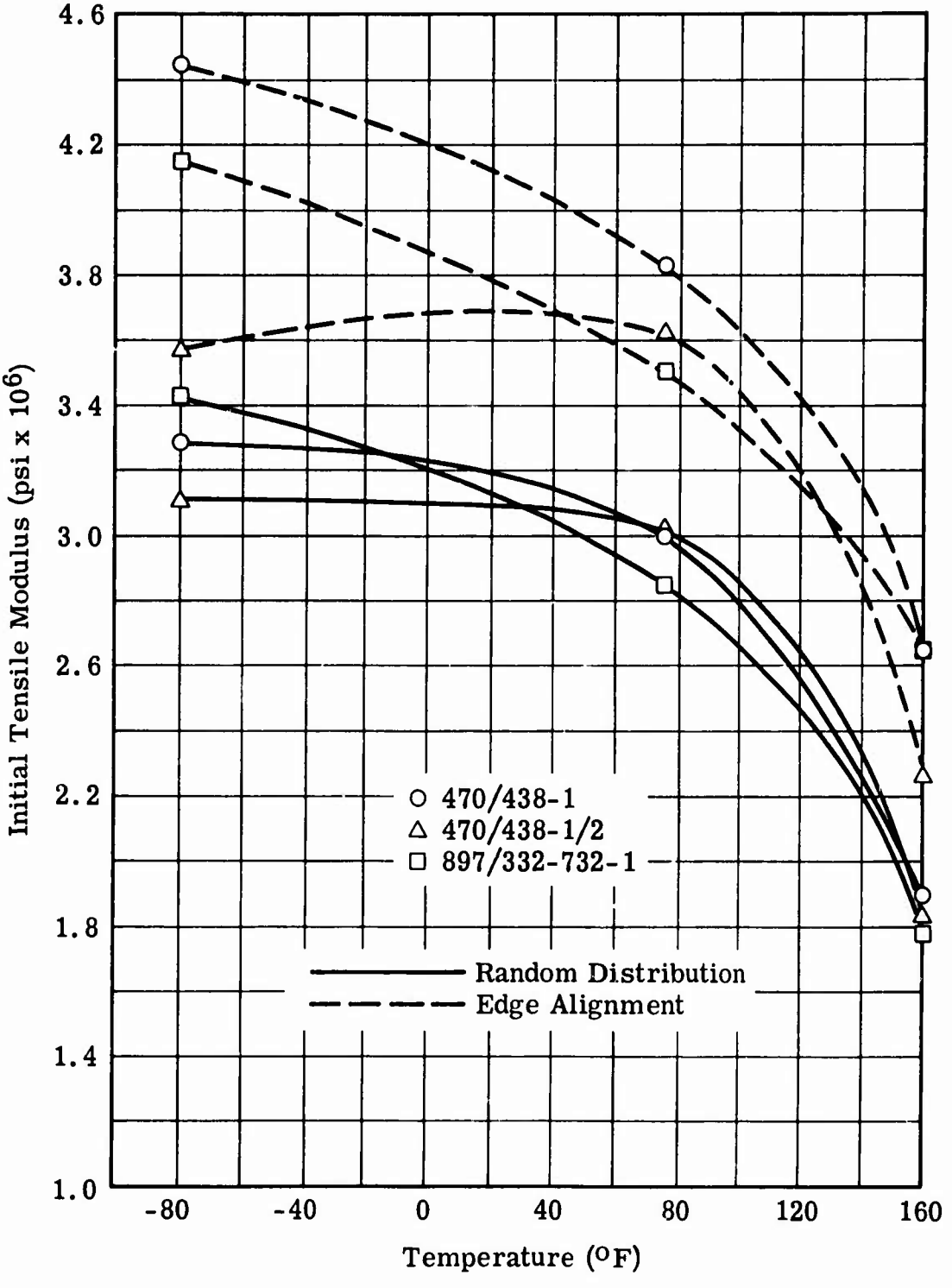

Figure 50. Effect of Temperature on Tensile Modulus of Undamaged Specimens.

The narrow specimen tensile test data reported in Table 40 were used to compute the edge-to-center ratios presented in Table 42 for strength and modulus at the three test temperatures. Although these ratios are not constant across all temperature levels for a particular composite, no definite trend is evident with respect to temperature. These variations in tensile property ratios were accepted as random occurrences. Therefore, the ratios were averaged for each composite and tensile property to obtain more representative values.

TABLE 42. EDGE-TO-CENTER TENSILE STRENGTH AND MODULUS RATIOS FOR UNDAMAGED SPECIMENS

Composite	Temp (°F)	Edge-to-Center Ratios	
		Strength	Modulus
470/438-1	-80	1.562	1.352
	75	1.345	1.277
	160	1.394	1.395
		1.434[a]	1.341[a]
470/438-1/2	-80	1.059	1.148
	75	1.159	1.202
	160	1.125	1.228
		1.114[a]	1.193[a]
897/332-732-1	-80	1.521	1.210
	75	1.521	1.228
	160	1.263	1.409
		1.435[a]	1.282[a]

[a]Ratios were averaged to obtain more representative values.

The degree of fiber alignment in composites with discontinuous reinforcements is suspected to be closely related to fiber length and independent of fiber or resin type. Interestingly, the average edge-to-center strength ratio across all temperatures is 1.43 for both composites with 1-inch fibers. Essentially this means that the 1/2-inch width at the edges of the standard 3.5-inch-wide specimen will carry 43 percent more load than a similar specimen cut from the center area. The average edge-to-center

modulus ratios were 1.34 and 1.28 for the 470/438-1 and 897/332-732-1 composites, respectively. The average edge-to-center strength and modulus ratios for the 470/438-1/2 composite were 1.11 and 1.19, respectively. These results confirm that the degree of fiber alignment along net-molded specimen edges is strongly influenced by fiber length.

Conclusions

The following conclusions can be drawn from the investigation of static tensile properties of undamaged specimens:

1. The transition section failure problem experienced in Task I has virtually been eliminated through the use of a modified preforming technique.

2. The tensile strength of net-molded, 3.5-inch-wide specimens of the 470/438-1 composite is approximately 16 percent higher than the same fiber glass and resin combination with 1/2-inch fibers.

3. The average tensile strength of 1/16-inch-thick, net-molded specimens of the 470/438-1 composite was lower than that obtained with 1/8-, 1/4-, and 3/8-inch-thick specimens.

4. A reduction in tensile strength and modulus of approximately 34 percent was experienced at 160°F compared with room-temperature values. This decrease is independent of composite type and specimen origin (center or edge cut).

5. Increases of about 15 and 8 percent in tensile strength and modulus, respectively, were obtained at -80°F over room-temperature values.

6. Edge material cut from net-molded, 3.5-inch-wide specimens with 1-inch fibers have approximately 43 percent more load-carrying capability than material from the center area. This is due to fiber alignment along the edges of the net-molded specimens.

7. The 470/438-1/2 composites have substantially less edge fiber alignment than composites with 1-inch fibers. The edge strength of the 470/438-1/2 specimens was only 11 percent greater than the center strength.

SUBTASK 2 - EFFECT OF BALLISTIC IMPACT CONDITIONS ON COMPOSITE DAMAGE AND LOAD CAPACITY

General

The objective of this investigation was to determine the effects of projectile type, impact velocity, and test temperature on the extent of ballistic damage and residual tensile load capacity of the three candidate composites. The most critical impact conditions would be determined from this study and used in subsequent Task II investigations.

Approach to the Problem

The basic test plan involved evaluation of the three candidate composites with two projectiles (caliber .50 AP M2 and tumbled caliber .30 ball M2) at three impact velocities (1500, 1800, and 2100 ft/sec) and three temperatures (-80°F, ambient, and 160°F). Three replicates of the 1/8-inch-thick standard specimens would be tested under each set of impact conditions. A grand total of 162 specimens, 81 with each projectile, were involved in the program. These specimens would be preloaded to 35 percent of the room temperature tensile strength of undamaged specimens. Consequently, the specimens of each composite type were tested under constant load rather than constant stress.

The post-ballistic test evaluation consisted of a visual damage assessment followed by residual tensile load capacity determination at room temperature. Rejection criteria previously discussed were applied to the test values prior to final data analysis.

Results of Caliber .50 AP M2 Projectile Impact Tests

A summary of visual area damage on both the front and back specimen surfaces resulting from untumbled caliber .50 AP M2 impacts is presented in Table 43. This table also includes damage volume, which was calculated by using the equation for a conical frustrum with bases corresponding to the front and back surface damage areas. This formula is defined in Equation (2) of the "Test and Evaluation Techniques" discussion.

The average front surface damage areas across all experimental levels for the 470/438-1, 470/438-1/2, and 897/332-732-1 composites were 0.629, 0.557, and 0.559 $in.^2$, respectively. All composites tend to exhibit the greatest front surface damage area at -80°F and the least at

TABLE 43. SUMMARY OF VISUAL BALLISTIC DAMAGE - CALIBER .50 AP M2 IMPACTED SPECIMENS

Velocity (ft/sec)	470/438-1			470/438-1/2			897/332-732-1		
	Temperature (°F)			Temperature (°F)			Temperature (°F)		
	-80	RT	160	-80	RT	160	-80	RT	160
	A. Front Surface Area (in.^{2})[a]								
1500	0.67	0.54	0.49	0.56	0.51	0.51	0.60	0.41	0.47
1800	0.63	0.61	0.58	0.65	0.50	0.59	0.58	0.49	0.64
2100	0.73[b]	0.64	0.77	0.59	0.52	0.58	0.57[b]	0.56	0.71
	B. Back Surface Area (in.^{2})[a]								
1500	2.06	2.03	1.83	1.51	1.40	1.36	1.63	1.37	1.31
1800	1.88	2.29	1.84	1.40	1.21	1.26	1.88	1.49	1.30
2100	2.21	1.56	1.72	1.32[b]	1.34	1.20	1.73[b]	1.45	1.40
	C. Volume (in.^{3})[a]								
1500	0.169	0.150	0.137	0.126	0.114	0.109	0.136	0.108	0.107
1800	0.153	0.170	0.149	0.124	0.101	0.110	0.147	0.117	0.117
2100	0.177[b]	0.134	0.159	0.115[b]	0.108	0.106	0.135[b]	0.120	0.130

[a] Values are based on three replicates except as noted.

[b] Values are based on six replicates.

room temperature. Damage area generally increases directly with velocity.

The longer fiber composites experience more back surface damage than composites reinforced with 1/2-inch-long fibers. The average back surface damage areas were 1.936, 1.333, and 1.507 in.^{2} for the 470/438-1, 470/438-1/2, and 897/332-732-1 composites, respectively. Damage area tended to increase indirectly with temperature and was generally unaffected by changes in velocity.

The results of damage volume were similar to the back surface damage area in temperature and velocity effects. The average damage volume was greatest with the 470/438-1 composite and least with the 470/438-1/2 composite. The average values were 0.1552, 0.1126 and 0.1241 in.^{3}, respectively, for the 470/438-1, 470/438-1/2, and 897/332-732-1 composites.

The transverse ballistic damage measurements summarized in Table 44 reflect the same relative composite performance as that observed for damage areas and volume. On the basis of grand averages for each composite type, the 470/438-1 composite exhibits the greatest transverse damage and the 470/438-1/2 composite exhibits the least damage.

The front surface transverse damage was generally lowest at room temperature. Damage tended to increase directly with impact velocity. The grand averages for the 470/438-1, 470/438-1/2, and 897/332-732-1 composites were 0.907, 0.859, and 0.903 inch, respectively.

The back surface transverse damage generally varied indirectly with both temperature and velocity. The influence of fiber length is typically more apparent on back surface damage (area or transverse) than on the impact surface. The average back surface transverse damage values across the entire experiment were 1.684, 1.374, and 1.526 inches for the 470/438-1, 470/438-1/2, and 897/332-732-1 composites, respectively.

TABLE 44. SUMMARY OF VISUAL TRANSVERSE BALLISTIC DAMAGE - CALIBER .50 AP M2 IMPACTED SPECIMENS

Velocity (ft/sec)	470/438-1			470/438-1/2			897/332-732-1		
	Temperature (°F)			Temperature (°F)			Temperature (°F)		
	-80	RT	160	-80	RT	160	-80	RT	160
	A. Front Surface Transverse Damage (in.)[a]								
1500	0.97	0.90	0.83	0.85	0.83	0.87	0.87	0.82	0.75
1800	0.90	0.81	0.85	0.90	0.80	0.94	0.88	0.81	1.03
2100	1.02[b]	0.89	0.99	0.82	0.84	0.88	0.90[b]	0.97	1.10
	B. Back Surface Transverse Damage (in.)[a]								
1500	1.78	1.85	1.50	1.50	1.37	1.50	1.57	1.70	1.42
1800	1.67	1.71	1.58	1.39	1.24	1.29	1.58	1.40	1.49
2100	1.90[b]	1.57	1.69	1.37[b]	1.36	1.35	1.56[b]	1.61	1.40
	C. Avg Front/Back Surface Transverse Damage (in.)[a]								
1500	1.38	1.37	1.17	1.19	1.10	1.18	1.21	1.26	1.08
1800	1.28	1.26	1.23	1.15	1.02	1.10	1.22	1.11	1.25
2100	1.46[b]	1.23	1.30	1.09[b]	1.10	1.10	1.22[b]	1.30	1.25

[a] Values are based on three replicates except as noted.

[b] Values are based on six replicates.

The average front/back surface transverse damage for the 470/438 composites was generally greatest at -80°F. The 897/332-732-1 composite was unaffected by changes in the test temperature. The impact velocity does not appear to have a significant effect on average transverse damage. The specimens reinforced with 1/2-inch fibers exhibited less damage than either of the composites with 1-inch fibers. The grand averages for the 470/438-1, 470/438-1/2, and 897/332-732-1 composites were 1.298, 1.114, and 1.211 inches, respectively.

In summary, maximum damage tends to occur at -80°F, where the composites are more brittle. No definite relationship was apparent between the extent of ballistic damage and impact velocity for all damage parameters. With respect to the influence of composite type, the 470/438-1 composite exhibited the greatest average damage and the 470/438-1/2 the least damage across all visual damage parameters.

The tensile load capacity of the caliber .50 AP M2 damaged specimens is summarized in Table 45. The reported values have been normalized to a 1/8-inch specimen thickness. It should be noted that seven specimens impacted at 160°F failed away from the ballistic wound during residual load capacity tests. In reviewing the damage records for these specimens, it was observed that structural degradation had occurred away from the perforation. This degradation manifested itself in the form of small, localized separation or cracks. The probable cause of these cracks was high stress in the impacted specimen, resulting from the initial preload and the reduced structural properties at 160°F. It was subsequently established from static strength tensile data at 160°F that the initial preload was approximately 50 percent of the average specimen strength. After nominal damage from a tumbled caliber .30 ball M2 projectile impact, the load in the residual material increased to 80 percent or more of the 160°F strength. Because these failures occurred away from the perforation and did not extend from the damaged area, it can be concluded that the effective ballistic damage was less critical at 160°F than at -80°F or room temperature. Therefore, the 160°F condition is not considered the temperature at which maximum damage occurs.

The average load capacity of the 470/438-1 composites was 10,500 pounds across the entire temperature-velocity experiment. The average undamaged tensile strength was 27,440 psi, or 12,030 pounds, for the standard 1/8-inch-thick specimen. Therefore, an average reduction in load capacity of 1530 pounds was experienced, or 12.6 percent of the undamaged load capacity. Actually, the average front surface transverse damage was 0.907 inch, or 25.8 percent of the standard specimen width. Even if effective damage was assumed to be equal to the projectile diameter, i.e., 0.50 inch, then a loss of 1/7, or 14.2 percent, in load capacity

TABLE 45. SUMMARY OF RESIDUAL LOAD CAPACITIES[a] FOR CALIBER .50 AP M2 IMPACTED SPECIMENS

Velocity (ft/sec)	470/438-1			470/438-1/2			897/332-732-1		
	Temperature (°F)			Temperature (°F)			Temperature (°F)		
	-80	RT	160	-80	RT	160	-80	RT	160
1500	9,567	9,270	10,923	7,203	7,930	7,173	9,157	8,157	10,390
1800	10,183	12,805[b]	11,373	7,305[b]	7,937	7,487	9,057	9,260	10,135[b]
2100	10,343	10,590	9,450	7,362[c]	8,150[b]	7,250	8,892[c]	10,025[b]	8,773

[a]Data normalized to a 1/8-inch specimen thickness. Values (in pounds) are based on three replicates except as noted.

[b]Values are based on two replicates.

[c]Values are based on six replicates.

would be expected. This apparent anomaly is due, in part, to the difference in load capacity between the center and edge materials. The ballistic impact destroys lower strength, randomly oriented material from the center section of the specimen. This center material has an average tensile strength of 25,370 psi compared to 27,440 psi for net-molded, 3.5-inch-wide specimens.

The strength retained by the 470/438-1 composite after caliber .50 AP M2 projectile impacts is extremely high compared with the 470/438-1/2 and 897/332-732-1 composites, which will be discussed in subsequent paragraphs. This is in direct conflict with the damage measurements, which consistently indicate more damage with the 470/438-1 composites. One possible explanation is that these ballistic specimens had an unusually high degree of fiber alignment along the edges and, consequently, possessed higher basic strength.

No definite trend in residual load capacity for the 470/438-1 composites is apparent with respect to either temperature or velocity. Both of the extreme values for the cells occurred at room temperature - the low value at 1500 ft/sec and the high at 1800 ft/sec.

The grand average for residual load capacity of 470/438-1/2 composites was 7533 pounds, with a maximum deviation of 617 pounds for any individual cell from the average. Based on an undamaged load capacity of 10,070 pounds, the caliber .50 AP M2 projectile impact caused a loss in load capacity of 2537 pounds, or 25.2 percent. With regard to the temperature effect on residual load capacity, it appears that ballistic impacts

at room temperature are less damaging than those at -80° or 160°F. The impact velocity has no significant effect on post-damage strength.

The 897/332-732-1 composites exhibited an average residual load capacity of 9316 pounds across the entire experiment. Based on an undamaged load capacity of 12,780 pounds (tensile strength of 29,120 psi), a loss of 3464 pounds, or 27.1 percent, in load capacity resulted from caliber .50 AP M2 projectile impacts. Within the range examined, test temperature and impact velocity do not have a significant effect on residual load capacity.

Results of Tumbled Caliber .30 Ball M2 Projectile Impact Tests

A cell-form summary of preliminary residual load capacity data, normalized to a 1/8-inch composite thickness, for tumbled caliber .30 ball M2 impacted specimens is presented in Table 46 for the three candidate composites. The cell values are averages of acceptable data after application of rejection criteria discussed earlier in this report. When these criteria were applied, 12 residual load capacity values were rejected. Replacement specimens were subsequently evaluated under the appropriate temperature-velocity test conditions. The results of the replacement testing are presented in a later portion of this subtask.

The Table 46 data indicate that the 470/438-1 composites generally exhibit higher residual load capacity than the 897/332-732-1 composites at corresponding temperature-velocity levels. The post-damage load capacity of the 470/438-1/2 composite is significantly lower than that of the composites with 1-inch fibers. Average load capacities across all temperature-velocity levels for the 470/438-1, 470/438-1/2, and 897/332-732-1 composites were 7,908, 5,704, and 7,528 pounds, respectively.

An examination of the residual load capacity data in Table 46 did not identify any one set of temperature-velocity conditions as being the most critical. It is evident, however, that the tumbled caliber .30 ball M2 projectile produces more extensive damage, as evidenced by the substantially lower load capacities compared with the caliber .50 AP M2 data.

Because no definite trend was evident between impact conditions and residual load capacity, the data from tumbled caliber .30 ball M2 impacted specimens were subjected to multiple regression analysis. Only the caliber .30 ball M2 data were considered since the damage is more severe with this projectile. In multiple regression analysis, a least-square fit of the data to a selected mathematical function is obtained. A general quadratic equation is commonly used when the relationship between the independent variables (velocity and temperature) and dependent

TABLE 46. PRELIMINARY SUMMARY OF RESIDUAL LOAD CAPACITIES[a] FOR TUMBLED CALIBER .30 BALL M2 IMPACTED SPECIMENS

Velocity (ft/sec)	470/438-1			470/438-1/2			897/332-732-1		
	Temperature (°F)			Temperature (°F)			Temperature (°F)		
	-80	RT	160	-80	RT	160	-80	RT	160
1500	7060[b]	7980	7527	6097	5810[b]	5820	6940[b]	7260[b]	8193
1800	7093	8913	6925[b]	6050	5795[b]	4973	7570	7420[b]	7313
2100	9223	8430	8017	5867	5367	5513	8640[c]	7590	6830[b]

[a] Data normalized to a 1/8-inch specimen thickness. Values (in pounds) are based on three replicates except as noted.

[b] Values are based on two replicates.

[c] Values are based on one replicate.

variable (residual load capacity) is unknown. The following quadratic equation was fitted to the individual specimen data:

$$Y = a_0 + a_1x_1 + a_2x_2 + a_{11}x_1^2 + a_{22}x_2^2 + a_{12}x_1x_2 \qquad (19)$$

where Y = residual load capacity, lb

x_1 = temperature, °R

x_2 = impact velocity, ft/sec

The values for the constant and coefficients are presented in Table 47. In addition, this table includes the coefficient of determination, $R^2 \times 100$, which is an estimate of the percentage of variability in the response data (Y) that has been accounted for by the equation.

The low $R^2 \times 100$ values are attributed, in part, to a high degree of data variability generally present within each experimental cell. Despite the relatively poor data fit, the residual load capacities predicted from the regression functions and reported in Table 48 agree reasonably well with the observed data (Table 46) for the corresponding velocity-temperature conditions.

TABLE 47. MULTIPLE REGRESSION COEFFICIENTS FOR PRELIMINARY RESIDUAL LOAD CAPACITY DATA

Composite	a_0	a_1	a_2	a_{11}	a_{22}	a_{12}	$R^2 \times 100$
470/438-1	-3,225.30	81.87	-11.37	-0.0583	0.0055	-0.0138	24.3
470/438-1/2	22,628.11	-9.71	-15.04	0.0079	0.0040	-0.0002	19.6
897/332-732-1	422.08	24.58	0.30	0.0073	0.0026	-0.0180	23.2

TABLE 48. SUMMARY OF PREDICTED RESIDUAL LOAD CAPACITIES[a] FOR TUMBLED CALIBER .30 BALL M2 IMPACTED SPECIMENS

Velocity (ft/sec)	470/438-1			470/438-1/2			897/322-732-1		
	Temperature (°F)			Temperature (°F)			Temperature (°F)		
	-80	RT	160	-80	RT	160	-80	RT	160
1500	7003	8260	7620	6307	6065	5679	6797	7495	7964
1800	7473	8085	7186	5796	5385	5254	7582	7278	7331
2100	8875	8963	7766	5907	5496	5347	8904	7506	7110

[a] Values are given in pounds.

The Table 48 data indicate that the minimum residual load capacity within the experimental range of the variables occurs at 1500 ft/sec and -80°F for both the 470/438-1 and 897/332-732-1 composites. A lower load capacity was predicted if the impact velocity were further reduced. The 897/332-732-1 composite at 160°F also shows a decreasing load capacity with increasing velocity. The 470/438-1/2 composite exhibited consistently lower load capacity values at 160°F than at the other two test temperatures. Although the minimum load capacity was predicted to occur at an impact velocity of 1800 ft/sec, the value at 2100 ft/sec was only marginally higher.

The multiple regression equations generally suggested that a further reduction in post-damage strength might be obtained at low temperature and low velocity as well as high temperature and high velocity. Consequently, additional ballistic tests were conducted with tumbled caliber .30 ball M2 projectiles at 1200 ft/sec and -80°F and at 2400 ft/sec and 160°F to explore this possibility.

The following discussions regarding the extent of damage and residual load capacity of tumbed caliber .30 ball M2 impacted specimens are based on the preliminary data reported above as well as the results of the replacement and the extended velocity-temperature testing.

The extent of area and volume damage experienced by the 1/8-inch-thick standard specimens as a result of tumbled caliber .30 ball M2 impacts is reported in Table 49. The average front surface damage areas across all test conditions were 1.278, 1.038, and 1.066 in.^{2} for the 470/438-1, 470/438-1/2, and 897/332-732-1 composites, respectively. Greater damage generally occurred at -80°F for the 470/438 composites and 160°F for the 897/332-732-1 composites. The ballistic impacts at room temperature caused less front surface damage area for all three candidate composites regardless of impact velocity. Damage tended to increase directly with projectile velocity irrespective of test temperature.

The overall average back surface damage areas for the 470/438-1, 470/438-1/2, and 897/332-732-1 composites were 4.567, 2.622, and 3.643 in.^{2}, respectively. Damage generally increased indirectly with temperature and was essentially unaffected by changes in impact velocity.

Since the 470/438-1 composites exhibit more front and back surface damage area than the other two composites, they also exhibit more volume damage. The 470/438-1/2 composite experienced the least damage, with the 897/332-732-1 composite showing intermediate volume damage. The average volume values across the entire experiment were 0.3445, 0.2236, and 0.2764 in.^{3} for the 470/438-1, 470/438-1/2, and 897/332-732-1 composites, respectively. Neither the test temperature nor the impact velocity appears to have a strong influence on damage volume. There is a subtle suggestion that greater damage occurs at low temperature and at high impact velocity.

The visual transverse damage sustained by the tumbled caliber .30 ball M2 impacted specimens is reported in Table 50. The grand averages for front surface transverse damage were 1.545, 1.466, and 1.465 inches for the 470/438-1, 470/438-1/2, and 897/332-732-1 composites, respectively. The transverse damage of the 470/438 composites appears to be unaffected by temperature changes, whereas damage is generally greater at 160°F for the 897/332-732-1 composites. All three candidate composites tend to exhibit more transverse damage with increased impact velocity.

The back surface transverse damage of the 470/438 composites is relatively insensitive to changes in either test temperature or impact velocity. On the other hand, the 897/332-732-1 composites generally

TABLE 49. SUMMARY OF VISUAL BALLISTIC DAMAGE - TUMBLED CALIBER .30 BALL M2 IMPACTED SPECIMENS

Velocity (ft/sec)	470/438-1			470/438-1/2			897/332-732-1		
	Temperature (°F)			Temperature (°F)			Temperature (°F)		
	-80	RT	160	-80	RT	160	-80	RT	160
	A. Front Surface Area (in.^{2})[a]								
1200	1.40[b]	-	-	1.00[b]	-	-	0.87[b]	-	-
1500	1.10[b]	1.00[c]	1.11	1.13	0.85[c]	0.97	0.83	0.70	1.14[d]
1800	1.48	1.11	1.29	1.16	0.93	1.14	1.32	0.85	1.26
2100	1.48	1.33	1.48	1.24	1.22	1.16[c]	1.19[b]	1.09	1.30[d]
2400	-	-	1.28	-	-	1.13[c]	-	-	1.18[b]
	B. Back Surface Area (in.^{2})[a]								
1200	4.53[b]	-	-	3.00[b]	-	-	4.07[b]	-	-
1500	4.50[b]	4.70[c]	4.46	2.49	2.40[c]	2.62	3.77	3.33	3.81[d]
1800	4.97	4.47	4.42	3.15	2.55	2.89	3.74	3.80	3.82
2100	5.31	4.56	4.25	2.54	2.50	2.34[c]	3.50[b]	3.38	3.83[d]
2400	-	-	4.07	-	-	2.36	-	-	3.02[b]
	C. Volume (in.^{3})[a]								
1200	0.353[b]	-	-	0.242[b]	-	-	0.282[b]	-	-
1500	0.322[b]	0.330[c]	0.326	0.221	0.195[c]	0.217	0.267	0.229	0.288[d]
1800	0.379	0.328	0.328	0.258	0.209	0.244	0.304	0.270	0.301
2100	0.411	0.347	0.353	0.231	0.226	0.211[c]	0.280[b]	0.261	0.307[d]
2400	-	-	0.313	-	-	0.206[c]	-	-	0.251[b]

[a]Values are based on three replicates except as noted.

[b]Values are based on five replicates.

[c]Values are based on four replicates.

[d]Values are based on two replicates.

TABLE 50. SUMMARY OF VISUAL TRANSVERSE BALLISTIC DAMAGE - TUMBLED CALIBER .30 BALL M2 IMPACTED SPECIMENS

Velocity (ft/sec)	470/438-1			470/438-1/2			897/332-732-1		
	Temperature (°F)			Temperature (°F)			Temperature (°F)		
	-80	RT	160	-80	RT	160	-80	RT	160
	A. Front Surface Transverse Damage (in.)[a]								
1200	1.66[b]	-	-	1.46	-	-	1.22[b]	-	-
1500	1.48[c]	1.40[b]	1.51	1.44	1.32	1.35	1.32	1.18	1.58[d]
1800	1.57	1.52	1.49	1.42	1.34[b]	1.04	1.61	1.30	1.51
2100	1.63	1.51	1.58	1.47	1.58	1.50[b]	1.45[c]	1.59	1.79[d]
2400	-	-	1.64	-	-	1.61[b]	-	-	1.57[c]
	B. Back Surface Transverse Damage (in.)[a]								
1200	2.63[b]	-	-	2.22	-	-	2.57[b]	-	-
1500	2.56[c]	2.54[b]	2.57	2.09	2.07	1.84	2.78	2.25	2.70[d]
1800	2.61	2.68	2.50[b]	2.21	2.17[b]	2.12	2.49	2.45	2.27
2100	2.54	2.64	2.54	1.94	2.02	1.96[b]	2.30[c]	2.35	2.28[d]
2400	-	-	2.36[b]	-	-	1.97[b]	-	-	2.30[c]
	C. Avg Front/Back Surface Transverse Damage (in.)[a]								
1200	2.15[b]	-	-	1.84	-	-	1.90[b]	-	-
1500	2.02[c]	1.97[b]	2.04	1.77	1.70	1.60	2.05	1.73	2.14[d]
1800	2.09	2.10	2.00	1.82	1.76[b]	1.88	2.05	1.87	1.90
2100	2.09	2.08	2.06	1.71	1.80	1.73[b]	1.87[c]	1.99	2.04[d]
2400	-	-	1.85	-	-	1.79[b]	-	-	1.93[c]

[a] Values are based on three replicates except as noted.

[b] Values are based on four replicates.

[c] Values are based on five replicates.

[d] Values are based on two replicates.

experienced greater damage at low temperature and low velocity. The average back surface transverse damage values across the entire experiment were 2.561, 2.055, and 2.431 inches for the 470/438-1, 470/438-1/2, and 897/332-732-1 composites, respectively.

The Table 50 data indicate that variations in temperature or velocity have a relatively insignificant effect on the average front/back surface transverse damage of the three candidate composites. The composites with 1-inch fibers experience greater transverse damage than the composite with the shorter length fibers. The grand averages for the 470/438-1, 470/438-1/2, and 897/332-732-1 were 2.041, 1.764, and 1.952 inches, respectively.

A cell-form summary of the tensile load capacities for the three candidate composites after tumbled caliber .30 ball M2 impacts is presented in Table 51. The cell values were linearly normalized to a specimen thickness of 1/8 inch. The average load capacities of damaged 470/438-1, 470/438-1/2, and 897/332-732-1 composites were 8128, 5547, and 7622 pounds, respectively. Based on undamaged tensile data discussed earlier, the respective values for percentage of strength retained are 67.6, 55.1, and 59.6. The higher strength retention values for the 470/438-1 and 897/332-732-1 composites are due to the greater degree of fiber alignment along the edges of the specimen. The ballistic impact eliminates the low-strength center material and leaves the high-strength edge material

TABLE 51. SUMMARY OF RESIDUAL LOAD CAPACITIES[a] FOR TUMBLED CALIBER .30 BALL M2 IMPACTED SPECIMENS

Velocity (ft/sec)	470/438-1			470/438-1/2			897/332-732-1		
	Temperature (°F)			Temperature (°F)			Temperature (°F)		
	-80	RT	160	-80	RT	160	-80	RT	160
1200	8975[b]	-	-	5320[b]	-	-	8477	-	-
1500	7680[c]	7683[c]	7527	6097	5610	5820	7320	7260	8100[b]
1800	7093	8913	7897	6050	5795[b]	4973	7520	7233	7313
2100	9223	8430	8017	5867	5367	5653[c]	8117	7590	6830[b]
2400	-	-	7965[b]	-	-	4463	-	-	8033

[a] Data normalized to a 1/8-inch specimen thickness. Values (in pounds) are based on three replicates except as noted.

[b] Values are based on two replicates.

[c] Values are based on four replicates.

undamaged. Consequently, composites with a high degree of edge fiber alignment parallel to the direction of tensile loading will exhibit high strength retention values.

The individual cell values indicate that no definite relationship exists between residual load capacity and either test temperature or impact velocity. Furthermore, there does not appear to be any correlation between visual damage and residual load capacity.

It was observed that degradation similar to that noted in caliber .50 AP M2 tests had occurred away from the perforation in a number of specimens impacted at 160°F. The cause was again attributed to a high stress developed in the impacted specimen. It was subsequently established from static tensile strength data at 160°F that the initial preload was approximately 50 percent of the specimen strength. After nominal tumbled caliber .30 ball M2 projectile damage, the load in the residual material increased to 80 percent or more of the 160°F strength.

Since there was substantial evidence that these high stresses caused specimen degradation that may have contributed to reduced load capacity, the 160°F test data were disregarded in establishing the most critical test temperature. The final determination of critical impact conditions was accomplished by numerically ranking the -80°F and room temperature data in Table 51 on an increasing residual load capacity basis. The cell with the lowest total of the individual rankings would be selected as representing the most critical impact conditions. The rankings are given in Table 52.

The results indicate that a tumbled caliber .30 ball M2 projectile impacting at 1500 ft/sec and room temperature will cause a near-maximum reduction in the load capacity of the 1/8-inch-thick standard specimen. In addition to having the lowest cumulative ranking, this velocity-temperature combination provided a more representative damage condition for all three candidate composites. This is apparent from the rankings of 3, 3, and 2 for the 470/438-1, 470/438-1/2, and 897/332-732-1 composites, respectively. Consequently, these conditions will be used to damage specimens intended for determining the cyclic fatigue properties of impacted composites in Subtask 3 of Task II.

Conclusions and Recommendations

The significant conclusions derived from the investigation for determining the effects of projectile type, impact velocity, and test temperature on the extent of damage and residual load capacity are as follows:

TABLE 52. RANKING OF RESIDUAL LOAD CAPACITIES FOR TUMBLED CALIBER .30 BALL M2 IMPACTED SPECIMENS

Velocity (ft/sec)	470/438-1	470/438-1/2	897/332-732-1	Cumulative
	A. Ranking of Composites at -80°F			
1200	6	1	7	14
1500	2	7	3	12
1800	1	6	4	11
2100	7	5	6	18
	B. Ranking of Composites at Ambient Temperature			
1200	← No data available →			
1500	3	3	2	8
1800	5	4	1	10
2100	4	2	5	11

1. The tumbled caliber .30 ball M2 projectile produced more extensive damage and resulted in lower tensile load capacity than the caliber .50 AP M2 projectile regardless of composite type, impact velocity, or specimen temperature.

2. On the average, the 470/438-1 composite exhibited the greatest area, volume, and transverse damage irrespective of projectile type, velocity, or temperature. The 470/438-1/2 composite consistently sustained less damage across all ballistic conditions.

3. The average residual load capacity of 470/438-1 composites was higher than that exhibited by the 470/438-1/2 and 897/332-732-1 composites after either caliber .50 AP M2 or caliber .30 ball M2 projectile impacts.

4. Greater damage of caliber .50 AP M2 impacted specimens generally occurred at -80°F. No correlation was evident between the extent of visual damage and impact velocity.

5. A significant number of specimens impacted at 160°F with caliber .50 AP M2 projectiles failed away from the ballistic wound during residual load capacity testing. Since no such failures occurred with specimens evaluated at -80°F or room temperature, this indicates that impacts at 160°F did not produce maximum damage.

6. No consistent relationship was found between visual damage and tumbled caliber .30 ball M2 impact conditions, i.e., velocity and temperature, across all damage parameters.

7. The average strengths retained by the 470/438-1, 470/438-1/2, and 897/332-732-1 composites after tumbled caliber .30 ball M2 impacts were 67.6, 55.1, and 59.6 percent, respectively. The presence of a higher degree of fiber alignment along the edges of specimens with 1-inch fibers is partly responsible for the greater strength retention.

8. Although no velocity-temperature combination with tumbled caliber .30 ball M2 projectiles resulted in minimum residual load capacity, impacts at 1500 ft/sec and room temperature produced near-minimum strength retention for all three candidate composites.

It was recommended that specimens intended for post-damage fatigue testing be impacted at room temperature with tumbled caliber .30 ball M2 projectiles at 0-degree obliquity and a nominal velocity of 1500 ft/sec. This recommendation was approved by the Eustis Directorate and implemented in the Subtask 3 program.

SUBTASK 3 - CYCLIC TENSILE FATIGUE PROPERTIES OF UNDAMAGED AND DAMAGED COMPOSITES

General

In designing flight control components for rotary- and fixed-wing aircraft, attention must be given to the repeated application of operational loads that might cause fatigue failure. When ballistic tolerance is incorporated into these components, the fatigue characteristics after projectile impact are equally important. The intent of this investigation was to determine the cyclic tensile properties of the three candidate composites in both the undamaged and ballistically damaged conditions.

Approach to the Problem

Net molded, 1/8-inch-thick standard specimens were subjected to tensile fatigue testing at room temperature on a Sonntag Machine at a cyclic loading rate of 30 cps. A fan was directed at the specimen to prevent excessive heating during testing. Generally, 15 specimens of each material were evaluated with the stress levels chosen to provide meaningful S-N (stress versus number of cycles to failure) data in the 10^4 to 10^7 cycle range. For the undamaged specimen, most of the fatigue tests were conducted at stress levels of 28 to 54 percent of the static ultimate tensile strength.

The specimens for post-ballistic damage testing were impacted at room temperature with tumbled caliber .30 ball M2 projectiles at 0-degree obliquity and a nominal velocity of 1500 ft/sec. During ballistic exposure, the composites were preloaded to 35 percent of their average static tensile strength at room temperature. Prior to fatigue testing, the extent of ballistic damage was measured using techniques previously discussed. Again, 15 specimens of each candidate composite were evaluated with most of the tests performed between 26 and 54 percent of the static tensile strength of ballistically damaged specimens. This corresponds to approximately 16 to 33 percent of the strength of undamaged specimens.

Discussion of Results

A summary of tensile fatigue test results on undamaged specimens of the three candidate composites is presented in Table 53. Fatigue testing of the 470/438-1 composite was conducted at seven stress levels ranging from 19.3 to 58.0 percent of the average undamaged ultimate tensile strength. As experience was gained in the fatigue behavior of short-fiber composites, it became possible to make more intelligent selections of the test stress levels that would provide meaningful S-N curves. Therefore, subsequent fatigue cycling of the 470/438-1/2 and 897/332-732-1 composites was conducted essentially at four stress levels.

The 470/438-1 specimen that was exposed at 19.3 percent of the ultimate tensile strength exhibited no evidence of cracking after 10,133,000 cycles. This specimen was then tested at a high stress level, 38.6 percent of ultimate, with failure occurring at 2,175,000 cycles. Five specimens were evaluated at the 38.6 percent stress level, with the double-exposure specimen exhibiting a fatigue life that was greater than the average. This indicates that a stress level asymptote (endurance limit) exists below which fatigue damage is insignificant. During the conduct of these fatigue tests, macrocracks appear in the form of scaling.

TABLE 53. SUMMARY OF FATIGUE TEST RESULTS ON UNDAMAGED SPECIMENS

Composite	Maximum Load			Thousands of Cycles to Failure				
				Replicate				
	Absolute (lb)	Stress Level (psi)	Percent of Ult	1	2	3	4	5
470/438-1	7,200	16,420	58.0	5.5	17	-	-	-
	5,990	13,650	48.3	31	31	28	54	-
	4,790	10,920	38.6	371	111	354	2,417	2,175[a]
	4,070	9,280	32.8	5,179	8,704	11,801	10,752	-
	3,590	8,190	29.0	3,931	-	-	-	-
	3,360	7,650	27.0	413	-	-	-	-
	2,400	5,460	19.3	>10,133	-	-	-	-
470/438-1/2	5,360	12,220	53.4	7	28	13	66	-
	4,510	10,270	44.9	37	35	119	156	-
	3,650	8,310	36.3	2,776	1,504	673	1,004	-
	3,220	7,330	32.0	2,997	942	4,732	-	-
	3,000	6,840	29.8	2,127	-	-	-	-
897/332-732-1	5,360	12,230	42.0	2	13	18	49	-
	4,860	11,080	38.0	193	94	16	-	-
	4,340	9,900	34.0	1,053	263	268	214	-
	3,580	8,150	28.0	8,646	2,093	854	5,117	-

[a]Specimen was previously tested at 19.3 percent of ultimate strength without failure.

Photographs were taken during fatigue testing to illustrate the rate of crack propagation in a selected specimen of each of the three candidate composites. The 470/438-1 specimen shown in Figure 51 failed after 54,000 cycles at a stress level corresponding to 48.3 percent of the ultimate strength. Cracks are evident at 2000 cycles, or within the first 4 percent of the fatigue life. Early crack formation is also apparent in the 470/438-1/2 specimen shown in Figure 52. This specimen, tested at 53.4 percent of the ultimate strength, failed at 13,000 cycles. The last two photographs (E and F), taken within a span of 20 seconds, indicate how rapidly cracks progress during the terminal phase of the fatigue life. Figure 53 shows a photographic record of a 897/332-732-1 specimen evaluated at 42.0 percent of the ultimate strength. Although not readily apparent in the photograph taken at 2000 cycles, cracks are present, particularly in the center of the test area. The first three photographs (A, B, and C) were taken with back lighting and are not as illustrative of crack formation and propagation rate as those photographs where the front surface of the specimen was illuminated. This particular 897/332-732-1 specimen failed after 18,000 cycles.

A relatively complete record was made of a 470/438-1 specimen stressed to 32.8 percent of ultimate strength to obtain information on crack formation and propagation rate. This specimen failed at 8,704,000

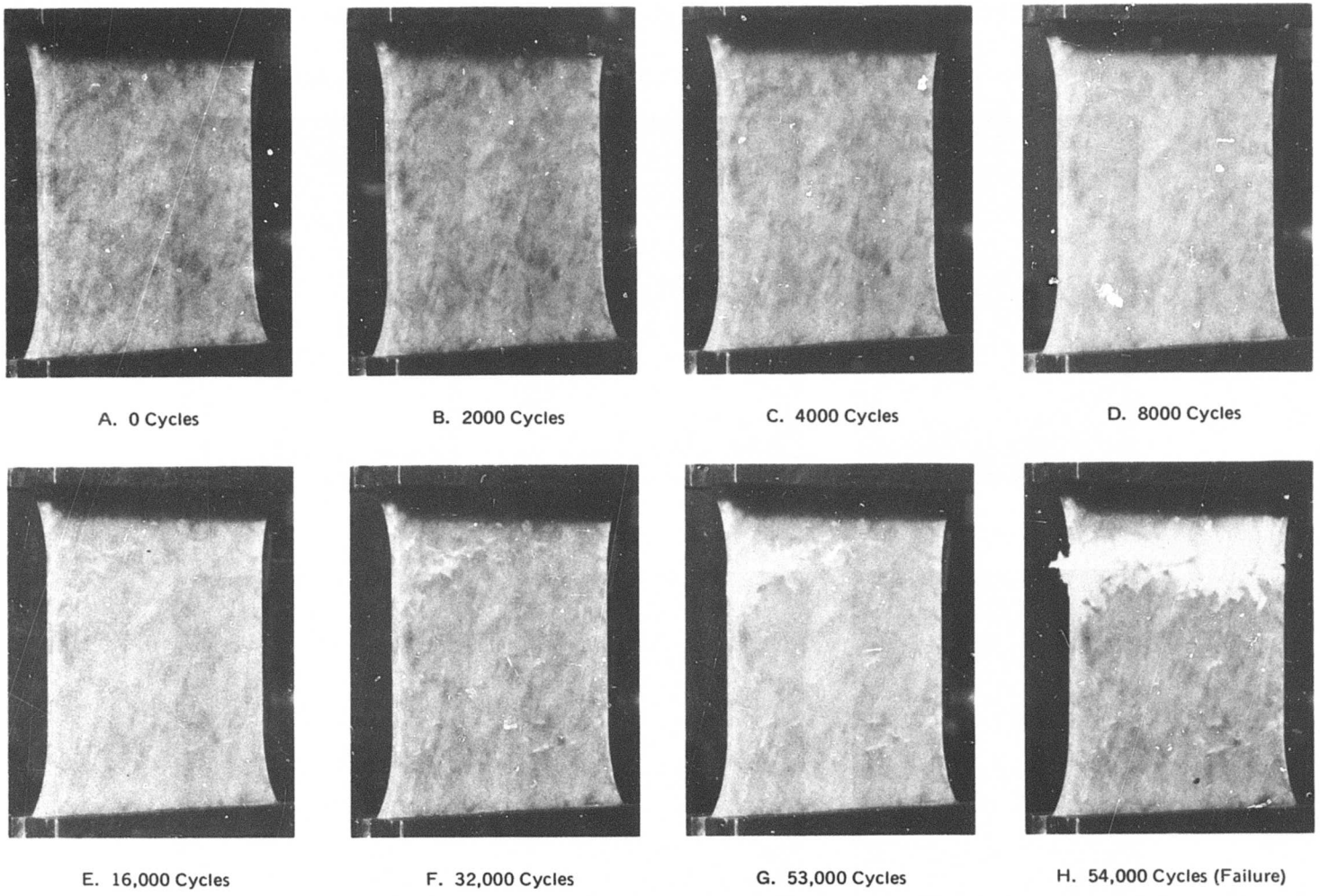

Figure 51. Tensile Cyclic Fatigue Test of Undamaged 470/438-1 Specimen.

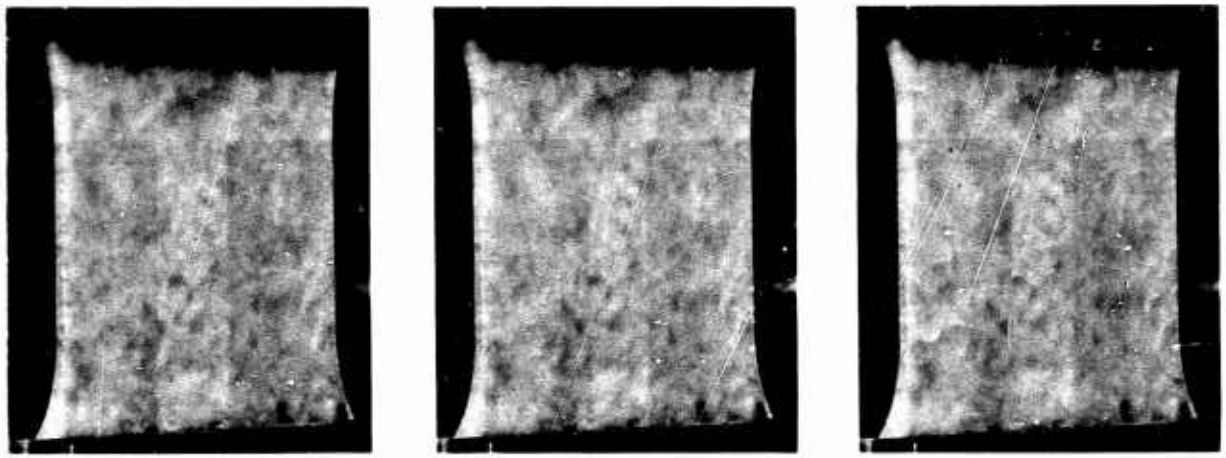

A. 0 Cycles

B. 2000 Cycles

C. 4000 Cycles

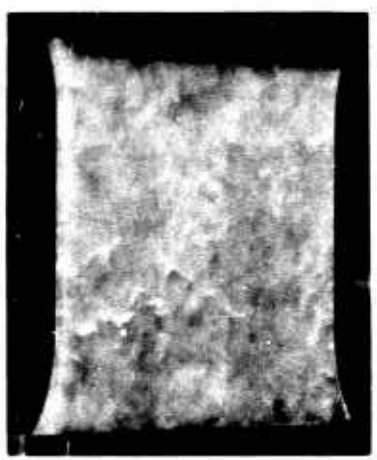

D. 8000 Cycles

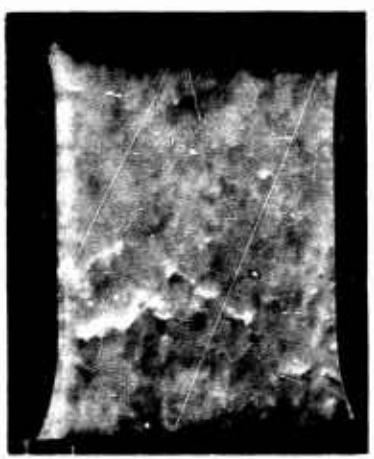

E. 13,000 Cycles

F. 13,000 Cycles (Failure)

Figure 52. Tensile Cyclic Fatigue Test of Undamaged 470/438-1/2 Specimen.

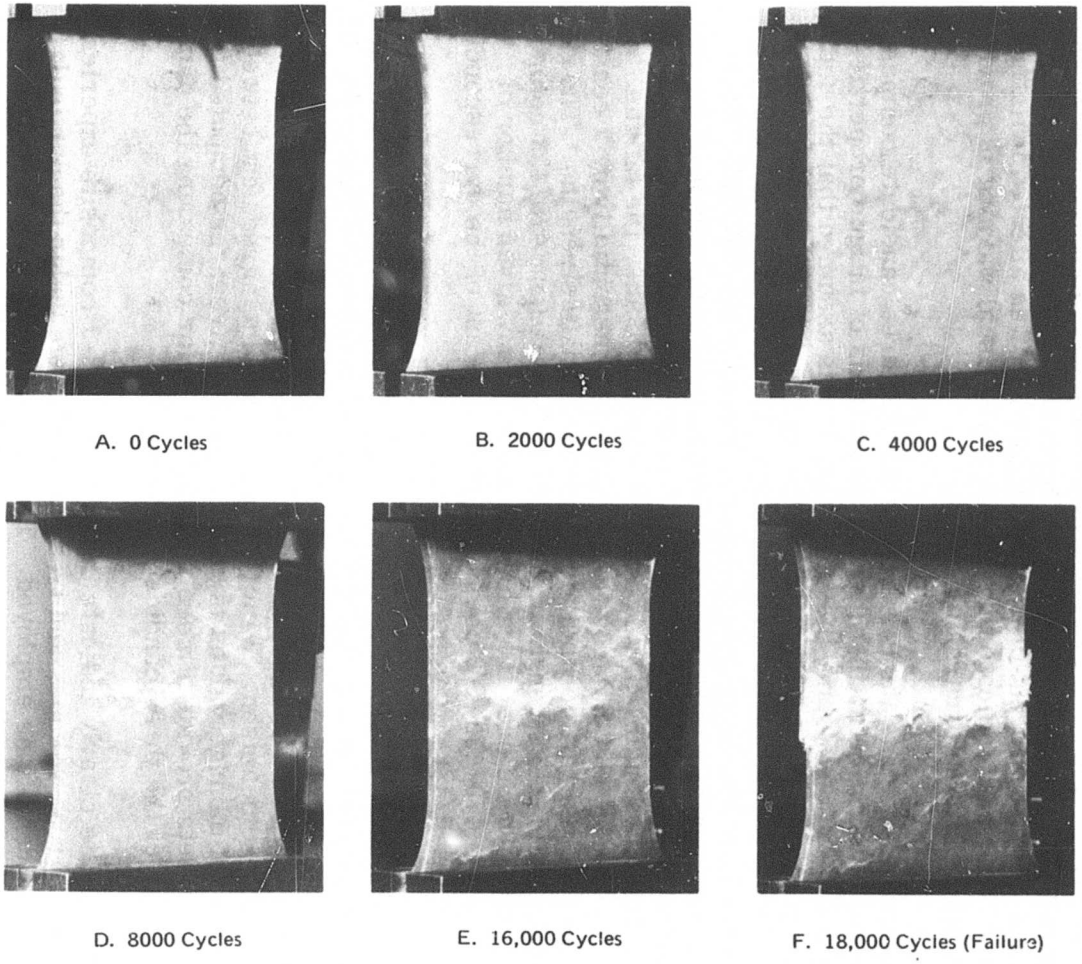

Figure 53. Tensile Cyclic Fatigue Test of Undamaged 897/332-732-1 Specimen.

cycles - only 6,000 cycles less than the average (logarithmic) fatigue life of all 470/438-1 specimens evaluated at this stress level. The initial measurements taken at 83,000 cycles (0.95 percent of the fatigue life) revealed that 28.3 percent of the specimen width was affected by fatigue cracks. After 468,000 cycles, or 5.38 percent of the fatigue life, the crack had propagated to 60.9 percent of the specimen width. Continued cycling resulted in crack growth at a decreasing rate. At 95 percent of the fatigue life, 88 percent of the specimen width was affected by fatigue cracks. These data indicate that considerable visual warning is provided before fatigue failure occurs.

Figure 54 presents the S-N curves for the three candidate composites in a single illustration so that direct comparisons of fatigue properties can be made. In developing these curves, it was assumed that the undamaged composites have a fatigue life of one cycle at a stress level corresponding to the static tensile load capacity. The curves for the 470/438 composites have the same general shape, whereas the 897/332-732-1 curve is substantially different. This indicates that the shape of the fatigue curve is governed by the fiber and resin constituents and is not influenced by fiber length. On an absolute capacity basis, the fatigue curves for the 470/438 composites are displaced essentially by a constant factor equal to the ratio of their undamaged ultimate strengths. The ratio of undamaged tensile strength of the 1/2- to 1-inch-long 470/438 composites is 0.81. Therefore, the allowable load for any given number of cycles with the 470/438-1/2 composite is 81 percent of the corresponding value for the 470/438-1 composite.

Measurements of visual damage exhibited by the ballistically impacted specimens for post-damage fatigue testing are reported in Tables 54, 55, and 56 for the 470/438-1, 470/438-1/2, and 897/332-732-1 composites, respectively. These tables also contain corresponding damage data from Subtask 2 for comparison. With few exceptions, the agreement between the two sets of damage values is good. Weighted averages computed from the two data sets provide a more accurate basis for comparing the damage response of the three candidate composites.

The results clearly indicate that the 470/438-1 composite experiences the greatest area, volume, and transverse damage under the particular ballistic test conditions employed. The 470/438-1/2 composite exhibits the least damage, with the values for the 897/332-732-1 composite generally falling between the extremes.

A summary of pertinent fatigue test data is given in Table 57. The maximum cyclic load was computed as a percentage of the static load capacity of damaged specimens. The residual load capacity values used

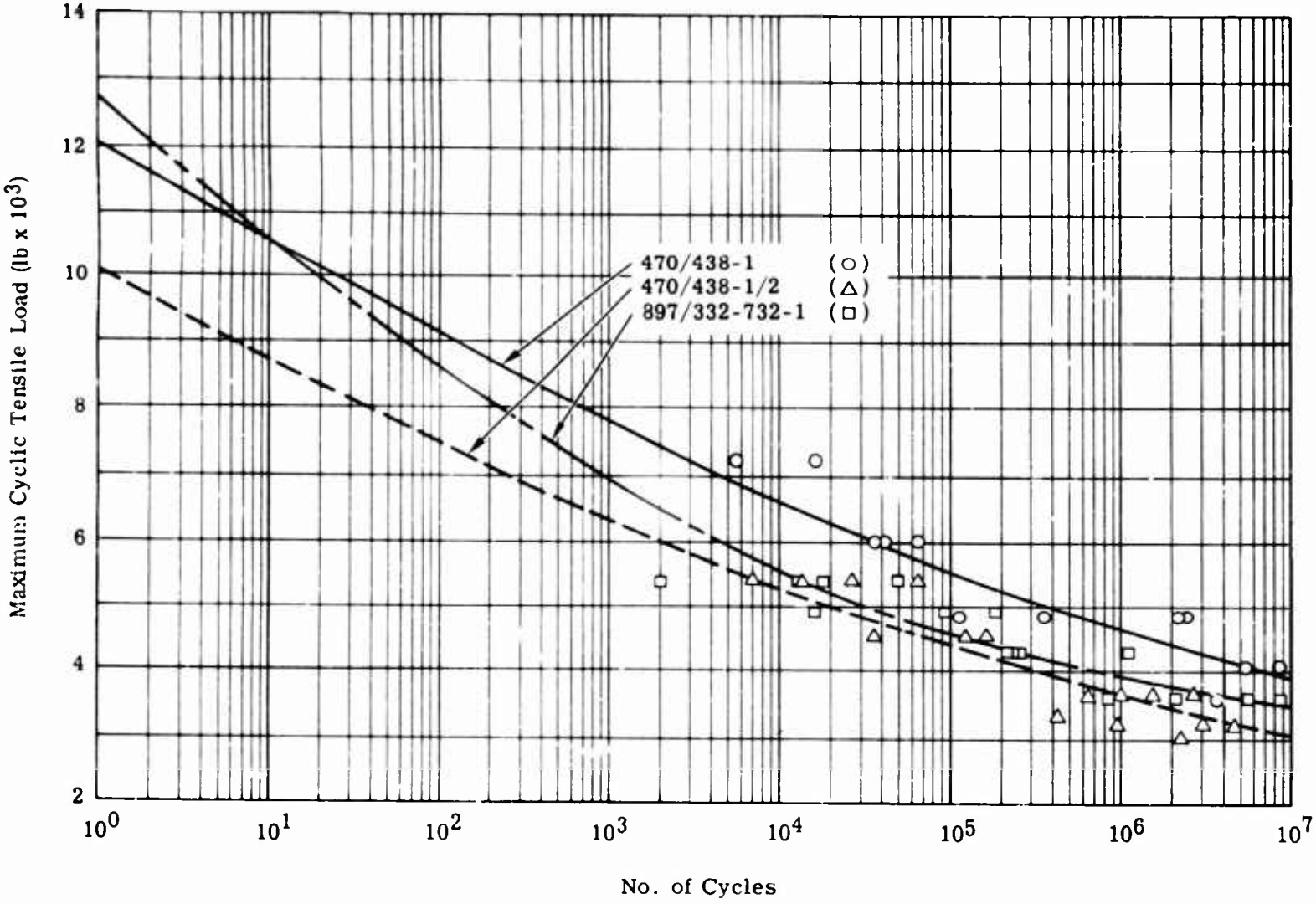

Figure 54. Load-N Curves for Undamaged Specimens of the Three Candidate Composites.

TABLE 54. COMPARISON OF DAMAGE AND RESIDUAL LOAD CAPACITY DATA FOR 470/438-1 COMPOSITES - TUMBLED CALIBER .30 BALL M2 IMPACTS AT 1500 FT/SEC (ROOM TEMPERATURE)

Parameter	Fatigue Study[a]	Subtask 2 Study[b]	Weighted Avg[c]
Front Surface Damage Area (i	1.02	1.00	1.02
Back Surface Damage Area (in.^{2})	4.17	4.70	4.28
Damage Volume (in.^{3})	0.293	0.330	0.301
Front Surface Transverse Damage (in.)	1.45	1.40	1.44
Back Surface Transverse Damage (in.)	2.66	2.54	2.64
Avg Front/Back Surface Transverse Damage (in.)	2.06	1.97	2.04
Residual Load Capacity (lb)	-	7683	7683[b]

[a]Values are based on 15 replicates.

[b]Values are based on four replicates.

[c]Values are based on a total of 19 replicates except as noted.

in this calculation were 7270, 6122, and 7060 pounds, respectively, for the 470/438-1, 470/438-1/2, and 897/332-732-1 composites at a 1/8-inch nominal thickness. These load capacity values are the weighted averages based on damaged specimens from Subtasks 2 and 5 that were impacted at room temperature with fully tumbled caliber .30 ball M2 projectiles at 1500 ft/sec and 0-degree obliquity.

Photographs were taken of representative specimens of the three candidate composites during fatigue testing. The particular 470/438-1 specimen photographed was evaluated at 47.9 percent of damaged ultimate strength and failed after 49,000 cycles. The series of photographs shown in Figure 55 shows the presence of fatigue cracks extending from the damaged area as early as 2000 cycles.

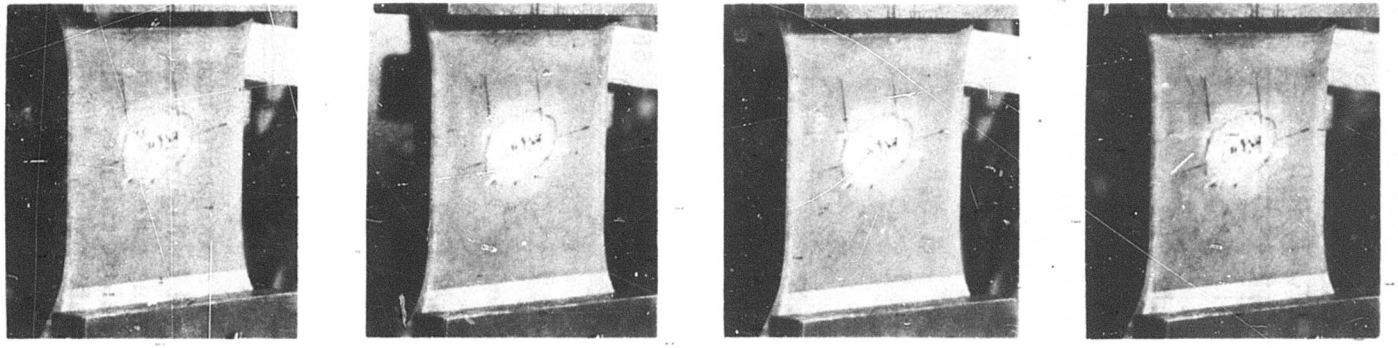

A. 0 Cycles B. 2000 Cycles C. 4000 Cycles D. 8000 Cycles

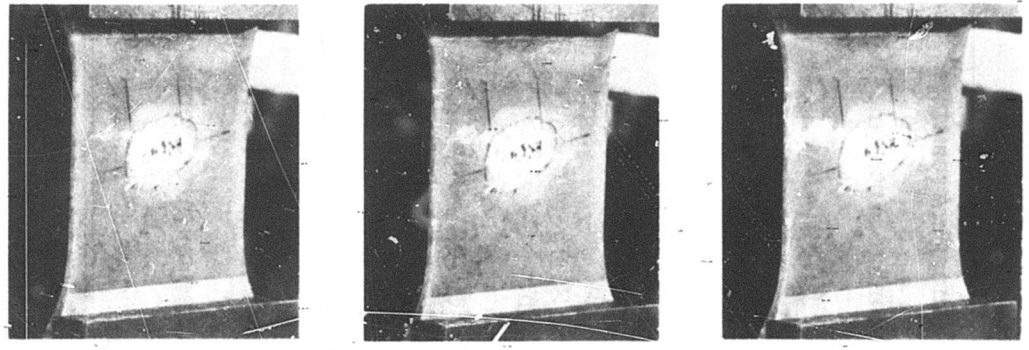

E. 16,000 Cycles F. 32,000 Cycles G. 48,000 Cycles

Figure 55. Tensile Cyclic Fatigue Test of Ballistically Damaged 470/438-1 Specimen.

TABLE 55. COMPARISON OF DAMAGE AND RESIDUAL LOAD CAPACITY DATA FOR 470/438-1/2 COMPOSITES - TUMBLED CALIBER .30 BALL M2 IMPACTS AT 1500 FT/SEC (ROOM TEMPERATURE)

Parameter	Fatigue Study[a]	Subtask 2 Study[b]	Weighted Avg[c]
Front Surface Damage Area (in.^{2})	0.86	0.85	0.86
Back Surface Damage Area (in.^{2})	2.38	2.40	2.38
Damage Volume (in.^{3})	0.197	0.195	0.197
Front Surface Transverse Damage (in.)	1.29	1.32[d]	1.30[e]
Back Surface Transverse Damage (in.)	1.98	2.07[d]	1.99[e]
Avg Front/Back Surface Transverse Damage (in.)	1.63	1.70[d]	1.64[e]
Residual Load Capacity (lb)	-	5610[d]	5610[d]

[a]Values are based on 15 replicates.

[b]Values are based on four replicates except as noted.

[c]Values are based on a total of 19 replicates except as noted.

[d]Values are based on three replicates

[e]Values are based on 18 replicates.

Evidence of fatigue cracks in the 470/438-1/2 composite tested at 46.9 percent of the damaged strength is apparent in Figure 56 after 4000 cycles. The last photograph in the series showing extensive fatigue damage was taken at 55,000 cycles, or 10 seconds before failure. The particular 897/332-732-1 specimen photographed was tested at a maximum stress of 52.7 percent of the static load capacity of ballistically damaged specimens. This series of photographs, shown in Figure 57, again indicates early fatigue crack formation (1000 cycles). Several of the cracks

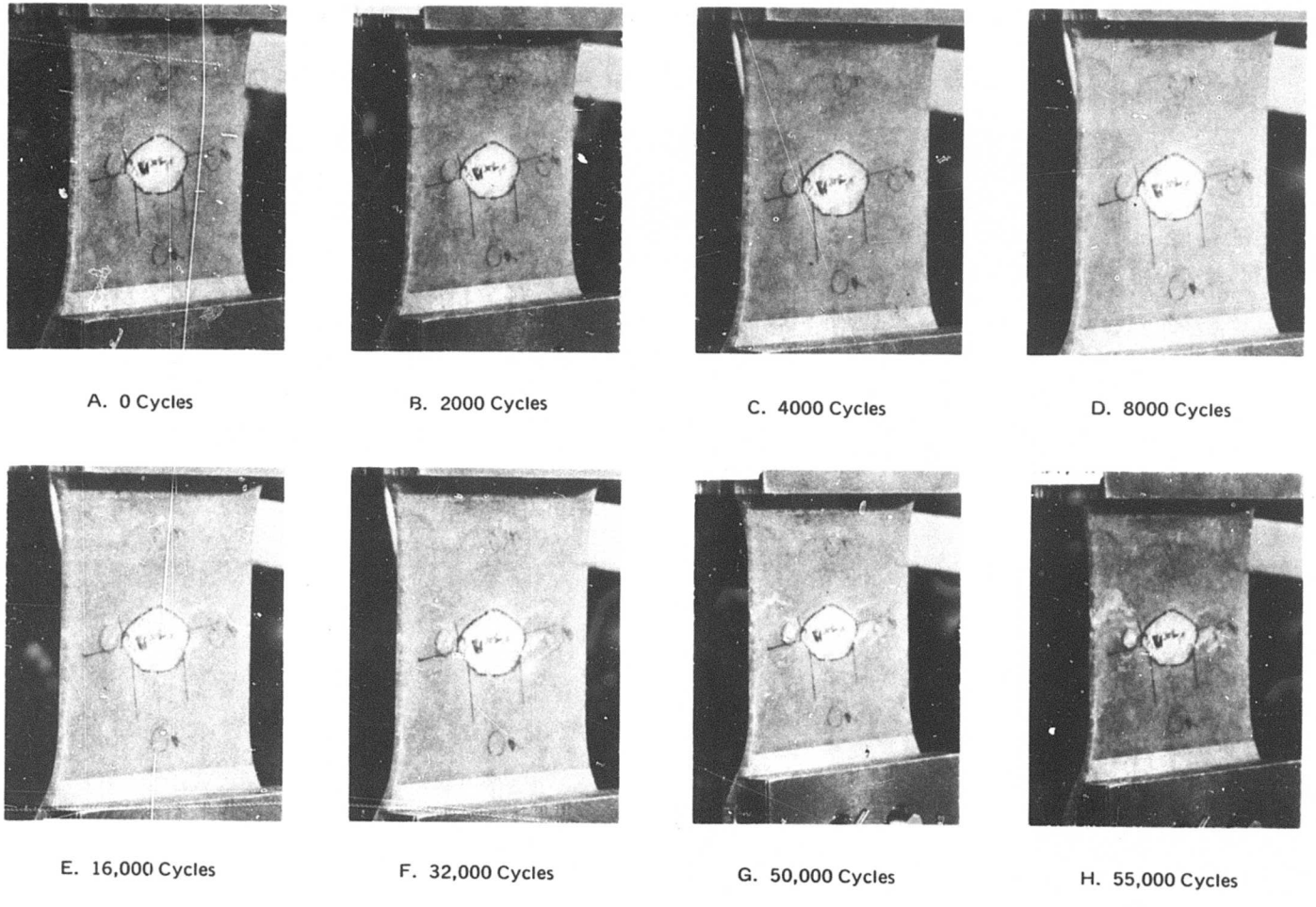

Figure 56. Tensile Cyclic Fatigue Test of Ballistically Damaged 470/438-1/2 Specimen.

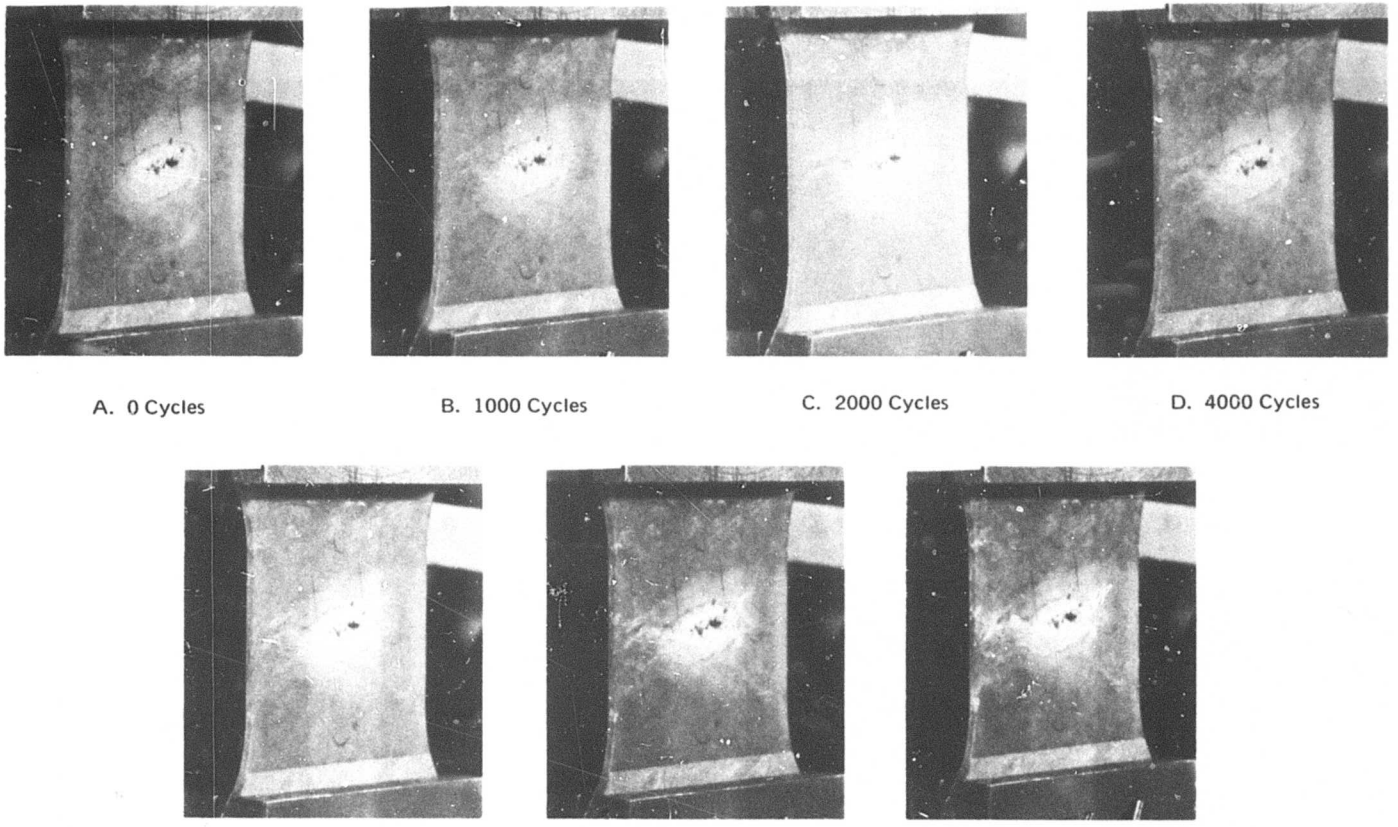

A. 0 Cycles B. 1000 Cycles C. 2000 Cycles D. 4000 Cycles

E. 8000 Cycles F. 16,000 Cycles G. 22,000 Cycles

Figure 57. Tensile Cyclic Fatigue Test of Ballistically Damaged 897/332-732-1 Specimen.

TABLE 56. COMPARISON OF DAMAGE AND RESIDUAL LOAD CAPACITY DATA FOR 897/332-732-1 COMPOSITES - TUMBLED CALIBER .30 BALL M2 IMPACTS AT 1500 FT/SEC (ROOM TEMPERATURE)

Parameter	Fatigue Study[a]	Subtask 2 Study[b]	Weighted Avg[c]
Front Surface Damage Area ($in.^2$)	0.96	0.70	0.91
Back Surface Damage Area ($in.^2$)	3.30	3.33	3.31
Damage Volume ($in.^3$)	0.246	0.229	0.243
Front Surface Transverse Damage (in.)	1.33	1.18	1.31
Back Surface Transverse Damage (in.)	2.39	2.25	2.36
Avg Front/Back Surface Transverse Damage (in.)	1.86	1.73	1.84
Residual Load Capacity (lb)	-	7260	7260[b]

[a] Values are based on 14 replicates.

[b] Values are based on three replicates

[c] Values are based on a total of 17 replicates except as noted.

evident at 1000 cycles have apparently originated away from the ballistic damage area. They are located, however, in an area where the section is reduced and higher stresses exist. The last photograph in the series was taken at 22,000 cycles, or 10 seconds before failure.

It is apparent from the data in Table 57 that the 470/438-1 composites exhibit more fatigue life variability than either of the other two systems. A three-decade difference in fatigue life was obtained for specimens evaluated at a common stress level (approximately 32 percent of the damaged static load capacity). Also, a change of about 20 percent in stress level (54.5 versus 34.8 percent) resulted in essentially the same fatigue life (about 40,000 cycles).

TABLE 57. SUMMARY OF FATIGUE TEST RESULTS ON BALLISTICALLY DAMAGED SPECIMENS

Max Cyclic Load (lb)	Percent of Static Strength of Damaged Specimens	Thousands of Cycles to Failure	Max Cyclic Load (lb)	Percent of Static Strength of Damaged Specimens	Thousands of Cycles to Failure	Max Cyclic Load (lb)	Percent of Static Strength of Damaged Specimens	Thousands of Cycles to Failure
A. 470/438-1 Specimens			B. 470/438-1/2 Specimens			C. 897/332-732-1 Specimens		
4500	63.8	<0.30	2804	45.8	37	3630	53.2	41
3994	54.5	48	2804	46.9	55	3630	52.7	22
3369	51.3	47	2804	45.8	27	3630	51.8	3
3369	45.7	25	2356	37.3	199	3049	43.2	1,276
3369	47.5	46	2356	37.3	267	3049	46.6	118
3369	47.9	49	2356	39.8	398	3049	42.2	631
2770	38.6	27	2356	39.4	1,130	3049	39.1	313
2770	38.2	157	2019	33.3	14*	2614	37.6	256
2770	36.2	15,987	2019	34.1	535	2614	37.9	1,181
2770	35.3	2,730	2019	33.3	647	2614	37.0	949
2310	31.8	13	2019	33.5	4,903	2614	38.6	927
2310	31.8	1,069	1683	26.5	12,328	2178	31.4	1,437
2310	32.1	10,417	1683	27.9	3,668	2178	31.4	18,040
2310	34.8	33	1683	24.7	>36,326	2178	31.6	2,667
1843	26.0	17,967	1683	28.4	>33,798	2178	30.8	21,858

*Fatigue machine malfunction.

The relative behavior of ballistically damaged specimens of the three candidate composites in a tensile cyclic fatigue environment is shown by the S-N curves presented in Figure 58. In generating these curves, the damaged specimens were assumed to have a fatigue life of one cycle at a stress level corresponding to the static residual load capacity. On an absolute load capacity basis, the 897/332-732-1 composites generally exhibit greater fatigue life than the other two candidate composites at corresponding stress levels. On the same basis, the 470/438-1/2 composites consistently show poorer fatigue characteristics.

Figure 59 illustrates the fatigue life of the three candidate composites as a function of their damaged static load capacities. These curves suggest that the 470/438-1/2 composite has greater fatigue life than the other composites when the maximum cyclic load is high, i.e., more than 62 percent of the damaged static load capacity. Below this stress level, the 897/332-732-1 composites exhibit superior fatigue properties. Actually, on the basis of percentage of damage load capacity, the differences in stress level are comparatively small across the fatigue life range shown (10^0 to 10^7 cycles).

Further analysis of the fatigue data using statistical techniques is given in the appendix.

Conclusions and Recommendations

The following conclusions can be drawn relative to the fatigue characteristics of undamaged and ballistically damaged composites:

1. An endurance limit (stress) exists below which cyclic tensile loading has no apparent effect on the composites.
2. Specimens tested above the endurance limit (10 - 20 percent ult) develop cracks within the first 4 percent of the fatigue life.
3. The fatigue curves for undamaged 470/438-1 and 470/438-1/2 composites are displaced by a constant factor equal to the ratio of their static ultimate strengths.
4. The fatigue characteristics of the undamaged 470/438-1 composites are superior to the other two composites.
5. For damaged specimens, the 897/332-732-1 composites generally exhibited the greatest fatigue life at all stress levels examined.
6. Differences in fatigue properties of damaged specimens of the three candidate composites are relatively minor when the stress

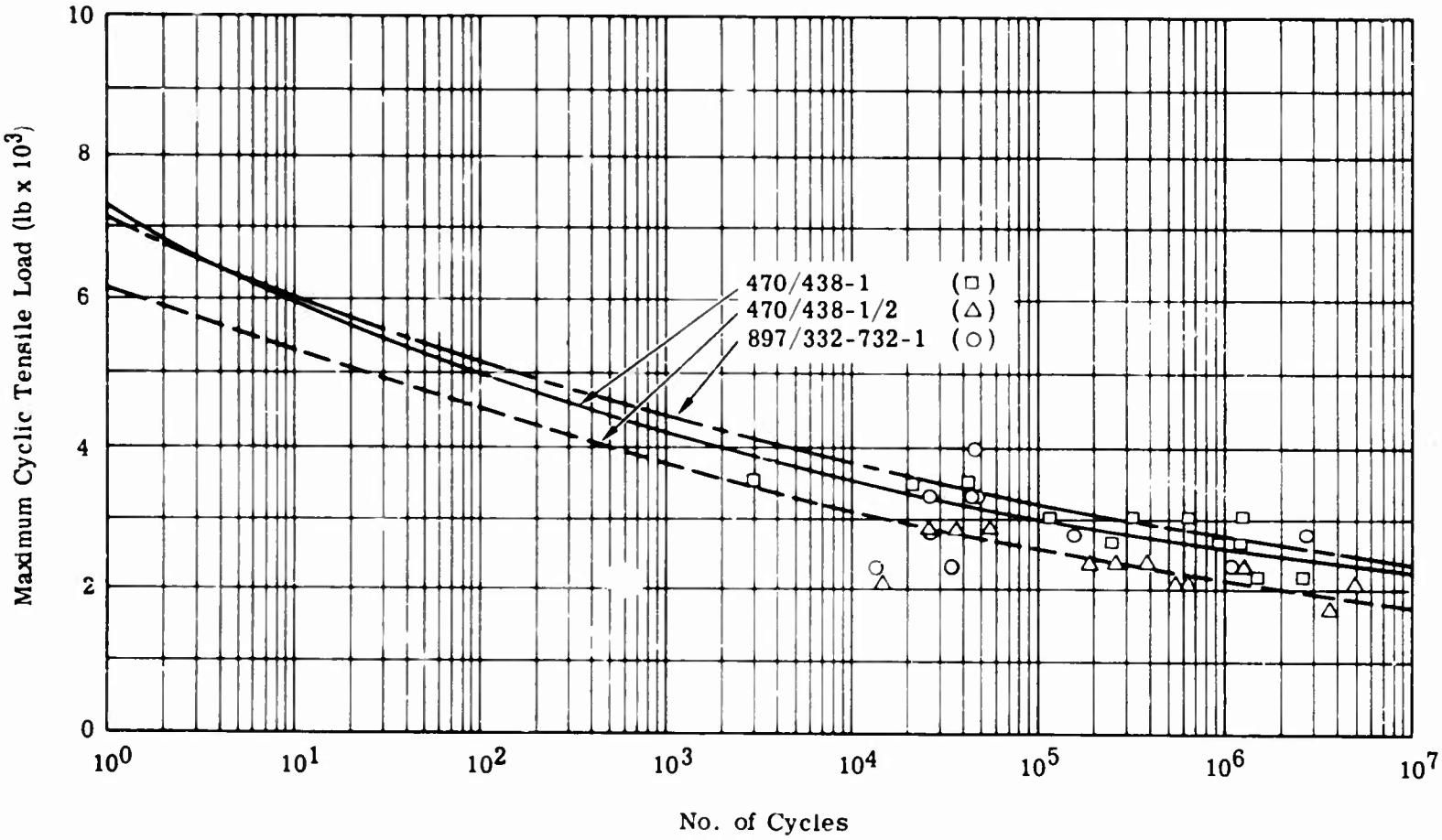

Figure 58. S-N Curves for Ballistically Damaged Specimens of the Three Candidate Composites.

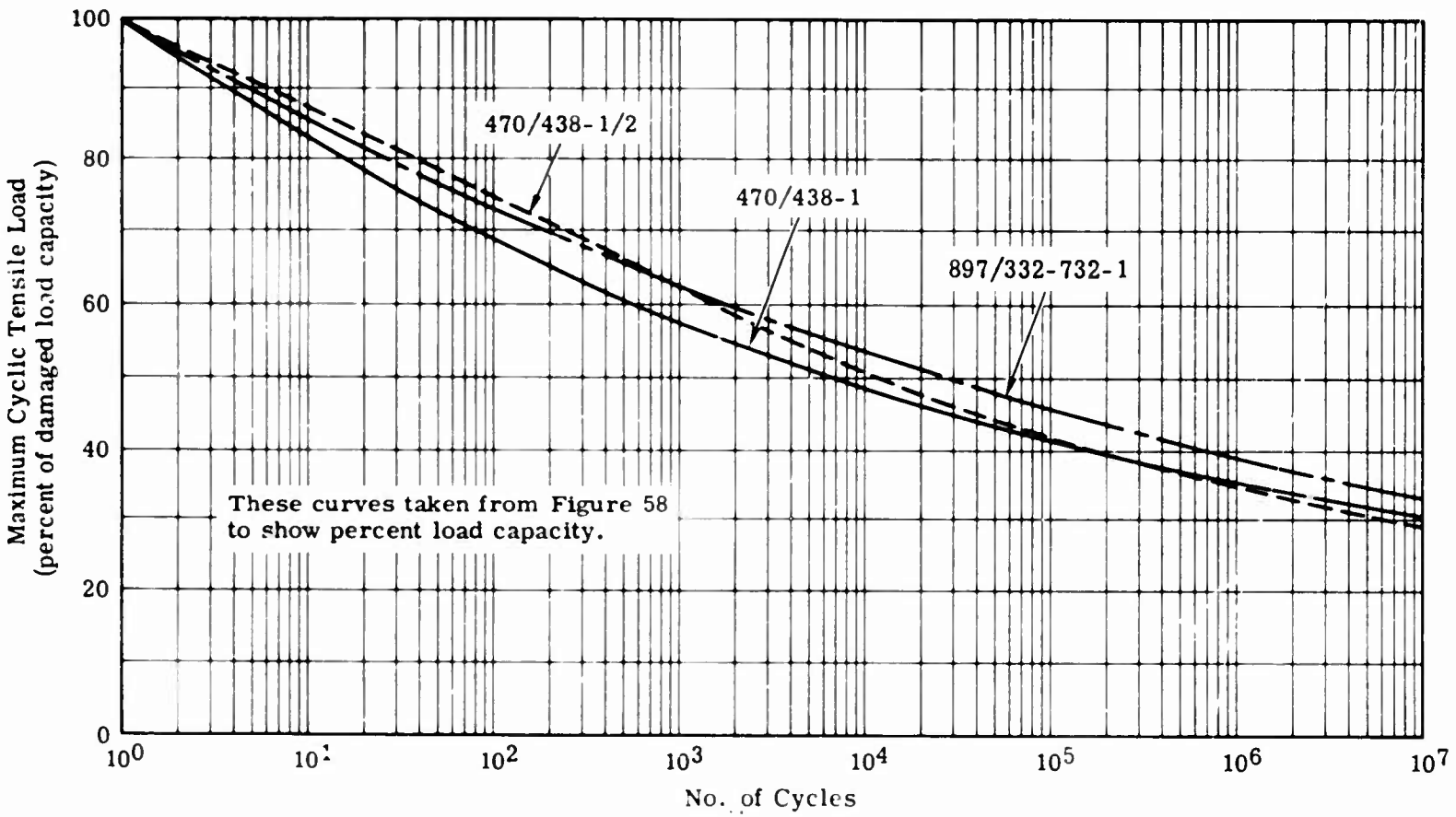

Figure 59. Fatigue Curves of the Three Candidate Composites (Percentage of Damaged Load Capacity).

level is reported as a percentage of the damaged static load capacity.

The superior fatigue characteristics of the 1-inch fiber composites on an absolute stress level basis are partly due to the presence of aligned fibers along specimen edges. If randomly oriented material had been evaluated, the differences in fatigue properties between the 1/2- and 1-inch composites would probably have been significantly reduced. This statement is substantiated, at least in part, by the similarity in fatigue life for the three candidate composites when the ordinate is the cyclic stress as a percentage of the damaged static load capacity. Therefore, the fatigue characteristics of the damaged and undamaged specimens do not, per se, constitute a strong basis for identifying the most promising composite.

SUBTASK 4 - COMPOSITE FRACTURE TOUGHNESS

General

The purpose of this investigation was to determine the fracture toughness, i.e., the crack propagation resistance, of net-molded specimens of the three candidate composite systems.

Approach to the Problem

The crack propagation resistance was established from standard 1/8-inch-thick specimens with a 1-inch simulated crack oriented transverse to the direction of the longitudinal axis of the specimen and the load path. This crack was produced by extending hacksaw cuts originating at a centrally located 1/2-inch-diameter hole with a jeweler's saw blade. The rate of slow crack propagation during tensile loading (at a load rate of .05 inch/minute) was marked on the specimen surface until the onset of rapid propagation. The effective crack length when instability occurred, the failure load, and the specimen width and thickness were used to calculate K, the fracture toughness factor. Fifteen specimens, five of each candidate composite, were used to compute an average toughness factor.

For additional details regarding the specimen and test procedure, refer to "Test and Evaluation Techniques," presented in an earlier portion of this report.

Discussion of Results

Some difficulty was experienced in differentiating between the cracks forming at the tip of the cut and the independent fractures occurring in the same general region. This problem is evident from the photographic record of a 897/332-732-1 composite at various stages of test (see Figure 60). The initial photograph taken at a tensile load of 8000 pounds indicates a major fracture near the right terminus of the cut. This fracture, however, is isolated from the crack at the tip of the cut. At a 9100-pound tensile load, the cracks have joined and the location of the fracture front is marked accordingly. The final photograph indicates that further crack extension had occurred on the left side before rapid propagation was experienced. The specimen failed at a tensile load of 9220 pounds.

The pertinent fracture toughness data generated in this investigation are reported in Table 58. The fracture toughness factor, K, was determined from the following mathematical expressions:

$$Y = X/B \tag{20}$$

where X = crack length at the onset of rapid fracture, in.

B = specimen width (3.51 inches)

$$Z = \frac{Y(2 + Y^4)}{(2 - Y^2 - Y^4)^2} \tag{21}$$

where Z = a geometry factor to correct for specimen width

$$K = \frac{P}{t}\sqrt{\frac{\pi Z}{B}} \tag{22}$$

where P = failure load, lb

t = specimen thickness, in.

Considering the problem of defining the location of the crack front, the fracture toughness values reported in Table 58 are reasonably consistent except in three cases where individual values deviate by more than 20 percent from the group average. The extremely high average toughness values indicate that short-fiber composites are extremely resistant to rapid crack propagation. The 438 and 332-732 resin systems without fiber glass reinforcement exhibited fracture toughness factors of 475 and 1080 lb/in.$^{3/2}$, respectively. Therefore, the reinforced composites are 50 to 120 times more crack resistant than the unfilled resins.

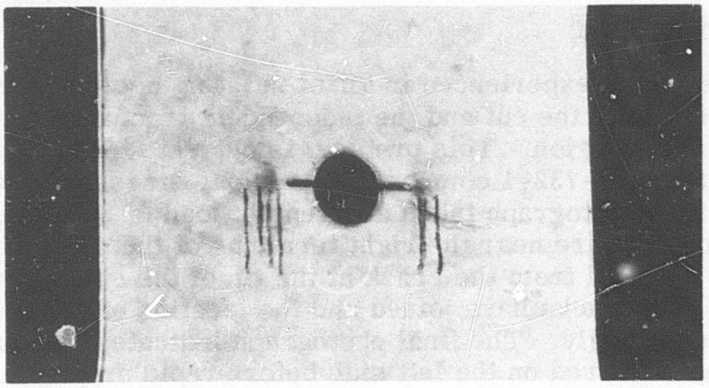

A. 8000-Pound Tensile Load

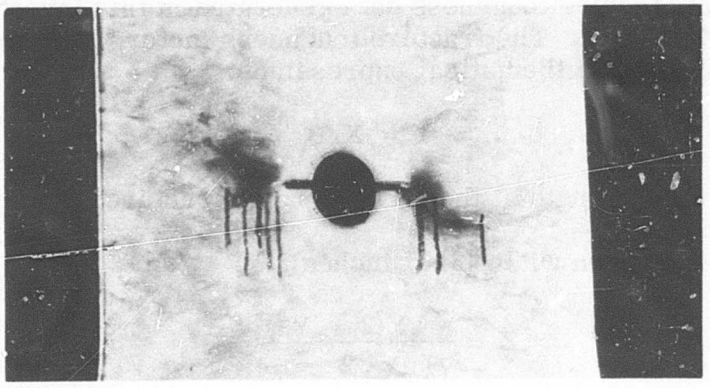

B. 9100-Pound Tensile Load

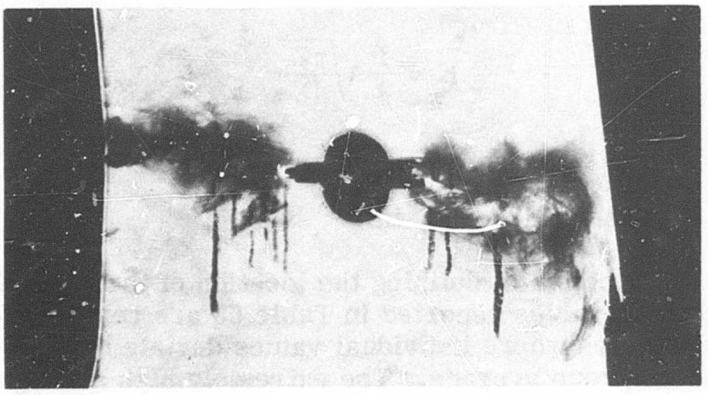

C. 9220-Pound Tensile Load

Figure 60. Fracture Toughness Test of 897/332-732-1 Composite.

TABLE 58. FRACTURE TOUGHNESS DATA FOR THE THREE CANDIDATE COMPOSITES

Composite	X (in.)	Y	Z	P (lb)	t (in.)	K (lb/in.$^{3/2}$)
470/438-1	1.19	0.339	0.195	9,100	0.117	32,500
	2.01	0.573	0.494	9,910	0.116	56,800
	1.94	0.554	0.454	11,580	0.127	58,100
	2.15	0.613	0.597	10,640	0.127	61,200
	2.32	0.661	0.769	11,600	0.121	79,500
						57,600[a]
470/438-1/2	1.88	0.536	0.420	7,360	0.120	37,600
	1.71	0.487	0.344	8,840	0.127	38,600
	1.75	0.499	0.361	7,770	0.131	33,900
	1.73	0.494	0.353	7,440	0.126	33,200
	1.92	0.547	0.440	8,390	0.123	42,800
						37,200[a]
897/332-732-1	2.53	0.721	1.118	8,670	0.128	67,700
	1.81	0.516	0.386	9,600	0.123	45,900
	2.05	0.584	0.519	7,190	0.120	40,900
	2.10	0.599	0.557	8,630	0.125	48,700
	1.99	0.566	0.478	9,220	0.124	48,600
						50,400[a]

[a]Average values

As expected, the data indicate that the 470/438-1 composite is substantially more crack resistant than the 470/438-1/2 composite. The greater fracture toughness of the 470/438-1 composite is due to the fact that only one-half the number of fiber ends are present and, on the average, a crack must travel along twice the fiber length before reaching the fiber end. Despite the higher toughness of the unfilled 332-732 resin system compared with the 438 resin, the 897/332-732-1 composite is less crack resistant than the 470/438-1 composite. The poorer performance of the 897/332-732-1 composite is attributed to the weaker resin-to-fiber glass interfacial bond resulting from the epoxy-incompatible finish (897) on the glass roving.

Additonal information was derived from the empirical data by conducting

a stress concentration analysis. The following discussion summarizes the results of this analytical effort.

The average ultimate load capacity of specimens with simulated cracks is given in Table 59 for each of the three candidate composites. These values are the average load capacities of the five replicates of each composite type given in Table 58. The undamaged ultimate tensile strength (σ_u) of these composites determined in Subtask 1 is also presented in Table 59.

The tensile strength of narrow specimens reported in Subtask 1 indicates that the edges of net-molded, 3.5-inch-wide test specimens carry a greater share of the load than the center area. It was shown that the edge-to-center strength ratios were 1.43 and 1.11 for composites with 1-inch and 1/2-inch-long fibers, respectively. A hypothetical model was also described earlier that related stress distribution to average specimen stress (σ_{avg}) as follows:

$$\sigma_{avg} = \frac{4}{7}\sigma_c + \frac{3}{7}\sigma_e \tag{23}$$

where σ_c = center stress, psi

σ_e = edge stress, psi

Substituting the edge-to-center strength ratio values in this expression yields

$$\sigma_{avg}]_{1"} = 1.184\ \sigma_c \text{ for 1-inch fiber composites} \tag{24}$$

$$\sigma_{avg}]_{1/2"} = 1.047\ \sigma_c \text{ for 1/2-inch fiber composites} \tag{25}$$

TABLE 59. STRESS CONCENTRATION FACTORS FROM FRACTURE TOUGHNESS DATA

Composite	Fracture Toughness Ult Load, P_{ft} (lb)	Thickness, t (in.)	Avg Ult Stress σ_u (psi)	Ult Center Stress, σ_c (psi)	Initial Crack, IC (in.)	Predicted Ult Load, P_{pre} (lb)	Stress Concentration Factor, KSC
470/438-1	10,550	0.1216	27,440	23,180	1.004	8880	0.84
470/438-1/2	7,960	0.1254	22,950	21,920	1.010	7320	0.92
897/332-732-1	8,660	0.1240	29,120	24,590	1.008	9604	1.11

The stress level (σ_c) at the center of the specimen at failure can be computed from Equations (24) and (25). The ultimate stress level (σ_u) is actually the average stress across the specimen when failure occurs. Substituting this value for σ_{avg} in Equation (23) results in the σ_c values reported in Table 59. The average initial crack length (IC) in the specimens prior to test is also presented. By reducing the undamaged ultimate strength of the specimens by an amount equal to the product of the crack length, specimen thickness, and computed center strength, then the predicted ultimate load capacities (P_{pre}) given in Table 59 are obtained.

The ratio of measured-to-predicted strength is the stress concentration factor (K_{SC}) associated with a particular flaw, in this case a simulated crack. These factors are given in Table 59 for the three candidate composites. True stress concentration factors must be equal to or greater than unity. Since the 470/438 composites exhibited stress concentration factors less than 1.0, this indicates that the strength distribution model may not be totally accurate or that composite variability may be responsible. The model is not the probable cause since an unrealistic strength distribution results when the factors for the 470/438 composites are set equal to unity. In the case of the 470/438-1 composite, for example, the edge and center strength values would become 51,300 and 9,500 psi, respectively, to satisfy a stress concentration factor of 1.0.

A more logical explanation is the presence of inherent variability in basic composite strength due to variations in the degree of edge fiber alignment. If the stress concentration factor were calculated on the basis of the highest ultimate tensile strength measured on any undamaged standard specimen, then the factors would be 1.01, 1.06, and 1.24 for the 470/438-1, 470/438-1/2, and 897/332-732-1 composites, respectively.

These results indicate that stress concentrations around cracks in the 470/438 composites have a negligible effect on tensile load capacity. On the other hand, the stress concentration factor is significant for the 897/332-732-1 composite. The load capacity of this composite is less, therefore, than would be expected from the actual crack dimensions.

The comparatively high stress concentration factor associated with the 897/332-732-1 composite may explain, at least in part, why unexpectedly low load capacities were obtained after ballistic impact. The 897/332-732-1 specimens exhibited marginally higher undamaged strength and significantly less visual ballistic damage than the 470/438-1 specimens. However, the latter composite gave slightly higher average residual load capacities than the 897/332-732-1 composite.

Conclusions

The results of the fracture toughness investigation disclosed that the three candidate composites are highly resistant to rapid crack propagation. These composites are 50 to 120 times more resistant than the basic unfilled resins used in their manufacture. The stress concentration factors associated with a simulated crack in the 470/438 composites were calculated to be near unity. The 897/332-732-1 composite exhibited a significantly higher factor, which may account for the apparent inconsistency between residual strength and extent of ballistic damage compared with the 470/438-1 composite.

SUBTASK 5 - EFFECT OF COMPOSITE THICKNESS ON BALLISTIC DAMAGE AND RESIDUAL LOAD CAPACITY

General

All ballistic testing up to this point in the Task II program was performed on 1/8-inch-thick specimens. The design of ballistically tolerant components with short-fiber composites would undoubtedly dictate other section thicknesses, depending on the magnitude of the local stresses. The primary purpose of Subtask 5 was to establish the extent of ballistic damage and residual load capacity as a function of composite thickness. A secondary objective was to determine if the velocity producing maximum damage and minimum residual load capacity was related to the projectile defeat capabilities (ballistic limit) of the composite.

Approach to the Problem

The composite thickness effects program was conducted in two distinct phases. The initial phase involved evaluation of 1/16-, 1/8-, 1/4-, and 3/8-inch-thick specimens (standard configuration) of the 470/438-1 composite at room temperature with tumbled caliber .30 ball M2 projectiles at 0-degree obliquity. Three specimens were tested at each of the 13 thickness and velocity combinations shown in Table 60.

Measurements of the residual velocity of the projectile were taken after specimen perforation to be used in calculating the ballistic limit. In addition, an assessment was made of visual ballistic damage prior to conducting the residual load capacity tests.

The combined effects of thickness and temperature on the ballistic response of the three candidate composites were determined during

TABLE 60. TEST PLAN FOR INITIAL PHASE OF THICKNESS EFFECTS PROGRAM

Thickness (in.)	Impact Velocity (ft/sec)
1/16	900 and 1200
1/8	900, 1200, and 1500
1/4	900, 1200, 1500, and 1800
3/8	1200, 1500, 1800, and 2100

the second phase of Subtask 5. The specific thickness and temperature conditions examined are given in Table 61. Three replicates were evaluated with tumbled caliber .30 ball M2 projectiles at 0-degree obliquity at each combination of thickness and temperature. The residual load capacity results from the initial phase were used to define the projectile impact velocity for the second phase tests.

TABLE 61. TEST PLAN FOR SECOND PHASE OF THICKNESS EFFECTS PROGRAM

Thickness (in.)	470/438-1		470/438-1/2			897/332-732-1		
	Temperature (°F)		Temperature (°F)			Temperature (°F)		
	-80	160	-80	RT	160	-80	RT	160
1/8	x	x	x	x	x	x	x	x
1/4	x	x	x	x	x	x	x	x
3/8	x	x	x	x	x	x	x	x

The impacts and residual velocities were measured during each test so that the ballistic limit could be calculated. After visual damage assessment, the residual strength of the specimens was determined at room temperature.

The specimens were prestressed during ballistic testing to 35 percent of their ultimate tensile strength at 160°F. The 35-percent prestress is approximately equivalent to 23 percent of the room temperature tensile strength. This is a departure from all previous tests where the specimens

were preloaded to 35 percent of the ambient strength. This latter condition resulted in extremely high stresses in the specimens after impact at 160°F. These stresses probably contributed to increased structural degradation that obscured the true effect of specimen temperature on the extent of ballistic damage and the residual load capacity.

Discussion of Results - Initial Phase of Thickness Effects Program

The average area and volume damage measurements for the 470/438-1 composites evaluated in the initial phase of Subtask 5 are summarized in Table 62. These data clearly indicate that ballistic damage increases directly with composite thickness. This is particularly evident on the back surface of the specimen and, consequently, in the volume of damage. With respect to velocity effects on area and volume damage, the results are not conclusive. Damage is relatively constant for a particular composite thickness at all impact velocities.

The transverse damage measurements given in Table 63 also show a definite correlation with thickness. The average front/back surface transverse damage of 3/8-inch-thick specimens is approximately 40 percent greater than that experienced by 1/16-inch-thick specimens. The extent of transverse damage is apparently unaffected by changes in impact velocity.

The residual load capacities for the 470/438-1 composites after application of the data rejection criteria are given in Table 64. These results indicate that post-damage strength increases directly with thickness but is insensitve to changes in impact velocity within the range examined.

In an effort to extract additional information from the data, multiple regression analysis was used to relate residual load capacity to specimen thickness and velocity. Individual specimen data were fitted to the following quadratic equation:

$$Y = a_0 + a_1x_1 + a_2x_2 + a_{11}x_1^2 + a_{22}x_2^2 + a_{12}x_1x_2 \qquad (26)$$

where Y = residual load capacity, lb

x_1 = specimen thickness, in.

x_2 = impact velocity, ft/sec

TABLE 62. SUMMARY OF VISUAL BALLISTIC DAMAGE - THICKNESS EFFECTS PROGRAM (INITIAL PHASE)

Velocity (ft/sec)	Thickness (in.)			
	1/16	1/8	1/4	3/8
	A. Front Surface Area (in.^{2})[a]			
900	1.09	1.35[b]	1.50	-
1200	1.21	1.15	1.27	1.32
1500	-	1.04	1.21	2.04
1800	-	-	1.51	2.52
2100	-	-	-	2.32
	B. Back Surface Area (in.^{2})[a]			
900	2.48	3.72[b]	6.62	-
1200	2.75	3.55	7.18	9.07
1500	-	4.52	6.04	8.07
1800	-	-	6.73	7.75
2100	-	-	-	7.57
	C. Volume (in.^{3})[a]			
900	0.108	0.290[b]	0.951	-
1200	0.121	0.273	0.960	1.722
1500	-	0.317	0.836	1.733
1800	-	-	0.956	1.792
2100	-	-	-	1.727

[a] Values are based on three replicates except as noted.

[b] Values are based on two replicates.

TABLE 63. SUMMARY OF VISUAL TRANSVERSE BALLISTIC DAMAGE - THICKNESS EFFECTS PROGRAM (INITIAL PHASE)

Velocity (ft/sec)	Thickness (in.)			
	1/16	1/8	1/4	3/8
	A. Front Surface Transverse Damage (in.)[a]			
900	1.46	1.40[b]	1.37	-
1200	1.43	1.38	1.36	1.64
1500	-	1.44	1.45	1.79
1800	-	-	1.67	2.06
2100	-	-	-	2.02
	B. Back Surface Transverse Damage (in.)[a]			
900	2.16	2.39[b]	3.01	-
1200	2.16	2.37	3.16	3.40
1500	-	2.65	2.74	3.27
1800	-	-	3.17	3.22
2100	-	-	-	3.16
	C. Avg Front/Back Transverse Damage (in.)[a]			
900	1.81	1.89[b]	2.20	-
1200	1.80	1.87	2.27	2.52
1500	-	2.05	2.09	2.53
1800	-	-	2.42	2.64
2100	-	-	-	2.59

[a] Values are based on three replicates except as noted.

[b] Values are based on two replicates.

TABLE 64. SUMMARY OF MEASURED RESIDUAL LOAD CAPACITIES[a] - THICKNESS EFFECTS PROGRAM (INITIAL PHASE)

Velocity (ft/sec)	Thickness (in.)			
	1/16	1/8	1/4	3/8
900	4190[b]	7440[c]	-	-
1200	3700	6760[c]	13,520	18,560
1500	-	6720	15,400[c]	25,760
1800	-	-	16,300	20,240
2100	-	-	-	22,910

[a] Data normalized to the nominal specimen thickness (1/8, 1/4, or 3/8 inch). Values (in pounds) are based on three replicates except as noted.

[b] Values are based on one replicate.

[c] Values are based on two replicates.

It was found that a good correlation resulted if only the linear thickness term (x_1) and the interaction term (x_1x_2) were used. The addition of the other terms of the equation had essentially no effect on the degree of fit. The resultant equation was

$$Y = 643.62 + 39,385.6\,x_1 + 10.840\,x_1x_2 \qquad (27)$$

The predicted values based on this expression for the 13 experimental cells are presented in Table 65(A). The agreement with the measured residual load capacities in Table 64 is generally good. The regression equation predicts that load capacity increases directly with impact velocity. For 1/8-inch-thick specimens, a 100-ft/sec increase in impact velocity produces a 136-pound increase in residual load capacity. This indicates that effective damage decreases with increasing velocity, although the influence is relatively small.

This regression analysis was repeated using additional compatible data from Subtask 2. Specifically, residual load capacity data were included on 1/8-inch-thick 470/438-1 composites impacted at room temperature at nominal velocities of 1500, 1800, and 2100 ft/sec. It was again

TABLE 65. PREDICTED RESIDUAL LOAD CAPACITIES - THICKNESS EFFECTS PROGRAM (INITIAL PHASE)

Velocity (ft/sec)	Thickness (in.)			
	1/16	1/8	1/4	3/8
	A. Capacities (in lb) Based on Subtask 5 Data			
900	3715	6786	12,959	-
1200	3918	7193	13,742	20,291
1500	-	7599	14,555	21,511
1800	-	-	15,368	22,730
2100	-	-	-	23,950
	B. Capacities (in lb) Based on Combined Data From Subtasks 2 and 5			
900	3851	6873	12,917	-
1200	4063	7296	13,762	20,229
1500	-	7719	14,608	21,497
1800	-	-	15,453	22,765
2100	-	-	-	24,034

determined that a reduced expression involving the linear thickness and thickness-velocity interaction terms produced a high degree of correlation. The regression equation based on the combined data was

$$Y = 829.36 + 38,201x_1 + 11.275x_1x_2 \qquad (28)$$

The constant and coefficients of this expression are only slightly changed from the original equation. Consequently, the predicted residual load capacities based on the revised equation and given in Table 65(B) are in close agreement with those given in Table 65(A) across the entire spectrum of conditions. The revised equation predicts that an increase of approximately 141 pounds in residual strength of a 1/8-inch-thick specimen will result from a 100-ft/sec increase in impact velocity.

The predicted values based on the modified equation are presented

graphically in Figure 61. The family of curves shown for the various impact velocities indicate that residual load capacity is extremely sensitive to thickness changes but relatively independent of velocity changes.

The ballistic test data from the initial investigation were used to estimate the projectile defeat capabilities of 1/16-, 1/8-, 1/4-, and 3/8-inch-thick 470/438-1 specimens using two different methods. The first method involved plots of impact versus residual velocities for specimens at two areal density levels, 2.54 and 3.76 lb/ft^2, corresponding to thicknesses of approximately 1/4 and 3/8 inch. The areal density values represent the weight per unit surface area (lb/ft^2) of the specimen in the test section and were calculated as follows:

$$\text{Areal density} = \frac{t\rho}{12} \tag{29}$$

where t = specimen thickness, in.

ρ = specimen density, lb/ft^3

These two areal density levels were selected because four empirical data points were available to define the impact-residual velocity relationship. The plotted data shown in Figure 62 suggests that these velocities are linearly related. The x-intercepts (residual velocity = 0) of these lines are estimates of the ballistic limit of the composites. These limits are 680 and 990 ft/sec for specimens with nominal thicknesses of 1/4 and 3/8 inch, respectively.

The second method for computing the ballistic limit involved the following mathematical expression:

$$\text{Ballistic limit} = \sqrt{V_I^2 - V_R^2} \tag{30}$$

where V_I = impact velocity, ft/sec

V_R = residual velocity, ft/sec

This equation was applied to individual ballistic test data at each thickness-velocity condition. These individual values were linearly normalized to areal density levels corresponding to the nominal specimen thicknesses. The normalized values were then averaged within each cell and reported in Table 66.

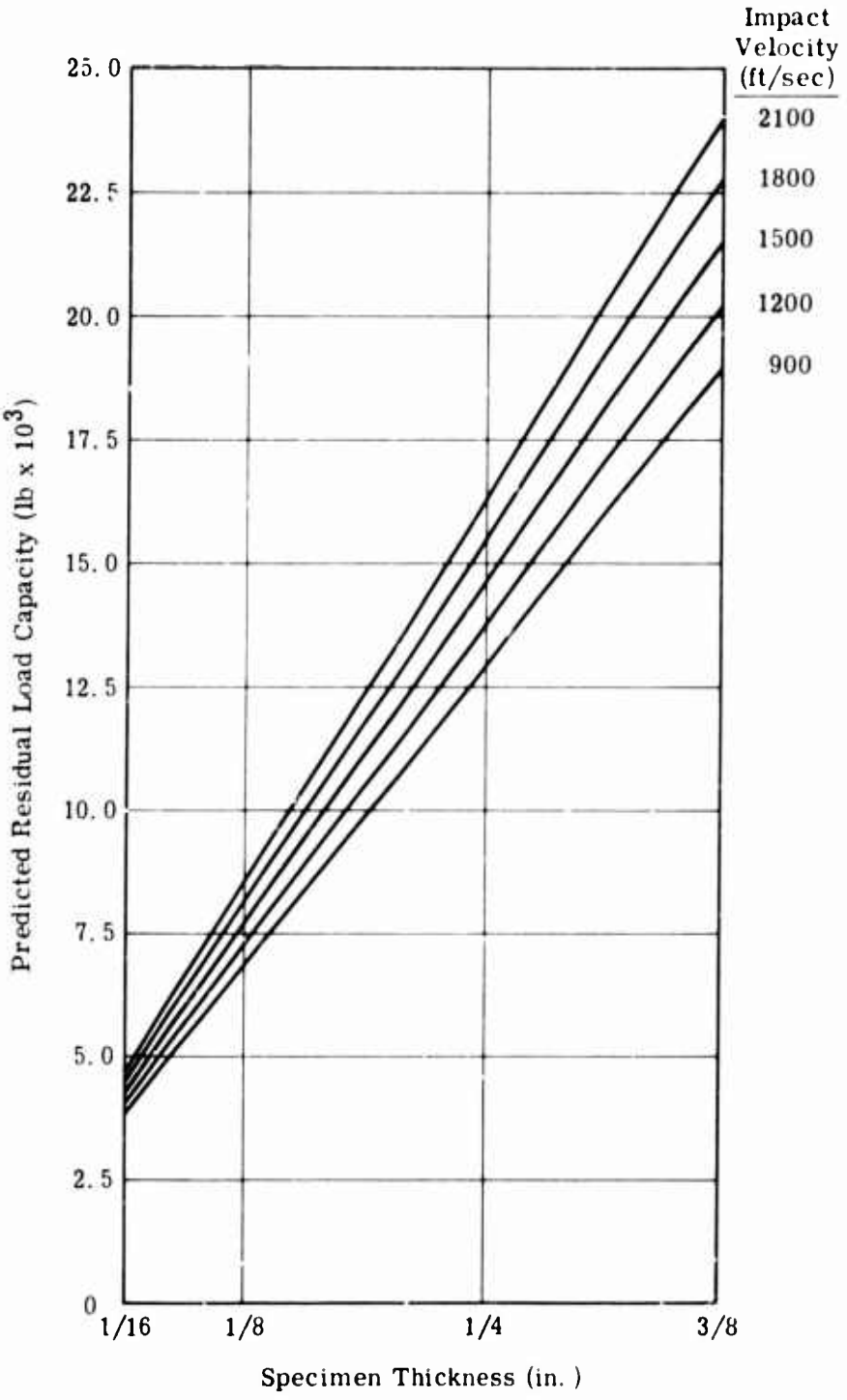

Figure 61. Relationship Between Specimen Thickness and Predicted Residual Load Capacity for 470/438-1 Composites.

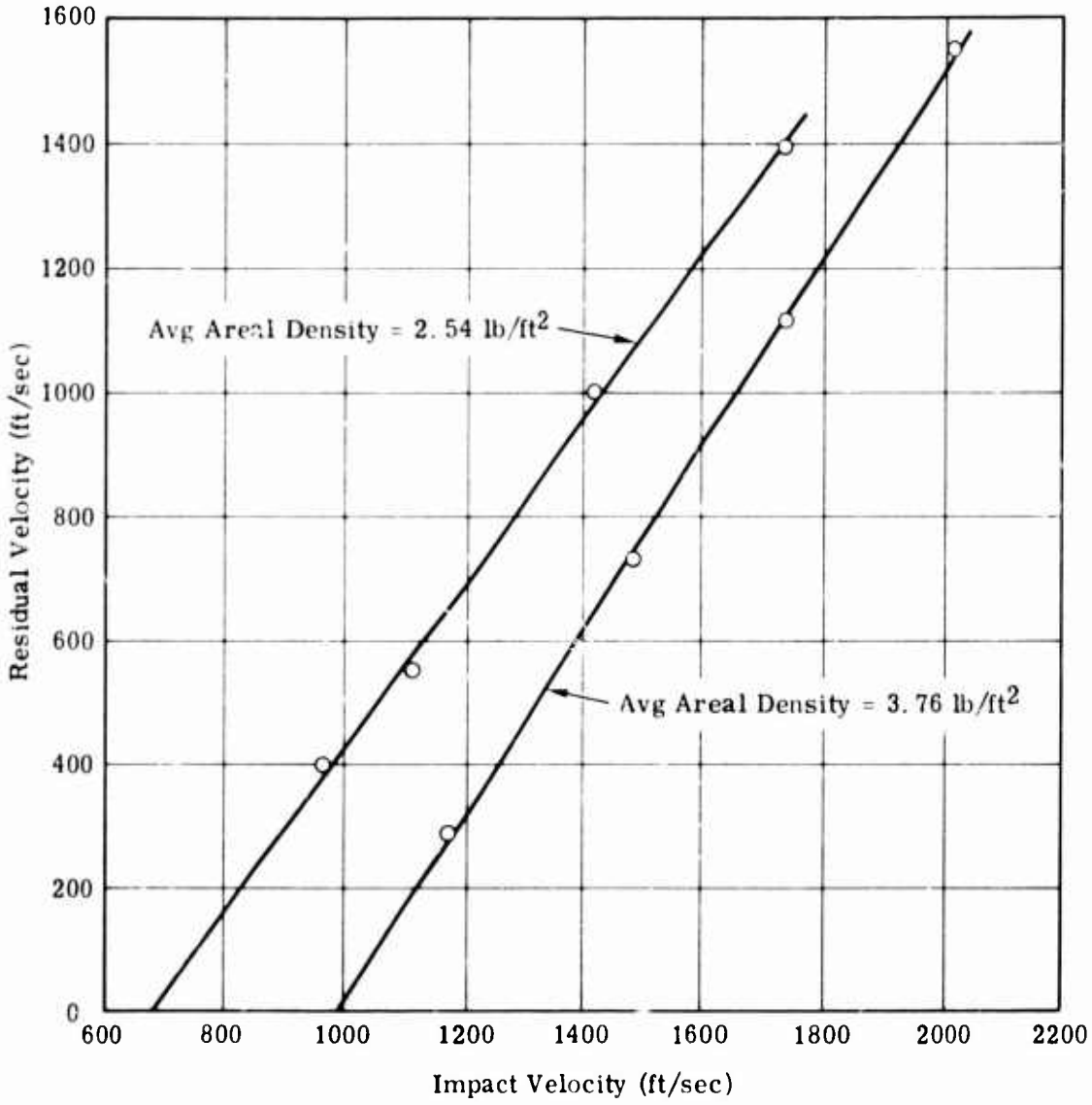

Figure 62. Relationship Between Impact and Residual Velocity for 470/438-1 Composites.

The minimum ballistic limit values for each areal density level are plotted in Figure 63. These minimum values were generally associated with the lowest impact velocity for each nominal specimen thickness. The ballistic limit curve based on the impact-residual velocity relationship is also shown in Figure 63. This latter curve probably defines the minimum value for the ballistic limit at the various thickness levels. This curve

TABLE 66. BALLISTIC LIMIT ESTIMATES BASED ON THICKNESS EFFECTS PROGRAM (INITIAL PHASE)

Nominal Thickness (in.)	Areal Density (lb/ft^2)	Ballistic Limit at Impact Velocity (ft/sec)				
		900	1200	1500	1800	2100
1/16	0.625	297	305	-	-	-
1/8	1.250	560	524	632	-	-
1/4	2.500	852	957	983	995	-
3/8	3.750	-	1106	1288	1351	1290

indicates that discontinuous fiber composites have low resistance to impacting projectiles and would, undoubtedly, be perforated under all realistic thickness-velocity conditions.

Although no definite relationship between residual load capacity and ballistic limit could be established, there is evidence that residual strength will be minimized at or near the ballistic limit. One group of 3/8-inch-thick specimens was tested at 1200 ft/sec, or approximately 20 percent higher than the minimum ballistic limit. The measured and predicted residual load capacities of this thickness-velocity condition were lower than those obtained with higher velocity impacts. Further reductions in load capacity would be expected at the ballistic limit where essentially all the impact kinetic energy would be absorbed by the specimen. Below the ballistic limit, decreased damage is anticipated with an attendant increase in residual load capacity.

Based on the results of the initial phase testing and data analysis, a decision was made with concurrence from the Eustis Directorate to conduct the second phase of Subtask 5 at a nominal impact velocity of 1500 ft/sec. Several factors were taken into account in arriving at this decision. First, the projectile impacts are inconsistent with respect to tumble and location at velocities below 1500 ft/sec. Second, the data indicate that residual load capacity values at 1500 ft/sec are representative of the average values predicted across the experimental velocity range (900 to 2100 ft/sec). Finally, this velocity was used for damaging the cyclic fatigue specimens and would therefore provide a common denominator for comparing composite response across several types of tests.

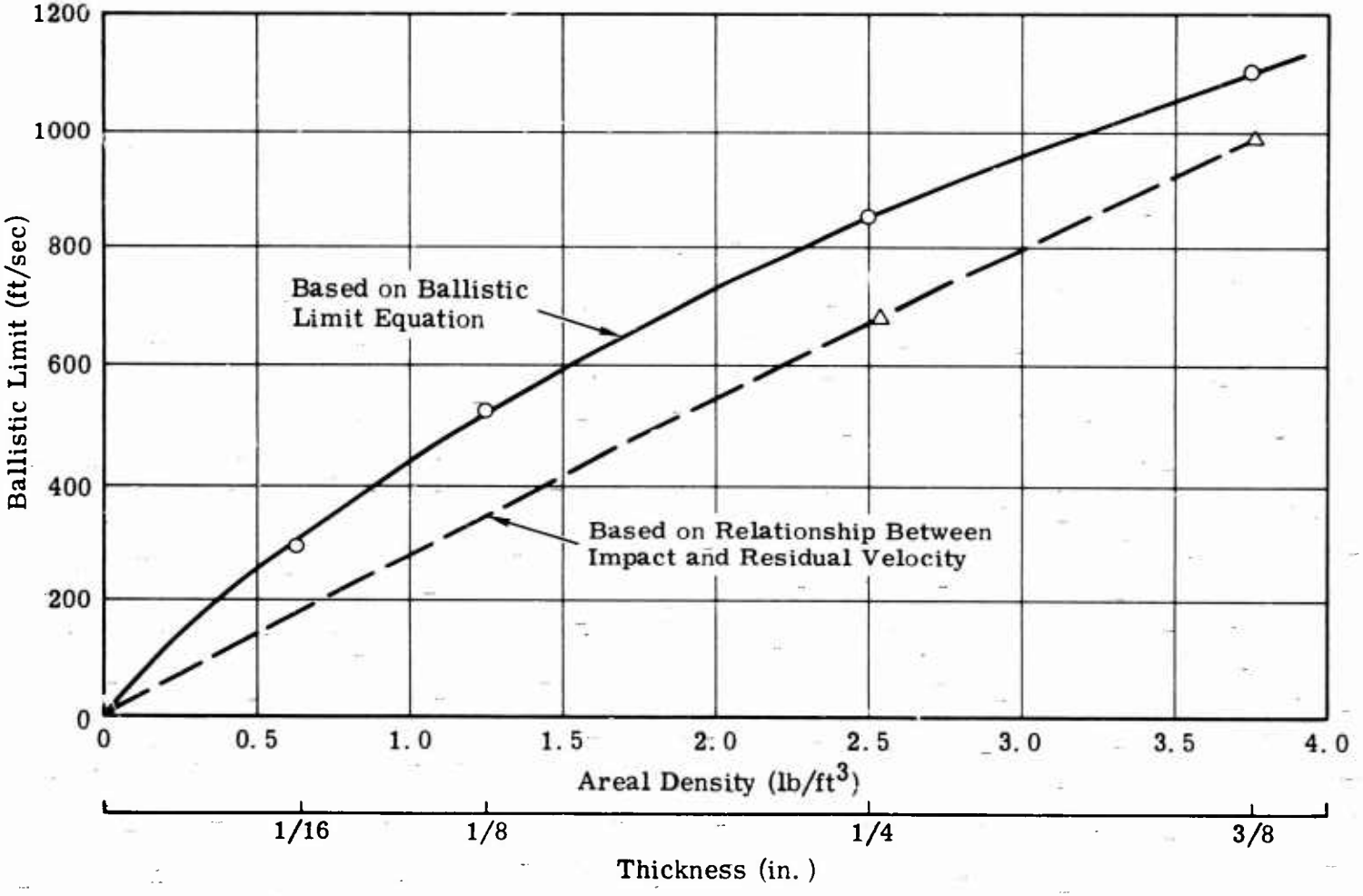

Figure 63. Relationship Between Ballistic Limit and Areal Density for 470/438-1 Composites.

Discussion of Results - Second Phase of Thickness Effects Program

Average damage areas (front and back surface) and volumes after application of data rejection criteria are given in Table 67 for the three candidate composites. Included in this table are damage measurements for the 470/438-1 composite at room temperature taken from the initial phase of Subtask 5. These results indicate that damage areas and volumes for the 470/438 composites with 1/2- or 1-inch fibers are relatively insensitive to changes in temperature over the experimental range. For 897/332-732-1 composites the average damage areas and volumes decrease with increasing temperature.

The effect of thickness on the extent of ballistic damage was established by averaging the cell values across all temperature levels. A graphical presentation of the front and back surface damage areas is given in Figure 64. These data indicate that the front surface damage area for 3/8-inch-thick specimens is approximately twice as great as the area measured on 1/8-inch-thick specimens. At any particular thickness level, the differences in front surface damage area among the three candidate material systems are relatively small on an absolute numerical basis.

With respect to back surface damage area, the composites with 1-inch fibers experience substantially more damage than 470/438-1/2 composites, particularly with the thicker specimens. For 3/8-inch-thick specimens, the 470/438-1 and 897/332-732-1 composites exhibit approximately twice the back surface damage area typical of the 470/438-1/2 composites. The damage area for both of the 470/438 systems at the 3/8-inch thickness level is about double the area measured on 1/8-inch-thick specimens. The back surface damage area for the 897/332-732-1 composite increases at approximately the same rate as thickness.

The effect of temperature and thickness on the extent of visual transverse damage is summarized in cell form in Table 68. The temperature effect was determined by averaging the damage values across all thickness levels. These average values indicate that temperature does not have a powerful influence on any of the transverse damage parameters regardless of composite type. The thickness effect is significant as evidenced from the curves shown in Figure 65. The front surface transverse damage for 3/8-inch-thick specimens is 26 to 45 percent greater than the damage associated with 1/8-inch-thick specimens. The back surface transverse damage experienced by 3/8-inch-thick composites is 32 to 50 percent greater than 1/8-inch-thick specimen damage. The 470/438-1 composite is least affected by changes in thickness, whereas the 897/332-732-1 composite reflects the greatest influence.

TABLE 67. SUMMARY OF VISUAL BALLISTIC DAMAGE[a] - THICKNESS EFFECTS PROGRAM (SECOND PHASE)

Thickness (in.)	470/438-1				470/438-1/2				897/332-732-1			
	Temperature (°F)				Temperature (°F)				Temperature (°F)			
	-80	RT	160	Avg	-80	RT	160	Avg	-80	RT	160	Avg
	A. Front Surface Area (in.^{2})[b]											
1/8	0.91	1.04	0.83[c]	(0.93)	0.85	0.76[c]	(0.81)	(0.81)	0.65	0.68	0.64[d]	(0.66)
1/4	1.39	1.21	1.35[c]	(1.32)	0.99	1.25[c]	1.33[c]	(1.19)	1.20	1.01	1.10[c]	(1.10)
3/8	1.80	2.04	1.64	(1.83)	1.58	1.55	1.49[c]	(1.54)	1.76	1.66	1.58	(1.67)
Avg	(1.37)	(1.40)	(1.27)		(1.14)	(1.19)	(1.21)		(1.20)	(1.12)	(1.11)	
	B. Back Surface Area (in.^{2})[b]											
1/8	3.99	4.52	3.65[c]	(4.05)	2.45	2.60[c]	(2.53)	(2.53)	3.48	3.08	2.54[d]	(3.03)
1/4	6.77	6.04	6.21[c]	(6.34)	3.51	3.71[c]	3.81[c]	(3.68)	5.98	5.68	4.66[c]	(5.44)
3/8	8.29	8.07	8.50	(8.29)	4.79	4.52	4.47	(4.59)	8.92	8.45	8.69	(8.69)
Avg	(6.35)	(6.21)	(6.12)		(3.58)	(3.61)	(3.60)		(6.13)	(5.74)	(5.30)	
	C. Volume (in.^{3})[b]											
1/8	0.288	0.317	0.263[c]	(0.289)	0.196	0.193[c]	(0.195)	(0.195)	0.233	0.217	0.163[d]	(0.204)
1/4	0.969	0.836	0.891[c]	(0.899)	0.545	0.579[c]	0.631[c]	(0.595)	0.840	0.780	0.672[c]	(0.764)
3/8	1.724	1.733	1.721	(1.726)	1.126	1.085	1.062	(1.091)	1.859	1.734	1.766	(1.786)
Avg	(0.994)	(0.962)	(0.958)		(0.622)	(0.619)	(0.629)		(0.977)	(0.910)	(0.867)	

[a] Specimens were impacted with tumbled caliber .30 ball M2 projectiles at a nominal velocity of 1500 ft/sec.

[b] Values are based on three replicates except as noted. Average values are shown in parentheses. Values other than "Avg" entries appearing in parentheses represent average values used for calculation in cases where data were rejected.

[c] Values are based on two replicates.

[d] Values are based on one replicate.

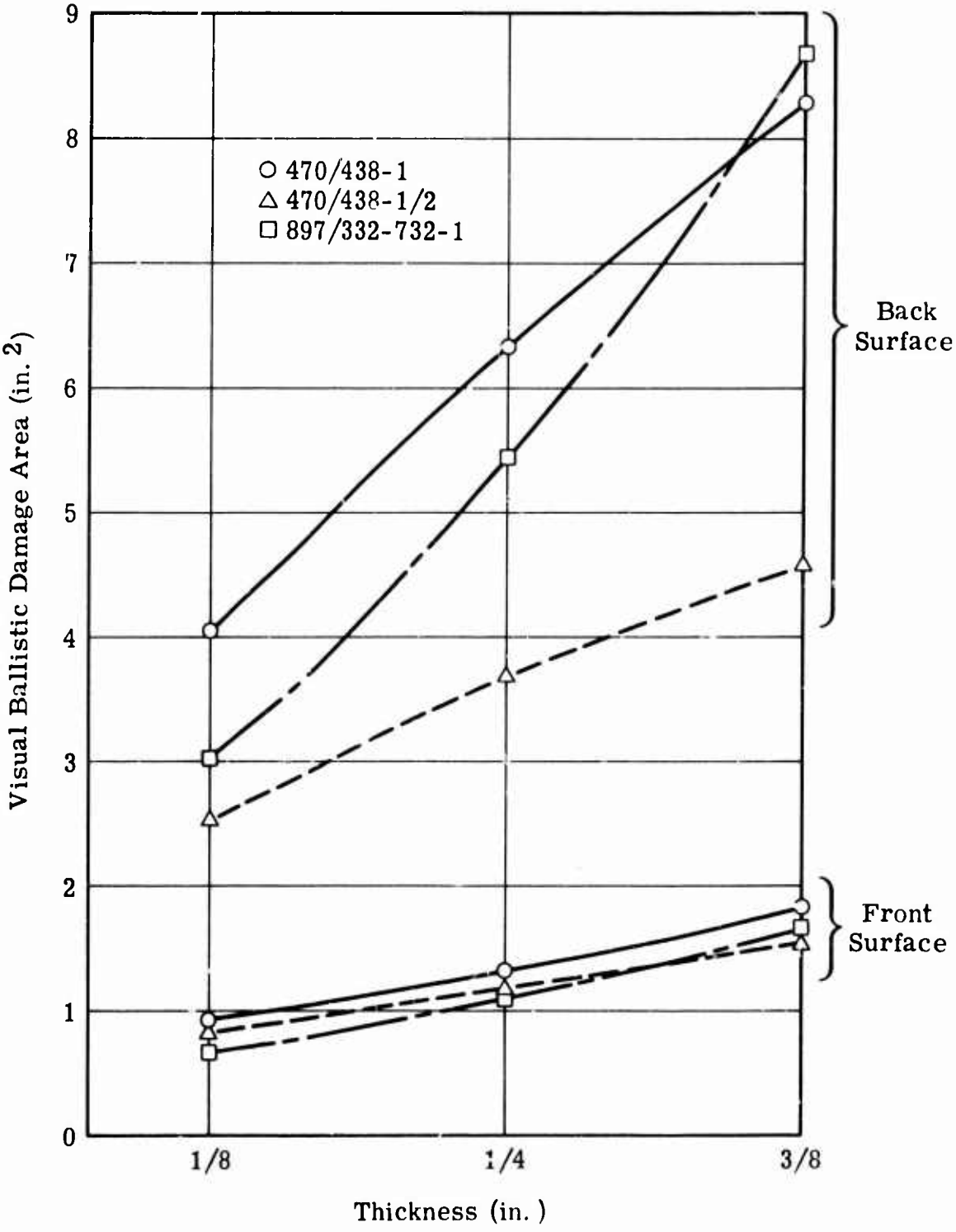

Figure 64. Relationship Between Specimen Thickness and Visual Ballistic Damage Areas for the Three Candidate Composites.

TABLE 68. SUMMARY OF VISUAL TRANSVERSE BALLISTIC DAMAGE[a] - THICKNESS EFFECTS PROGRAM (SECOND PHASE)

Thickness (in.)	470/438-1				470/438-1/2				897/332-732-1			
	Temperature (°F)			Avg	Temperature (°F)			Avg	Temperature (°F)			Avg
	-80	RT	160		-80	RT	160		-80	RT	160	
	A. Front Surface Transverse Damage (in.)[b]											
1/8	1.45	1.44	1.25[c]	(1.38)	1.30	1.08[c]	(1.19)	(1.19)	1.21	1.25	1.31[d]	(1.26)
1/4	1.70	1.45	1.61[c]	(1.59)	1.38	1.51	1.54[c]	(1.48)	1.47	1.26	1.44[c]	(1.39)
3/8	1.76	1.79	1.67	(1.74)	1.74	1.62	1.61	(1.66)	1.88	1.87	1.72	(1.82)
Avg	(1.64)	(1.56)	(1.51)		(1.47)	(1.40)	(1.45)		(1.52)	(1.46)	(1.49)	
	B. Back Surface Transverse Damage (in.)[b]											
1/8	2.61	2.65	2.32[c]	(2.53)	2.00	1.94[c]	(1.97)	(1.97)	2.41	2.22	2.01[d]	(2.21)
1/4	3.00	2.74	3.17[c]	(2.97)	2.43	2.51	2.49[c]	(2.48)	3.12	2.90	2.80[c]	(2.94)
3/8	3.37	3.27	3.40	(3.35)	2.77	2.69	2.62	(2.69)	3.30	3.31	3.35	(3.32)
Avg	(2.99)	(2.89)	(2.96)		(2.40)	(2.38)	(2.36)		(2.94)	(2.81)	(2.72)	
	C. Avg Front/Back Surface Transverse Damage (in.)[b]											
1/8	2.03	2.05	1.79[c]	(1.96)	1.65	1.51[c]	(1.58)	(1.58)	1.81	1.74	1.66[d]	(1.74)
1/4	2.35	2.09	2.39[c]	(2.28)	1.91	2.01	2.02[c]	(1.98)	2.30	2.08	2.12[c]	(2.17)
3/8	2.57	2.53	2.54	(2.55)	2.26	2.16	2.12	(2.18)	2.59	2.59	2.54	(2.57)
Avg	(2.32)	(2.22)	(2.24)		(1.94)	(1.89)	(1.91)		(2.23)	(2.14)	(2.11)	

[a] Specimens were impacted with tumbled caliber .30 ball M2 projectiles at a nominal velocity of 1500 ft/sec.

[b] Values are based on three replicates except as noted. Average values are shown in parentheses. Values other than "Avg" entries appearing in parentheses represent average values used for calculation in cases where data were rejected.

[c] Values are based on two replicates.

[d] Values are based on one replicate.

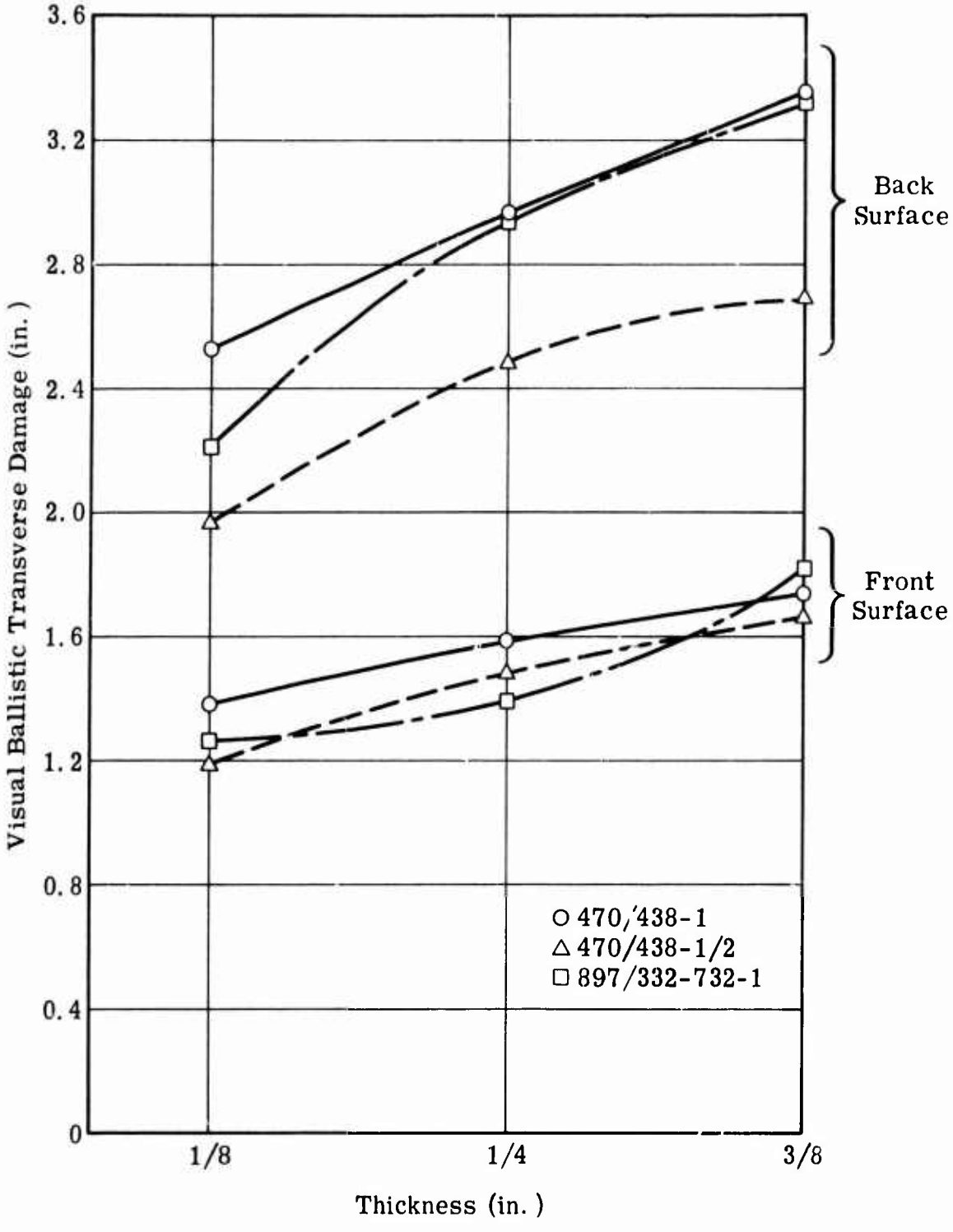

Figure 65. Relationship Between Specimen Thickness and Visual Transverse Ballistic Damage for the Three Candidate Composites.

The residual load capacities of the three candidate material systems as affected by temperature and thickness changes are reported in Table 69. The values reported for the 470-438/1 composites at room temperature were obtained from the initial phase of the thickness investigation. The effect of temperature was established by averaging all cell values in a vertical direction; thickness effects were derived by horizontal cell averaging.

The temperature effect appears to be relatively minor, particularly on the 470/438-1/2 composites. The temperature insensitivity of the 470/438-1/2 composites is evident from both the average and within-cell values. The 470/438-1 composites generally exhibit lower post-damage load capacities after ballistic impact at 160°F than at -80°F or room temperature. The residual load capacity of the 897/332-732-1 composites was consistently lower after impact at -80°F.

A comparison of the effect or thickness on residual load capacity for the three materials is shown graphically in Figure 66. The calculated stress levels are based on total net cross-sectional area without any attempt to access damaged area.

The 470/438-1 composites retained 58.7, 53.5, and 59.0 percent of the undamaged load capacity for the 1/8-, 1/4-, and 3/8-inch thick specimens, respectively. These values are based on undamaged strength data reported in Subtask 1 of Task II. These retention values suggest that changes in specimen thickness do not significantly influence the extent of effective ballistic damage on the 470/438-1 material. From Figure 66 it would appear that the 897/332-732-1 and the 470/438-1/2 materials are adversely affected by the change in thickness.

During the second phase of the thickness study, measurements were taken of the residual projectile velocity after specimen perforation. The specimens were impacted at 0-degree obliquity with tumbled caliber .30 ball M2 projectiles at a nominal impact velocity of 1500 ft/sec. The measured impact and residual velocities were used to estimate the ballistic limit of the composites from the mathematical expression given in Equation (30).

The ballistic limit values were then linearly normalized to areal density (weight per unit area) levels of 1.25, 2.50, and 3.75 lb/ft^2 for the 1/8-, 1/4-, and 3/8-inch-thick specimens, respectively. The resultant values are summarized in cell form in Table 70 and presented graphically in Figure 67. The room temperature values for the 470/438-1 composites were taken from the initial phase of the thickness investigation.

TABLE 69. SUMMARY OF RESIDUAL LOAD CAPACITIES[a] - THICKNESS EFFECTS PROGRAM (SECOND PHASE)

Thickness (in.)	470/438-1				470/438-1/2				897/332-732-1			
	Temperature (°F)				Temperature (°F)				Temperature (°F)			
	-80	RT	160	Avg	-80	RT	160	Avg	-80	RT	160	Avg
1/8	7,357	6,720	7,115[b]	(7,064)	5,043	6,890[b]	(5,967)	(5,967)	6,387	6,860	8,260[c]	(7,169)
1/4	14,600[c]	15,400[b]	11,535[b]	(13,845)	10,537	10,430	10,180[b]	(10,382)	11,820	13,710	13,460[b]	(12,997)
3/8	22,930[b]	25,760	18,500[b]	(22,397)	15,650[b]	15,203	16,123	(15,659)	16,530	19,143	18,453	(18,042)
Avg	(14,962)	(15,969)	(12,383)		(10,410)	(10,841)	(10,757)		(11,579)	(13,238)	(13,391)	

[a]Specimens were impacted with tumbled caliber .30 ball M2 projectiles at a nominal velocity of 1500 ft/sec. Data are normalized to the nominal specimen thickness (1/8, 1/4, or 3/8 inch). Values (in pounds) are based on three replicates except as noted. Average values are shown in parentheses. Values other than "Avg" entries appearing in parentheses represent average values used for calculation in cases where data were rejected.

[b]Values are based on two replicates.

[c]Values are based on one replicate.

TABLE 70. SUMMARY OF ESTIMATED BALLISTIC LIMITS[a] - THICKNESS EFFECTS PROGRAM (SECOND PHASE)

Thickness (in.)	470/438-1				470/438-1/2				897/332-732-1			
	Temperature (°F)				Temperature (°F)				Temperature (°F)			
	-80	RT	160	Avg	-80	RT	160	Avg	-80	RT	160	Avg
1/8	731	633	635	(666)	589	578[b]	(584)	(584)	665[b]	635	665	(655)
1/4	1053	982	1140	(1058)	978	956	1017[b]	(984)	1024	1000	1031	(1018)
3/8	1302	1288	1243	(1278)	1231[b]	1188	1216	(1212)	1265	1282	1294	(1260)
Avg	(1029)	(968)	(1006)		(933)	(907)	(939)		(985)	(972)	(997)	

[a]Specimens were impacted with tumbled caliber .30 ball M2 projectiles at a nominal velocity of 1500 ft/sec. Data are normalized to areal densities of 1.25, 2.50, and 3.75 lb/ft^2 for the 1/8-, 1/4-, and 3/8-inch-thick specimens, respectively. Values (in ft/sec) are based on three replicates except as noted. Average values are shown in parentheses. Values other than "Avg" entries appearing in parentheses represent average values used for calculation in cases where data were rejected.

[b]Values are based on two replicates.

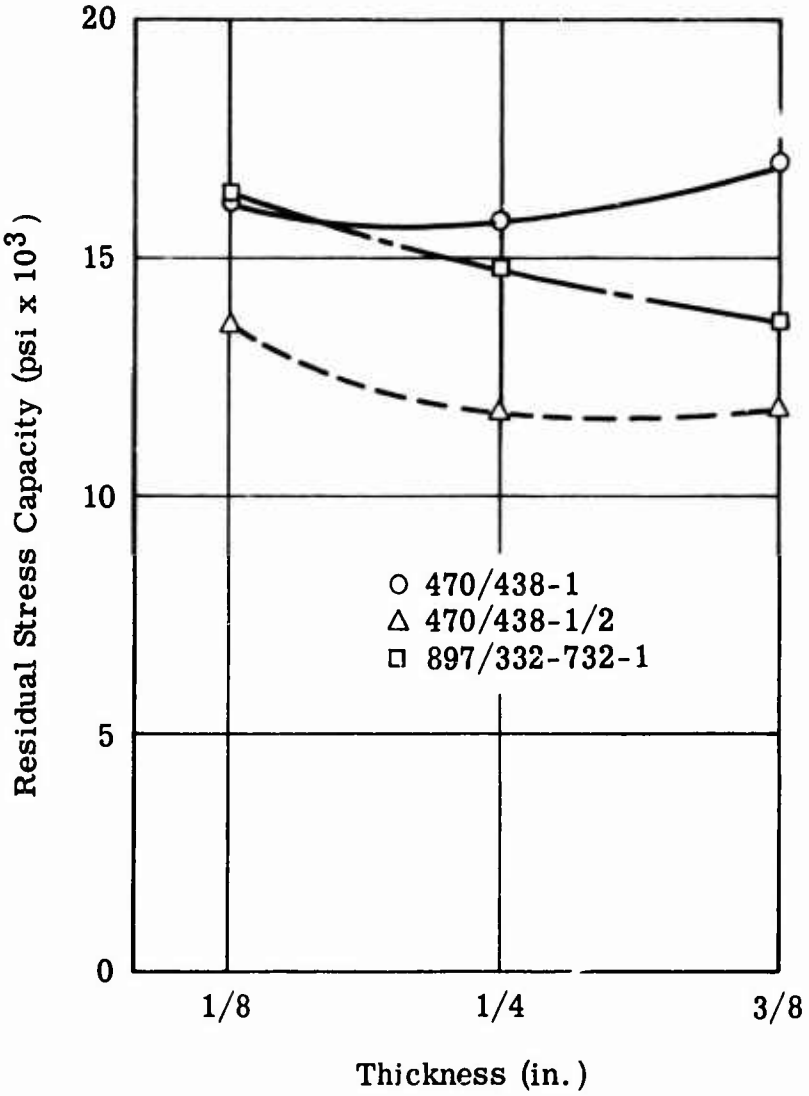

Note: Stress Calculations Based on Full Cross-Sectional Area

Figure 66. Relationship Between Specimen Thickness and Residual Stress Capacity for the Three Candidate Composites.

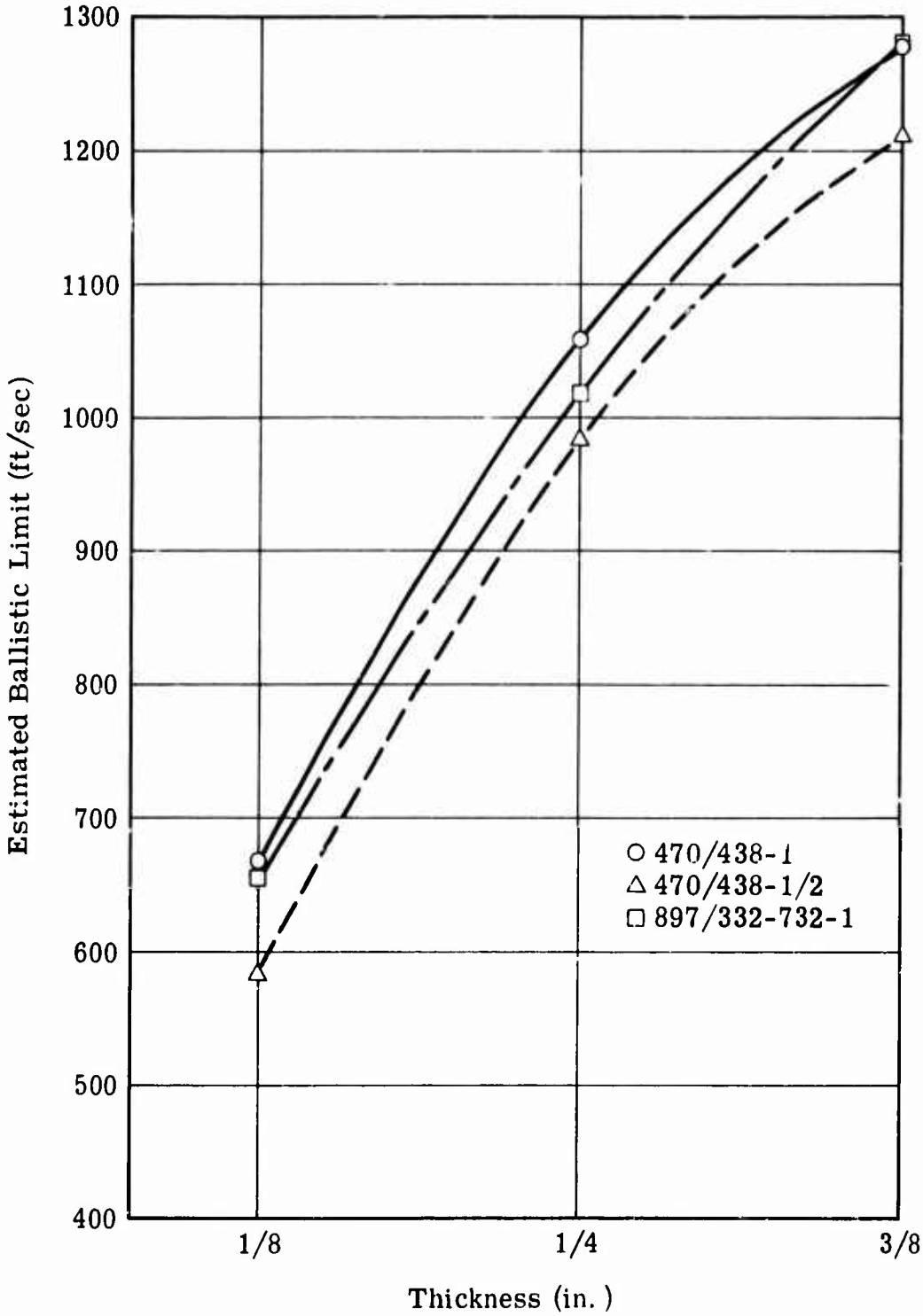

Figure 67. Relationship Between Specimen Thickness and Estimated Ballistic Limit for the Three Candidate Composites.

The effect of temperature on the estimated ballistic limit is minimal as evidenced by the small differences in averages shown parenthetically at the bottom of each column. The ballistic limit versus thickness curves in Figure 67 indicate a very strong thickness effect, as expected. The 3/8-inch-thick specimens exhibit approximately twice the projectile defeat capabilities typical of 1/8-inch-thick specimens irrespective of composite type. The composite with shorter fibers, 470/438-1/2, is more easily perforated than the two composites with 1-inch fibers. The absolute differences in ballistic limit capabilities among all three candidate material systems are relatively small.

A substantial amount of damage and residual load capacity data was generated on 1/8-inch-thick standard specimens under one set of ballistic conditions during Subtasks 2, 3, and 5. Specifically, the set of conditions involved the tumbled caliber .30 ball M2 projectile impacting at 1500 ft/sec and 0-degree obliquity. Data were obtained at three test temperatures (-80°F, ambient, and 160°F) with each of the three candidate composites. A summary of these data based on weighted averages is presented in cell form in Table 71. Because the damage and residual load capacity values are based on a larger sample than available within any investigation, more reliable comparisons of temperature effects and relative composite performance are possible.

The data indicate that the extent of ballistic damage and the residual load capacity of the 470/438-1 composite are relatively unaffected by changes in temperature. Minimum damage was consistently associated with ballistic impacts at 160°F, although differences in damage across the three temperature levels were generally less than 5 percent. The ballistic damage and residual load capacity of the 470/438-1/2 specimens are also generally insensitive to variations in temperature. Damage tends to be least at room temperature, and this is manifest in higher post-damage load capacities. Greatest transverse damage was experienced at -80°F, which resulted in low residual load capacities. The 897/332-732-1 composite sustains more front surface damage at 160°F and more back surface damage at -80°F. Although significant differences exist in damage parameter values across the temperature spectrum examined, no definite trend is apparent. The residual load capacity of specimens impacted at 160°F was 15 to 20 percent higher than those impacted at -80°F or room temperature.

The 470/438 composite with 1-inch fibers exhibited greater damage and residual load capacity than the composite reinforced with 1/2-inch fibers. The greater damage was particularly evident in the back surface measurements. The residual load capacity of the 470/438-1 specimens is about 20 to 35 percent higher than that of the 470/438-1/2 specimens. The

TABLE 71. GRAND SUMMARY OF DAMAGE AND RESIDUAL LOAD CAPACITY DATA[a] FOR STANDARD CANDIDATE COMPOSITES IMPACTED WITH TUMBLED CALIBER .30 BALL M2 PROJECTILES AT 1500 FT/SEC AND 0-DEGREE OBLIQUITY

Parameter	470/438-1			470/438-1/2			897/332-732-1		
	Temperature (°F)			Temperature (°F)			Temperature (°F)		
	-80	RT	160	-80	RT	160	-80	RT	160
Front Surface Damage Area ($in.^2$)[b]	1.03	1.02	1.00	0.99	0.85	0.97	0.74	0.88	0.97
Back Surface Damage Area ($in.^2$)[b]	4.31	4.31	4.14	2.47	2.40	2.62	3.63	3.28	3.39
Damage Volume ($in.^3$)[b]	0.309	0.303	0.301	0.209	0.197	0.217	0.250	0.239	0.246
Front Surface Transverse Damage (in.)[c]	1.47	1.44	1.41	1.37	1.28	1.35	1.27	1.30	1.50
Back Surface Transverse Damage (in.)[c]	2.58	2.64	2.46	2.05	1.99	1.84	2.60	2.34	2.47
Avg Front/Back Surface Transverse Damage (in.)[c]	2.02	2.04	1.94	1.71	1.63	1.60	1.93	1.82	1.98
Residual Load Capacity (lb)[d]	7542	7270	7361	5570	6122	5820	6854	7060	8153

[a] Includes data from Subtasks 2, 3, and 5 of Task II.

[b] Values are based on 8, 22, 5, 6, 21, 3, 6, 20, and 3 replicates for cells 1 through 9, respectively.

[c] Values are based on 8, 22, 5, 6, 20, 3, 6, 20, and 3 replicates for cells 1 through 9, respectively.

[d] Values are based on 7, 7, 5, 6, 5, 3, 6, 6, and 3 replicates for cells 1 through 9, respectively.

897/332-732-1 composite generally experienced damage that was intermediate between the two 470/438 composites. At -80°F and room temperature, the 897/332-732-1 composite exhibited a slightly lower residual load capacity than the 470/438-1 composite. At 160°F, however, the 897/332-732-1 specimens had a 10 percent higher residual load capacity than the 470/438-1 specimens.

Conclusions

The following conclusions can be drawn from the data generated in the thickness effects investigation:

1. Ballistic damage increases directly with specimen thickness. However, residual stress capacity is only slightly affected.

2. Projectile velocity does not have a significant effect on visual damage.

3. Statistical analysis indicates that residual load capacity of

the 470/438-1 composite increases directly with impact velocity. An increase of approximately 20 percent in post-damage strength is obtained for a 1200-ft/sec increase (2100 versus 900 ft/sec) in impact velocity.

4. The specimen temperature during ballistic impact does not have a powerful influence on either the extent of damage or the residual load capacity.

5. The ballistic limit, i.e., the projectile defeat capability, of the three candidate composites increases directly with thickness but is essentially unaffected by changes in temperature. The 3/8-inch-thick specimens, regardless of composite type, exhibit ballistic limits that are approximately twice those of 1/8-inch-thick specimens.

6. The ballistic limit of the composites with 1-inch fibers is higher than that computed for the 470/438-1/2 composites. For tumbled caliber .30 ball M2 projectile impacts at 0-degree obliquity, the ballistic limits for 3/8-inch-thick specimens generally fell in the 1200 to 1300 ft/sec range. This indicates that the composites have low resistance to impacting projectiles and would therefore be perforated under all realistic impact velocity and material thickness conditions.

SUBTASK 6 - EFFECT OF COMBINED STRESS AND BALLISTIC IMPACT CONDITIONS (THRESHOLD)

General

This investigation was conducted to determine the threshold stress level at which 1/8-inch-thick specimens of the three candidate composites would fail catastrophically when impacted with tumbled caliber .30 ball M2 projectiles.

Approach to the Problem

Nine standard specimens of each composite type were impacted at 160°F with tumbled caliber .30 ball M2 projectiles at 0-degree obliquity and a nominal velocity of 1500 ft/sec. The 160°F condition was chosen because it represents the most critical temperature with respect to the static strength properties of the composites. Since flight control components must function under the required load conditions regardless of temperature, the composite will be stressed to a higher percentage of its ultimate

strength at 160°F than at any lower temperature. Therefore, the component design will be governed, to a large extent, by the composite properties at elevated temperature, and the generation of combined stress-impact data at 160°F is highly desirable. Testing at this critical temperature will contribute to a higher degree of confidence in the final component design.

The initial specimen of each candidate composite was prestressed to approximately 90 percent of the damaged strength at 160°F. An up-and-down method was then employed, wherein the prestress level was changed based on the response of the preceding specimen. If the previous specimen failed catastrophically, the prestress was reduced for the following specimen. Conversely, if the preceding specimen survived, the prestress was increased for the next test. After each reversal in response (failure/no failure/failure), a constantly decreasing change was made in prestress level.

The threshold stress was determined by arithmetically averaging the highest individual prestresses resulting in specimen survival with a like number of the lowest prestresses producing catastrophic failure. An arbitrary limit of 1000 psi was imposed on the maximum permissible spread between extreme individual values used in this computation.

Discussion of Results

The results of the individual tests and estimates of threshold stress are presented in Table 72 for the three candidate composites. The threshold stress for the 470/438-1/2 composite could not be determined by using the technique described above because the spread between the highest stress for survival and lowest stress for failure was 2833 psi (9424 versus 6591 psi). An estimate of the threshold stress at 160°F was obtained from the following expression:

$$\sigma_{ts(470/438\text{-}1/2)} = \sigma_{ts(470/438\text{-}1)} \left[\frac{\sigma_{u(470/438\text{-}1/2)}}{\sigma_{u(470/438\text{-}1)}}\right] \qquad (31)$$

where σ_{ts} = threshold stress at 160°F, psi

σ_u = undamaged tensile strength at 160°F, psi

By substituting the known values, the expression becomes

$$\sigma_{ts(470/438\text{-}1/2)} = 8043 \left(\frac{14,620}{17,480}\right) = 6727 \text{ psi} \qquad (32)$$

TABLE 72. SUMMARY OF THRESHOLD STRESS TEST DATA[a] FOR THE THREE CANDIDATE COMPOSITES

Prestress (psi)	Time to Failure After Impact (sec)	Threshold Stress (psi)	Min Failure Stress (psi)
	A. 470/438-1 Specimens		
11,033	90	8043[b]	7844
* 7,844	3		
4,738	No failure after 300 sec		
6,278	No failure after 420 sec		
8,830	3		
7,147	No failure after 420 sec		
* 8,351	192		
* 7,730	No failure after 840 sec		
* 8,206	No failure after 600 sec		
	B. 470/438-1/2 Specimens		
9,224	No failure after 300 sec	8008[b],	6591
10,543	Failed before impact	6727[c]	
* 9,424	No failure after 420 sec		
10,556	Failed before impact		
7,906	No failure after 420 sec		
8,561	No failure after 540 sec		
9,230	5		
* 6,591	414		
5,401	No failure after 900 sec		
	C. 897/332-732-1 Specimens		
11,719	38	7367[b]	7206
8,357	12		
4,511	No failure after 420 sec		
* 7,206	28		
5,689	No failure after 1200 sec		
6,694	No failure after 420 sec		
* 7,702	15		
* 7,036	No failure after 5400 sec		
* 7,522	No failure after 1200 sec		

[a] Specimens were impacted at 160°F with tumbled caliber .30 ball M2 projectiles at a nominal velocity of 1500 ft/sec and 0-degree obliquity.

[b] Computed from asterisked prestress values.

[c] Revised value based on Equation (31).

This value seems reasonable based on the minimum stress for failure of 6591 psi.

Of the 27 specimens evaluated in this program, two failed before and 10 failed after ballistic impact. Both of the failures prior to impact were obtained with 470/438-1/2 composites prestressed to approximately 72 percent of their undamaged strength at 160°F. This was the highest percentage of prestress used throughout the combined stress-impact test program. All specimens were generally under load about 30 seconds before impact. This period of time was required to clear the range, load the round in the weapon, and fire the projectile. None of the impacted specimens failed immediately, although three failed in the first five seconds after impact. Failure of the other 7 specimens occurred 12 to 414 seconds after projectile perforation.

It is evident from the time-to-failure after impact data that discontinuous fiber composites are susceptible to creep rupture. This phenomenon was observed during evaluation of the first specimen, the 470/438-1 composite, at a prestress of 11,033 psi. This specimen did not fail until 90 seconds after impact. It was decided at this point to mount a dial indicator on the load fixture to obtain rough measurements of specimen elongation. Generally, the first dial indicator reading was made 20 seconds after impact. No readings could be taken on the 897/332-732-1 composites that failed after 28 and 38 seconds because the specimens were creeping at an extremely high rate. With the 470/438-1 and 470/438-1/2 specimens that failed 192 and 414 seconds respectively after impact, an increasing creep rate with time was observed.

In reviewing the elongation data, it was determined that the 470/438-1/2 composite prestressed to 7906 psi was creeping at an increasing rate when the test was terminated (420 seconds). It is highly probable that failure would have occurred within a reasonable period of time if the load had been maintained. In all other cases, the creep rate was decreasing at the conclusion of the test, although some elongation was still taking place. Generally, the creep rate during the terminal phase of the test was less than 1 μin./in./sec (0.36 pct/hr).

The effect of combined stress-impact conditions can best be illustrated by comparing the threshold stress with the strength of specimens that were impacted under low prestress and tensile tested at 160°F. The average residual load capacities of 470/438-1, 470/438-1/2, and 897/332-732-1 specimens impacted at 160°F and tested at room temperature were 7361, 5820, and 8153 pounds, respectively. To adjust to a 160°F condition, these loads must be multiplied by 0.637 for the 470/438 composites and 0.710 for the 897/332-732-1 composite. The resultant values are

4689, 3707, and 5789 pounds for the 470/438-1, 470/438-1/2, and 897/332-732-1 composites, respectively. The corresponding values for threshold stress converted to load capacity are 3530, 2950, and 3230 pounds. The ratio of residual load capacity to threshold preload represents the stress intensity factor associated with the combined effects of prestress and ballistic conditions.

The stress intensity factors for the 470/438-1, 470/438-1/2, and 897/332-732-1 composites are 1.33, 1.26, and 1.79, respectively. These factors indicate that the 470/438 composites are less vulnerable to combined stress-impact conditions than the 897/332-732-1 composite. These results closely parallel those obtained during Subtask 4, where higher stress concentrations were found at the ballistic damage area of 897/332-732-1 composites compared to the 470/438 composites.

On an absolute basis, the 470/438-1 specimens can tolerate higher prestress conditions (8043 psi) before catastrophic failure will occur. The lowest threshold value, 6724 psi, was obtained with the 470/438-1/2 specimens. The 897/332-732-1 composite exhibited a threshold prestress of 7206 psi, which was intermediate between the two 470/438 composites.

Conclusions and Recommendations

It can be concluded from the results of this investigation that the three candidate composites are susceptible to creep rupture. This phenomenon was observed in both undamaged and damaged specimens. No conclusive statements can be made relative to the precise magnitude of this problem since the investigation was not designed to provide this information.

It can also be concluded that the load capacities of the three candidate composites are significantly reduced under combined stress-ballistic impact conditions. This is particularly evident with the 897/332-732-1 composite where the ratio of static load capacity after damage to threshold stress, converted to load capacity, for catastrophic failure was 1.79. The corresponding ratios for the 1- and 1/2-inch 470/438 composites were 1.33 and 1.26, respectively, indicating a lesser effect of combined stress-impact. On an absolute basis the 470/438-1, 470/438-1/2, and 897/332-732-1 specimens exhibited threshold preloads of 3530, 2950, and 3230 pounds, respectively. These values apply for 1/8-inch-thick standard specimens impacted with fully tumbled caliber .30 ball M2 projectiles at 1500 ft/sec, 0-degree obliquity, and 160°F.

Since discontinuous fiber composites exhibit tensile creep that must

be considered in component design, it is recommended that appropriate tests be conducted to measure this property at 160°F. Specifically, these tests should be performed in accordance with Method 1063, Tensile Time-Fracture and Creep, of Federal Test Method Standard No. 406. The long-term creep properties will be established by this method since a minimum test duration of 1000 hours is required.

SUBTASK 7 - SELECTION OF THE MOST PROMISING COMPOSITE

General

The objective of this subtask was to choose the most promising composite for characterization in Task III and for subsequent use in the fabrication of ballistically tolerant flight control components. This selection would be made from the three candidate composites (470/438-1, 470/438-1/2, and 897/332-732-1) and would be based primarily on information generated in the Task II program.

Approach to the Problem

All three candidate composites can be used in ballistically tolerant components if properly designed so that the material section remaining after projectile impact can carry the operational loads. The most effective composite, however, is obviously the one requiring the minimum original section, assuming that the composites have similar densities.

Determination of the required original section demands a knowledge of two factors; namely, the basic strength of the composite and the amount of material elminated as a result of ballistic impact under various test conditions. This latter factor relates to the extent of effective rather than visual damage. The term "effective damage length" is introduced to represent the theoretical length of composite material, transverse to the load path, that is lost due to perforation and accounts for the attendant reduction in specimen strength.

The residual load capacity and, consequently, the effective damage length are potentially influenced by test and material variables. These variables include the prestress level, the projectile velocity and orientation, as well as the specimen temperature and thickness. Although a few of these variables could be precisely controlled during testing, the majority deviated from nominal due to inherent test or material variablility. Because of these random variations, the true effect of the variables could be estimated only by using statistical procedures; namely, multiple regression

analysis. The residual load capacity data for tumbled caliber .30 ball M2 impacted specimens of each composite type were analyzed separately. These data included those values normally excluded by the rejection criteria.

The residual load capacity data were initially fitted to a regression equation involving 28 terms considered to have a potential effect on composite response. In general form, the regression equation used was

$$\text{Residual load capacity (lb)} = a_0 + a_i x_i + a_{ii} x_{ii}^2 + a_{iii} x_{iii}^3 + a_{ij} x_i x_j \quad (33)$$

The univariate (x_i, x_{ii}, x_{iii}) and interaction ($x_i x_j$) terms of this equation are presented in Table 73. The coefficients (a-values) and the constant (a_0) were determined from at least-squares fit of the test data.

The resultant equation was used to calculate the residual load capacity for various data sets in which one variable was changed while all others were held constant. Since the load capacity of the undamaged composite was known, the effective damage length could readily be computed from the loss in specimen strength.

Effective damage lengths were also determined for ballistically damaged specimens at two fatigue life levels: 2000 and 10,000,000 cycles. The loss in strength was obtained by subtracting the maximum cyclic stress corresponding to each of these fatigue life levels from the load capacity of undamaged fatigue specimens.

A similar procedure was employed to compute the effective damage lengths for specimens subjected to the combined effects of prestress and ballistic impact conditions at 160°F. In order to eliminate the influence of temperature, the 160°F strength of undamaged specimens was used as the base-line value. The difference between the base-line value and the threshold stress causing catastrophic failure represented the loss in strength.

A comparison was then made of the width required for a 1/8-inch-thick specimen of the three candidate composites to carry various loads before and after projectile impact. The results of this analysis provided the basic for selecting the most efficient composite.

Discussion of Results

A compilation of pertinent Task II test results was prepared to assist in selecting the composite material for the balance of the contractual

TABLE 73. TERMS OF THE MULTIPLE REGRESSION EQUATION

Variable	Description	Symbol	Level[a]
Temperature	Specimen temperature (^{o}F)	T	T T * T
Velocity	Projectile impact velocity (ft/sec)	V	V V * V V * V * V
Prestress	Specimen prestress as a fraction of undamaged strength at the test temperature	PRE	PRE PRE * PRE
Footprint Length	Measure of the degree of projectile tumble at time of impact (in.)	FP	FP FP * FP
Thickness	Average specimen thickness in test area (in.)	TH	TH TH * TH TH * TH * TH
Sine of Projectile Rotation Angle	In-plane rotational angle of projectile. Tip of projectile at 12 o'clock, angle = 0^{o}; at 3 o'clock (transverse), angle = 90^{o}.	SIN (ROT)	SIN (ROT) SIN^2 (ROT)
Off-Centerness Factor	Measure of projectile displacement from the longitudinal axis of specimen. For centered impact, factor = 1.000.	KF	KF KF * KF
Specific Gravity	Measured specific gravity of the specimen	SG	SG SG * SG
Temperature-Velocity	Interaction term	-	T * V

[a]Asterisks in this column designate multiplication.

TABLE 73 - Continued

Variable	Description	Symbol	Level[a]
Temperature-Prestress	Interaction term	-	T * PRE
Temperature-Thickness	Interaction term	-	T * TH
Velocity-Prestress	Interaction term	-	V * PRE
Prestress-Thickness	Interaction term	-	PRE * TH
Footprint Length-Thickness	Interaction term	-	FP * TH
Footprint Length-Sine of Rotation Angle	Interaction term	-	FP * SIN (ROT)
Thickness-Specific Gravity	Interaction term	-	TH * SG

[a]Asterisks in this column designate multiplication.

effort. Table 74 presents a summary of tensile strength and modulus data for undamaged specimens. Included are the effects of temperature, fiber alignment, thickness, and cyclic loading. Also presented are strength factors that represent the ratio of each property to the basic value which is the tensile strength at room temperature.

The effect of ballistic and composite variables on residual load capacity is given in Table 75 for tumbled caliber .30 ball M2 impacted specimens. These data were obtained by substituting appropriate values for the variables in the multiple regression equation. The constant and coefficients for the regression equation are summarized in Table 76 for the 470/438-1, 470/438-1/2, and 897/332-732-1 composites. One term, T * TH, was omitted from the equation because it did not improve the degree of fit as measured by the coefficient of determination. This coefficient, $R^2 \times 100$, defines the percentage of test data variability that is

TABLE 74. ENVIRONMENT AND LOADING EFFECTS ON TENSILE PROPERTIES OF UNDAMAGED COMPOSITES

Parameter	Property Value			Strength Factor		
	470/438-1	470/438-1/2	897/332-732-1	470/438-1	470/438-1/2	897/332-732-1
1. Undamaged Ultimate Tensile Strength (psi)						
a. Basic Value, σ_S[a]	27,440	22,950	29,120	1.000	1.000	1.000
b. Temperature Effect						
At -80°F	29,470	24,650	38,350	1.074	1.074	1.317
At 75°F	27,440	22,950	29,120	1.000	1.000	1.000
At 160°F	17,480	14,620	20,680	0.637	0.637	0.710
c. Edge Alignment						
Center, σ_c	23,140	21,800	24,600	0.843	0.950	0.845
Edge, σ_e	33,200	24,400	35,200	1.210	1.063	1.209
d. Thickness Effect						
1/16 inch	24,800	22,400	26,300	0.904	0.976	0.903
1/4 inch	29,550	23,400	31,300	1.077	1.020	1.075
3/8 inch	28,880	23,200	30,700	1.052	1.011	1.054
2. Modulus of Elasticity (psi x 10^6)						
a. Basic Value, E_S[a]	3.50	3.59	3.47	1.000	1.000	1.000
b. Temperature Effect						
At -80°F	3.96	3.61	3.96	1.131	1.006	1.141
At 160°F	2.32	2.21	2.54	0.663	0.616	0.732
c. Edge Alignment						
Center	3.06	3.32	3.20	0.874	0.925	0.922
Edge	4.10	3.84	4.11	1.171	1.070	1.184
3. Density (lb/in.^{3})	0.0691	0.0690	0.0711	-	-	-
4. Fatigue Strength (psi)[a]						
At 2,000 cycles	16,960	13,710	14,743	0.618	0.597	0.506
At 100,000 cycles	12,663	10,011	10,423	0.461	0.436	0.358
At 10,000,000 cycles	8,869	6,949	7,863	0.323	0.303	0.270

[a] Standard specimens, 1/8 inch thick and 3.5 inches wide, at 75°F.

TABLE 75. INFLUENCE OF TEST VARIABLES ON THE RESIDUAL LOAD CAPACITY AND EFFECTIVE DAMAGE LENGTH OF TUMBLED CALIBER .30 BALL M2 IMPACTED SPECIMENS

Variable	Level	470/438-1		470/438-1/2		897/332-732-1	
		Load (lb)	Damage Length (in.)	Load (lb)	Damage Length (in.)	Load (lb)	Damage Length (in.)
Temperature (°F)	-80	7,875	1.440	5,762	1.564	7,890	1.579
	-5	7,568	1.534	5,846	1.533	7,933	1.565
	70[a]	7,420	1.584	5,767	1.562	7,819	1.601
	115	7,407	1.588	5,641	1.607	7,675	1.645
	160	7,451	1.573	5,457	1.674	7,476	1.706
Velocity (ft/sec)	900	6,653	1.827	-	-	-	-
	1200	6,768	1.792	5,123	1.793	7,112	1.812
	1500[a]	7,420	1.584	5,767	1.562	7,819	1.601
	1800	8,332	1.282	6,084	1.463	8,069	1.522
	2100	9,227	0.973	5,929	1.503	9,663	1.015
Prestress (percent of ultimate)	15	7,169	1.666	5,893	1.516	7,895	1.577
	25[a]	7,420	1.584	5,767	1.562	7,819	1.601
	35	7,875	1.440	6,260	1.398	8,073	1.520
	45	8,534	1.212	7,371	0.990	8,659	1.342
Footprint Length (in.)	1.10[a]	7,420	1.581	5,767	1.562	7,819	1.601
	1.00	8,158	1.323	5,601	1.622	7,987	1.548
	0.90	8,819	1.114	5,521	1.651	8,156	1.506
	0.80	9,402	0.912	5,524	1.650	8,324	1.451
Thickness (in.)	0.125[a]	7,420	1.584	5,767	1.562	7,819	1.601
	0.250	13,552	1.934	10,605	1.765	14,387	1.930
	0.375	19,612	1.958	13,920	1.979	19,650	2.059
Rotation Angle (deg)	90[a]	7,420	1.584	5,767	1.562	7,819	1.601
	75 or 105	7,336	1.611	5,659	1.601	7,882	1.561
	60 or 120	7,206	1.654	5,374	1.703	8,067	1.522
Off-Centerness Factor	1.000[a]	7,420	1.584	5,767	1.562	7,819	1.601
	1.043	6,533	1.863	5,225	1.756	6,642	1.944
	1.094	5,574	2.136	4,835	1.894	5,942	2.126
	1.158	3,515	2.400	4,741	1.927	6,181	2.067

[a]Level at standard conditions. When the effect of one variable was determined, the balance of the variables were held constant at standard conditions. Specific gravities used in computation were 1.907 for the 470/438 composites and 1.972 for the 897/332-732-1 composite.

TABLE 76. CONSTANT AND COEFFICIENTS FOR THE REGRESSION EQUATION - TUMBLED CALIBER .30 BALL M2 IMPACTED SPECIMENS

Term	470/438-1		470/438-1/2		897/332-732-1	
T	-0.184996	02[a]	0.300858	02	-	
T * T	0.140985	-01	-0.145451	-01	-0.138861	-01
V	-0.156413	02	0.119051	02	0.912700	02
V * V	0.914945	-02	0.221190	-02	-0.525470	-01
V * V * V	-0.171233	-05	-0.895396	-06	0.111131	-04
PRE	0.533020	05	0.349642	05	0.325187	05
PRE * PRE	0.102239	05	0.309231	05	0.165536	05
FP	0.176853	05	-0.283736	05	-	
FP * FP	-0.389747	04	0.423092	04	-	
TH	-0.465871	05	0.454079	06	-	
TH * TH	0.139663	06	0.381651	06	-0.417521	05
TH * TH * TH	-0.189320	06	-0.573860	06	-	
SIN (ROT)	0.455247	04	-0.365769	05	-	
SIN^2 (ROT)	0.866426	04	0.253226	04	-	
KF	-0.632747	05	-0.120204	06	-0.327193	06
KF * KF	0.209237	05	0.526898	05	0.146808	06
SG	0.131559	06	0.843316	06	-	
SG * SG	-0.355627	05	-0.208367	06	-	
T * V	0.968735	-02	0.458358	-02	0.786155	-02
T * PRE	-0.475753	02	-0.924218	02	-0.149909	02
T * TH	-		-0.465886	01	0.329179	02
V * PRE	-0.115506	02	-0.457712	01	-0.213074	02
V * TH	0.212993	01	-0.967999	02	-0.550987	02
PRE * TH	-0.987669	05	0.580544	05	-	
FP * TH	0.396651	04	-0.838182	05	-	
FP * SIN (ROT)	-0.173833	05	0.316230	05	-0.168536	04
TH * SG	0.425349	05	-0.141778	06	0.676480	05
Constant	-0.811335	05	-0.783476	06	0.124466	06

[a]Floating point notation; e.g., -0.184996 02 is -0.184996 x 10^2, or -18.4996.

accounted for by the form of the equation and the terms included. The coefficient of determination was 88.0 percent for the 470/438-1 regression equation.

The full 28-term expression was used to relate residual load capacity

to the various independent variables for the 470/438-1/2 composite. The value for $R^2 \times 100$ of 94.1 percent indicates that the regression equation closely approximates reality, within the experimental range of the variables. Ten terms were omitted from the equation for the 897/332-732-1 composite without affecting the degree of fit. The coefficient of determination with the simplified expression was 95.3 percent, the highest correlation obtained in the multiple regression analysis.

The predicted load capacities from the regression equations were then used in computing the effective damage lengths reported in Table 75. Two different methods were utilized in making these computations, depending on the extent of ballistic damage. In those cases where effective damage was confined to randomly oriented material, i.e., the central 1.5-inch width of the specimen, the calculation was based on the following equation:

$$l_e = \frac{P_u - P_d}{t\sigma_c} \tag{34}$$

where l_e = effective damage length, in.

P_u = undamaged load capacity, lb

P_d = residual load capacity, lb

t = specimen thickness, in.

σ_c = strength of center material, psi

When damage was greater than 1.50 inches, as determined from Equation (34), the effective damage length was obtained from the curves shown in Figure 68. These curves are based on the hypothetical strength distribution model discussed earlier in this report and represent solutions to the quadratic expressions

$$-0.5\left(\frac{\sigma_e}{\sigma_c} - 1\right)l_e^2 + \left(1.5\frac{\sigma_e}{\sigma_c} - 2.5\right)l_e + \left(\frac{\sigma_e}{\sigma_c} + 2.5\right) - 0.625\left(\frac{\sigma_e}{\sigma_c} - 1\right) - b_c = 0 \tag{35}$$

and

$$b_c = \frac{P_d}{t\sigma_c} \tag{36}$$

where σ_e = strength of edge material

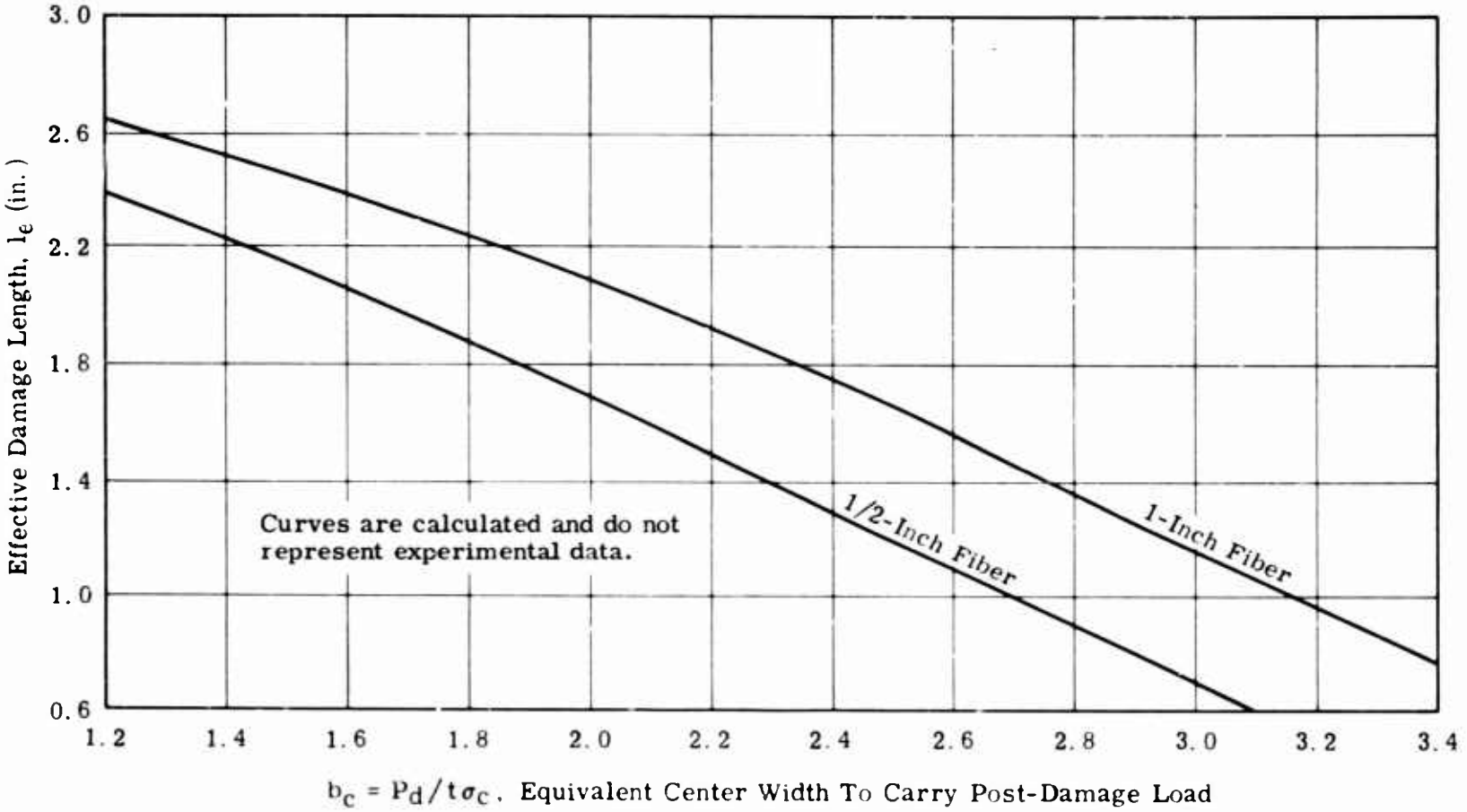

Figure 68. Effective Damage Length From Ultimate Load Data.

Two curves are presented in Figure 68 since the edge-to-center strength ratio, σ_e / σ_c, is different for the two fiber lengths involved. The strength ratios for the 1- and 1/2-inch fiber composites are 1.435 and 1.114, respectively.

The data in Table 75 indicate that residual load capacities and, consequently, effective damage length are relatively insensitive to changes in specimen temperature during ballistic impact regardless of composite type. Residual load capacity generally increases directly with both impact velocity and prestress irrespective of composite type. The effect of the latter variable seems contrary to the combined stress-impact results discussed in Subtask 6. It is important to recognize that there was one significant difference in test procedure between the combined stress-impact investigation and the balance of the ballistic tests conducted in Task II. In the combined stress-impact investigation, the specimen prestress was maintained for at least 5 minutes unless failure occurred earlier. In all other Task II tests, the preload was removed within 20 seconds after ballistic impact.

Since the trend to higher residual load capacities with increasing prestress if below the threshold stress was consistent across all composite types, this adds credence to the general relationship observed. One possible explanation for this trend is that the effective stiffness of the specimen increases directly with prestress. This would reduce the amount of damage caused by bending in the specimen.

Changes in projectile footprint length did not have a similar effect on the three candidate composites. The effective damage length for the 470/438-1 composite decreased dramatically as the footprint length became shorter. The 897/332-732-1 composite also exhibited reduced effective damage with decreased footprint length, but this reduction was substantially less than that manifested by the 470/438-1 composite. The 470/438-1/2 composite was essentially unaffected by variations in footprint length. No explanation is apparent for the difference in the behavior of the three candidate composites.

Effective damage length increases directly with specimen thickness regardless of composite type. Actually, the differences in absolute values are relatively small at corresponding thicknesses for the three candidate composites. Variations in rotation angle of the projectile have only a minor influence on effective damage length. The geometry of the projectile - the small l/d ratio and the cylindrical base - probably is responsible for this minor effect. An angular rotation of 30 degrees reduces the effective length of the projectile only 7 percent compared with 13.5 percent for an infinitely large l/d ratio.

Residual load capacity decreases significantly with increasing off-centerness or displacement of the impacts from the longitudinal axis of the specimen. This is true regardless of composite type, although the effect is more pronounced with the 1-inch fiber composites. An off-centerness factor of 1.000 indicates that the projectile is symmetrically located about the longitudinal axis of the specimen. For each successive level of off-centerness given in Table 75, the projectile is displaced an additional 0.10 inch. Therefore, the factor of 1.158 corresponds to a lateral displacement of 0.30 inch for a fully tumbled projectile impacting transverse to the load path.

Selected residual load capacity and effective damage length values from Table 75 are summarized in Table 77 to show the effects of temperature, thickness, and velocity. Also presented are the appropriate values for damage fatigue and combined stress-impact conditions. Effective damage lengths of the 470/438-1/2 and 897/332-732-1 composites are less than that of the 470/438-1 composite for both the 2000 and 10,000,000 fatigue cycles. The effective damage lengths of these composites are based on the reduction in strength from the undamaged fatigue strengths, and the 897/332-732-1 composite exhibited the greatest reduction in strength in undamaged fatigue. If selection is based on the center strength of an undamaged, unfatigued specimen, the 470/438-1/2 composite is clearly superior to the 897/332-732-1. With respect to combined stress-impact effects, Table 27 shows that the 470/438-1/2 composite, with an effective damage length of only 1.960, is superior to both the 470/438-1 and 897/332-732-1 composites, which have effective damage lengths of 2.150 and 2.470 respectively.

The data reported in Tables 74 and 76 were utilized to establish the part width required to carry various loads before and after tumbled caliber .30 ball M2 projectile impact. In this analysis, it was assumed that the composite would be 1/8 inch thick and consist only of randomly oriented material. This latter constraint was imposed since there is no assurance that a significant degree of fiber alignment will be present in the compression-molded flight control components.

The load-carrying abilities of the three candidate composites are presented in Table 78 for six operational conditions. The first condition, static strength at 75°F, represents the simple case where the composite is not subjected to ballistic impact. The part widths required to carry the static tensile loads are determined, therefore, from undamaged specimen property data. Consequently, a wider part is required for the 470/438-1/2 composite because of its lower undamaged strength.

When the composites are impacted at room temperature with fully tumbled caliber .30 ball M2 projectiles at 1500 ft/sec, the part width must be increased by an amount equal to the effective damage length given in Table 78 under these ballistic conditions. The required widths given

TABLE 77. ENVIRONMENT AND LOADING EFFECTS ON TENSILE PROPERTIES OF TUMBLED CALIBER .30 BALL M2 IMPACTED SPECIMENS

Parameter	Property Value			Effective Damage Length		
	470/438-1	470/438-1/2	897/332-732-1	470/438-1	470/438-1/2	897/332-732-1
1. Undamaged Ultimate Tensile Load, P_u (lb)	12,030	10,070	12,780	-	-	-
2. Post-Damage Load, P_d (lb)[a]						
a. Temperature Effect at 1500 Ft/Sec						
At -80°F	7,875	5,762	7,890	1.440	1.564	1.579
At 75°F	7,420	5,767	7,819	1.584	1.562	1.601
At 160°F	7,451	5,457	7,476	1.573	1.674	1.706
b. Thickness Effect at 75°F and 1500 Ft/Sec						
1/8 inch	7,420	5,767	7,819	1.584	1.562	1.601
1/4 inch	13,552	10,605	14,387	1.934	1.765	1.930
3/8 inch	19,612	13,920	19,650	1.958	1.979	2.059
c. Velocity Effect at 75°F						
At 1500 ft/sec	7,420	5,767	7,819	1.584	1.562	1.601
At 1800 ft/sec	8,332	6,084	8,069	1.282	1.463	1.522
At 2100 ft/sec	9,227	5,929	9,663	0.973	1.503	1.015
3. Damaged Fatigue at 75°F						
At 2,000 cycles	3,995	3,600	4,210	1.910	1.480	1.435
At 10,000,000 cycles	2,200	1,730	2,310	1.790	1.590	1.380
4. Combined Stress-Impact: Load Capacity at Catastrophic Failure (lb)[a]	3,530	2,950	3,230	2.150	1.960	2.470

[a] Standard specimens, 1/8 inch thick and 3.5 inches wide.

TABLE 78. COMPARISON OF LOAD-CARRYING ABILITIES OF THE THREE CANDIDATE COMPOSITES[a]

Condition	Load (lb)	Required Width (in.)		
		470/438-1	470/438-1/2	897/332-732-1
Static Strength at 75°F	Basic strength →	23,140 psi	21,800 psi	24,600 psi
	1,000	0.346	0.367	0.325
	2,000	0.692	0.734	0.650
	5,000	1.729	1.835	1.625
	10,000	3.460	3.670	3.250
Post-Damage Strength at 75°F[b]	Damage length →	1.584 in.	1.562 in.	1.601 in.
	1,000	1.930	1.929	1.926
	2,000	2.276	2.296	2.251
	5,000	3.313	3.397	3.226
	10,000	5.044	5.232	4.851
Fatigue Strength at 75°F and 2000 Cycles	Fatigue strength →	14,300 psi	13,020 psi	12,470 psi
	1,000	0.560	0.614	0.642
	2,000	1.120	1.228	1.284
	5,000	2.800	3.070	3.210
	10,000	5.600	6.140	6.420
Post-Damage Fatigue Strength at 75°F and 2000 Cycles[b]	Damage length →	1.910 in.	1.480 in.	1.435 in.
	1,000	2.470	2.094	2.077
	2,000	3.030	2.708	2.719
	5,000	4.710	4.550	4.645
	10,000	7.510	7.620	7.855
Static Strength at 160°F	160°F strength →	14,720 psi	13,900 psi	17,480 psi
	1,000	0.543	0.576	0.458
	2,000	1.086	1.152	0.916
	5,000	2.715	2.880	2.290
	10,000	5.435	5.760	4.580
Combined Stress-Impact at 160°F[b]	Damage length →	2.150 in.	1.960 in.	2.470 in.
	1,000	2.693	2.536	2.928
	2,000	3.236	3.112	3.386
	5,000	4.865	4.840	4.760
	10,000	7.585	7.720	7.050

[a]All specimens are assumed to be 1/8-inch-thick center material.

[b]Specimens were impacted with tumbled caliber .30 ball M[illegible] projectiles at 1500 ft/sec and 0-degree obliquity.

under the second condition, post-damage strength at 75°F, indicate negligible differences for the three candidate composites for loads up to 2000 pounds. Beyond this load level, the 1-inch fiber composites are superior.

The third condition defines the width of composite required to sustain 2000 fatigue cycles at various load levels before projectile impact. The fatigue strength of randomly oriented material reported in Table 78 was determined from property data on undamaged specimens given in Table 74. Specifically, the values were obtained by multiplying the fatigue strength of the standard specimens by the strength factor for center material. The part width data indicate that the 470/438-1 composite is the most efficient material system at all load levels.

If 2000 cycles are applied to the composites after ballistic damage, the part widths associated with the fourth condition are needed to carry the loads indicated. These widths were determined by adding the effective damage length given in Table 78 to the part width required for the undamaged fatigue condition. The results indicate that a negligible difference exists in required part width between the 470/438-1/2 and 897/332-732-1 composites for 1000- and 2000-pound loads. These composites are clearly superior to the 470/438-1 system at the two lower load levels. At a 5000-pound load, the 470/438-1/2 composite is more efficient than either of the 1-inch fiber composites. At 10,000 pounds, the highest load level considered, the 470/438-1 composite is superior to the other two material systems.

The 897/332-732-1 composite is definitely superior to the other two composites if the design is based on the fifth condition, static strength at 160°F. This superiority results from the fact that the 897/332-732-1 composite has significantly higher elevated temperature strength than either of the 470/438 composites.

The final condition relates to the situation where the part is ballistically impacted while under tensile load at 160°F. The analysis indicates that the 470/438-1/2 composite is the most efficient system under these combined stress-impact conditions for loads up to 2000 pounds. Beyond this level, the 897/332-732-1 composite is superior because of its higher static tensile strength at 160°F.

Since flight control components must continue to function during and after ballistic attack, the combined stress-impact and damage fatigue properties of the composite are vitally important design considerations. The operating flight loads on these components are generally less than 2000 pounds. Under these conditions, the components can be designed most efficiently with the 470/438-1/2 composite. Another advantage of

this composite is that the 1/2-inch fibers are less susceptible to crippling during molding than 1-inch fibers. Consequently, the 470/438-1/2 composite was recommended to the Eustis Directorate and subsequently adopted for use in ballistically tolerant flight control components.

The residual load capacity data for 470/438-1/2 composites impacted with untumbled caliber .50 AP M2 projectiles were subsequently analyzed using multiple regression techniques. The regression equation defined in Table 73 was modified by excluding all terms involving the sine of the projectile rotation angle. The empirical data were then fitted to the regression equation by using a least-squares technique. A number of terms that had an insignificant effect on the fit were subsequently eliminated from the modified equation. The constant and coefficients for this reduced equation are summarized in Table 79.

TABLE 79. CONSTANT AND COEFFICIENTS FOR THE REGRESSION EQUATION - CALIBER .50 AP M2 IMPACTED SPECIMENS

Term	470/438-1/2	
V	0.48260820	03[a]
V * V	-0.23614397	00
V * V * V	0.43528544	-04
TH	0.57182296	07
TH * TH	0.55014927	08
TH * TH * TH	-0.20204779	09
KF	0.13048620	06
KF * KF	-0.62096951	05
SG	-0.13779474	08
SG * SG	0.37856088	07
T * V	0.59010030	-02
T * TH	-0.26406678	02
V * PRE	-0.17564076	02
V * TH	-0.44585350	03
PRE * TH	0.22189173	06
TH * SG	-0.48008602	07
Constant	0.12154970	08

[a] Floating point notation; e.g., 0.48260820 03 is 0.48260820 x 10^3, or 482.60820.

This equation was used to determine the effects of temperature, velocity, prestress, and off-centerness on residual load capacity. The load capacities predicted from the regression equation were then utilized to compute effective damage length for various levels of the independent variables.

The residual load capacities and associated damage lengths for 1/8-inch-thick standard specimens are presented in Table 80. These data

TABLE 80. INFLUENCE OF TEST VARIABLES ON THE RESIDUAL LOAD CAPACITY AND EFFECTIVE DAMAGE LENGTH OF CALIBER .50 AP M2 IMPACTED SPECIMENS

Variable	Level	470/438-1/2	
		Load (lb)	Damage Length (in.)
Temperature (°F)	-80	6685	1.238
	5	7102	1.086
	70[a]	7518	0.933
	115	7768	0.842
	160	8017	0.751
Velocity (ft/sec)	1500[a]	7518	0.933
	1800	7842	0.815
	2100	7970	0.768
Prestress (percent of ultimate)	25	7378	0.984
	35[a]	7518	0.933
	45	7657	0.882
	55	7796	0.832
Off-Centerness Factor	1.000[a]	7518	0.933
	1.018	7610	0.900
	1.038	7668	0.878
	1.062	7669	0.878

[a] Level at standard conditions. In determining the effect of one variable, the balance of the variables were held constant at the standard conditions. Projectile footprint length used in computations was 0.50 inch. Also, a specific gravity value of 1.907 was used in residual load capacity calculations.

clearly indicate that the caliber .50 AP M2 projectile is less damaging than tumbled caliber .30 ball M2 projectiles. The results also show that effective damage length decreases significantly with increasing specimen temperature and impact velocity. The influence of prestress was consistent with regression data for tumbled caliber .30 ball M2 impacted specimens; i.e., damage length decreased with increasing prestress. The effect of off-centerness, which indicates less damage with increased ballistic asymmetry, is contrary to the expected result. However, absolute differences are small between the residual load capacities at the various levels of off-centerness, indicating that this variable has a relatively insignificant effect.

Conclusions and Recommendations

It was concluded from the Subtask 7 study that the 470/438-1/2 composite is the most efficient material for use in ballistically tolerant flight control components. Compared to the 1-inch fiber composites, the 470/438-1/2 material system sustains less or equivalent effective damage during ballistic impact. The superiority of the 1/2-inch fiber composite is particularly evident under combined stress-impact conditions. It was further concluded that the 470/438-1/2 composite requires equivalent or less part width to carry loads up to and including 2000 pounds after ballistic damage than either of the 1-inch composites.

Because of the superior properties of the 470/438-1/2 composite after projectile impact, this material system was recommended to the Eustis Directorate for characterization in Task III and ultimate use in flight control components. This recommendation was subsequently adopted.

TASK III - DESIGN ALLOWABLE PROPERTIES EVALUATION STUDY

GENERAL

The design of ballistically tolerant flight control components requires a thorough knowledge of the ballistic response and structural properties of the selected material of construction, in this case the 470/438-1/2 composite. The ballistic behavior of this composite was established from exhaustive Task II testing. The limited mechanical property data obtained in Task II were inadequate for design purposes. Consequently, the Task III study was conducted to generate the necessary structural data for the reliable design of flight control components.

APPROACH TO THE PROBLEM

The mechanical properties of the 470/438-1/2 composite were determined at -80°F, room temperature, and 160°F, using test specimens and methods that are appropriate for discontinuous fiber composites. The following specific properties were measured:

1. Interlaminar shear strength
2. Flexural strength and modulus
3. Tensile strength and modulus
4. Compressive strength and modulus
5. Panel shear strength and modulus
6. Bearing strength

Drawings of the various test specimen configurations and setups used in determining the structural properties are shown in Figure 69. The test methods including mathematical equations used in computing the mechanical property values are discussed in the following paragraphs.

Interlaminar Shear Strength

This property of the 470/438-1/2 composite was determined from a short-beam flexural test. The 1/8-by-1/2-by-1-inch specimen was tested at a crosshead speed of 0.05 in./min. The interlaminar shear strength, SS, was computed from the following equation:

$$S_S = \frac{3P}{4bd} \tag{37}$$

where P = breaking load, lb

b = specimen width, in.

d = specimen thickness, in.

Flexural Strength and Modulus

The flexural properties of the 470/438-1/2 composite were established from 1/8-by-1/2-by-4-inch specimens tested at a crosshead speed of 0.05 in./min. Simultaneous readings of load and deflection were taken during testing. Deflection was measured by a dial indicator located under and in contact with the center of the 2-inch span. The ultimate flexural strength, S_F, was calculated from the following mathematical expression:

$$S_F = \frac{3PL}{2bd^2} \tag{38}$$

where P = breaking load, lb

L = span, in.

b = specimen width, in.

d = specimen thickness, in.

Load-deflection curves were plotted to determine the modulus of elasticity in flexure. The following equation was used to compute the flexural modulus, E_B:

$$E_B = \left(\frac{L^3}{4bd^3}\right)\left(\frac{\Delta P}{\Delta y}\right) \tag{39}$$

where y = deflection, in.

Tensile Strength and Modulus

The tensile properties of the 470/438-1/2 composite were measured on flat specimens of the configuration shown in Figure 69. An extensometer with a 2-inch gage length was mounted on the specimen to obtain a load-elongation (stress-strain) curve. The load was applied at a crosshead separation rate of 0.05 in./min. The ultimate tensile strength, S_T, was calculated from the following equation:

1. INTERLAMINAR SHEAR

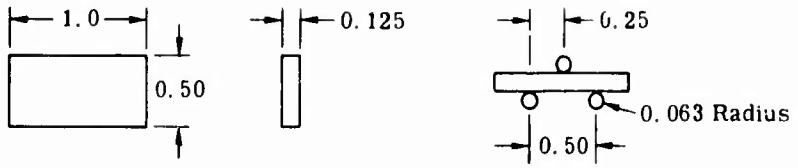

2. FLEXURE

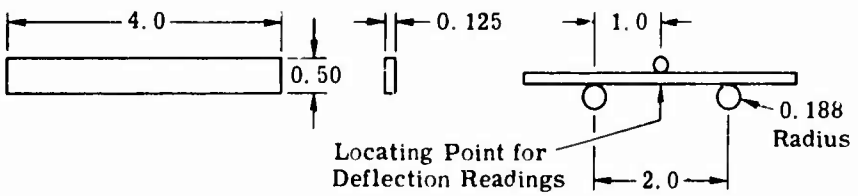

3. TENSION

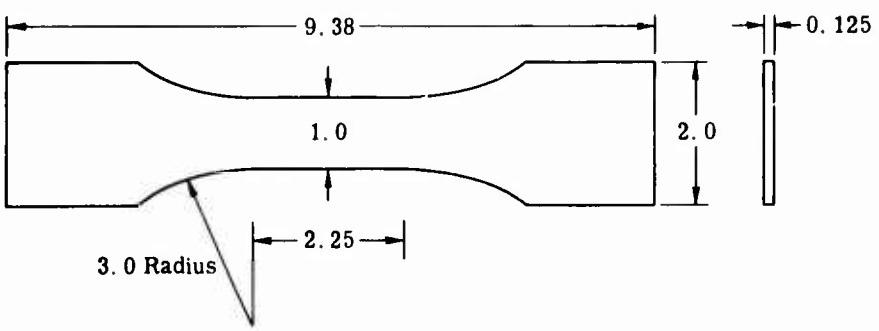

4. COMPRESSION

A. Ultimate

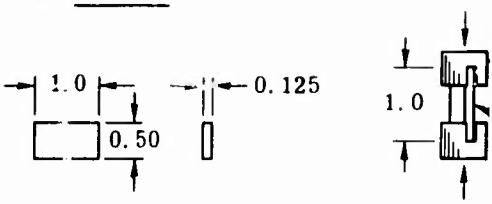

5. PANEL RAIL SHEAR

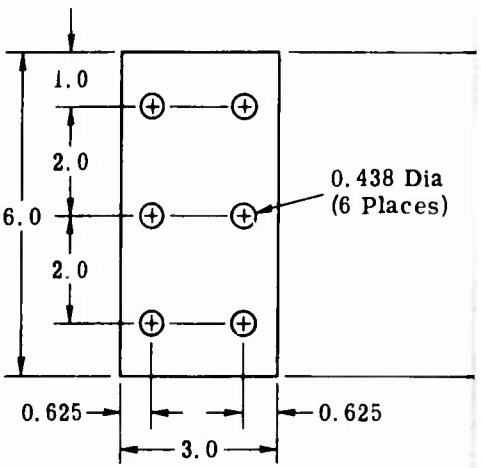

6. BEARING

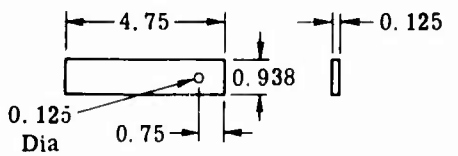

X = 4% of Hol

Figure 69. Mechanical Property Specimens and Test Setups.

4. COMPRESSION

A. Ultimate

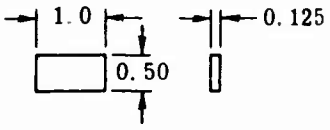

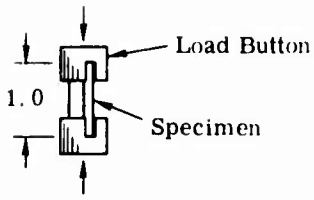

B. Modulus

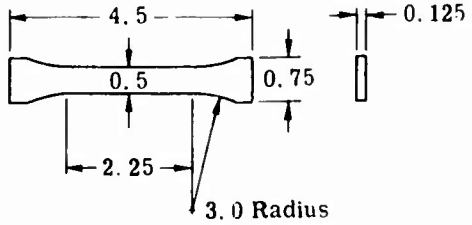

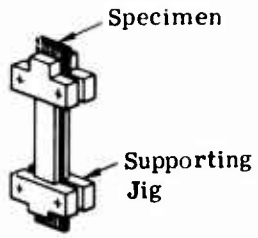

5. PANEL RAIL SHEAR

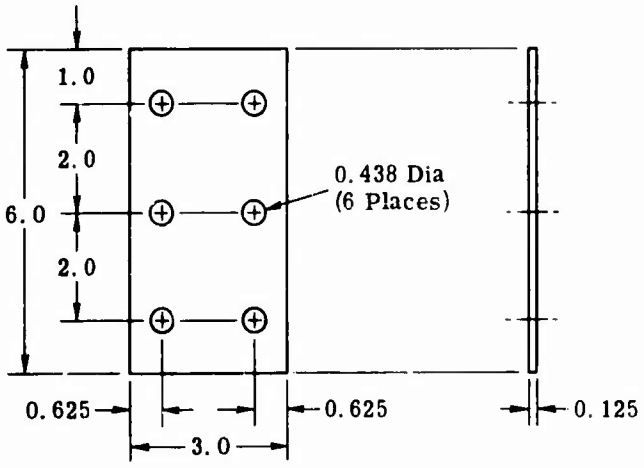

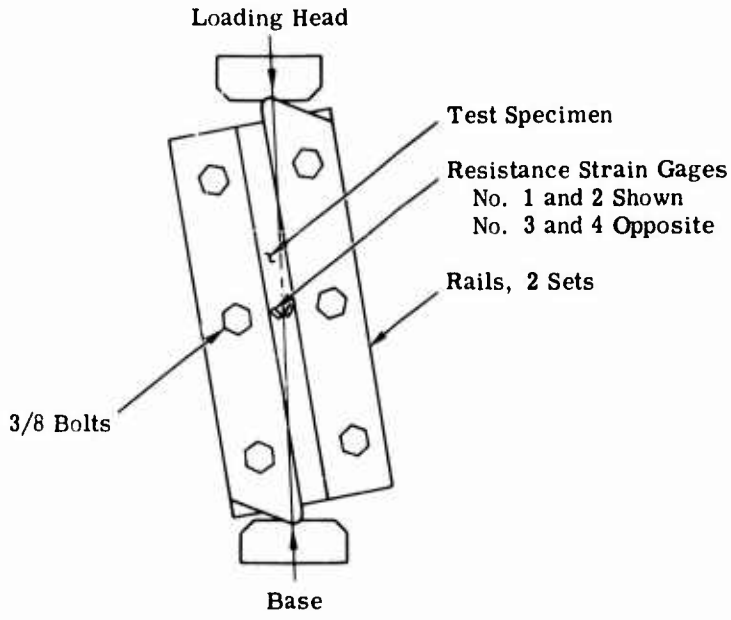

6. BEARING

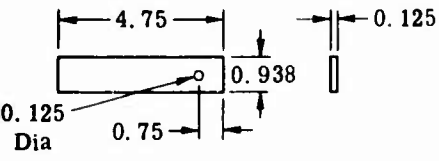

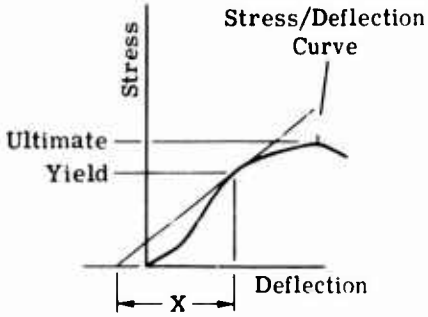

X = 4% of Hole Dia

Note: All dimensions are in inches.

$$S_T = \frac{P}{bd} \tag{40}$$

The modulus of elasticity in tension, E_T, was determined from the initial slope of the load-elongation curve.

Compressive Strength and Modulus

Separate test specimens as shown in Figure 69 were used to establish the compressive strength and modulus of the 470/438-1/2 composite. Both types of specimens were tested at a crosshead speed of 0.05 in./min. The ends of the ultimate compressive specimens were inserted into button fixtures and then potted with an epoxy resin to eliminate premature failure at the loading surfaces due to local crushing. This assembly was mounted in a compression fixture to ensure axial loading. The ultimate compressive strength, S_C, was determined as follows:

$$S_C = \frac{P}{bd} \tag{41}$$

The compression modulus fixture shown in Figure 69 is designed so that the specimen extends 1/8 inch above and below the fixture. Also, the edges of the specimen extend beyond the edges of the center supports so that an extensometer (2-inch gage length) could be attached. The modulus was determined from the initial slope of the stress-strain curve derived from the extensometer plots.

Panel Shear Strength and Modulus

The test specimen and fixture used to measure the panel shear properties of the 470/438-1/2 composite are shown in Figure 69. The specimens were clamped between two sets of steel rails to which coarse sandpaper had been bonded to increase the friction between the specimen and rails. Sufficient torque was applied to each of the 3/8-inch bolts to prevent slippage without crushing the specimen. Four resistance strain gages, two on each specimen surface, were mounted at 45 degrees to the longitudinal axis as shown in Figure 69. The specimen was loaded at a crosshead speed of 0.05 in./min through special seats that were machined to accommodate the ends of the rails. The panel shear strength, S_{PS}, was computed from the following expression:

$$S_{PS} = \frac{P}{ld} \tag{42}$$

where P = breaking load, lb

l = specimen length, in.

d = specimen thickness, in.

The oscillograph record of the response of the strain gages was used to plot a stress-strain curve. The shear modulus, G, was calculated from the initial slope of this curve.

Bearing Strength

The bearing strength testing was performed in accordance with method 1051 of Federal Test Method Standard No. 406. The specimen shown in Figure 69 was tested at a crosshead speed of 0.05 in./min. A 2-inch gage length extensometer was used to measure the movement of the free end of the specimen with relation to the bearing pin in the tension loading fixture. A constant record of load versus elongation was obtained up to a total strain of 0.005 inch, i.e., 4 percent of the bearing hole diameter. The test was continued until maximum stress was sustained in the specimen. The bearing yield strength was computed as follows:

$$S_{By} = \frac{P}{dD} \tag{43}$$

where P = load at a total strain of 4 percent of the bearing hole diameter, lb

d = specimen thickness, in.

D = bearing hole diameter, in.

The bearing ultimate strength was calculated from the same equation except that P = the maximum load, in pounds, sustained by the specimen.

The test specimens were prepared from compression molded, 1/8- by 12- by 12-inch panels. Each specimen was generally taken from a prescribed area of the panel as shown in Figure 70. When necessary, specimen locations were shifted to exclude anomalies present in critical areas of the moldings that might influence the test values. Also, the original test plan did not include any provisions for determining the bearing strength of the 470/438-1/2 composite. Because this property is important in component design, a decision was made to modify the engineering plan accordingly. However, this decision was reached after all other test specimens had

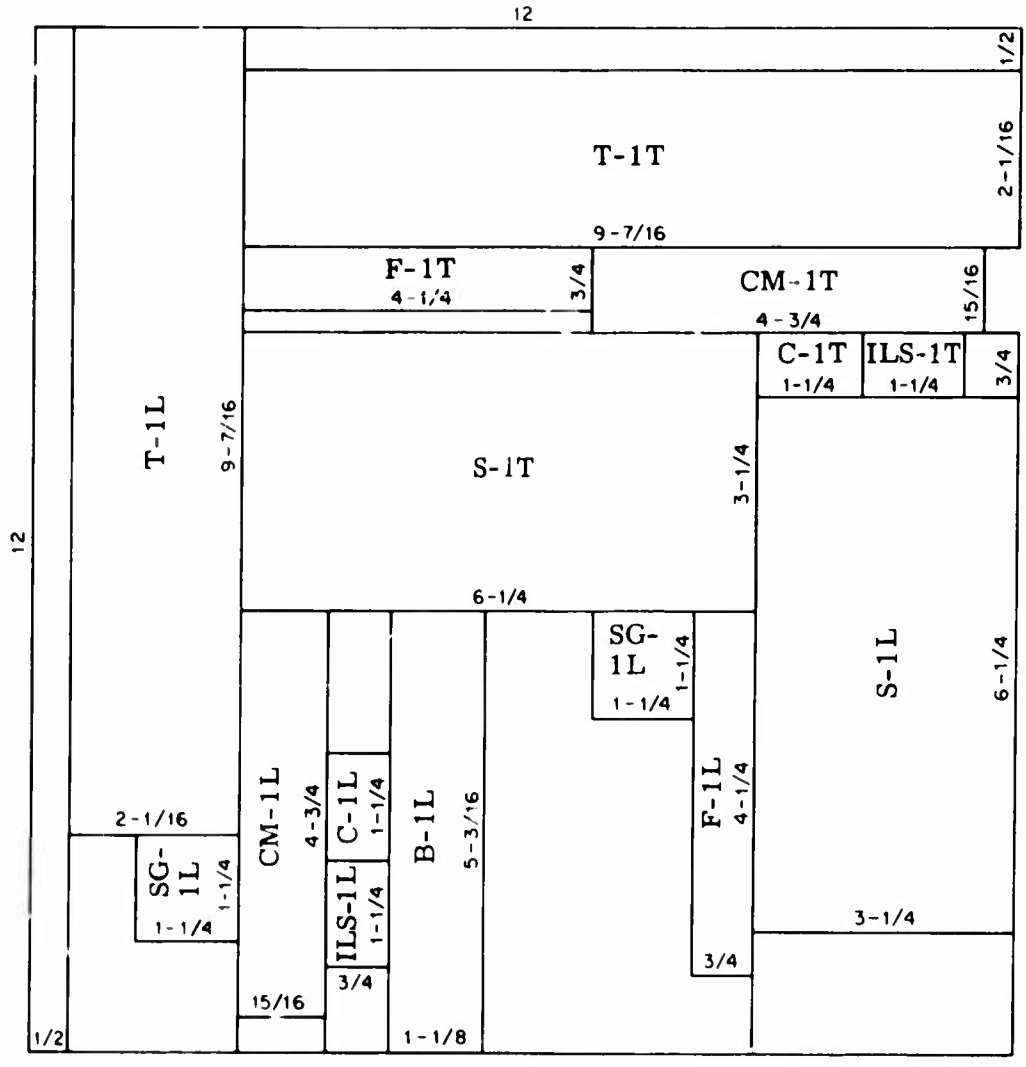

Notes:
1. All dimensions are in inches.
2. Letter prefixes define type of specimen:
   - T - tension
   - C - compression
   - CM - compression modulus
   - SG - specific gravity (also used for fiber content)
   - F - flexure
   - S - panel rail shear
   - ILS - interlaminar shear
   - B - bearing
3. Digits define panel numbers.
4. Letter suffixes define orientation:
   - L - longitudinal
   - T - transverse

Figure 70. Panel Layout for Mechanical Property Specimens.

been rough-cut from the moldings. Consequently, the bearing strength specimens were prepared from acceptable areas of the residual molded material.

The edges of the compression-molded panels contain aligned fibers that would affect the structural property values. Therefore, the specimens were removed either from the inboard panel area or from an area such that the aligned fibers were present outside the test section, such as the end of a tensile specimen. Furthermore, both longitudinal and transverse specimens were taken for each mechanical property, except bearing strength, to minimize the influence of fiber alignment that might exist in the central panel area. Six replicates, equally distributed between longitudinal and transverse specimens, were generally evaluated for each property at all temperature levels.

In order for the structural data to be of maximum value to the designer, it must be reported on a basis (or bases) that is completely understandable and readily usable. Therefore, the design allowable data will be presented on two bases having associated statistical assurances. These bases, which are also used in MIL-HDBK-5A*, are defined below.

1. A Basis - The A mechanical property value is the value above which at least 99 percent of the population of values is expected to fall, with a confidence of 95 percent.

2. B Basis - The B mechanical property value is the value above which at least 90 percent of the population of values is expected to fall, with a confidence of 95 percent.

The statistical parameters, mean and standard deviation, along with the sample size are required to define the A and B basis values. Multiple regression analysis was employed to derive the statistical parameters for each mechanical property across all temperature levels. This is accomplished by fitting the test data to a quadratic equation having a single independent variable; namely, temperature. The following quadratic equation will be used:

$$Y = a_0 + a_T T + a_{TT} T^2 \qquad (44)$$

---

* METALLIC MATERIALS AND ELEMENTS FOR AEROSPACE VEHICLE STRUCTURES, MIL-HDBK-5A, Dept of Defense, Washington, D.C., 8 February 1966.

where Y = mechanical property value

T = absolute temperature, ^{o}R

The constant, a_0, and coefficients for the linear and quadratic temperature terms were obtained from a least-squares fit of the data. The variation in test data from the regression curve provides the standard deviation for the entire experiment. The advantage of using this approach in computing the A and B basis values lies in the magnitude of the sample size. Since test data at three temperature levels are involved, the sample size is essentially three times as large as that available when the statistical parameters are determined at each temperature level. Actually, three degrees of freedom are used to obtain the values for the constant and coefficients of the regression equation. Therefore, the final sample size is three less than the total number of test points for each mechanical property.

Statistical tolerance limits which are analogous to engineering tolerance limits were then computed from the regression data. The lower 99 and 90 percent tolerance limits were determined at a confidence probability of 95 percent. These limits correspond to the A and B basis levels. Design allowables are considered conservatively low, due to small sample size and related statistical approach.

DISCUSSION OF RESULTS

A total of 13 panels, 1/8 by 12 by 12 inches, were produced from 470/438-1/2 molding compound for fabrication of the mechanical property specimens. Two of these panels, numbers 8 and 9 in the molding sequence, were initially set aside because of the presence of a significant number of internal flaws. However, the defect-free areas of these panels were subsequently used in the preparation of several of the specimens for bearing strength determination.

The specific gravity, density, resin content, and fiber content data generated on the 13 panels used in this investigation are reported in Table 81. The specific gravity was determined by the water-displacement technique. The density value was then computed from the measured specific gravity. The resin content on a weight basis was obtained by the loss-on-ignition method. The resultant value along with the density of the unfilled 438 resin was used to calculate the resin content on a volume basis. The fiber content is simply the difference between 100 percent and the percentage of resin content.

These data indicate that the average fiber content of the 13 panels deviated only 0.1 percent from the target value of 52.0 v/o. Also, the variability

TABLE 81. SPECIFIC GRAVITY, DENSITY, AND FIBER CONTENT OF 470/438-1/2 COMPOSITE

Specimen No.	Specific Gravity	Density ($lb/in.^3$)	Percent Resin (by wt)	Resin Content (v/o)	Glass Content (v/o)
SG-1L	1.903	0.0688	30.5	46.4	53.6
SG-1T	1.899	0.0686	30.6	46.5	53.5
SG-2L	1.897	0.0685	30.8	46.8	53.2
SG-2T	1.898	0.0686	31.5	47.5	52.5
SG-3L	1.891	0.0683	31.6	47.7	52.3
SG-3T	1.892	0.0684	31.0	47.0	53.0
SG-4L	1.891	0.0683	32.1	49.2	50.8
SG-4T	1.894	0.0684	31.7	47.8	52.2
SG-5L	1.893	0.0684	31.5	47.5	52.5
SG-5T	1.897	0.0685	33.7	50.0	50.0
SG-6L	1.891	0.0683	32.3	48.5	51.5
SG-6T	1.893	0.0684	31.5	47.5	52.5
SG-7L	1.889	0.0682	32.1	48.2	51.8
SG-7T	1.891	0.0683	31.6	47.7	52.3
SG-8L	1.877	0.0678	32.2	48.3	51.7
SG-8T	1.875	0.0677	32.2	48.3	51.7
SG-9L	1.878	0.0678	32.1	48.2	51.8
SG-9T	1.874	0.0677	32.3	48.4	51.6
SG-10L	1.887	0.0682	31.4	47.3	52.7
SG-10T	1.889	0.0682	32.7	49.0	51.0
SG-11L	1.889	0.0682	32.5	49.7	50.3
SG-11T	1.892	0.0684	31.2	48.2	51.8
SG-12L	1.893	0.0684	32.3	49.5	50.5
SG-12T	1.888	0.0682	31.5	47.5	52.5
SG-13L	1.885	0.0681	32.2	49.4	50.6
SG-13T	1.888	0.0682	32.1	49.2	50.8
Avg	1.890	0.0683	31.8	48.1	51.9

in specific gravity was extremely small between panels. The minimum and maximum values differed by only 0.029 (1.874 versus 1.903), or approximately 1.5 percent of the grand average of 1.890.

As indicated earlier in this section, multiple regression analysis was used to determine the statistical parameters (mean and standard deviation) for each of the mechanical properties. The empirical data were fitted to a general quadratic equation in one independent variable, temperature.

The constant and coefficients for the regression equations are presented in Table 82 for each structural property. Also reported is the coefficient of determination, which indicates the percentage of variability in the test data that has been explained by the form of the equation and the terms included in the fit. In all but one case, shear modulus, the test data fit the equation reasonably well.

The individual test values, the statistical parameters derived from regression analysis, and the design allowable values (A and B bases) are presented for each mechanical property in the series of tables that follow. The standard deviation reported in each table applies at each test temperature level.

The interlaminar shear results given in Table 83 indicate that mean strength decreases significantly at 160°F compared with either -80°F or room temperature values. At the most critical temperature level, 160°F, the A and B design allowable values are 2654 and 3587 psi, respectively. For the A-basis value, this means that at least 99 percent of all future values will exceed 2654 psi with a confidence of 95 percent.

The ultimate flexure strength data reported in Table 84 disclose that strength decreases with increasing temperature. At 160°F the A

TABLE 82. CONSTANT AND COEFFICIENTS FOR THE MECHANICAL PROPERTY REGRESSION EQUATIONS

Mechanical Property	Constant, a_0	Coefficient, a_T	Coefficient, a_{TT}	Coefficient of Determination, $R^2 \times 100$
Interlaminar Shear Strength	-0.227281 05*	0.134097 03	-0.143875 00	79.0
Ultimate Flexure Strength	-0.731875 05	0.590906 03	-0.672968 00	62.7
Flexure Modulus	-0.819875 01	0.491243 -01	-0.514785 -04	76.6
Ultimate Tensile Strength	0.301450 05	-0.752933 01	-0.210679 -01	66.0
Tensile Modulus	-0.202376 01	0.274535 -01	-0.323424 -04	82.2
Ultimate Compressive Strength	0.238946 05	0.170895 03	-0.275472 00	89.4
Compressive Modulus	-0.389886 00	0.165043 -01	-0.195182 -04	74.2
Panel Shear Strength	0.542082 05	-0.108410 03	0.738773 -01	93.0
Shear Modulus	0.232896 01	-0.431061 -02	0.385436 -05	47.3
Bearing Yield Strength	-0.105143 06	0.668383 03	-0.727717 00	70.2
Ultimate Bearing Strength	-0.228952 05	0.539634 03	-0.697451 00	89.3

*Floating point notation; e.g., -0.227281 05 is -0.227281×10^5, or -22,728.1.

TABLE 83. RESULTS OF INTERLAMINAR SHEAR STRENGTH TESTS ON 470/438-1/2 COMPOSITE

Specimen No.	Test Temp (°F)	Interlaminar Shear Strength (psi)	Multiple Regression Data (psi)		Design Allowables (psi)*	
			Mean	Std Deviation	A Basis	B Basis
ILS-10L	-80	8100				
ILS-11L	-80	6950				
ILS-13L	-80	7610	7453		5000	5933
ILS-11T	-80	8900				
ILS-12T	-80	6740				
ILS-13T	-80	6420				
ILS-1L	75	7670				
ILS-2L	75	6940				
ILS-4L	75	8250	7833	682	5380	6313
ILS-2T	75	8020				
ILS-4T	75	7880				
ILS-5T	75	8240				
ILS-5L	160	5160				
ILS-6L	160	4660				
ILS-7L	160	5870	5106		2654	3587
ILS-6T	160	4380				
ILS-7T	160	5400				
ILS-10T	160	5170				

* Design allowables are considered conservatively low, due to small sample size and related statistical approach.

TABLE 84. RESULTS OF FLEXURE STRENGTH TESTS ON 470/438-1/2 COMPOSITE

Specimen No.	Test Temp (°F)	Ultimate Flexure Strength (psi)	Multiple Regression Data (psi)		Design Allowables (psi)*	
			Mean	Std Deviation	A Basis	B Basis
F-11L	-80	50,900				
F-12L	-80	49,100				
F-13L	-80	50,080	54,180		28,258	38,118
F-10T	-80	65,680				
F-11T	-80	61,070				
F-12T	-80	48,250				
F-1L	75	53,280				
F-2L	75	42,870				
F-3L	75	50,860	50,326	7,203	24,405	34,264
F-1T	75	42,390				
F-2T	75	54,000				
F-7T	75	58,560				
F-6L	160	27,480				
F-7L	160	28,960				
F-10L	160	41,410	34,485		8,563	18,423
F-4T	160	30,740				
F-5T	160	46,770				
F-13T	160	31,550				

* Design allowables are considered conservatively low, due to small sample size and related statistical approach.

mechanical property value is 8563 psi, or only about 30 percent of the A-basis value at room temperature. Because of the relatively large standard deviation, the mean strength values must be reduced by approximately 26,000 psi to obtain the corresponding A mechanical property values.

The flexure modulus data for the 470/438-1/2 composite are summarized in Table 85. The data indicate that the modulus is highest at room temperature and lowest at 160°F. The mean value of 2.47×10^6 psi at 160°F represents a decrease of approximately 25 percent from the room temperature modulus of 3.35×10^6 psi. The A and B design allowable values at the most severe temperature condition are 1.68×10^6 and 1.98×10^6 psi, respectively.

The ultimate tensile strength data given in Table 86 reveal that increased temperature results in decreased strength. At 160°F the mean tensile strength is about 82 percent of the mean value at room temperature. To obtain the A and B mechanical property values, the mean strength must be reduced approximately 8000 and 5000 psi, respectively, regardless of test temperature.

Typical stress-strain curves obtained during tensile testing of the 470/438-1/2 composite at -80°F, room temperature, and 160°F are shown in Figure 71. These curves disclose that the modulus, as determined from the initial slope, decreases with increasing temperature. On the other hand, the total elongation at failure increases directly with test temperature. A 1.23-percent elongation at failure was observed at 160°F compared with 0.91 percent at room temperature. The tensile modulus results are summarized in Table 87. The minimum A and B mechanical values of 1.66×10^6 and 2.00×10^6 psi, respectively, were obtained at 160°F.

The ultimate compressive strength of the 470/438-1/2 composite decreases substantially with increased temperature as evidenced from the test data given in Table 88. The mean compressive strengths at room temperature and 160°F are approximately 75 and 50 percent, respectively, of the mean value at -80°F. This marked reduction in strength is also evident in both the A and B compressive strength values. For the A-basis condition, the design allowable strengths are 35,169, 22,589, and 10,071 at -80°F, room temperature, and 160°F, respectively. Designing for the elevated temperature condition will ensure satisfactory performance of the component at either room temperature or -80°F.

Figure 72 presents typical stress-strain curves obtained on compression modulus specimens of the 470/438-1/2 composite at the three test temperatures. A definite reduction in modulus was obtained with increasing

TABLE 85. RESULTS OF FLEXURE MODULUS TESTS ON 470/438-1/2 COMPOSITE

Specimen No.	Test Temp (°F)	Flexure Modulus (psi x 10^6)	Multiple Regression Data (psi x 10^6)		Design Allowables* (psi x 10^6)	
			Mean	Std Deviation	A Basis	B Basis
F-11L	-80	3.21	3.04	0.22	2.24	2.54
F-12L	-80	2.94				
F-13L	-80	2.73				
F-10T	-80	3.19				
F-11T	-80	3.29				
F-12T	-80	2.85				
F-1L	75	3.39	3.35		2.56	2.86
F-2L	75	3.14				
F-3L	75	3.50				
F-1T	75	3.15				
F-2T	75	3.49				
F-7T	75	3.42				
F-6L	160	2.02	2.47		1.68	1.93
F-7L	160	2.40				
F-10L	160	2.64				
F-4T	160	2.48				
F-5T	160	2.79				
F-13T	160	2.49				

*Design allowables are considered conservatively low, due to small sample size and related statistical approach.

TABLE 86. RESULTS OF TENSILE STRENGTH TESTS ON 470/438-1/2 COMPOSITE

Specimen No.	Test Temp (°F)	Ultimate Tensile Strength (psi)	Multiple Regression Data (psi)		Design Allowables (psi)*	
			Mean	Std Deviation	A Basis	B Basis
T-10L	-80	26,230	24,241	2,220	16,253	19,292
T-11L	-80	25,020				
T-13L	-80	23,160				
T-11T	-80	24,390				
T-12T	-80	19,310				
T-13T	-80	27,340				
T-1L	75	20,590	20,086		12,098	15,137
T-2L	75	18,210				
T-3L	75	20,290				
T-2T	75	21,190				
T-4T	75	19,400				
T-5T	75	20,840				
T-5L	160	16,370	17,378		9,390	12,429
T-6L	160	18,540				
T-7L	160	14,580				
T-6T	160	19,030				
T-7T	160	20,590				
T-10T	160	15,160				

*Design allowables are considered conservatively low, due to small sample size and related statistical approach.

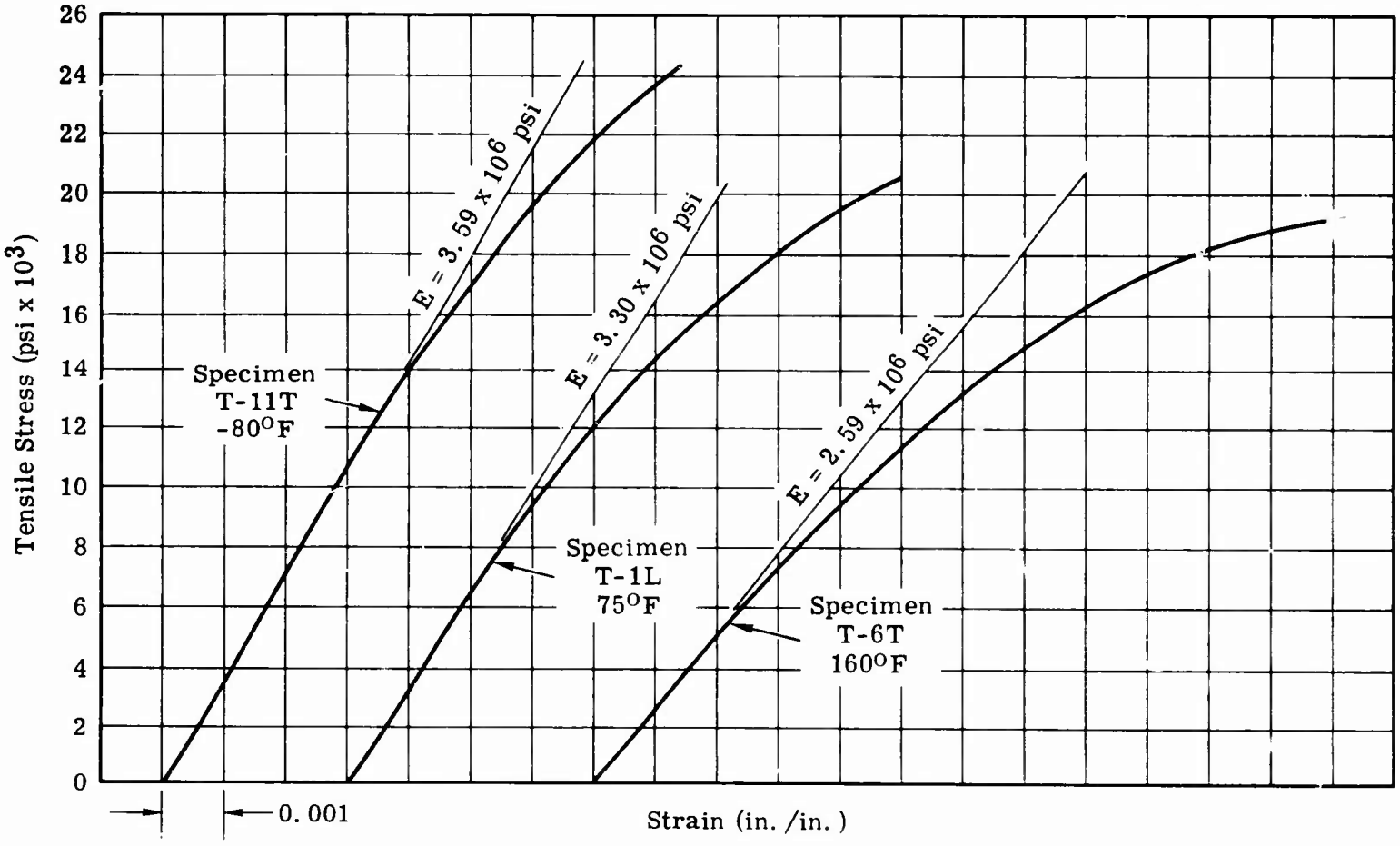

Figure 71. Typical Tensile Stress-Strain Curves for 470/438-1/2 Composite.

TABLE 87. RESULTS OF TENSILE MODULUS TESTS ON 470/438-1/2 COMPOSITE

Specimen No.	Test Temp (°F)	Tensile Modulus (psi x 10^6)	Multiple Regression Data (psi x 10^6)		Design Allowables* (psi x 10^6)	
			Mean	Std Deviation	A Basis	B Basis
T-10L	-80	4.10	3.74	0.25	2.83	3.17
T-11L	-80	3.52				
T-13L	-80	3.77				
T-11T	-80	3.59				
T-12T	-80	3.70				
T-13T	-80	3.75				
T-1L	75	3.30	3.41		2.50	2.85
T-2L	75	3.57				
T-3L	75	3.40				
T-2T	75	3.33				
T-4T	75	3.28				
T-5T	75	3.56				
T-5L	160	2.29	2.57		1.66	2.00
T-6L	160	2.77				
T-7L	160	2.09				
T-6T	160	2.59				
T-7T	160	3.13				
T-1(	160	2.52				

*Design allowables are considered conservatively low, due to small sample size and related statistical approach.

TABLE 88. RESULTS OF COMPRESSIVE STRENGTH TESTS ON 470/438-1/2 COMPOSITE

Specimen No.	Test Temp (°F)	Ultimate Compressive Strength (psi)	Multiple Regression Data (psi)		Design Allowables (psi)*	
			Mean	Std Deviation	A Basis	B Basis
C-11L	-80	47,620	49,056	3,860	35,169	40,451
C-12L	-80	49,700				
C-13L	-80	42,110				
C-11T	-80	51,450				
C-12T	-80	53,180				
C-13T	-80	50,280				
C-1L	75	39,910	36,476		22,589	27,871
C-2L	75	35,030				
C-5L	75	35,980				
C-1T	75	32,520				
C-2T	75	31,340				
C-3T	75	44,080				
C-6L	160	23,100	23,958		10,071	15,353
C-7L	160	23,660				
C-10L	160	23,540				
C-4T	160	28,900				
C-6T	160	20,980				
C-10T	160	23,570				

*Design allowables are considered conservatively low, due to small sample size and related statistical approach.

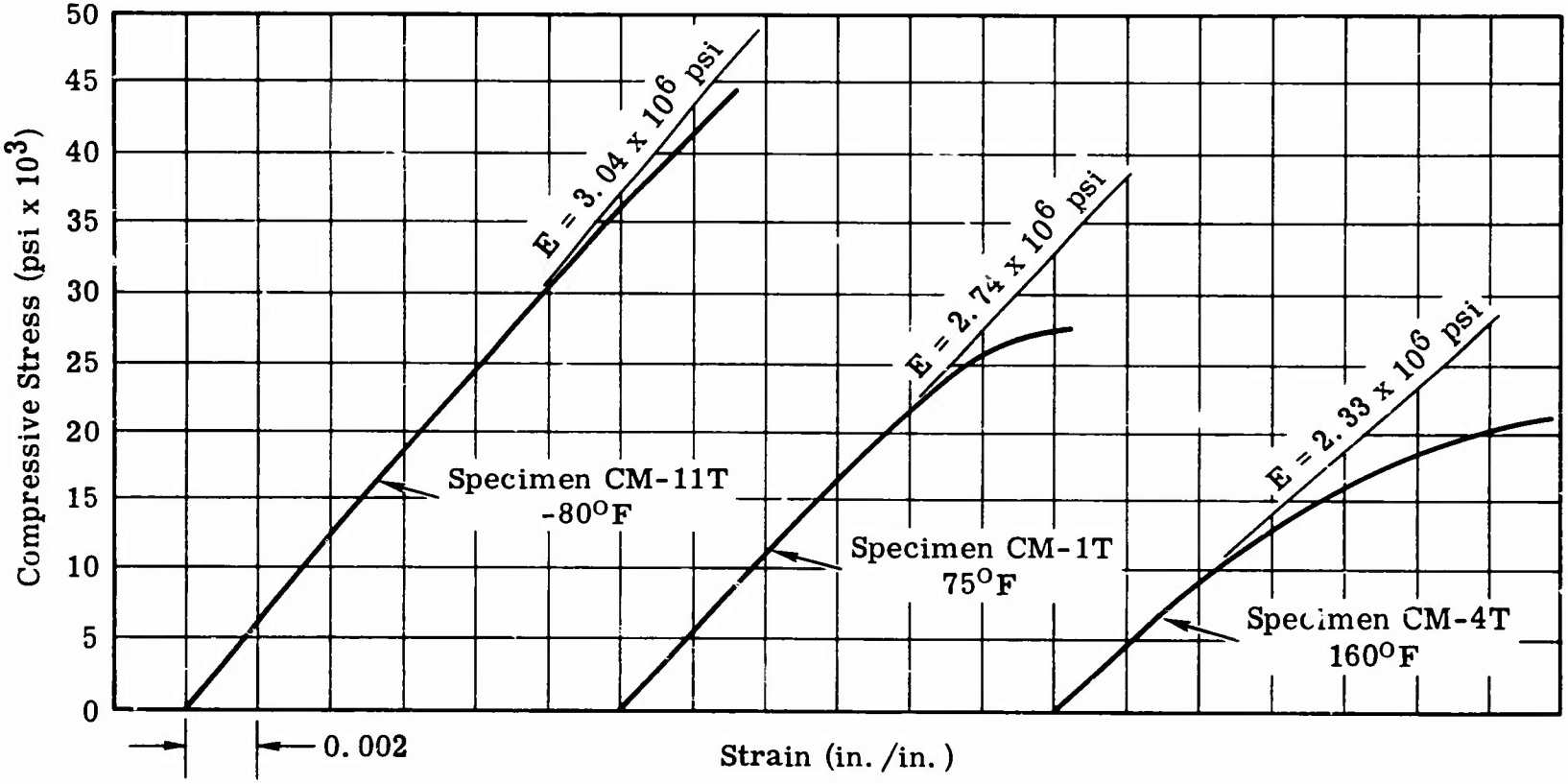

Figure 72. Typical Compressive Stress-Strain Curves for 470/438-1/2 Composite.

temperature, but not of the magnitude observed in the ultimate compression tests. Actually, the percentage decrease in modulus was about one-half that experienced in compressive strength tests at the corresponding temperature levels. The compressive modulus test results are summarized in Table 89. These data indicate that the minimum design allowable values are experienced at the elevated temperature condition. The A and B compression modulus values at 160°F are 1.63 x 10^6 and 1.90 x 10^6 psi, respectively.

The panel shear data reported in Table 90 disclose that increased test temperature produces a decrease in shear strength. This same trend is reflected at both design allowable levels. At 160°F, where the shear strength is lowest, the A and B values are 11,319 and 12,867 psi, respectively.

Typical stress-strain curves obtained from panel shear data are shown in Figure 73. These curves suggest that shear modulus is higher at -80°F than at either room temperature or 160°F. This is also apparent from the test data summary presented in Table 91. The mean modulus values at room temperature and 160°F are essentially identical (1.13 x 10^6 versus 1.14 x 10^6 psi). The minimum A and B shear modulus values of 0.88 x 10^6 and 0.98 x 10^6 psi, respectively, were obtained at room temperature. This is the only instance in the Task III program where the lowest design allowable values did not occur at 160°F.

The bearing yield data reported in Table 92 indicate that the strength of the 470/438-1/2 composite is similar at -80°F and room temperature but decreases approximately 33 percent at 160°F. Because of a relatively large standard deviation, both the A and B bearing yield values are substantially lower than the mean value. This is most apparent at 160°F, where the A design allowable value of 10,753 psi is only 36.3 percent of the mean bearing yield strength.

The results of the ultimate bearing strength tests on the 470/438-1/2 composite are given in Table 93. These data reveal a substantial reduction in strength with increasing test temperature. This trend is also evident in the design allowable values. At 160°F the A bearing ultimate value, 20,757 psi, is approximately 35 percent of the corresponding value at -80°F. It is abundantly clear that components designed for the elevated temperature condition will perform satisfactorily at either room temperature or -80°F.

TABLE 89. RESULTS OF COMPRESSIVE MODULUS TESTS ON 470/438-1/2 COMPOSITE

Specimen No.	Test Temp (°F)	Compressive Modulus (psi x 10^6)	Multiple Regression Data (psi x 10^6)		Design Allowables* (psi x 10^6)	
			Mean	Std Deviation	A Basis	B Basis
CM-10L	-80	2.99	3.06	0.20	2.36	2.63
CM-11L	-80	2.99				
CM-13L	-80	3.03				
CM-11T	-80	3.04				
CM-12T	-80	3.22				
CM-13T	-80	3.11				
CM-1L	75	3.10	2.85		2.15	2.41
CM-2L	75	2.77				
CM-3L	75	2.83				
CM-1T	75	2.74				
CM-2T	75	2.97				
CM-10T	75	2.71				
CM-4L	160	2.00	2.34		1.63	1.90
CM-6L	160	2.08				
CM-7L	160	2.37				
CM-4T	160	2.33				
CM-6T	160	2.82				
CM-7T	160	2.44				

* Design allowables are considered conservatively low, due to small sample size and related statistical approach.

TABLE 90. RESULTS OF PANEI SHEAR STRENGTH TESTS ON 470/438-1/2 COMPOSITE

Specimen No.	Test Temp (°F)	Ultimate Panel Shear Strength (psi)	Multiple Regression Data (psi)		Design Allowables (psi)*	
			Mean	Std Deviation	A Basis	B Basis
S-7L	-80	22,830	23,680	1,052	19,542	21,072
S-10L	-80	23,750				
S-3T	-80	25,450				
S-5T	-80	22,690				
S-2L	75	18,110	17,350		13,281	14,829
S-5L	75	17,980				
S-1T	75	18,450				
S-2T	75	16,990				
S-13T	75	15,240				
S-11L	160	15,310	15,390		11,319	12,867
S-12L	160	15,760				
S-7T	160	15,700				
S-11T	160	15,380				
S-12T	160	14,810				

* Design allowables are considered conservatively low, due to small sample size and related statistical approach.

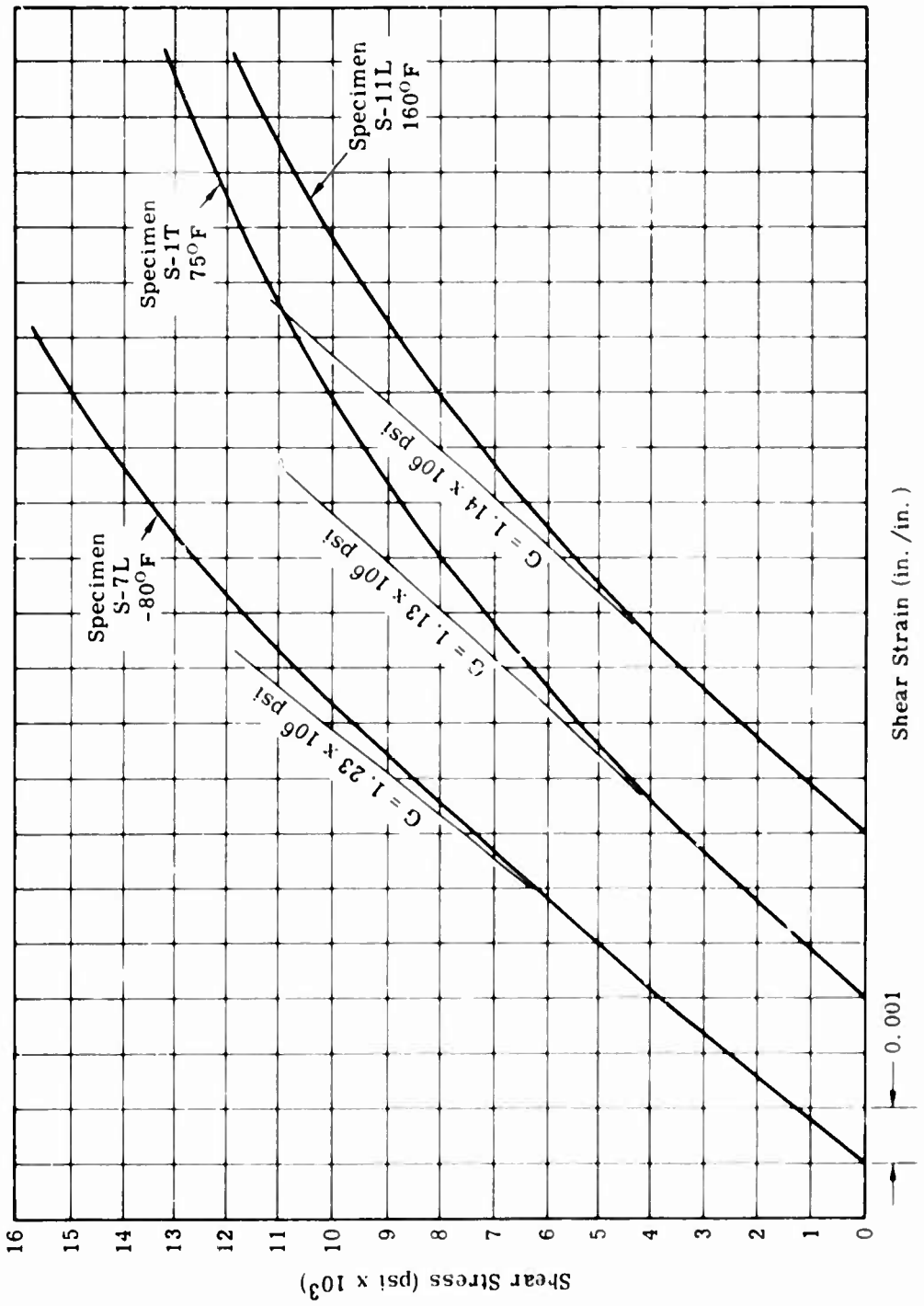

Figure 73. Typical Panel Shear Stress-Strain Curves for 470/438-1/2 Composite.

TABLE 91. RESULTS OF PANEL SHEAR MODULUS TESTS ON 470/438-1/2 COMPOSITE

Specimen No.	Test Temp (°F)	Shear Modulus (psi x 10^6)	Multiple Regression Data (psi x 10^6)		Design Allowables* (psi x 10^6)	
			Mean	Std Deviation	A Basis	B Basis
S-7L	-80	1.28	1.25	0.06	1.00	1.09
S-10L	-80	1.31				
S-3T	-80	1.17				
S-5T	-80	1.23				
S-2L	75	1.17	1.13		0.88	0.98
S-5L	75	1.09				
S-1T	75	1.13				
S-2T	75	1.05				
S-13T	75	1.19				
S-11L	160	1.14	1.14		0.90	0.99
S-12L	160	1.20				
S-7T	160	1.21				
S-11T	160	1.08				
S-12T	160	1.06				

* Design allowables are considered conservatively low, due to small sample size and related statistical approach.

TABLE 92. RESULTS OF BEARING YIELD STRENGTH TESTS ON 470/438-1/2 COMPOSITE

Specimen No.	Test Temp (°F)	Bearing Yield Strength (psi)	Multiple Regression Data (psi)		Design Allowables (psi)*	
			Mean	Std Deviation	A Basis	B Basis
B-3	-80	43,100	43,760	4,939	24,998	32,086
B-8	-80	54,400				
B-9	-80	42,900				
B-9	-80	40,300				
B-13	-80	38,100				
B-1	75	49,200	44,010		25,375	32,459
B-2	75	40,000				
B-8	75	43,200				
B-9	75	47,800				
B-12	75	40,000				
B-2	160	29,200	29,520		10,758	17,846
B-3	160	33,000				
B-9	160	26,800				
B-9	160	33,800				
B-13	160	24,800				

* Design allowables are considered conservatively low, due to small sample size and related statistical approach.

TABLE 93. RESULTS OF ULTIMATE BEARING STRENGTH TESTS ON 470/438-1/2 COMPOSITE

Specimen No.	Test Temp (°F)	Ultimate Bearing Strength (psi)	Multiple Regression Data (psi)		Design Allowables (psi)*	
			Mean	Std Deviation	A Basis	B Basis
B-3	-80	82,460	81,460	6,007	58,633	67,255
B-8	-80	78,700				
B-9	-80	84,450				
B-9	-80	83,580				
B-13	-80	78,080				
B-1	75	64,000	65,970		43,344	51,960
B-2	75	65,630				
B-8	75	64,840				
B-9	75	79,400				
B-12	75	56,000				
B-2	160	41,270	43,580		20,757	29,379
B-3	160	47,010				
B-9	160	40,300				
B-9	160	51,150				
B-13	160	38,160				

* Design allowables are considered conservatively low, due to small sample size and related statistical approach.

CONCLUSIONS AND RECOMMENDATIONS

The following conclusions can be drawn from the determination of design allowable properties for the 470/438-1/2 composite in the Task III study:

1. The mean mechanical properties of the 470/438-1/2 composite are substantially lower at 160°F than at room temperature or -80°F. The only exception to this trend occurred in the panel shear modulus testing, where the room-temperature and 160°F values were essentially identical.

2. The design allowable values exhibit a similar trend with respect to temperature as the mean property values. Consequently, designs based on the 160°F allowable data will have increased structural margins of safety at room temperature and -80°F.

A summary of design allowable data at -80°F, room temperature, and 160°F is presented in Table 94. These data are reported on two standard bases having associated statistical assurances. Table 94 also contains information on the mean, standard deviation, and number of specimens used to compute the design allowable values.

It is recommended that the A-basis design allowable values be employed

in the structural design of flight control components. The A-basis value is that value above which at least 99 percent of the population of values will fall, with a confidence of 95 percent.

TABLE 94. DESIGN ALLOWABLES FOR 470/438-1/2 COMPOSITE

Mechanical Properties	Test Temp (°F)	Multiple Regression Data (psi)		No. of Specimens	Design Allowables (psi)[a]	
		Mean	Std Deviation		A Basis[b]	B Basis
Interlaminar Shear	-80	7,453	682	18	5,000	5,933
	75	7,833			5,380	6,313
	160	5,106			2,654	3,587
Flexure Strength (Ultimate)	-80	54,180	7,203	18	28,258	38,118
	75	50,326			24,405	34,264
	160	34,485			8,563	18,423
Flexure Modulus	-80	3.04×10^6	0.22×10^6	18	2.24×10^6	2.54×10^6
	75	3.35×10^6			2.56×10^6	2.86×10^6
	160	2.47×10^6			1.68×10^6	1.98×10^6
Tensile Strength (Ultimate)	-80	24,241	2,220	18	16,253	19,292
	75	20,086			12,098	15,137
	160	17,378			9,390	12,429
Tensile Modulus	-80	3.74×10^6	0.25×10^6	18	2.83×10^6	3.17×10^6
	75	3.41×10^6			2.50×10^6	2.85×10^6
	160	2.57×10^6			1.66×10^6	2.00×10^6
Compressive Strength (Ultimate)	-80	49,056	3,860	18	35,169	40,451
	75	36,476			22,589	27,871
	160	23,958			10,071	15,353
Compressive Modulus	-80	3.06×10^6	0.20×10^6	18	2.36×10^6	2.63×10^6
	75	2.85×10^6			2.15×10^6	2.41×10^6
	160	2.34×10^6			1.63×10^6	1.90×10^6
Panel Shear Strength (Ultimate)	-80	23,680	1,052	14	19,542	21,072
	75	17,350			13,281	14,829
	160	15,390			11,319	12,867
Shear Modulus	-80	1.25×10^6	0.06×10^6	14	1.00×10^6	1.09×10^6
	75	1.13×10^6			0.88×10^6	0.98×10^6
	160	1.14×10^6			0.90×10^6	0.99×10^6
Bearing Strength (Ultimate)	-80	81,460	6,007	15	58,633	67,255
	75	65,970			43,344	51,960
	160	43,580			20,757	29,379

[a] Design allowables are considered conservatively low, due to small sample size and related statistical approach.

[b] Recommended for design use.

SUMMARY OF RESULTS

General trends in extent of damage and residual strength after ballistic damage in relation to the major parameters evaluated are summarized below and in chart form in Table 95.

1. The tensile strength of short fiber-glass-reinforced composites increases significantly with increasing fiber length.

2. The residual strength after ballistic damage and the extent of that damage are directly and significantly proportional to the fiber length. Composites of one-inch-long fibers have approximately 1-1/2 times the residual strength of 1/2-inch-long fibers and twice the strength of 1/4-inch-long fibers after ballistic damage. The extent of back surface damage is in approximately the same ratios.

3. Fiber finish, resin matrix, fiber-to-resin ratio, and fiber diameter do not have a pronounced effect on either extent of ballistic damage or residual strength. Trends of the effect of these parameters on extent of damage and residual strength were empirically derived, using statistical methods, and the optimum combination of materials was selected for use in the design of ballistic-tolerant components.

4. Visual or measured extent of damage is not a reliable criterion for a judgment of post-ballistic damage properties of short-fiber mold composites. Minimum damage does not necessarily indicate maximum residual strength.

5. Caliber .50 AP M2 untumbled projectiles cause significantly less damage at any ballistic velocity-temperature condition than caliber .30 ball M2 fully tumbled projectiles.

6. Short-fiber composites have low resistance to perforation (complete penetration) on ballistic impact and will be perforated at all realistic thickness-velocity-temperature impact conditions.

7. Ballistic impacts at elevated temperatures (+160°F) tend to produce small localized separations or cracks in the composite away from the ballistic impact perforation. Such cracks contribute to degradation of the residual load capacity.

8. Short-fiber, compression-molded materials have potential manufacturing and process problems in fiber alignment at the edges and fiber crippling in areas of thickness change. These problems must be carefully considered in the design and analysis of flight control components.

9. Flight control components must continue to function in the stress-thermal environment before, during, and after ballistic impact. Hence such factors as the effect of combined stress-impact and the undamaged and damaged operational fatigue properties of the components are vitally important design considerations. The 470/438-1/2 material exhibits minimum fiber-crippling and minimum fiber-alignment problems, plus superior or equivalent combined stress-impact properties and lower damage fatigue properties than the one-inch-long fiber materials. Therefore, considering all factors relating to both fabrication and physical behavior, it appears that the 470/438-1/2 fiber material offers the optimum trade-off in this application, and it is recommended for use in the design of ballistic-damage-tolerant flight control components.

TABLE 95. GENERAL TRENDS IN REGARD TO MAJOR PARAMETERS

Parameter	Tensile Stress (Undamaged)	Modulus E	Visual Ballistic Damage	Crack Propagation Rate	K_C Stress Intensity Factor	Strength-to-Weight Ratio	Crippling of Fiber	Residual Stress (Post-Damage)
Increasing Fiber Length	↑	—	↑	↓	↑	↑	↑	↑
Increasing Fiber Diameter	↑	—	↑	○	○	↑	○	↑
Increasing K_C, Resin	—	—	—	—	—	—	—	—
Increasing Specimen Thickness	↑	—	↑	○	○	○	↓	—
Fiber Finish, Incompatible to Compatible	↑	↓	—	↓	↑	—	—	—
Fiber Type, E to S	↑	↑	—	○	○	↑	—	↑
Increasing Temperature	↓	↓	—	○	○	↓	—	—
Increasing Ballistic Velocity	—	—	—	○	○	—	—	↑
Increasing Fiber Content	↑	↑	—	○	○	—	↑	↑

LEGEND

↑ Values increasing — Insignificant change

↓ Values decreasing ○ Not evaluated

APPENDIX
TENSILE FATIGUE DATA ANALYSIS

BACKGROUND

Another approach to fatigue data analysis using the statistical techniques that were effectively used in other analyses was employed at the end of Phase I of this program. In the original analyses described in subtask 3 of Task II, the fatigue data had been generated and the analysis conducted in a conventional manner. Tensile fatigue testing was conducted on both undamaged and ballistically damaged specimens by establishing several tensile load levels and by fatigue cycling approximately four specimens, at each set of conditions, to failure under that load. Load-N curves were then drawn for both the undamaged and damaged conditions. No attempt was made to determine the lower tolerance limits, inasmuch as the data did not lend itself to this type of analysis. The reason for this is that standard deviations and tolerance limits for structural property values are generated from data where the test values of stress in tension, compression, etc., are the dependent variables, whereas in fatigue testing, the stress is an independent variable and the number of cycles to failure is the dependent variable. No test techniques can be devised for fatigue testing wherein each specimen tested within a group can be caused to fail at a fixed number of cycles with the stress level as the dependent variable.

It can readily be seen that if the conventional type of data, with N as the independent variable, is subjected to statistical analysis and the lower tolerance limit established, the results would be a value for the number of cycles above which at least 99 percent of all future N values would fall with a confidence of 95 percent. Such data are not readily useful to a designer who wants to know the structural capability under cyclic load. It is desired to know the lower tolerance limits of the stress level that will survive a specified fatigue life.

This novel, inverse prediction problem has arisen before; it was solved in an article by R. G. Easterling and published in the Journal of the American Statistical Association.* The solution method given was quite unwieldy and was modified here so that a computer could be programmed to provide an efficient solution.

---

* Easterling, R. G., DISCRIMINATION INTERVALS FOR PERCENTILES IN REGRESSION, Journal of the American Statistical Association, Vol. 64, No. 327, September 1969, pp. 1031-1041.

THE FUNCTION USED FOR FITTING

A Weibull function was the equation provided for fitting the controlled peak stress, S_{max}, of a sinusoidally applied load and the response cycles, N. Equation (45) is the form of that function.

$$S_{max} = (\sigma_u - S_E)\ e^{-k\ (\log_e N)^M} + S_E \qquad (45)$$

where σ_u = ultimate stress

S_E = endurance limit load (asymptote)

k = an unknown constant to be established

M = an unknown constant to be established

Although σ_u and S_E are also unknown, they were fixed by examination of a plot of the test data; this was done so that the problem could be simplified to a tractable linear regression as required in Easterling's article. Thus, the two unknown constants, k and M, are to be estimated by linear regression. To accomplish this, Equation (45) must be solved for log-log N. By rearrangement and taking the natural logarithm twice, log-log N can be solved.

$$\text{log-log } N = \frac{-\log k}{M} + \frac{1}{M}\ \text{log-log}\left(\frac{\sigma_u - S_E}{S_{max} - S_E}\right) \qquad (46)$$

Now Equation (46) is in the linear regression form:

$$y = \hat{\beta}_0 + \hat{\beta}_1 x \qquad (47)$$

where $\hat{\beta}_0 = \dfrac{-\log k}{M}$

$\hat{\beta}_1 = \dfrac{1}{M}$

Therefore, after Equation (46) is fitted and the $\hat{\beta}_0$ and $\hat{\beta}_1$ regression coefficients are evaluated, the following expressions are obtained:

$$M = 1/\hat{\beta}_1 \qquad (48)$$

$$k = e^{-\hat{\beta}_0/\hat{\beta}_1} \qquad (49)$$

TOLERANCE LIMIT CALCULATION

For any specified limit of the response (fatigue cycles), the lower tolerance level, X_0, for the load S_{max} is sought. To do this, we must find the root, X_0, of Equation (7) in Easterling's article.

$$D\left\{\frac{Y_{\underline{P}} - \hat{\beta}_0 - \hat{\beta}_1 X_0}{SD} - Z_\alpha \left[1 + \frac{(Y_{\underline{P}} - \hat{\beta}_0 - \hat{\beta}_1 X_0)^2}{2(n-2)\, S^2 D^2}\right]^{1/2}\right\} - Z_{\underline{P}} = 0 \quad (50)$$

where $$D = \sqrt{\frac{1}{n} + \frac{X_0^2}{\Sigma X^2}}$$

n = sample size of regression

ΣX^2 = sum of squares of controlled variable, S_{max}, in regression data

S = standard error from regression calculation

$Z_{\underline{P}}$ is implicitly defined by:

$$\underline{P} = \int_{-\infty}^{Z_{\underline{P}}} f(x)dx, \text{ where } f(x) \text{ is}$$

the Gaussian probability density.

Z_α is obtained from $\alpha = \int_{-\infty}^{Z_\alpha} f(x)dx.$

Since Equation (50) is nonlinear, it must be solved by iterative methods that start with an initial estimated value of X_0 and converge to the root. This is a time-consuming operation; therefore, a computer program was developed to provide the solution.

The assumptions made in the development of Equation (50) are as follows:

1. The population of the response values has a Gaussian (normal) distribution for the fixed load level. This assumption is not verifiable with small sample sizes.

2. For every value of the controlled variable, the population standard error of the response variable is homoscedastic. This assumption is verifiable by testing the hypothesis that the sample standard error, at each level of the controlled variable, came from populations with the same response standard error. To check this assumption, an F-test of the largest and smallest variances of log-log N was conducted, and they were found to be homoscedastic.

DISCUSSION OF RESULTS

The fitting of the data for undamaged specimen fatigue testing to Equation (46) was accomplished using the regression analysis technique. The results were as follows:

1. Confidence level = 95%
2. Regression coefficient, $\hat{\beta}_0$, = 2.4447 (log-log N)
3. Regression coefficient, $\hat{\beta}_1$, = 0.6054 (log-log N)
4. Constant, k, = 0.01760
5. Constant, M, = 1.653
6. Standard error, S, = 0.07022 (log-log N)
7. Ultimate load, σ_u, = 10,068 lb
8. Endurance limit, S_E, = 1250 lb

The fundamental function, Equation (45), is then defined as follows:

$$L_{max} = 8818\, e^{-0.01760\,(\log_e N)^{1.653}} + 1250 \qquad (51)$$

The mean values and the lower tolerance limits were computed from the regression function. The data were plotted in Figure 74, which is a typical Load-N curve of the undamaged fatigue mean values with the A and B design allowable levels shown. Figure 75 shows the same type of information for the damaged fatigue values.

In the development of these functions for the statistical analysis, it was necessary to assume a one-cycle load value and an endurance limit

load value. For the one-cycle load, an average of the static test data was used. The variability of this point could not be included in the mathematics used to develop the regression function and therefore was not included. As a result, the lower tolerance limit for low number of cycles does not appear entirely reasonable. A further examination of the data used in Figures 74 and 75 is made in Figure 76, which plots the same information as a percentage of the one-cycle strength, and it can be seen that undamaged and damaged curves are almost identical. This would indicate that if the one-cycle value is known, a curve of load versus number of cycles can be developed based on Figure 76. Therefore, to develop a conservative design allowable for fatigue throughout the total range from one to 10^7 cycles, the following approach was used. The lower tolerance limit from the static load information was used as the lower tolerance value for one cycle, and the complete lower tolerance curve was developed from the mean value curve of Figure 76. This curve is superimposed over the lower tolerance curve developed from the fatigue data and the lower values are used for the design curve. With proper correction factors applied for random fiber orientation center material, temperature, and preload, the curves of allowable stress versus number of cycles can be computed and are shown in Figure 77. As an example, Figure 78 shows a design load curve for the standard 3.5-inch-wide specimen, damaged at 160°F, based on the 160°F allowable stress/cycle curve of Figure 77, and the established damage length, and the mean and lower tolerance values based on the test data of the damaged specimens adjusted for center material only and 160°F. It can be seen that at 2000 cycles, which is the design requirement for the post-damage loads, the established design curve is below the lower tolerance limit of the test data.

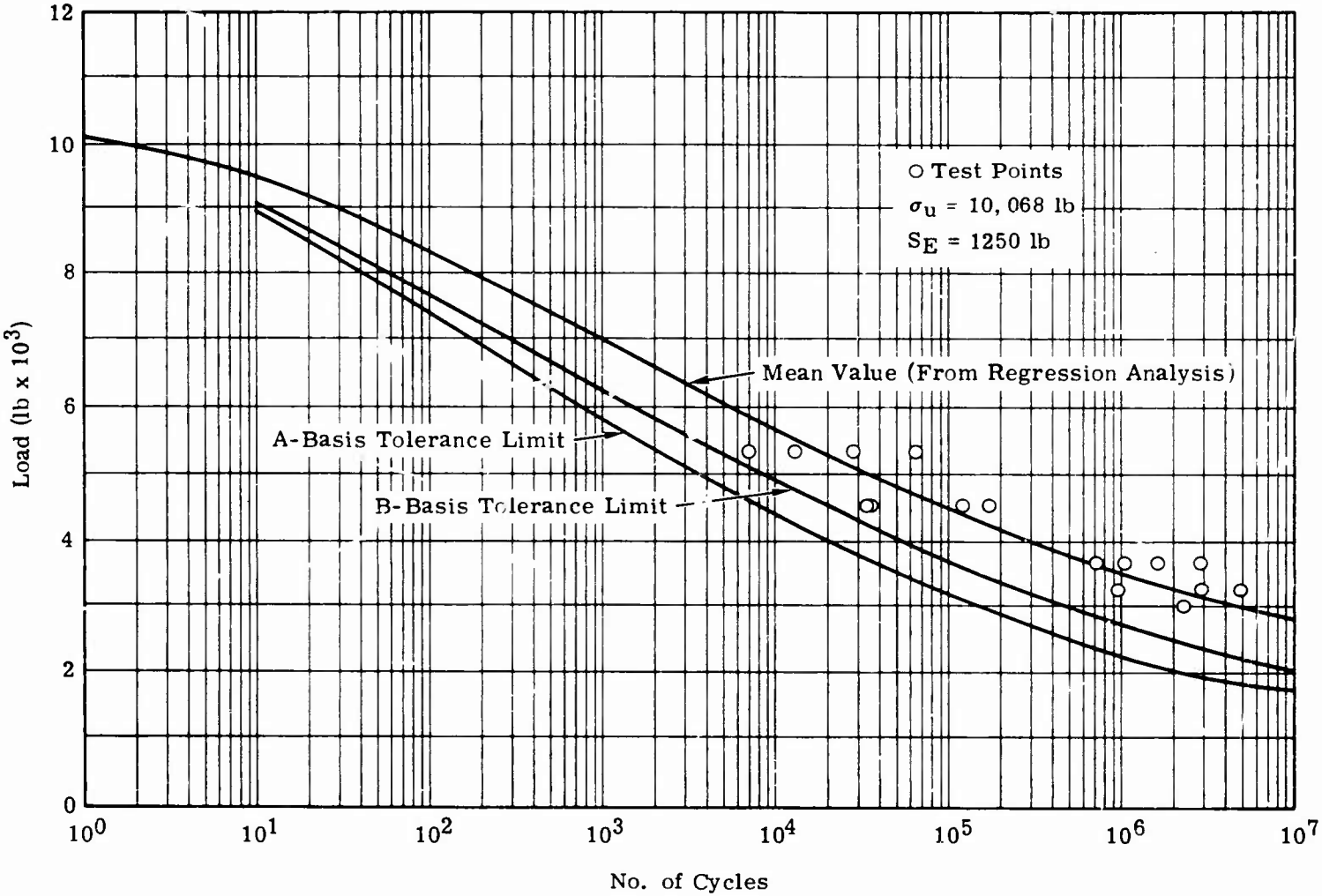

Figure 74. Fatigue Curves for Undamaged 470/438-1/2 Composite Load Capacity Showing A- and B-Basis Tolerance Limits.

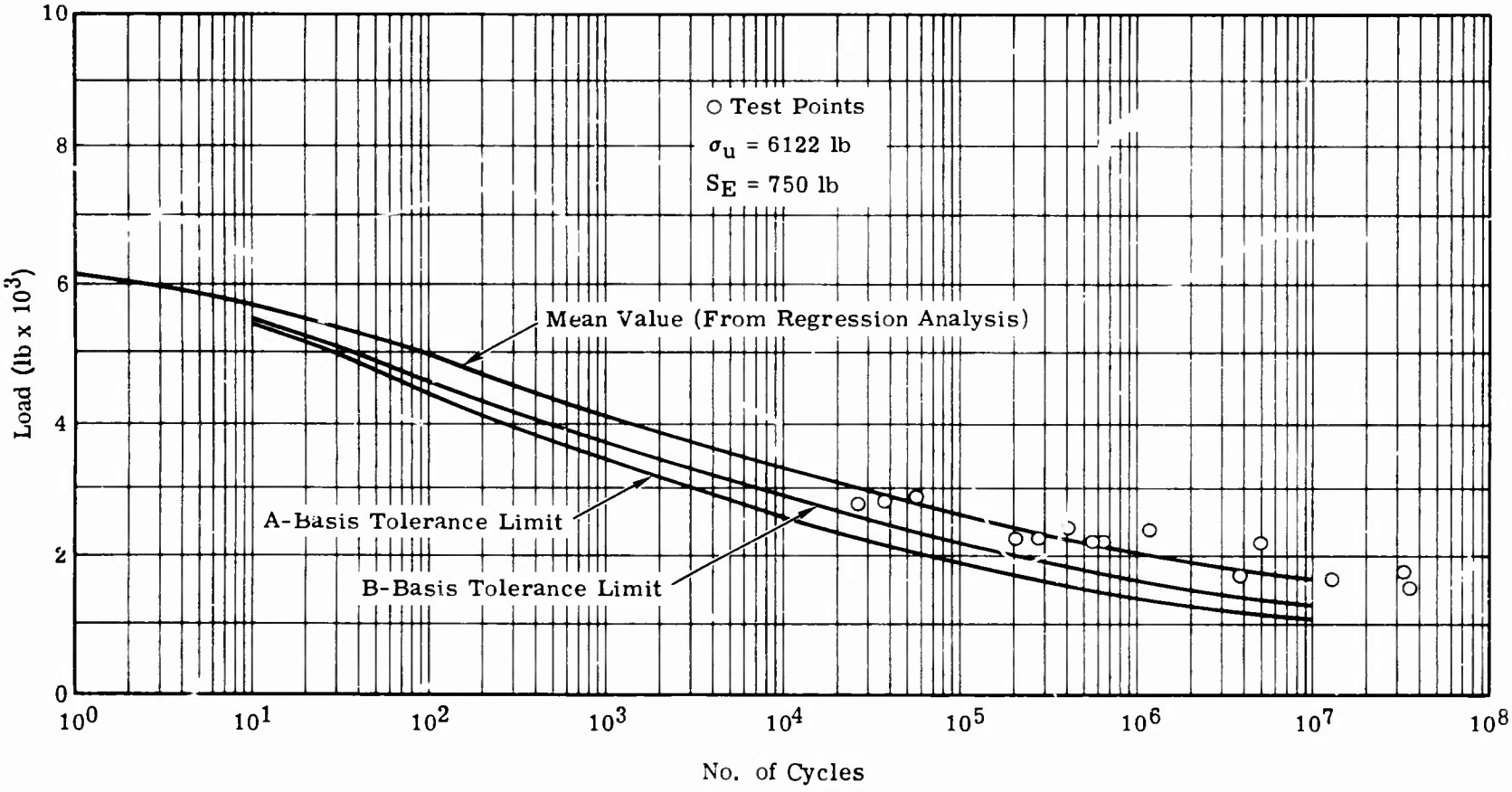

Figure 75. Fatigue Curves for Damaged 470/438-1/2 Composite Load Capacity Showing A- and B-Basis Tolerance Limits.

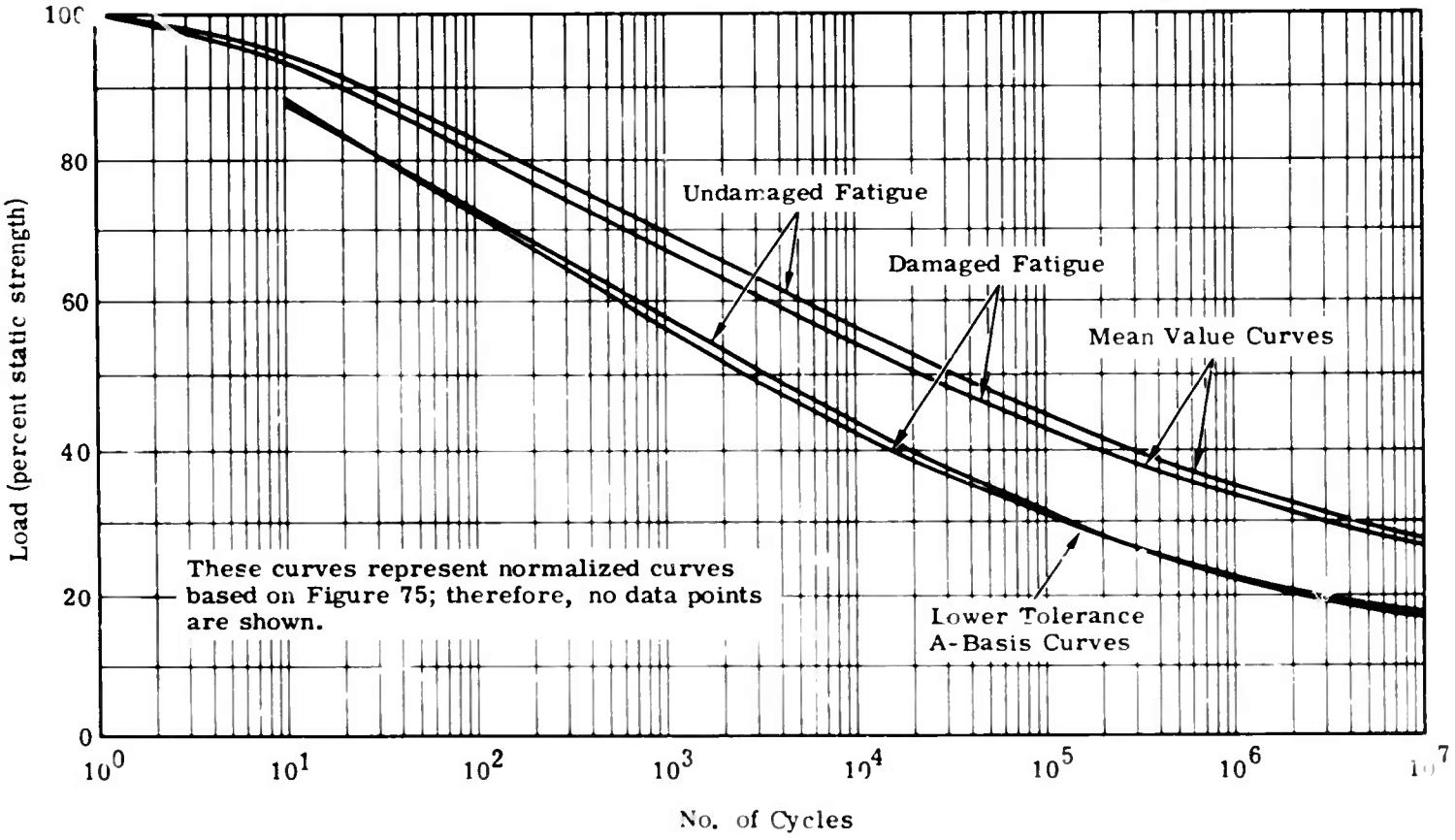

Figure 76. Fatigue Curves for 470/438-1/2 Composite as a Percentage of Static Load.

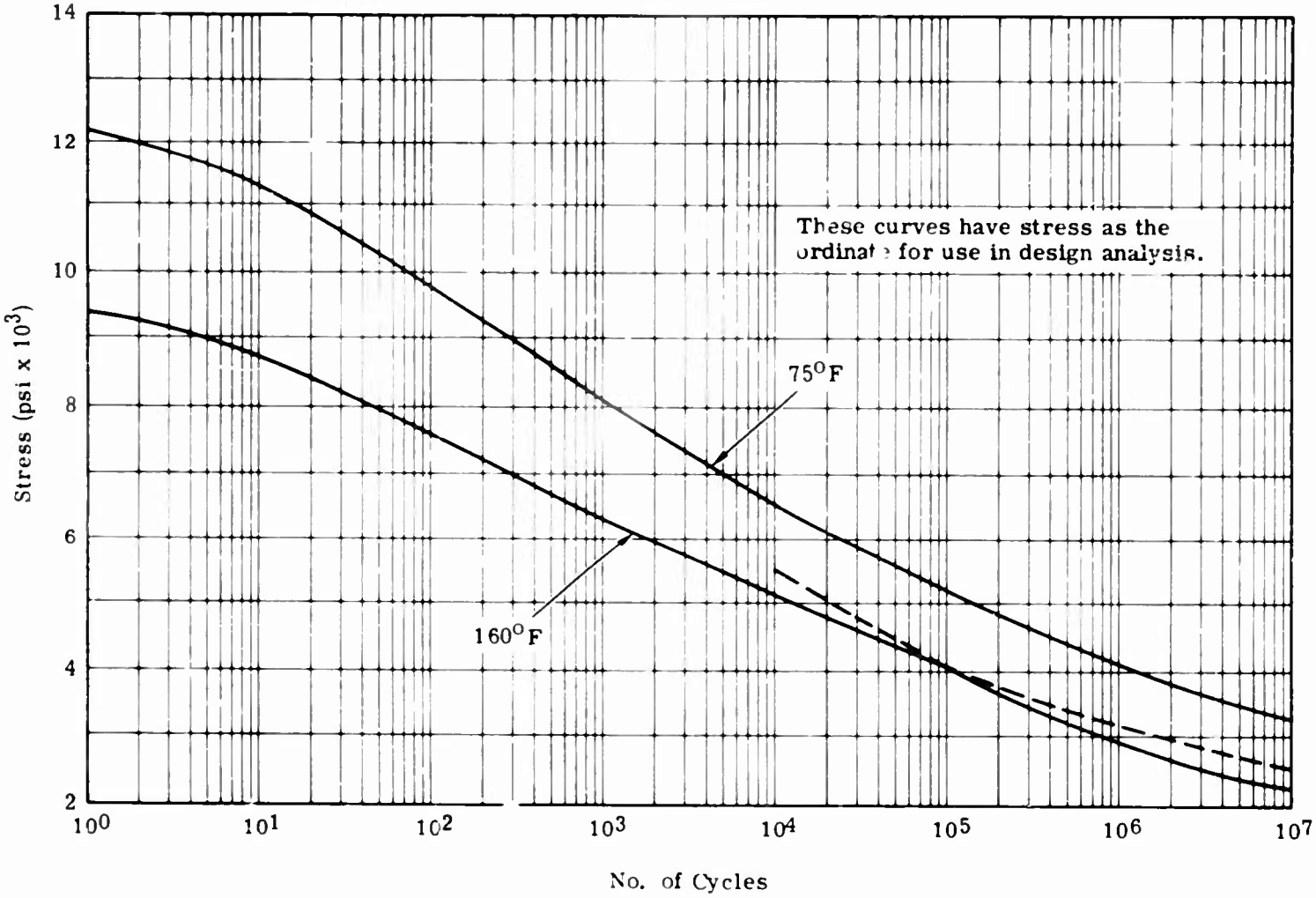

Figure 77. Fatigue Design Curves (A Basis) for 470/438-1/2 Composite.

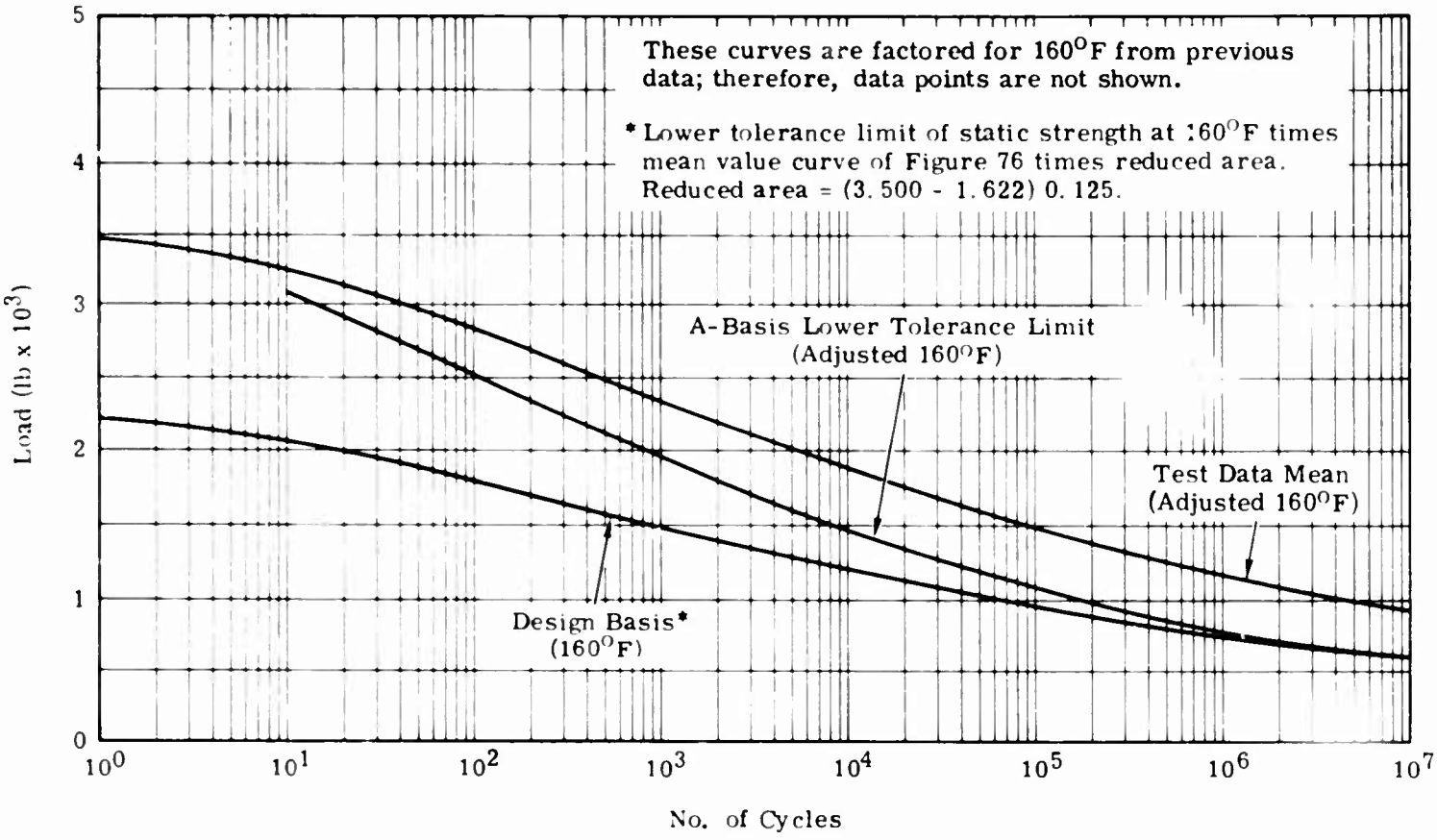

Figure 78. Typical Fatigue Design Curve for 470/438-1/2 Composite (Based on 3.5-Inch Minimum Width).